Role of non-vesicular secretion in neuronal development

Alessandra Gallo

Université de Paris
Ecole doctorale BioSPC (562)

Trafic membranaire dans le cerveau normal et pathologique
Institut de Psychiatrie et Neuroscience de Paris (IPNP), INSERM U1266, Paris, France

Role of non-vesicular secretion in neuronal development

Par **Alessandra Gallo**

Thèse de doctorat de **Neurobiologie**

Dirigée par **Thierry Galli**

Présentée et soutenue publiquement le **30 Septembre 2019**

Devant un jury composé de :

Mme. Catherine JACKSON Président du jury

Mme. Michela MATTEOLI Rapporteur

M. Ludger JOHANNES Rapporteur

M. Carlos DOTTI Examinateur

M. Etienne MOREL Examinateur

M. Thierry GALLI Directeur de thèse

Paris, September 2019

I would like to thank and acknowledge all the people that helped and motivated me during these years.

First and foremost, I wish to thank my thesis supervisors, Thierry Galli and Christian Vannier. Their wisdom and advices have been instrumental in my development and maturation as a researcher. In different and complementary ways, they both have transmitted to me their enthusiasm and passion for science.
I thank Christian "pour les recreations" on Neuroastronomy.

I am grateful to the members of the jury for their work, evaluation and helpful feedback on my work.

I owe my deepest gratitude to the Ecole des Neurosciences de Paris (ENP), for giving me the opportunity to do this great experience.
.
Thanks to all my lab mates, for making our shared space a wonderful place. Thanks to Sole and Francesca, I could not have done this without them.

To my Parisian sisters, Marta (my real sister), Flavia, Sara and Roberta, for the best moments of these six years in Paris.

Finally, a special thanks is for Mamma and Papà for letting me fly independently, supporting all my decisions. Grazie per la fiducia che avete sempre avuto nei miei confronti.

Alessandra

Contents:

ABSTRACT:

The growth of axons and dendrites during neuronal development requires a massive increase of surface area via the insertion of new proteins and lipids. This event occurs through the fusion of secretory vesicles with the plasma membrane, the final step of the secretory pathway. Recently, non-vesicular transfer of lipids at contact sites between the endoplasmic reticulum (ER) and the plasma membrane was shown to contribute to membrane expansion. Members of the ER-integral membrane protein Extended-Synaptotagmin (E-Syt) family have been identified as Ca^{2+}-dependent lipid transfer proteins at ER-plasma membrane contact sites, and shown to transfer glycerophospholipids via their lipid binding domains (SMP domains). The laboratory previously found that a novel ER-plasma membrane SNARE complex, composed of the ER-resident Sec22b and the neuronal plasmalemmal Syntaxin-1 (Stx1), is involved in neurite growth despite being unable to mediate membrane fusion. However, how this complex participates to neurite extension remained to be elucidated. In yeast, Sec22 interacts with lipid transfer proteins of the OSH family, enriched at the ER- plasma membrane contact sites, supporting a role for Sec22b-populated ER- plasma membrane junctions in non-vesicular lipid transport between these bilayers.

Based on these observations, our starting hypothesis was that E-Syts-mediated non-vesicular lipid transfer at Sec22b-populated ER- plasma membrane contact sites, might contribute to neurite outgrowth. The goal of my PhD project was to explore this hypothesis with two specific questions: 1/ What are the partners of Sec22b complexes which might be involved in the unconventional mechanisms of membrane expansion? 2/ What is the mechanism by which the non-fusogenic SNARE Sec22b/Stx1 complex acts in neuronal development?

Here we show that Sec22b interacts with E-Syt2 and Stx1 in PC12 cells and with E-Syt2, E-Syt3 and Stx3 in HeLa cells. Sec22b/E-Syt2 interaction appeared to depend on the presence of the Longin amino-terminal domain of Sec22b. Overexpression of E-Syt2 stabilized Sec22b-Stx3 association, whereas silencing of E-Syt2 had the opposite effect. Overexpression of E-Syt2 full length, but not the mutant forms which are unable to transfer lipids or attach to the ER, increased the formation of filopodia particularly in the growing axon. Finally, this effect was inhibited by a clostridial neurotoxin cleaving Stx1, by the expression of Sec22b Longin domain and a by a Sec22b mutant with extended linker between SNARE and transmembrane domains.

In conclusion, the results presented in this thesis support the hypothesis that Sec22b/Stx1 contact sites may contribute to membrane expansion via an interaction with phospholipid transfer proteins like E-Syts.

KEYWORDS: Endoplasmic reticulum-plasma membrane contact sites, non-vesicular lipid transfer, SNAREs, lipid transfer proteins, membrane expansion, neuronal development

RESUME:

La croissance des axones et des dendrites au cours du développement neuronal nécessite une expansion de la membrane plasmique via l'insertion de nouveaux lipides et protéines. Cet événement se produit à la suite de la fusion des vésicules de sécrétion avec la membrane plasmique. Cependant, plusieurs études ont montré que le transfert non-vésiculaire de lipides au niveau des sites de contact entre le réticulum endoplasmique (RE) et la membrane plasmique joue aussi un rôle dans la croissance des cellules. Des membres de la famille de synaptotagmines étendues (E-Syts) ont été identifiés comme protéines de transfert des lipides dépendantes du Ca^{2+} au niveau des sites de contact RE- membrane plasmique.

Nous avons récemment découvert qu'un nouveau complexe SNARE aux sites de contact RE-membrane plasmique, composé par Sec22b et Syntaxin-1 (Stx1), est impliqué dans la croissance des neurites bien qu'il soit incapable de favoriser la fusion membranaire. Cependant, la manière dont ce complexe participe à l'extension des neurites reste à élucider. Chez la levure, Sec22 interagit avec les protéines de transfert des lipides de la famille OSH, enrichis aux sites de contact RE- membrane plasmique.

Sur la base de ces observations, notre hypothèse est que le transfert non-vésiculaire de lipides induit par E-Syts au niveau des jonctions RE-membrane plasmique contenant Sec22b pourrait contribuer à la croissance neuronale. L'objectif de mon projet de thèse était d'explorer cette hypothèse. Nous montrons que Sec22b interagit avec E-Syt2 et Stx1 dans les cellules PC12 et avec E-Syt2, E-Syt3 et Stx3 dans les cellules HeLa. L'interaction Sec22b / E-Syt2 dépend du domaine Longin de Sec22b.

La surexpression des E-Syts stabilise l'association Sec22b / Stx1, alors que l'inactivation des E-Syts provoque l'effet inverse. La surexpression de E-Syt2 de type sauvage, mais pas des mutants incapables de transférer les lipides ou non fixés au RE, augmentent la formation de filopodes axonaux et la ramification de neurites dans les neurones en développement. Cet effet est inhibé par une neurotoxine clostridiale clivant Stx1, par l'expression du domaine Sec22b Longin et par un mutant Sec22b ayant une extension entre les domaines SNARE et transmembranaire.

En conclusion, les résultats présentés dans ma thèse soutiennent l'idée que les sites de contact Sec22b / Stx1 contribuent à l'expansion de la membrane via une interaction avec des protéines de transfert de phospholipides comme E-Syts.

MOTS CLEFS: Sites de contact réticulum endoplasmique- membrane plasmique, transfert non-vésiculaire de lipides, protéines SNARE, protéines de transfert de lipides, expansion membranaire, développement neuronal

PREFACE

Just like the skin for animals, the plasma membrane (PM) is for cells not only a protective barrier, but also the interface with the exterior and crucial player in many physiological and pathological processes. Being an integral part of the cell, it expands its surface in concert with cell growth and development. Coined Neuron's Herculean task by Karl Pfenninger, neuronal PM expansion is a massive phenomenon because these cells grow long and elaborated axons and dendrites, which can extend up to meters from the cell body. Hence, compared to other cell types, developing neurons have to face a formidable challenge of adding new membrane to appropriate locations in a manner that requires both high processivity and fine regulation. Membrane expansion during neuronal development is mainly thought to occur through the fusion of secretory vesicles with the PM. However, non-vesicular mechanisms of membrane traffic could contribute to PM expansion.

The main goal of my PhD project, performed in the laboratory of Thierry Galli at the Institut Jacques Monod and Institute de Psychiatry and Neurosciences of Paris, has been to characterize the role of SNAREs and their partners, residing at membrane contacts between endoplasmic reticulum (ER) and PM, in membrane expansion during neuronal growth. The starting point was the previous work by Maja Petkovic, who showed in her article published in *Nature Cell Biology* in 2014 that the R-SNARE Sec22b, a conserved ER-localized SNARE involved in vesicle fusion within the early secretory pathway, had a novel non-fusogenic function in promoting PM expansion during polarized growth (Petkovic et al. 2014). This additional unexpected function of Sec22b is achieved *via* its interaction with the neuronal Q-SNARE Syntaxin-1 (Stx1) at ER-PM contact sites in neuronal growth cones. Interestingly, in collaboration with the team of Cathy Jackson, this article also showed that Sec22 interacted with proteins involved in the non-vesicular lipid transfer of phosphoinositides between PM and ER in yeast. These results raised the simple question: "What is the mechanism whereby the non-fusogenic Sec22b-Stx1 complex is involved in neuronal growth?" and such question became the motivation of the work presented here. The hypothesis is that Sec22b-Stx1 complex associates with lipid transfer proteins (LTPs), which drive lipid transfer, rather than classical vesicular fusion, to mediate membrane expansion during neuronal development.

To test this hypothesis I have combined diverse approaches, from molecular biology and biochemistry, to characterize the molecular composition of SNARE complexes at ER-PM

contact sites, to experiments in cultured neurons and cell lines, involving drug treatment and imaging (live-microscopy, confocal microscopy, STED), to characterize the phenotype elicited by such associations. These approaches allowed me to demonstrate that Sec22b interacts with proteins belonging to the family of the ER-resident Extended-Synaptotagmins (E-Syts), which reside at ER-PM contact sites where they function as LTPs. In addition, I found that the overexpression of E-Syt2 increased the formation of filopodia in developing neurons, particularly in the growing axons. Interestingly, such E-Syt2 mediated morphogenetic effect seems to be dependent on Sec22b and Stx1, as impairing the correct function of these two proteins abolished the enhanced growth promoted by E-Syt2 overexpression. These findings support the idea that Sec22b-Stx1 contact sites may contribute to membrane expansion via the interaction with phospholipid transfer proteins like E-Syts.
This work benefited from a collaboration with the group of Francesca Giordano in expanding the scope of the study to non-neuronal cell types, as plasma membrane expansion during cellular growth is a conserved mechanism among all types of tissues development, as well as in pathological conditions like cancer.

The present manuscript is organized in three main sessions: introduction, results and discussion. The introduction aims at providing a solid background necessary to contextualize my scientific work and it is divided into two main chapters. Chapter 1 introduces the concepts of biological membranes and synthesis and metabolism of membrane lipids. It then reports on structure and functions of ER-PM contact sites, putting a particular accent on lipid trafficking between membranes. Chapter 2 summarizes the large body of literature on neuronal development, focusing on the conventional and the unconventional mechanisms by which the addition of newly synthesized membrane occurs during neurite outgrowth.

Abbrevations:

APC: Adenomatous polyposis coli

aPKC: Atypical protein kinase C

BDNF: Brain derived neurotrophic factor

BoNT: Botulinum neurotoxin

Cer: Ceramide

cER: Cortical ER

CERT: Ceramide transfer protein

Chol: Cholesterol

CL: Cardiolipin

CRMP-2: Collapsin-response mediator protein-2

DIV: Days *in vitro*

EM: Electron microscopy

ER: Endoplasmic reticulum

E-Syts: Extended Synaptotagmins

GDP: Guanine difosfate

GlcCer: Glucosylceramide

GPI: Glycosylphosphatidylinositol

GSK-3β: Glycogen synthase kinase 3 Beta

GSL: Glycosphingolipid

GTP: Guanine trifosfate

IGF-1: Insulin-like growth factor-1

JPH: Junctophilin

KD: Knock-down

KO: Knock-out

LD: Lipid droplet

LN: Laminin

LTP: Lipid-transfer protein

MCSs: Membrane contact sites

ngCAM: Neuron–glia cell adhesion molecule

NGF: Nerve growth factor

NSF: N-ethylmaleimide-sensitive-factor

ORP: oxysterol binding protein (OSBP)-related protein

OSBP: oxysterol binding protein

PA: Phosphatidic acid

PC: Phosphatidylcholine

PE: Phosphatidylethanolamine

pER: Perinuclear ER

PG: Phosphatidilglycerol

$PI(3,4,5)P_3$: Phosphatidylinositol-(3,4,5)-trisphosphate

$PI(3,5)P_2$: Phosphatidylinositol-(3,5)-bisphosphate

$PI(4,5)P_2$: Phosphatidylinositol-(4,5)-bisphosphate

PI: Phosphatidylinositol and

PI3K: Phosphoinositide 3-kinase

PI4P: Phosphatidylinositol-4-phosphate

PIP: Phophoinositide

PIS: Phosphatidylinositol synthase

PITP: phosphatidylinositol transfer protein

PLL: Poly-L-lysine

PM: Plasma membrane

PPVs: Plasmalemmal precursor vesicles

PS: Phosphatidylserine

PTEN: Tensin homologue deleted on chromosome 10 protein

rER: Rough ER

sER: Smooth ER

SM: Sphingomyelin

SMP: Synaptotagmin-like mitochondrial lipid binding protein domain

SMS: Sphingomyelin synthase

SNAP: Soluble NSF-attachment proteins

SNARE: Soluble N-ethylmaleimide-sensitive-factor (NSF) attachment protein receptor

SOCE: Store-operated Ca2+ entry

Stx1: Syntaxin-1

Tcbs: Tricalbins

TeNT: Tetanus neurotoxin

TG: Triglycerides

TGN: *Trans*-Golgi network

TMD: Transmembrane domain

VAPs: VAMP-associated proteins

Chapter 1

Lipid metabolism and membrane contact sites between ER and PM

The distinctive cellular architecture of eukaryotes is defined by membrane-delimited intracellular compartments. In animals, approximately half of the volume of a cell is membrane-enclosed, and in plants the vacuole can make up to 95% of the total cellular volume. If the plasma membrane (PM) organizes the cell as a unit and defines its internal volume, the intracellular membranes allow the optimization of cellular activities, by increasing the working surface and isolating domains with specific biochemical properties. Compared to prokaryotes, eukaryotic cells have indeed a much smaller surface area to volume ratio, and the PM area is presumably too small to sustain the many vital functions for which membranes are required. The system of internal membranes can be therefore considered as an adaptation that eukaryotes have evolved to alleviate this imbalance. Nevertheless, intracellular membranes do more than just providing increased membrane area. The advantage of elaborating specific compartments, during evolution, is the segregation of otherwise incompatible chemical reactions which then can be contained into compartments providing the appropriate and specialized aqueous spaces for a particular function to occur. Such compartmentalization is coupled to a coordination of cellular activities by the establishment of inter-organelle trafficking of signal and metabolites Communication has so far being thought to be ensured only by intracellular membrane traffic which is the process whereby exchanges between membrane-enclosed organelle and their lumen is mediated by carrier vesicles. More recently has emerged that notion that transfer of molecules could take place in specialized regions, namely membrane contact sites (MCSs), where membranes of two organelles are closely apposed and harbor molecular bridges.

An abundant literature has been dedicated to the biology of MCSs formed between the various compartments of eukaryotic cells. In this chapter I will develop functional relationships between endoplasmic reticulum (ER) and PM since MCSs established between these two compartments provide a powerful model for understanding molecular mechanisms driving inter-organelle exchanges and signaling. Several reviews highlight well characterized functions of ER-PM contacts in the control of Ca^{2+} dynamics (Helle et al. 2013), the regulation of signaling pathways (Haj et al. 2012, Stefan et al. 2011). Another important functional

specialization of these sites with regards to inter-compartment exchanges is their ability to perform lipid shuttling (Prinz 2014, Stefan et al. 2013).

In the first chapter of this thesis manuscript I will develop our current view on ER-PM contact sites with a particular emphasis on lipid-related activities. Topics such as membrane structure and/or dynamics, largely beyond the scope of this manuscript, will not be included as they constitute the subject of many recent reviews. Therefore, a first chapter of the introduction will be focused on the major involvements of membrane-bound compartments in lipid metabolism. The general characteristic of MCSs will be described as well as how several protein families are involved in the formation of these contacts. On the basis of the most recent discoveries, the functions orchestrated by ER-PM junctions will be discussed. The lipid trafficking events between membranes will be stressed out to understand how this process has been lately involved in neurite outgrowth, which is the subject of my thesis work.

1.1) Biochemical composition of biological membranes

Biological membranes are formed by the continuous addition of newly-synthesized components to a pre-existing one. These must then be transported and delivered to the correct compartment. The question as to how cells distribute newly produced proteins and lipids across membrane compartments to their proper destination has been central in cell biology. With regards to lipids, new molecules assembled on the cytoplasmic leaflet of the ER membrane can then be translocated to the luminal leaflet by flippases, a family of proteins which is in part responsible for adjusting the lipid composition of each layer of the membrane. Membrane components then leave the ER and travel through the secretory pathway for distribution to various subcellular compartments including the PM.
Notwithstanding the importance of membrane proteins in cellular function, a topic such as their biology and physiology will not be addressed in the context of this thesis. The current focus will be the structural organization and function of lipids within biological membranes.

Membranes are composed of several thousands of different lipids present in various amounts and proportions. Lipid structural and local abundance diversity can be observed from the scale of a membrane leaflet to that of a whole organism, suggesting that it is an essential features in determining the membrane identity. Furthermore, a large number of genetic diseases associated with mutations in enzymes involved in lipid metabolism, remodeling and modification,

suggests that membrane lipids fulfil many cellular functions (Klose et al. 2013, Lamari et al. 2013, van Meer et al. 2008). In cells, lipids first represent an essential energy storage device in the form of triglycerides (TG), which can be mobilized when demand for energy arises (Nakamura et al. 2014). This storage is also a source used as a reservoir of fatty acid and sterol components for membrane biogenesis. Second, cellular membranes are composed of amphipathic lipids, which consist of a hydrophobic "tail" region, with the propensity for self-association, and a hydrophilic "head" group, able to interact with aqueous environments and with each other. Due to their amphipathicity, membrane lipids spontaneously associate into bilayers in aqueous medium. This fundamental principle enabled the building of a primordial cell by segregating its internal constituents from the external environment, as well as to compartmentalize specific chemical reactions in order to increase biochemical efficiency (van Meer et al. 2008). In addition to a barrier function, lipids such as diacylglycerol and phosphoinositides act as signaling molecules (Shimizu 2009), molecular hubs for protein recruitment in cellular processes (Saliba et al. 2015) and substrates for post-translational protein fatty acylation (Resh 2016).

1.1.1) The repertoire of membrane lipids

The major structural lipids in eukaryotic membranes are glycerophospholipids, which account for 40-60 mol % of the total lipid fraction. These molecules are composed of a glycerol backbone, esterified on sn-1 and sn-2 carbons by two fatty acid chains, respectively. The carbon in position sn-3 generated by the double esterification by a phosphate on the sn-3 hydroxyle and an alcohol moiety. Glycerophospholipids can be classified according to the nature of the polar head groups. Phosphatidylcholine (PC), which is the most represented in eukaryotic membrane, has a choline molecule bound to the phosphate (Fig. 1a). Ethanolamine, serine, inositol and glycerol can replace choline, giving rise to phosphatidylethanolamine (PE), phosphatidylserine (PS), phosphatidylinositol and (PI) phosphatidilglycerol (PG), respectively (Escribá et al. 2008, Harayama & Riezman 2018, Klose et al. 2013, van Meer et al. 2008).

Sphingolipids constitute a second class of structural lipid accounting for the 10–15% of total membrane lipids. They are composed of a sphingoid-base backbone on which is linked a relatively long (up to 24 carbon atoms) saturated fatty acid chain. Acylated sphingosines are referred to as ceramides. Sphingomyelin (SM) (the only nonglycerol phospholipid in cell

membranes) and glycosphingolipids (GSLs) result from the attachment of a choline molecule and an oligosaccharide to the hydroxyl group of ceramides, respectively (Fig. 1b).

Sterols are present in most of eukaryotic cell membranes. While relatively long aliphatic chains constitute the hydrophobic moiety of most of membrane lipids, sterols essentially correspond to polycyclic structures, i.e. amphipathic four-ring isoprenoid-based hydrocarbons. Cholesterol (Chol) is the most abundant sterol in mammalian cells being able to enrich up to 50% of the total lipid composition in the PM. Its rigid hydrophobic backbone, which interacts with phospholipid acyl chains, harbors a hydroxyle group that interacts with the phosphate head of phospholipids (Fig. 1c). These interactions modulate membrane fluidity, membrane packing and the formation of microdomains. Ergosterol and lanosterol are two other representatives of the sterol class which exhibit a structure similar to that of Chol. They are respectively found in the membranes of fungi, yeasts and protozoans (Brennan et al. 1974) and in prokaryotes (Henriksen et al. 2006).

Biological membranes contain lipid-anchored proteins resulting from a post-translational modification consisting in linking a lipid group to newly synthesized proteins. These fatty acids give rise to myristoylation, palmitoylation, isoprenylation and take place in the membrane cytoplasmic leaflet. Glypiation correnspponds to the acquisition of a glycosylphosphatidylinositol (GPI) anchor on the extra-cytoplasmic leaflet.

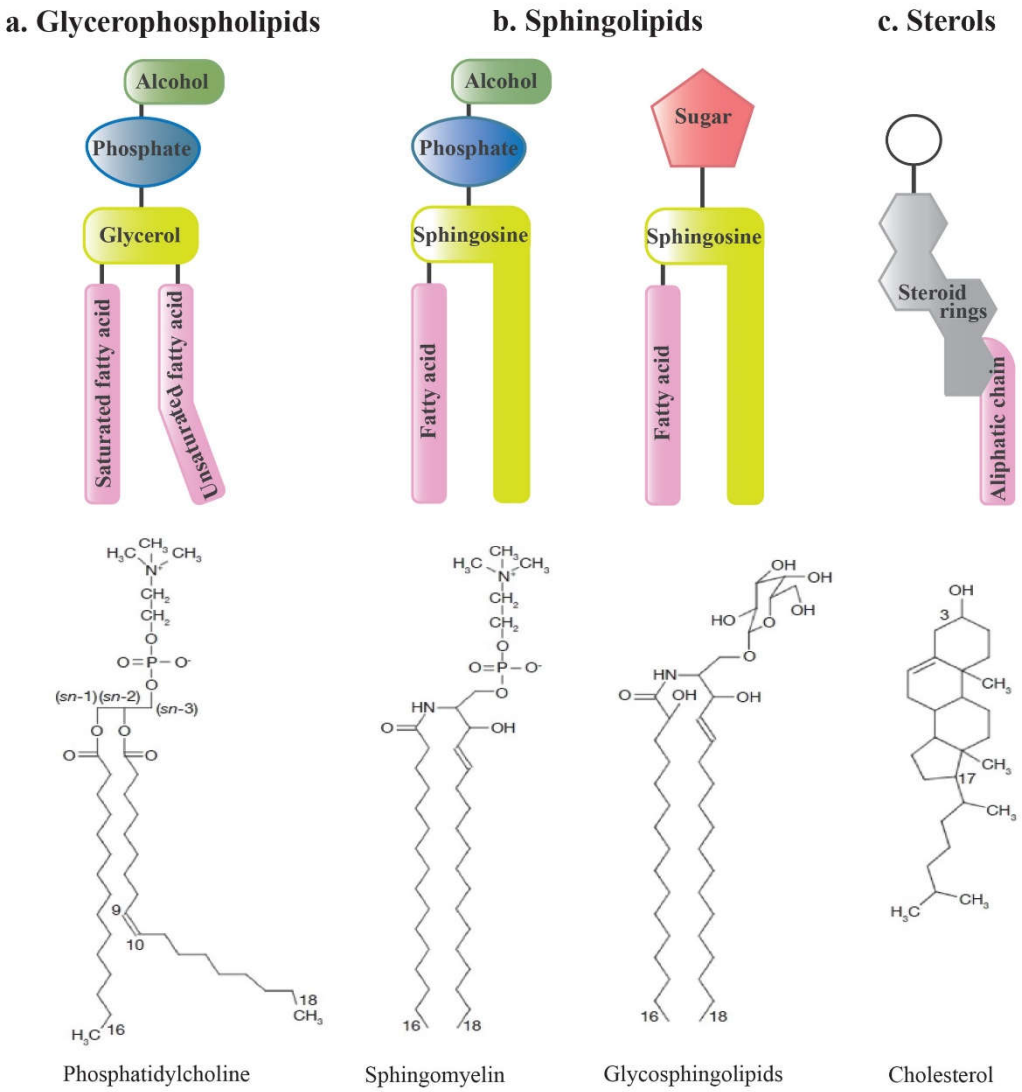

Figure 1. The molecular diversity of lipid species. Biological membranes comprise three major classes of lipids: glycerophospholipids (a), sphingolipids (b) and sterols (c).

1.1.2) Lipid metabolism and compositional diversity of membrane compartments

According to current estimates, the mammalian lipidome is comprised of 10,000 to 100,000 individual species of lipid molecules, which vary depending on their headgroups and aliphatic chains. In eukaryotic cells, lipids synthesis and catabolism are compartmentalized in several organelles, including the ER, the Golgi complex and the PM. The geographical restriction of lipid metabolism is the first determinant of the unique compositions of organelles and, consequently, of their downstream biological functions (Shevchenko & Simons 2010). Compartmentalization exists even at the suborganellar level, as shown by the enrichment of

many lipid-related enzymes in ER-mitochondria MCSs (Vance 2014). There is thus a need for more precise information on the localization of enzymes related to lipid synthesis and metabolism. Stable isotope labelling and mass spectrometry are the classical techniques used to monitor the kinetics of lipid biosynthesis and turnover. However, because of limitations in these techniques, such as the lack of robust and readily available data analysis software, new methodologies are required (Brandsma et al. 2017). Fluorescent analogues of fatty acids or lipid precursors that closely resemble the physicochemical properties of endogenous compounds, can be generated by bioorthogonal click chemistry reactions and used to understand how lipid distribution and composition are regulated (Izquierdo & Delgado 2018, Neef & Schultz 2009). Furthermore, some lipids can be directly imaged in tissues by mass spectrometry (MALDI-MSI) (Hankin et al. 2011, Mohammadi et al. 2016, Sparvero et al. 2012).

1.1.2.1) The ER: the major site of lipid synthesis

The vast majority of cellular lipids is synthetized by ER-localized enzymes. Hence, the ER represents the organelle that mainly influences cellular lipid biomass. ER-localized lipid synthesis provides cells with membrane lipids for growth, proliferation, and differentiation, as well as maintenance of membrane homeostasis.

The ER encloses about half of the total membrane area of an animal cell. It is organized into a labyrinthine membrane-bound network of branching tubules and flattened sacs that extends throughout the cytosol. Tubules and sacs interconnect, and their membrane is continuous with the outer nuclear membrane. Based on its ultrastructural appearance, it can be divided into three domains: “rough ER (rER)” whose name comes from its rough appearance due to the presence of membrane bound ribosomes, “smooth ER (sER)” and the double-membrane “nuclear envelope” surrounding the nucleus. It can also form additional discrete functional domains such as organelle contact sites, ER exit sites of secretory pathway and sites where lipid droplets bud (Jacquemyn et al. 2017, Lynes & Simmen 2011).

The largest portion of enzymes involved in lipid synthesis are transmembrane domain proteins spanning ER membranes. However, due to the large size of the ER, it is still challenging to determine their exact localization. Lipid synthesis is classically considered as a function of the sER. Nevertheless, this cannot be considered as the exclusive site of lipid production. Many evidences support the concept that some lipid synthesis reactions concentrate in functionally defined ER domains, such as ER–organelle contact sites. It has been shown, both in yeast and

mammalian cells, that ER-mitochondria and ER-PM contact sites exhibit a high capacity to synthesize certain phospholipids, especially PS and PI (Pichler et al. 2001, Vance 1990).

The ER is the site of synthesis of the main bulk of structural phospholipids and Chol, as well as of non-structural lipids such as triacylglycerol and cholesteryl esters (Fig. 2). The synthesis of glycerophospholipids is triggered by the acylation of glycerol 3-phosphate to form phosphatidic acid (PA), from which all other glycerophospholipids are formed by the addition of a polar head group (Blom et al. 2011). Sphingolipid synthesis spans from the ER, where it begins, to the Golgi complex, where it ends. Synthesis of the sphingosine and ceramide (Cer) intermediates occurs in the cytosolic side of the ER. Cer is then transferred to the Golgi apparatus in two manners, and each mode determines whether it is converted into either SM or glucosylceramide (GlcCer). While Cer transferred *via* vesicular transport is converted in GlcCer, Cer for the synthesis of SM is non-vesicularly transported by ceramide the transfer protein (CERT) at ER-Golgi contact sites (Blom et al. 2011, Hanada et al. 2003, Hannun & Obeid 2018). Even though *de novo* Chol is mainly synthesized in the ER, this lipid is rapidly transported to other organelles. Indeed, the ER, which is situated at the beginning of the secretory pathway, displays very low concentrations of sterols and complex sphingolipids. The resulting flexible and non-rigid membrane is consistent with its function in the insertion and transport of newly synthesized lipids and proteins (Jackson et al. 2016, van Meer et al. 2008).

1.1.2.2) Lipid synthesis in other membrane compartments

Besides the ER, other membrane-bound compartments, such as the Golgi apparatus, the PM, lipid droplets (LDs) and mitochondria, also contribute to the generation of the lipid spectrum within cellular membranes.

The Golgi apparatus functions as a factory in which proteins received from the ER are further processed and sorted for transport to their final destinations. In electron micrographs, the Golgi apparatus looks like a set of flattened membrane-enclosed sacs, also called cisternae. Vesicles that bud off from the ER fuse with the closest Golgi membranes, called the *cis*-Golgi. Afterwards, molecules travel through the medial and *trans* compartments of the Golgi stack, within which most metabolic activities of the Golgi apparatus take place. The modified proteins then move to the *trans*-Golgi network (TGN), which acts as a sorting and distribution center, directing molecular traffic to lysosomes, the PM, or the cell exterior (Bankaitis et al. 2012, Farquhar & Palade 1981).

In addition to its activities in processing and sorting glycoproteins, the Golgi apparatus functions in lipid synthesis and metabolism (Fig. 2). SM and GSLs are synthesized from Cer in the Golgi apparatus. SM is synthesized by the transfer of a phosphorylcholine group from PC to Cer through the action of sphingomyelin synthases (SMSs). There are two mammalian SMS: SMS1 and SMS2. SMS1 only resides in the Golgi apparatus, whereas SMS2 exists both in the Golgi and in the PM (Li et al. 2007, Tafesse et al. 2007). Alternatively, Cer generated in the ER can be glycosylated by glucosylceramide synthase to produce GlcCer, which serves as a precursor of complex glycosphingolipids (Hanada et al. 2003, Hannun & Obeid 2018). SM is synthesized on the lumenal surface of the Golgi, but glucose is added to Cer on the cytosolic side. GlcCer then flips, and additional carbohydrates are added on the lumenal side of the membrane (Jeckel et al. 1992).

The PM is highly enriched in sphingolipids and sterols compared to other cellular membranes. This lipid composition responds to the need of being rigid and tightly packed in order to act as impermeable barrier and to resist mechanical stress. Moreover, the PM also needs to be able to curve, a property enabled by enrichment of anionic glycerophospholipids, such as PI and PS, in the inner leaflet of the membrane due to their affinity for sphingolipids and Chol (Jackson et al. 2016, van Meer et al. 2008). The PM is not primarily involved in the synthesis of its structural lipids. However, some metabolic reactions for lipids that are involved in signaling can occur within this organelle (Fig. 2). For example**,** PI is normally produced by the phosphatidylinositol synthase (PIS) residing in cytosolic side of the ER. Nevertheless, a significant part of its synthesis is associated with a mobile PIS-containing membranes that are capable of making contacts with a variety of organelles, including the PM and the Golgi, allowing a direct PI synthesis in such compartments (Kim et al. 2011). A second example regards the synthesis of SM. As previously mentioned, the localization of the SMS2 on the extracellular leaflet of the PM implies that a certain amount of SM is locally produced within this organelle (Li et al. 2007, Tafesse et al. 2007).

LDs have a unique architecture consisting of a hydrophobic core of neutral lipids, which is separated from the aqueous cytosol by a monolayer of surface phospholipids. Their main functions include lipid storage for energy generation and membrane synthesis. Furthermore, LDs serve as organizing centers for the synthesis of specific lipids including for example TGs and ergosterol (Fig. 2) (Kuerschner et al. 2008, Walther & Farese 2012).

Mitochondria synthesize PA and PG, which are used for the synthesis of cardiolipin (CL), a phospholipid found almost exclusively in mitochondria (Fig. 2). Decarboxylation of PS produces mitochondrial PE, which is then exported to other organelles (Choi et al. 2005). The level of sphingolipids and sterols is generally low in mitochondria, whereas the high percentage of CL in the inner membrane, in addition to its high PE / PC ratio, recalls the bacterial origin of this organelle (Daum 1985).

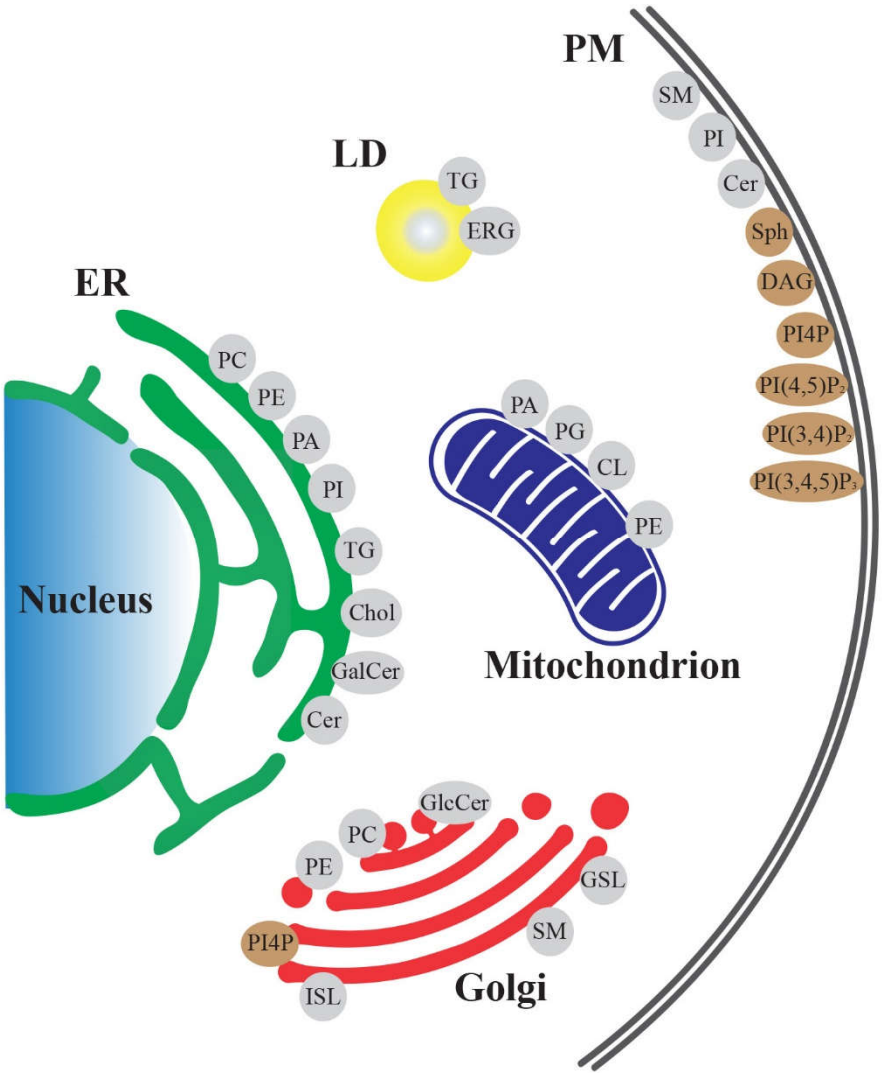

Figure 2. Lipid synthesis in the different membrane compartments. The figure illustrates the site of synthesis of the major phospholipids (grey) and lipids that are involved in signalling pathways (brown). The major glycerophospholipids assembled in the ER are phosphatidylcholine (PC), phosphatidylethanolamine (PE), phosphatidylinositol (PI), phosphatidylserine (PS) and phosphatidic acid (PA). In addition, the ER synthesizes Ceramide (Cer), galactosylceramide (GalCer) and cholesterol (Chol). Triacylglycerol (TG) synthesis occurs both in the ER and in LDs. The Golgi lumen is the site of synthesis of sphingomyelin (SM), complex glycosphingolipids (GSLs) and yeast inositol

sphingolipid (ISL) synthesis. PC is also synthesized in the Golgi, and may be coupled to protein secretion at the level of its diacylglycerol (DAG) precursor. Approximately 45% of the phospholipid in mitochondria (mostly PE, PA, phosphatidylglycerol (PG) and cardiolipin (CL)) is autonomously synthesized by the organelle. The PM is the site where lipids involved in signaling pathway are generetaed, including phosphatidylinositol-(3,5)-bisphosphate (PI(3,5)P2), phosphatidylinositol-(4,5)-bisphosphate (PI(4,5)P2), phosphatidylinositol-(3,4,5)-trisphosphate (PI(3,4,5)P3) and phosphatidylinositol-4-phosphate (PI4P). Based on articles cited in the paragraph 1.1.2.

1.2) Membrane contact sites: Historical overview

The first evidence of the existence of contacts between membrane-bound organelles came from the pioneering work of Porter and Palade (Porter & Palade 1957), describing by electron microscopy (EM) of muscle cells, structures in which ER and PM in close proximity generated small gaps filled by electrodense material. Such loci were later shown to regulate the flux of Ca^{2+} during excitation-contraction coupling in muscles (Endo 2009). Five years after Porter and Palade, Rosenbluth reported on the existence of similar structures in neurons, defined as an "intimate association" of subsurface ER cisternae with the neuronal plasmalemma. Their apparent absence in neighboring, non-neuronal cells and their occurrence in sensory and muscle cells, which, as neurons, generate or conduct electrical potential changes, led to the idea that these structures were present exclusively in such specialized cells (Rosenbluth 1962). In the following years, ER-PM junctions were morphologically recognized in a variety of organisms and cell types (Golovina 2005, Hayashi et al. 2008, Levy et al. 2015, Manford et al. 2012, Wu et al. 2017). The quest for their molecular composition then started.

The first observations of ER-PM contacts paved the way for further discoveries of physical links between the ER and various cellular organelles. Notwithstanding the well characterized vesicle trafficking between ER and Golgi, the two compartments are also linked by MCSs. ER-Golgi contacts were identified during the 1970s (Novikoff 1971), but their main function was only recently delineated: as a lipid transfer zone between the two organelles (Hanada et al. 2003, Kannan et al. 2015, Mesmin et al. 2013). The existence of ER-mitochondria MCSs was suggested by co-sedimentation of ER particles and mitochondria, and by electron microscopic proofs of close associations between mitochondria and ER (Mannella et al. 1998, Shore & Tata 1977). The seminal work was the discovery that ER adherent to mitochondria was

biochemically specialized for this function (Vance 1990). More recently, contacts between ER and other cell compartments were described in both yeast and mammals (Fig. 3).

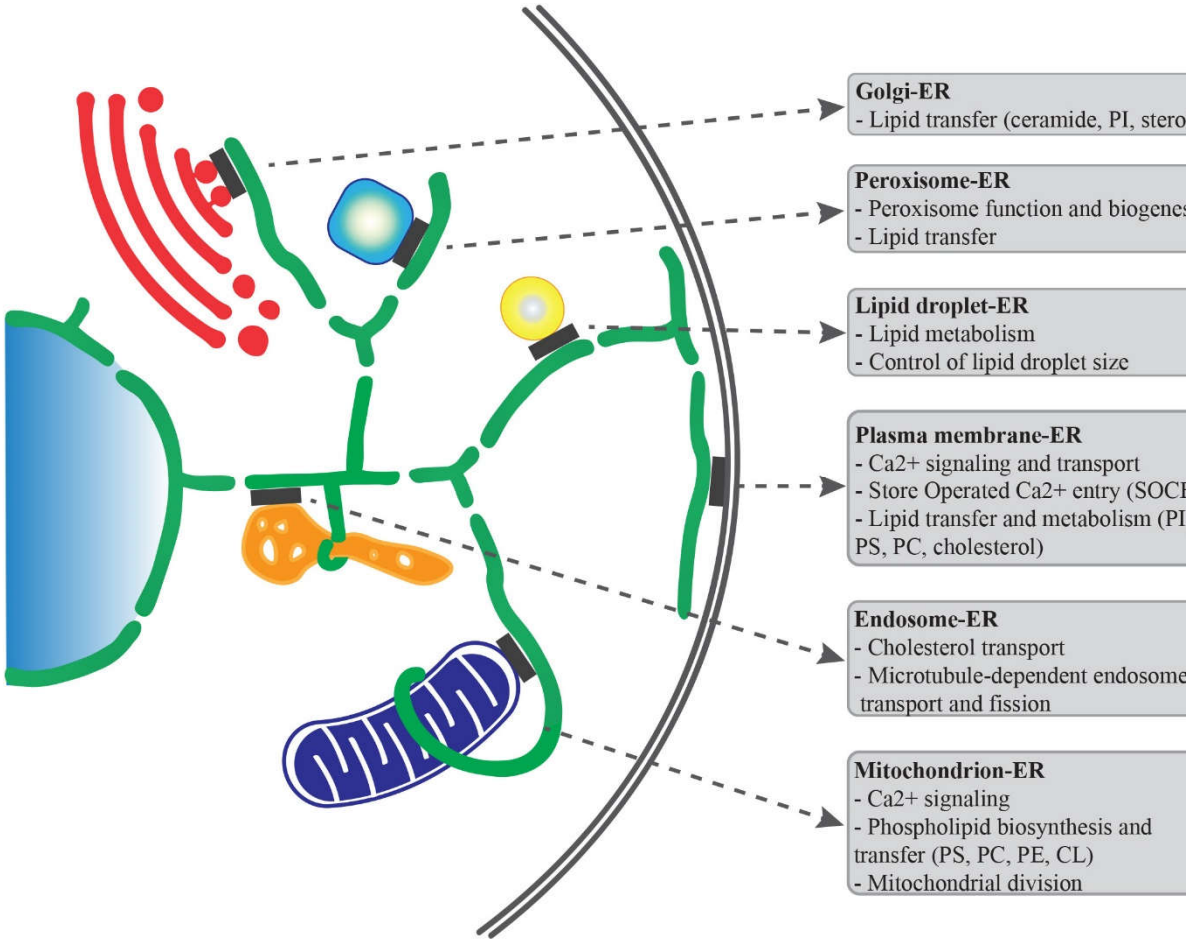

Figure 3. Schematic representation of MCSs. ER forms contacts with various cellular compartments including PM, Golgi, mitochondrion, endosomes, peroxisomes and lipid droplets (Jacquier et al. 2011, Raiborg et al. 2015, Schrader et al. 2015). These connections are necessary for multiple cellular processes, mainly related to lipid and Ca^{2+} metabolism, but also for organelle biogenesis and maturation, such as endosome and mitochondrial division.

1.3) General features of membrane contact sites

MCSs are classically defined as domains of close apposition between ER and a second organelle. Despite different intracellular localizations, MCSs display the following common properties: 1) the two membranes participating in the contact are in tight association with an interspace ranging from 7 to 30 nm; 2) this narrow apposition can modify ER membrane curvature and excludes ribosomes from its cytoplasmic face; 3) complete fusion between

membranes has never been described, implying that membrane identity is likely maintained; 4) a protein composition characterizes MCS microdomains (Prinz 2014, West et al. 2011).

MCSs are dynamic structures, which may appear as stable or transient on different time scales. STIM-ORAI interactions at ER-PM contacts display a very dynamic behavior: STIM1 rapidly forms oligomers in the ER membrane after Ca^{2+} store depletion. This oligomerization is followed by translocation of STIM1 to preexisting ER-PM junctions, which can enlarge to some extent (~50%) (Wu et al. 2006), and where it recruits the plasmalemmal Ca^{2+}-specific channel Orai1 to restore the physiological Ca^{2+} level in the ER lumen, a process that finally causes the dissociation of the transient STIM-ORAI interaction (Carrasco & Meyer 2011, Liou et al. 2007). Stability can further vary not only between different classes of MCSs, but also within a contact formed by the very same protein family. The ERMES complex appears as a stable structure linking ER and outer mitochondrial membrane in *S. cerevisiae* (Nguyen et al. 2012). These observations raise the question of what are the molecular determinants of MCS stability and further studies in this direction will be necessary to address such still open question.

Our knowledge of MCSs ultrastructure has until now derived from high-resolution EM, which revealed morphological diversity among different species or with respect to their function. ER-PM junctions provide an example of how the architecture of a contact site is related to its specific function. A recent cryo-electron tomography analysis of ER–PM contacts in mammalian cells highlighted the diverse structures of Extended Synaptotagmins (E-Syts) – and STIM1-mediated connections. On one hand, contacts formed by E-Syts (thought to exchange phospholipids at MCSs, see paragraph 1.5) displayed an electron-dense layer between the two membranes, likely formed at least in part by the cytosolic domains of E-Syts, which mask the hydrophobic side chains of phospholipids during their transfer (Fig. 4a). On the other hand, filamentous structures perpendicular to the membranes occurring in STIM1-dependent ER-PM junctions, formed upon reduction of luminal Ca^{2+}, had no intermediate density (Fig. 4b) (Fernández-Busnadiego et al. 2015, Soboloff et al. 2012). This shows that MCSs have a structure related to their function: lipid transfer or store-operated Ca^{2+} entry (SOCE).

In the following paragraphs, I will mainly focus on structure and functions of the most studied class of MCSs: the ER-PM contact sites.

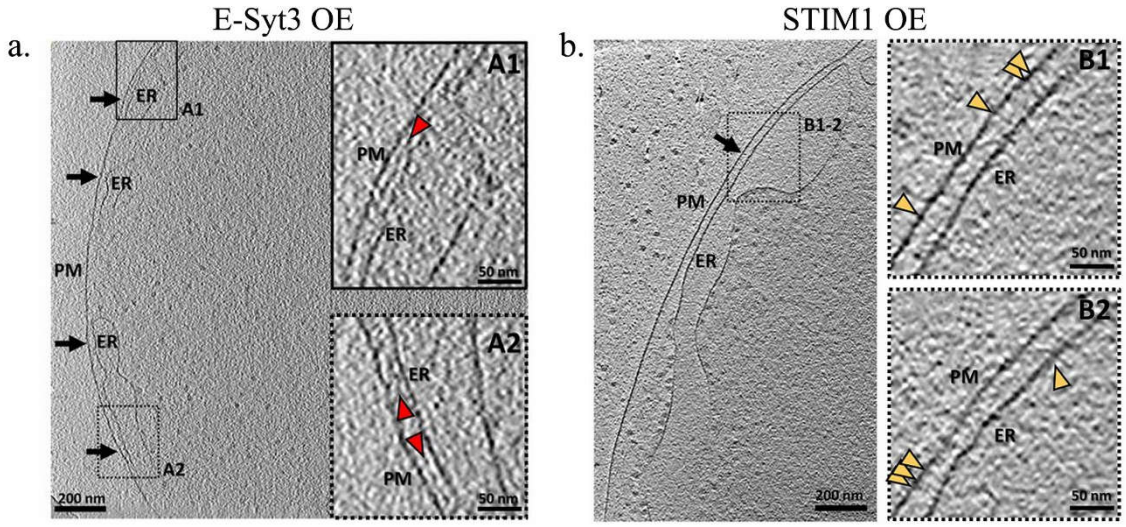

Figure 4. Tomographic slices of ER–PM contacts in COS-7 cells. (a) ER–PM contacts (black arrows) in a cell overexpressing Myc-E-Syt3 (E-Syt3 OE). (A1 and A2) Higher-magnification of the ER–PM contact in the regions labeled in A. The intermediate density is indicated by red arrowheads. (b) ER–PM contact (black arrow) in a cell transfected with mRFP-STIM1 (STIM1 OE). (B1 and B2) Higher-magnification of the ER–PM contact in the region labeled in A. Filaments bridging the ER and the PM are indicated by yellow arrowheads (Images adapted from Fernández-Busnadiego et al. 2015).

1.4) Proteins operating at ER-PM junctions

Despite half a century passed since their first identification, still little is known about the molecular mechanisms governing biogenesis, dynamics, structure and function of ER-PM contacts. The last decade has seen a renewed interest in MCS biology, particularly with the identification of proteins establishing connections between membranes. The formation of a functional ER-PM junction requires a well-tuned recruitment of proteins. A simple view of MCSs would consider tethering proteins setting the initial connection between the two bilayers. This would then create a unique microenvironment, favoring the recruitment of a second class of proteins performing functions specific of that particular contact (Helle et al. 2013). While attractive, this simplistic view may not be so real because very few proteins can be exclusively listed into only one of the two categories. In particular, no proteins have been found that merely tether, with no other role, but a more complex scenario prevails, in which almost all proteins operating at ER-PM junctions have more than one function.

Particular criteria define a tethering protein:

a) From a structural viewpoint, a single element tether includes an ER-anchoring domain and a lipid- or protein-binding domain distal from the first (Henne et al. 2015). The presence of these two modules should allow for the simultaneous binding of the two membranes. There is an exception however when tethering is mediated by *trans*-interactions of proteins residing in the two opposite bilayers (Petkovic et al. 2014).
b) From a functional viewpoint, overexpression of a tether should result in an increase of ribosome-free ER elements closely apposed to the PM, and, on the contrary, inactivation should at least in part disassemble the contact. However, in some cases, several independent proteins contribute to establishing a single junction (Takeshima et al. 2000). Such functional redundancy might compensate the lack of a component in order to maintain a stable membrane connection. Three families of structurally unrelated ER-PM tethering proteins have been identified in yeast: Ist2 (related to the mammalian TMEM16 family of ion channels), the tricalbins (Tcb1/2/3, C2 domain-containing proteins similar to the extended synaptotagmin-like proteins E-Syt1/2/3), and Scs2 and Scs22 (vesicle-associated membrane protein-associated proteins). The absence of all six tethering proteins results in morphological alterations of the cortical ER: the network of sheets and tubes attached to the PM is largely lost and ER accumulates in the cytoplasm while absence of only one has at best partial effects (Manford et al. 2012).

The above list can be extended by including proteins known to act as potential tethers in yeast and in mammals, namely Junctophilins, Sec22-Sso1 (orthologs of mammalian Sec22b-Stx1 complexes) and Kv2.1 potassium channels (Fox et al. 2015, Giordano et al. 2013, Petkovic et al. 2014, Takeshima et al. 2000, Wolf et al. 2012) (Fig. 5). In this paragraph I will present these protein families, providing details on their structure and function at ER-PM MCSs. The difference in their domain organization and cellular pathway may explain how the diversity of protein-based structures elaborated by the cells can converge in bridging ER and PM membranes and, conversely, how MCSs become the hubs for numerous intracellular signals.

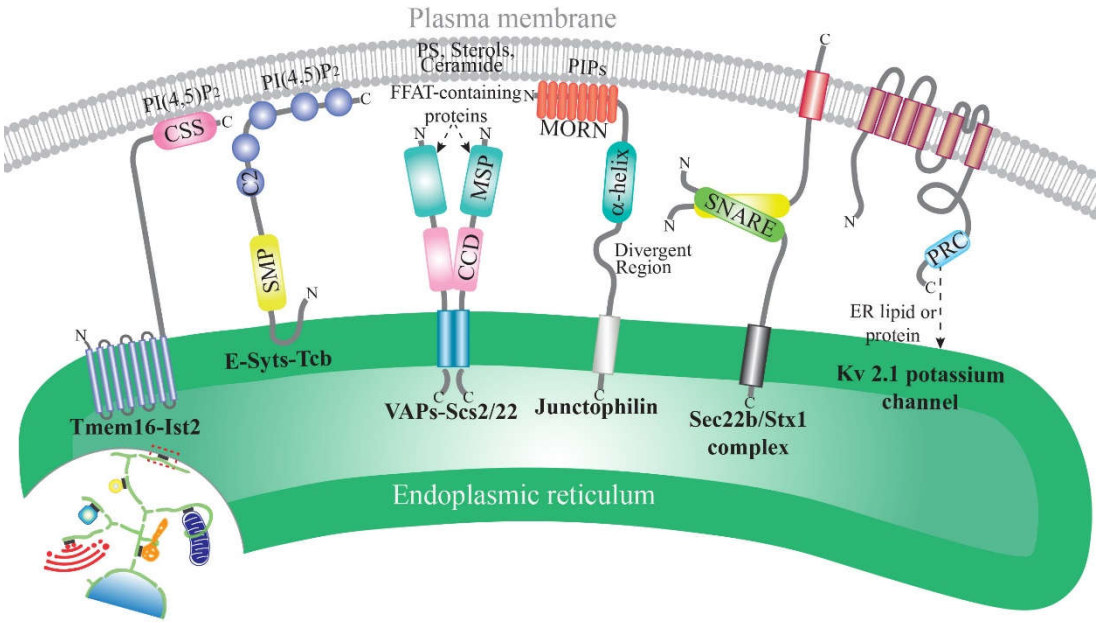

Figure 5. Domain organization and topology of ER-PM tethering proteins. Members of six different protein families are proposed to be tethers between the ER and PM in metazoa and/or yeast. Abbreviations: CCD, coiled-coil domain; CSS, cortical sorting signal; E-Syt, extended synaptotagmin; ER, endoplasmic reticulum; FFAT, double phenylalanine in an acidic tract; MORN, membrane occupation and recognition nexus; MSP, major sperm protein; PIP, undefined phosphoinositide; PI(4,5)P2, phosphatidylinositol 4,5-bisphosphate; PM, plasma membrane; PRC, proximal restriction and clustering; PS, phosphatidylserine; SMP, synaptotagmin-like mitochondrial lipid-binding protein; Tcb, tricalbin; VAP, VAMP-associated protein (modified from (Gallo et al. 2016).

1.4.1) Tmem16 (Ist2 in Yeast)

In *S. cerevisiae,* ER apparatus forms three domains, the perinuclear ER (pER), the cortical ER (cER) and occasional strands that link them. cER appears as tubules and small cisternae apposed to the PM. The ER membrane protein Ist2 interacts with phophoinositides (PIPs) of the PM (Fischer et al. 2009).

Based on sequence homology, Ist2, an octaspanning integral protein of the ER, is a member of the TMEM16 or anoctamin (ANO) Ca^{2+}-activated chloride-channels protein family (Hartzell et al. 2009). Its accumulation at PM-associated ER loci is mediated by a C-terminal polybasic stretch rich in lysine and histidine (the cortical sorting signal of Ist2, CSSIst2), interacting with PM PI(4,5)P_2 and other lipids (Fischer et al. 2009). A recent study showed that an intrinsically disordered (ID) domain of 300 amino acids is interposed between the transmembrane domain (TMD) and the CSSIst2 (Fig. 5). Such ID region, lacking persistent secondary or tertiary

structures, is highly flexible, and too long to span the distance between- and link cER and PM (Kralt et al. 2015).
Massive over-expression of Ist2 in mammalian cells leads to a patch-like localization of the ER at the cell periphery, and similar results are seen with over-expression of STIM, which has a similarly long linker, indicating that Ist2 functions as a tether from yeast to metazoans (Ercan et al. 2009), perhaps for long-distance interactions.

In addition to its bipartite lipid binding ability, Ist2 fulfills the other typical characteristics of a tether protein: its overexpression leads to an increased association between ER and PM. Conversely, the amount of PM-associated cER at less than 30 nm is reduced from 48% of WT cells to only 8% in ist2Δ cells, and the distance between the two membranes is increased in the latter (Wolf et al. 2012). Another study found however no significant loss of cER in Ist2 single mutants (Manford et al. 2012).
Moreover, yeast growth is sensitive to the abundance of Ist2 protein (Wolf et al. 2012), supporting an involvement of ER-PM contacts in cell growth. In line with their contribution to cell growth, recent studies have shown that the mammalian TMEM16F/Ano6, a particular member of the TMEM16 family that function either as a Ca^{2+}-activated ion channel or as a lipid scramblase, induces a massive surface membrane expansion without involvement of classical exocytic pathways (Bricogne et al., 2018; Fine et al., 2018). Further details on this function will be provided in the context of alternative pathways of membrane trafficking in neuronal development (see paragraph 2.4).

1.4.2) Extendend Synaptotagmins (E-Syts, Tcbs in Yeast)

E-Syts are Ca^{2+}-regulated ER-integral membrane proteins named from their similarity to the synaptotagmin protein family, which also includes ferlins (Lek et al. 2012). The founding members of this family, Synaptotagmins 1 and 2 are crucial Ca^{2+} sensor acting in synaptic vesicle exocytosis (Min et al. 2007). Analysis of vertebrate sequences uncovered three evolutionarily conserved, closely related E-Syt proteins (E-Syt1, E-Syt2 and E-Syt3) (Fig. 6A) considered to be yeast Tcbs' orthologues (Creutz et al. 2004, Lee & Hong 2006). E-Syts contain an N-terminal "hairpin" region, penetrating without entirely crossing the ER bilayer, a cytosolic synaptotagmin-like mitochondrial lipid binding protein (SMP) domain, and either five (E-Syt1) or three (E-Syt2 and E-Syt3) C2 modules acting as $Ca^{2+/}$phospholipid-binding domains and/or

as protein–protein interaction domains (Rizo & Südhof 1998) (Fig. 5). The C2-domains are independent modules of 80–160 residues assembled into the β-sandwich conformation as originally described for the synaptotagmin-1 C2A-domain, the first whose atomic structure and Ca^{2+}-binding mode were determined, and the only one where the entire sequence required for Ca^{2+} binding is conserved (Min et al. 2007, Xu et al. 2014).

A potential role of E-Syts in promoting ER-PM junctions formation is supported by structure/function studies showing that their last C-terminal C2 domains, namely C2C (E-Syt2, E-Syt3) and C2E (E-Syt1), mediate the binding to $PI(4,5)P_2$, a phosphoinositide concentrated in the PM (Di Paolo & De Camilli 2006, Reinisch & De Camilli 2016). Hence, since the amino-terminus of E-Syts is embedded in ER membranes, binding of C2 domains to the PM induces the formation of short-distance MCSs. In the case of E-Syt2 and E-Syt3, that are constitutively bound to the PM, C2C domain-dependent ER-PM association only requires the presence of $PI(4,5)P_2$ (Giordano et al. 2013, Min et al. 2007). The C2A and C2B domains then regulate the tightness and the topology of this binding in response to cytosolic Ca^{2+} concentration. In contrast, the recruitment of E-Syt1 to the PM requires elevation Ca^{2+} levels to the micromolar range and the action of the Ca^{2+}-dependent C2C domain in combination with the C2E domain. Similarly to E-Syt2 and 3, Ca^{2+}-dependent PM association of E-Syt1 is then regulated by the C2A and C2B domains, again allowing a dynamic tightening to the PM (Fig. 6B) (Chang et al. 2013, Giordano et al. 2013, (Herdman & Moss 2016), Idevall-Hagren et al. 2015).

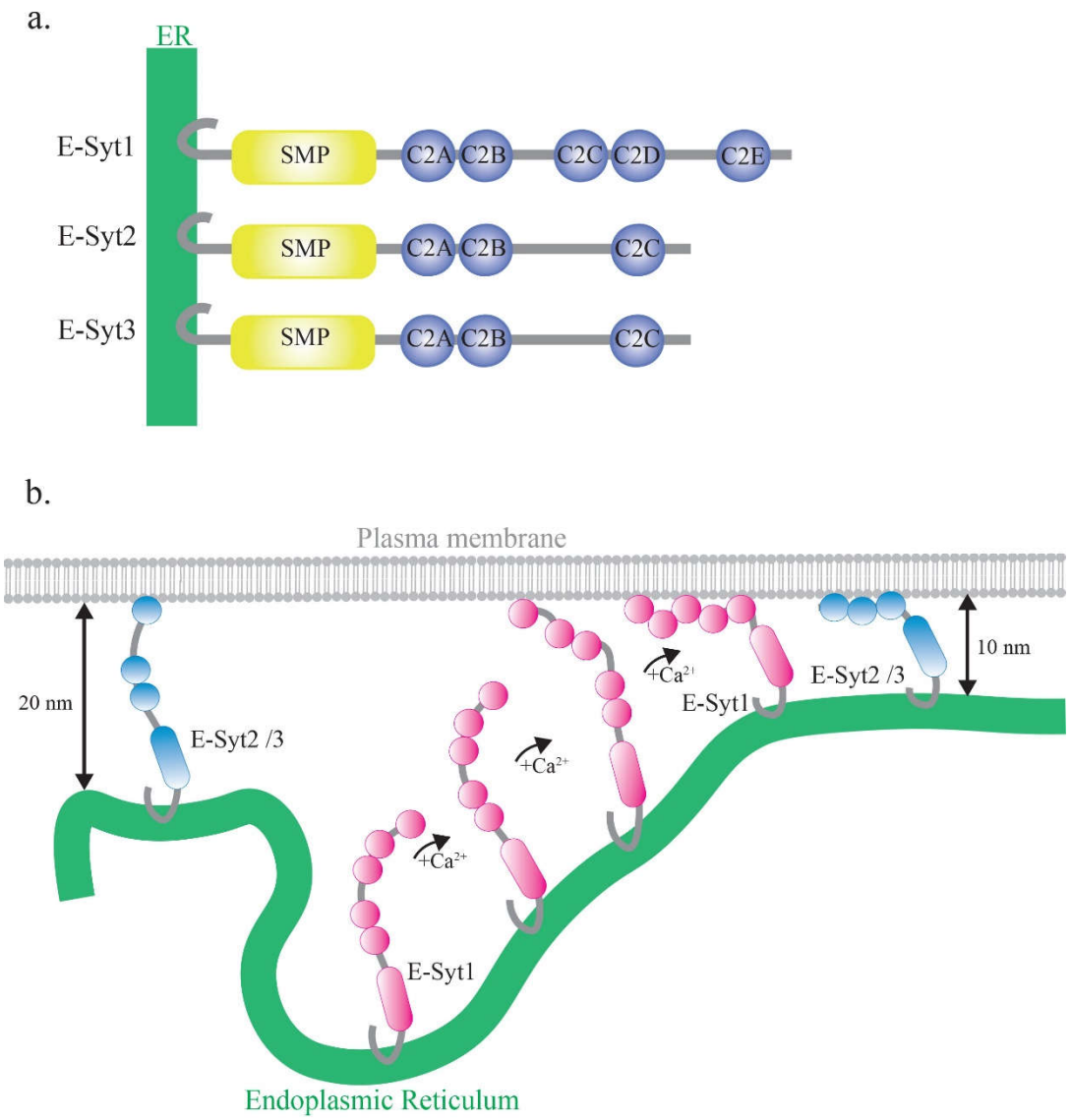

Figure 6. Architecture and Ca^{2+}-dependent regulation of E-Syts. (A) Schematics showing the domain structure of mammalian E-Syts. The E-Syts are anchored in the ER by an N-terminal beta-hairpin. Their cytosolic portion consists of an SMP domain and five or three C2 domains in E-Syt1 and E-Syt2/3, respectively. (B) Coordination between C2 domains regulates the tightness of the ER-PM contact sites. E-Syt2/3 (in blue) bind the PM through its C2C domain in a semi-constitutive manner. An increase in cytosolic Ca^{2+} would then tighten binding by enhancing the C2A/C2B interaction with PM phospholipids. E-Syt1 (in pink) does not significantly interact with the PM at low cytosolic Ca^{2+}, but could also bind in a progressively tighter manner at enhanced cytosolic Ca^{2+}. Based on articles cited in the paragraph 1.4.2.

Remarkably, due to their ability to homo- or heterodimerize, E-Syt activity can be modulated by Ca^{2+} acting on homo- or hetero-dimers containing E-Syt1 (Giordano et al. 2013, Reinisch & De Camilli 2016). Contrary to what happens in mammals, in yeast no Ca^{2+}-dependent function in ER-PM tethering has been attributed to Tcbs (Manford et al. 2012). Post-translational

modifications and association with other proteins are also likely to be involved in modulating E-Syt functions, but these have yet to be studied in detail.

Consistent with the tether criteria, deletions of C2C domain abolish E-Syt2 PM localization (Min et al. 2007), whereas E-Syts overexpression increases ER-PM contacts (Giordano et al. 2013). Surprisingly, genetic deletion of E-Syt genes results in a mild phenotype in mouse, suggesting that E-Syts are functionally redundant with other ER-PM tethering proteins (Herdman et al. 2014). Furthermore, E-Syts/Tcbs function at ER-PM contacts cannot solely be reduced to tethering the two membranes. The presence in E-Syts of a SMP domain, predicted to accommodate a lipid within a hydrophobic groove (Kopec et al. 2010), and the capability of homo- or heterodimerization able to create a hydrophobic bridge between two bilayers or operate as a shuttle (Schauder et al. 2014), have suggested a role of E-Syts in lipid transfer between ER and PM (Schauder et al., 2014; Yu et al., 2016; Saheki et al., 2016). This will be detailed in paragraph 1.5.

1.4.3) VAMP-Associated Proteins (VAPs, Scs2/22 in Yeast)

VAMP-associated proteins (VAPs) are integral ER membrane proteins named after their initial identification as interactors of the vesicular SNARE synaptobrevin/VAMP in *A. punctate* (Skehel et al. 1995). Besides their classical ER localization, VAPs were found in a wide variety of contact sites between ER and organelles, such as Golgi and PM, assessing a role for these proteins in the establishment of MCSs (Lev et al. 2008).

Mammals express two VAP isoforms sharing a similar primary organization: VAP-A and –B, encoded by two distinc genes, and an alternative spliced variant of VAP-B, VAP-C. These proteins consist in two conserved domains, namely an N-terminal immunoglobulin-like β sheet (MSP domain) and a C-terminal TMD domain harboring a putative dimerization motif. An additional domain consists in a coiled-coil motif (CCD), similar to those found in SNAREs, in mammalian E-Syts (Nishimura et al. 1999) (Fig. 5). In S. cerevisiae the two VAP homologues, Scs2 and Scs22, contain neither the coiled-coil nor the dimerization motifs and, consequently, these proteins do not form dimers (Loewen et al. 2003).

VAPs bind a wide number of intracellular lipid-binding proteins, such as oxysterol binding protein (OSBP)-related proteins (ORPs), CERT proteins, PI-transfer domain-containing

proteins and retinal degeneration-B protein (RdgB) (Kawano et al. 2006, Loewen et al. 2003). The evolutionary conserved FFAT (double phenylalanine in an acidic tract)-motif is necessary and sufficient for binding to VAPs and it allows ER targeting via VAP binding (Loewen et al. 2003). FFAT modif is found in many proteins, suggesting that VAPs may be present in a large number of MCS types involving the ER membrane (Levine 2004, Murphy & Levine 2016). The crystal structure of the rat VAP-A/ORP1 FFAT motif revealed how a specific molecular interaction is conserved from yeast to mammals (Kaiser et al. 2005). Part of the FFAT binding site of the Scs2p has been identified by a mutagenic screen. This showed that the FFAT motif recognizes a positively charged patch of several basic residues on the surface of the MSP domain (Loewen & Levine 2005). *In vitro* studies demonstrated that the Scs2p MSP domain also binds with high affinity the PM-enriched phosphoinositides PI4P and PS, suggesting a role for Scs2p at ER-PM contact sites (Kagiwada & Hashimoto 2007).

A large number of FFAT-motif containing proteins have domains allowing the simultaneous binding of ER via VAPs and PM via phospholipids, thus contributing to the establishment of contacts between these two bilayers. For example, the phosphatidylinositol transfer protein (PITP) Nir2, mammalian orthologue of D. melanogaster RdgB, binds VAPs in the ER and translocates from the cytosol to E-Syt1-induced ER-PM junctions formed in response to elevation of cytosolic Ca^{2+}. At these sites, Nir2 promotes via its PITP activity, the replenishment of $PI(4,5)P_2$ at the PM after receptor-induced hydrolysis (Chang et al. 2013). The presence of FFAT proteins at ER-PM junctions reveals the biological significance of VAPs in tethering the two bilayers, a function further confirmed by the reduced number of ER-PM contacts in yeast cells lacking Scs2p (Loewen et al. 2007). However, VAP proteins do more than just tether ER and PM: they actively participate in MCS function as occurs, for instance, at yeast ER-PM contacts, where the VAP orthologs Scs2/22 are key regulators of PI4P metabolism (Stefan et al. 2011). Furthermore, Scs2 is specifically located at sites of polarized growth, suggesting that VAPs, similarly to Ist2, act in cell growth and in polarized functions of the ER, both in yeast and in higher eukaryotes (Loewen et al. 2007).

1.4.4) Junctophilins

Junctophilins (JPHs) anchor the endo/sarcoplasmic reticulum to the PM in excitable cells, both muscles and neurons. A phylogenetic study suggested that the JPH family is conserved among metazoan species: invertebrates contain a single JPH gene, while mammals express four JPH isoforms (JPH1-JPH4) arisen by ancestral gene via duplication and divergence mechanisms. Isoforms are tissue-selective: JPH1 and JPH2 are expressed in skeletal and cardiac muscle respectively, whereas JPH3 and JPH4 are mainly expressed in neuronal tissues. The same analysis revealed that JPH subtypes share conserved sequences of 14 amino acid residues, termed MORN (membrane occupation and recognition nexus) motifs, repeated eight times in the amino-terminal region (Garbino et al. 2009). The MORN motifs mediate binding to the PM through interaction with PM-specific phospholipids, such as PIPs. Their transmembrane C-terminal domain anchors JPHs to the ER. Their N-and C-termini are linked by an α-helix of 100 amino acids, thought to control ER-PM distance, and a less evolutionarily conserved divergent region, whose role is still unclear (Landstrom et al. 2014, Takeshima et al. 2000, 2015) (Fig. 5).

Among all the putative tethers, JPHs were initially considered as the only proteins with a pure structural function in holding together intracellular membranes. However, emerging evidence suggests that they are also critical for proper Ca^{2+} signaling in excitable cells. In the muscle physiology context, JPHs interact with the ryanodine receptors (RyRs), which mediate Ca^{2+} release within the SR during the excitation-contraction coupling. Genetic manipulations in mouse established the key role of JPH1 and JPH2 in controlling Ca^{2+} utilization in sketetal and cardiac muscle cells exhibiting impaired communication between dihydropyridine receptors (DHPRs) and RyRs and morphologically abnormal junctions (Ito et al. 2001, Takeshima et al. 2000).

JPH3 and JPH4 may play roles in mediating motor control through maintenance of efficient Ca^{2+} signaling in the brain. Supporting this hypothesis, the functional communication between NMDA receptors, RyRs, and small-conductance Ca-activated K channels is disconnected because of junction disassembly in JPH3/JPH4 double knock-out (KO) mouse neurons (Ito et al. 2001).

Overall, these studies have been instrumental in revealing that specific interactions between JPHs and Ca^{2+}-channels are needed for physiological Ca^{2+} signaling.

1.5) Functions orchestrated at ER-PM junctions

A well-established function for MCSs in metazoan cells involves the trafficking of calcium and lipids between two compartments. Additional roles of MCS have emerged only recently. These novel functions mainly regard the control of organelle shape and morphology, intracellular signaling and cell stress responses. From the pioneering observations to the most recent discoveries, I will discuss the mechanisms so far disclosed for non-vesicular lipid exchange between ER and PM. These may involve lipid-transfer proteins (LTPs), catalyzing transport of lipid molecules between the two membranes. The structure of LTPs will be described with regards to how their domain organization can account for their lipid-binding specificity and transfer capability.

1.5.1) Discovery and features of non-vesicular lipid transport

The non-homogeneous distribution of lipids throughout compartments in eukaryotic cells is determined by complex mechanisms of intracellular lipid transport allowing amphipathic molecules to shuttle between membranes inside the aqueous milieu of the cell. Canonical intracellular membrane trafficking accounts for protein and lipid transport between ER, Golgi, and PM (Kaplan & Simoni 1985a, Schekman 2002). This participates in the non-homogenous distribution of lipids because sorting mechanisms apply in donor compartments to both proteins and lipids, and lipid modifying enzymes are targeted to specific compartments (Blom et al. 2011). However, intracellular lipid trafficking does not solely rely on vesicular lipid transport. Indeed, several studies have demonstrated the existence of transport mechanisms occurring independently from the conventional secretory pathway.

The first evidence in support of a non-vesicular transport of lipids come from pharmacological studies. Colchicine and brefeldin A, two agents known to interrupt protein secretion had no effect on the movement of lipids, such as PC, PE, Chol, GlcCer, from the ER to the PM (Kaplan & Simoni 1985a,b; Sleight & Pagano 1983, Urbani & Simoni 1990, Vance et al. 1991, Warnock et al. 1994). These original findings were reinforced by genetic studies in yeast. Cells with impaired Sec18p, a key protein for most vesicle trafficking out of the ER, did not exhibit altered

transport of the newly-synthesized ergosterol, the major yeast sterol (Baumann et al. 2005). These results suggested a high capacity of non-vesicular lipid transport mechanisms. These facts may be particularly relevant in bulk growth of the PM.

Complementary to vesicular trafficking, non-vesicular lipid transport represents a main source of lipids for organelles not connected to the secretory pathway (mitochondria, chloroplasts and lipid droplets). This ensures a rapid control of lipid levels (such as Chol), lipid metabolism regulation and cell signaling while avoiding toxic effects (Prinz 2010).

1.5.2) Molecular mechanisms of non-vesicular lipid transport

Non-vesicular movement of lipids takes place through three general processes: lateral diffusion, trans-bilayer flip flop and monomeric lipid exchange (Fig. 7).

Lateral diffusion applies to lipids moving in the membrane bilayer plane, whereas *trans*-bilayer flip flop between leaflets of one membrane occurs either spontaneously or with the help of specialized proteins, such as flippases (Holthuis & Levine 2005, Lev 2010). These two processes operate within one bilayer. Monomeric lipid exchange can consist in the spontaneous desorption of a lipid from a membrane into the aqueous phase and its insertion into another membrane. Such process is usually influenced by aqueous-phase solubility of lipids and membrane curvature (Lev 2010).

Spontaneous lipid exchange can also occur during a mechanism of simple or activated collision of two membranes. In the second case, a lipid, referred to as activated, extends from the bilayer, increasing the probability of its transfer during collision (Steck et al. 2002). The spontaneous movement of most lipid species is extremely slow. For example, PC is exchanged between artificial membranes with a half-time above two days. Moreover, spontaneous movements would randomize the content of lipids within membranes rather than establish differential lipid composition, essential for organelles identity. Therefore, it seems unlikely that such mechanism plays a significant role in membrane biogenesis and maintenance unless proteins intervene to control the reactions.

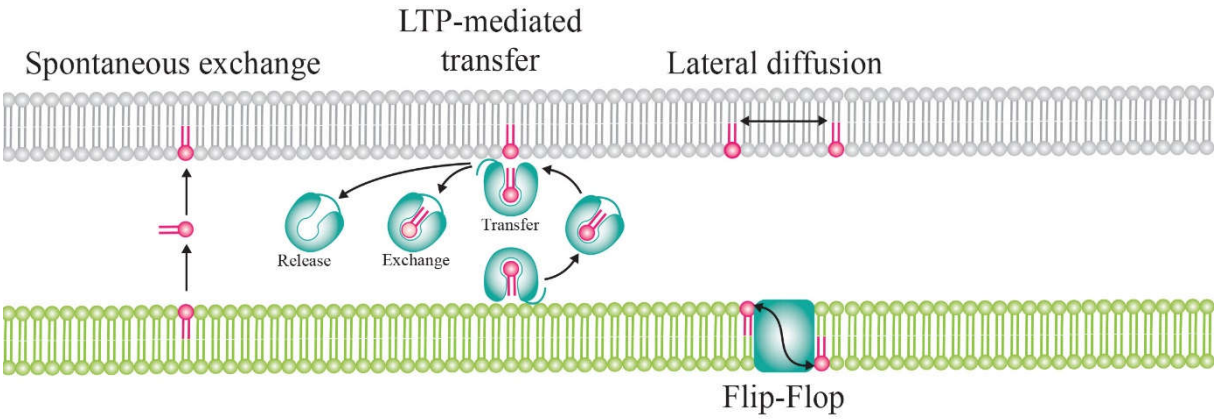

Figure 7. Mechanisms of non-vesicular lipid transfer. There are three mechanisms involved in non-vesicular lipid transport: monomeric lipid exchange, lateral diffusion and transbilayer flip-flop. Monomeric lipid exchange can be spontaneous or mediated by lipid-transfer proteins (LTPs). LTPs can transfer a lipid to the acceptor membrane or exchange it with a lipid of the acceptor membrane. Lateral diffusion occurs in the lateral plane of the membrane. Transbilayer flip-flop can be either spontaneous (not shown) or mediated by proteins such as flippases and translocases. Based on articles cited in the paragraph 1.5.2.

1.5.3) Lipid transfer proteins to facilitate the spontaneous lipid exchange

Due to the hydrophobicity of lipids and the low rate of spontaneous movement through an aqueous environment, LTPs are required to facilitate their non-vesicular transport as well as bilayer close proximity.

Performing *in vitro* studies, Lalanne & Ponsin demonstrated that LTPs accelerate the spontaneous monomeric lipid exchange by increasing the rate of lipid desorption from the donor membrane (Lalanne & Ponsin 2000). MCSs are the preferential location of LTP-mediated non-vesicular lipid transport because they provide a short distance between the two lipid-exchanging membranes (less than 30 nm). A working model for LTPs that have domains allowing them to bind both the correct donor and acceptor membranes is that both domains simultaneously engage their targets at MCSs in order to control their specific lipid shuttling (Levine 2004). This occurs by accommodating a lipid monomer into a hydrophobic pocket (1:1 stoichiometry) specific for a particular class of lipids (Fig. 7). Thus, an organelle-selective localization of LTPs would contribute to preserving the composition and identity of intracellular compartments.

Whereas LTPs are subdivided in phospholipid-, sterol- and sphingolipid-transfer proteins, the diversity of their lipid-binding domains corresponds to six structural families: SEC14, PITP, STAR-related lipid transfer (START), glycolipid-transfer protein (GLTP), SCP-2 (non-specific LTPs), and OSBP/ORP (D'Angelo et al. 2008, Lev 2010). The crystal structure of at least one member for each family, in association with its specific lipid ligand has been resolved (Im et al. 2005, Kudo et al. 2008, Schaaf et al. 2008, Yoder et al. 2001). Despite heterogeneity in lipid recognition, the variety of LTP structures converge to a similar feature in their lipid binding domain, generally composed of a central β-sheet surrounded by several α-helices. Such packed structure creates a hydrophobic tunnel with shape and size varying among the different families, depending on their specific ligand structure (Lev 2010).

1.5.4) Mechanisms of LTP-mediated lipid exchange at MCSs

As already mentioned, LTPs probably act efficiently at MCSs because this allows them to mediate short-range transfer of lipids between apposed bilayers.

LTP-mediated lipid exchange at MCSs can be simplified as sequential events starting when a lipid from a donor membrane is accommodated into the LTP's lipid binding pocket. A conformational change would then occur, resulting in a closed configuration of LTP structure, masking the lipid from the aqueous phase. LTP interaction with an acceptor membrane would reverse the conformation to transfer the lipid to the acceptor membrane (Fig. 7) (Lev 2010). This theoretical model is complicated by the fact that several factors must be taken into account in order to preserve the difference in lipid composition between two connected membranes. First, LTPs must be selectively targeted to specific MCSs. Therefore, in addition to their lipid-specialized hydrophobic pocket, they possess topological sorting signals or domains which impose an interaction with specific membranes. In some instances, such domains account for a direct interaction of LTPs with the MCS membranes. For example, some classes of integral ER LTPs can interact with the second organelle through pleckstrin homology (PH) or C2 domains. In other cases, the LTP-membrane interaction is protein-mediated. This is the case for OSBP and CERT, harbouring FFAT motifs, which bind members of the ER-resident VAP family of proteins (Fig. 8b). Additionally, in most cases, lipid exchange must be vectorial, and as such, often necessitates to overcome a concentration gradient. To perform vectoriality, LTPs take advantage of two general mechanisms: heterotypic exchange and trapping (Holthuis & Menon

2014, Lahiri et al. 2015). Heterotypic exchange involves the ability of some LTPs to bind two different lipids and exchange them in opposite directions across two bilayers. In trapping, a particular lipid is restrained in one of the two membranes composing the MCS and chemically modified (metabolic trapping), or restrained by its high affinity for and/or preferential association with a protein or another lipid in the membrane. A good example of metabolic trapping occurs at MCSs between trans-Golgi and ER during ceramide traffic. As described in paragraph 1.1, in mammalian cells, Cer, the precursor of all sphingolipids, is synthesized in the ER and directionally translocated to the Golgi compartment by CERT proteins owing to their membrane targeting determinants (FFAT motif to bind VAP in the ER and PH domain to bind PI4P in Golgi). Within the Golgi, it is converted to SM by SMS enzymes, a modification enabling the continuous one-way delivery of Cer without accumulation (Hanada et al. 2003).

ER-PM contact sites provide the major prototypes for thermodynamic trapping and heterotypic exchange. The mechanism of anterograde movement of sterols and PS from ER to PM involves their thermodynamic retention in the PM: sterols produced within the ER, accumulate in the PM because of their preferential interaction with saturated phospholipids species, which are more abundant within the PM than in the ER (Baumann et al. 2005). Similarly to sterols, PS synthesized in the ER relocalizes into the inner leaflet of the PM by virtue of a preferential association with specific PM protein microdomains. PS transport against an apparent concentration gradient is mediated by the LTPs Osh6 and Osh7, which define a unique OSBP subfamily with structural features adapted for PS recognition (Maeda et al. 2013). Recent studies however, demonstrated that the trapping system is not the only way to transport and enrich PS at the PM. OSBP-related proteins (ORPs) utilize a counter transport of PI4P to drive lipids from ER toward the PM against concentration gradients (Chung et al. 2015, Moser von Filseck et al. 2015a). This example of heterotypic exchange occurring at MCSs between ER and PM will be detailed below.

1.5.4.1) ORP/Osh-mediated counter-transport of lipids at ER-PM contact sites

The ORP family includes numerous LTPs conserved from yeast to mammals, thought to function in vesicular trafficking, intracellular signaling, and non-vesicular lipid transport between ER and PM (Raychaudhuri & Prinz 2010). The structure of the yeast ORP Osh4p/Kes1p in complex with cholesterol or ergosterol is typical of LTPs: its lipid-binding domain, called ORD, forms a hydrophobic cavity accommodating lipids covered by a “lid”

domain (Im et al. 2005). A role for ORP/Osh proteins in lipid transfer is supported by functional studies showing reduced sterol transport rate in cells lacking Osh (Raychaudhuri et al. 2006). The yeast Osh6 and Osh7 bind PS rather than sterol, indicating that, depending on the structural features of their hydrophobic pocket, different classes of lipids are ligands of specific ORD-containing proteins (Fig. 8a) (Maeda et al. 2013). In addition to ORDs, many ORPs contain other domains, including pleckstrin homology (PH) domains, which bind PIPs (in combination with ARF small GTPases), and FFAT motifs, which bind the ER proteins VAPs, enabling ORPs to preferentially function at ER-PM contacts (Loewen et al. 2003) (Fig. 8b). Furthermore, it has been demonstrated that both sterol extraction and transfer by Osh4p are PI(4,5)P2-dependent *in vitro* and *in vivo* (Raychaudhuri et al. 2006). The current view is based on *in vitro* studies showing that Osh4p acts as sterol/PI4P exchanger compensating the transfer of sterol from ER to Golgi with PI4P counter-transport in the opposite direction (de Saint-Jean et al. 2011), posits the existence of a link between Osh/ORPs-mediated lipid transport and PI metabolism. Using FRET-based assays with high temporal resolution to measure lipid exchange processes between liposomes, Moser von Filseck and colleagues found that Osh4 moves sterols from ER to Golgi against its concentration gradient, by dissipating the energy of a PI4P gradient, which is maintained by the hydrolysis by Sac1p of PI4P in the ER. This study provides further details in support to the hypothesis of the occurrence of a cyclic lipid exchange mediated by Osh4p at ER-Golgi interface (Moser von Filseck et al. 2015b). The PI4P-recognition site in Osh4p overlaps with the sterol-binding pocket, meaning that Osh4p can carry only one lipid at a time. However, only the amino-acid residues making contacts with the PI4P headgroups, and not those which bind sterols, are conserved among all ORD-containing proteins (de Saint-Jean et al. 2011, Mesmin et al. 2013). This strongly supports the idea that PI4P could be a common ligand for all ORP/Osh proteins, and that PI4P countercurrent could also drive the transport of other lipids, such as that of PS toward the PM at ER-PM contact sites. PI4P/PS counter-transport mediated by ORP/Osh proteins has been investigated by two groups in yeast and in mammalian cells (Chung et al. 2015, Moser von Filseck et al. 2015a), confirming that in yeast PS is transferred from ER to PM by Osh6 and Osh7. A phylogenetic analysis in metazoans revealed that the closest mammalian relatives of the Osh6/Osh7 clade are ORP5 and ORP8, which display a high degree of sequence conservation for PS specific binding (Maeda et al. 2013). Both in yeast and in mammals these LTPs are preferentially located at ER-PM contacts (Chung et al. 2015, Moser von Filseck et al. 2015a). Furthermore, in HeLa cells the cortical

pool of expressed GFP-ORP5 and GFP-ORP8, increases upon overexpression of enzymes responsible for PI4P synthesis, suggesting that PI4P is involved in the binding of ORP5 and ORP8 to the PM, via their PH domains (Chung et al. 2015). To examine PS and PI4P counter-transport mediated by Osh6, an *in vitro* assay has been developed, combining FRET technique and the use of lipid sensors selective for PS and for PI4P respectively (Moser von Filseck et al. 2015a). Similarly, an assay testing the transfer of these two lipids between "heavy" and "light" liposomes displaying different lipid proportions, in the presence of WT or mutant ORDORP8, demonstrated the ability of ORP8 to function as PS/PI4P exchanger (Chung et al. 2015). Remarkably, in both systems the ORP/Osh-mediated cyclic lipid transport at the ER-PM interface is guaranteed by dephosphorylation of PI4P operated by Sac1p, which maintains the necessary PI4P gradient (Fig. 8b). Collectively, the data obtained so far allow defining a general mechanism whereby specific LTPs operate at MCSs to drive a selective trafficking of lipids.

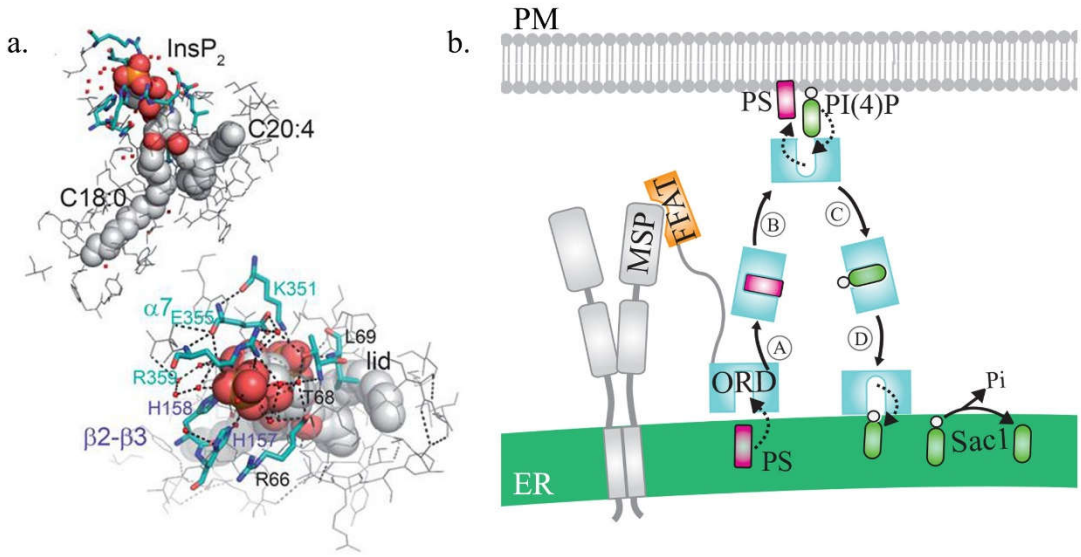

Figure 8. Mechanisms of Osh/ORPs-mediated lipid exchange at ER-PM contacts. (a) Structure of PI4P-bound Osh (Osh6p) (PI4P in sphere). Close-up view: key residues coordinating the head group. Red dots, water molecules; dashed lines, H bonds (Images adapted from Moser von Filseck et al., 2015). (b) Proposed model for PS/PI4P cyclic exchange mediated by Osh proteins (ORP5 or ORP8 in mammals, Osh6 or Osh7 in yeast). The ORD of Osh binds PS in the ER and transfers it to the PM (A, B) in exchange for PI4P in reversed reactions (C,D). The activity of Sac1 maintains the PI4P gradient necessary to drive PS transport. Based on articles cited in the paragraph 1.5.4.1.

1.5.4.2) E-Syts: a novel class of LTPs at ER-PM junctions

Besides their well characterized C2 domains allowing ER-PM tethering (Giordano et al. 2013), E-Syts also contain a SMP domain which has been proposed to mediate lipid transfer.

A crystal structure analysis of an E-Syt2 fragment revealed that the SMP domain consists in a β-barrel composed by a highly twisted β-sheet and three α-helices. The E-Syt2 fragments assemble in dimers both in solution and in the crystal, likely by virtue of the interaction of their SMP modules (Fig. 9a,b) (Schauder et al. 2014; Reinisch & De Camilli 2016). Bioinformatics studies established that SMP domains are homologous to the large TULIP superfamily of proteins which bind lipids and other hydrophobic ligands (Kopec et al. 2011). SMP dimers of E-Syt2 adopt a tubular structure similar to that of the TULIP proteins BPI (bactericidal/permeability-increasing protein, a PC-binding protein) and CETP (cholesteryl ester-transfer protein, acting in lipoprotein metabolism), which, contrary to E-Syts, are monomers and contain a TULIP module tandem forming a tube (Reinisch & De Camilli 2016, Schauder et al. 2014, Wong and Levine, 2017).

The SMP domains of E-Syts are thought to possess the capability to bindlipids , as their structure allows E-Syts to host glycerolphospholipids. This has been confirmed by *in vitro* assays demonstrating the ability of PC to displace NMD-PE from E-Syt2. In addition, mass spectrometry analyses in mammalian cells expressing E-Syt2 also confirmed the binding of glycerophospholipids to the protein (Schauder et al. 2014). These evidences have been instrumental in hypothesizing a role for the SMP domain of E-Syts in lipid transfer between ER and PM bilayers. It is important to note that E-Syt1 requires Ca^{2+} elevations not only to establish ER-PM junctions, but also to function as LTP (Yu et al., 2016; Saheki et al., 2016). By using a set of liposome-based assays, Bian and colleagues have shown that the binding of Ca^{2+} to the C2A domain of E-Syt1 enables lipid transport by releasing a charge-based auto-inhibitory interaction between this domain and the SMP (Bian et al., 2018; Bian et al., 2019b).

Hitherto, two different possibilities, namely a “tunnel model” and a “shuttle model”, have been proposed for the mechanism by which E-Syt SMP dimers move lipids at ER-PM contacts (Schauder et al. 2014, Wong and Levine 2017). As shown in figure 10c, in the tunnel model the SMP dimer forms a hydrophobic bridge between the two apposed membranes, through which lipid are transferred, functioning similarly to the tunnel formed by CETP (Zhang et al. 2012). The weakness of such mechanism lies in the fact that the SMP channel is too short (90-Å -long)

to entirely span the MCS distance except at closest range MCS (obviously less than 9 nm) and additional multimerization to form longer tetrameric tubes is unlikely given geometrical constraints imposed by linker sequence lengths (Reinish and De Camilli, 2016). In the second model, the SMP domains move within the ER-PM junction, extracting a lipid from one membrane and delivering it to the second. This model is in accordance with the typical system by which classical LTPs mediate lipid exchange at MCSs. In order to determine the distance between bilayers at which SMP-mediated lipid transport might occur, Bian and colleagues (2019a) took advantage of the DNA-origami nanostructures (Douglas et al., 2009; Rothemund, 2006) to develop a distance-dependent lipid transfer assay between DNA origami organized-liposomes. In this system, two DNA-ring-templated liposomes (donor and acceptor) are docked via a rigid DNA pillar, which determines their distance. The SMP of E-Syt1 was anchored to the donor liposome and the transfer of lipids between the two bilayers was measured using a FRET-based assay. By using this elegant technique, the authors have shown that lipid transfer can occur over distances that exceed the length of the SMP dimer, compatible with a shuttle model. On the other hand, in other studies, small puncta-like closer appositions of the two bilayers (<10 nm), which would be compatible for the tunnel model, have been observed (Fernàndez-Busnadiego et al., 2015). Therefore, deeper investigations will be necessary to definitely assess which mechanism E-Syts use to transfer lipids at ER-PM contact sites.

Interestingly, contrary to most of LTPs, E-Syts bind glycerophospholipids with any apparent preference. This may result in net, unidirectional bulk of lipid transfer required for membrane expansion or contraction. Hence, E-Syts might play a role in polarized cell growth occurring for example during neuronal development.

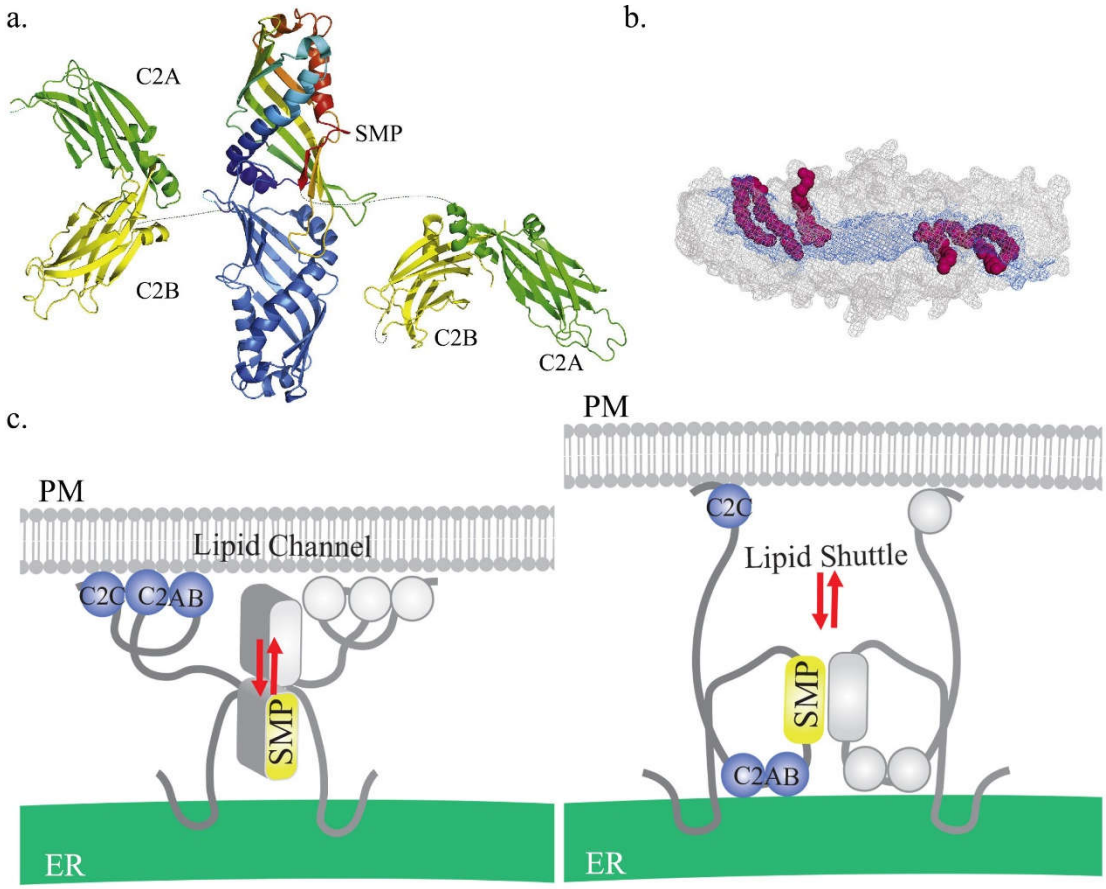

Figure 9. Mechanisms of E-Syts-mediated lipid exchange at ER-PM contacts. (a) Structure of an E-Syt2 fragment containing the SMP domain, C2A, and C2B. One SMP module in the SMP dimer is blue; the other is colored from blue at the N-terminus to red at the C-terminus. (b) Mesh representation of the SMP dimer. Hydrophobic residues lining the channel along the length of the dimer are blue. In the structure, the dimer binds two glycerophospholipids and two detergent molecules, such that hydrophobic and hydrophilic portions are in the channel and extruded into the solvent, respectively. Hydrophilic portions are disordered and were not modeled. (Images in (a) and (b) adapted from Reinisch & De Camilli 2016). (c) Two possible prototypes of E-Syt dimer–mediated lipid transport are depicted: a tunnel model (left), in which a bridge formed by the dimer allows for the transfer of lipids between the two bilayers, and a shuttle model (right), in which the SMP domains of E-Syts bind and move lipids from one membrane to another. Based on articles cited in the paragraph 1.5.4.2.

1.6) Contacts between the ER and PM in neurons

The ER network extends into all neuronal compartments without any interruptions, although rER is mainly present in the cell body (Linsdey et al., 1985). Remarkably, this continuity persists even in narrow compartments, like dendritic spines (Spacek and Harris, 1997; Martone et al., 1993) and thin branches of terminal axons (Renvoise et al., 2010), where single thin tubules of ER remain fully connected to the rest of the network. Given its wide distribution

within the whole cell, it is not surprising that contacts between ER other organelles also occurs in neurons. As a matter of facts, ER cisternae closely apposed to the PM in neuronal cells were among the first ER–PM contacts reported (Rosenbluth, 1962), and proteins implicated in MCSs are expressed in neurons. A detailed map of abundance and distribution of MCSs within neurons has been recently reconstructed in 3D by using focused ion beam-scanning electron microscopy (FIB-SEM) (Wu et al., 2017). The authors found that contacts between the ER and the PM were ubiquitously distributed (Fig. 10). In the cell body, these contacts are particularly prominent in size, covering a large fraction of the PM (Fig. 10b). Possibly, this is related to lower surface-(PM) to-volume (cytoplasm) ratio in the cell body, so that increasing their abundance in cell bodies may help these contacts to function correctly, supporting a greater volume of cytosol. In dendrites, the ER is mostly tubular, with occasional small cisternae. It also populates dendritic spines, stopping at the neck of the thinner ones and only reaching the head of the larger ones, such as mushroom spines (Fig. 10c-d). In axon, the ER creates a system of anastomosed tubules, whereas in thin axonal segments it generally forms a single continuous tubule (Fig. 10e). Both in dendrites and axons, ER-PM contact sites can be depicted; however, the contact area between the two membranes appears much smaller than the contact area in cell bodies.

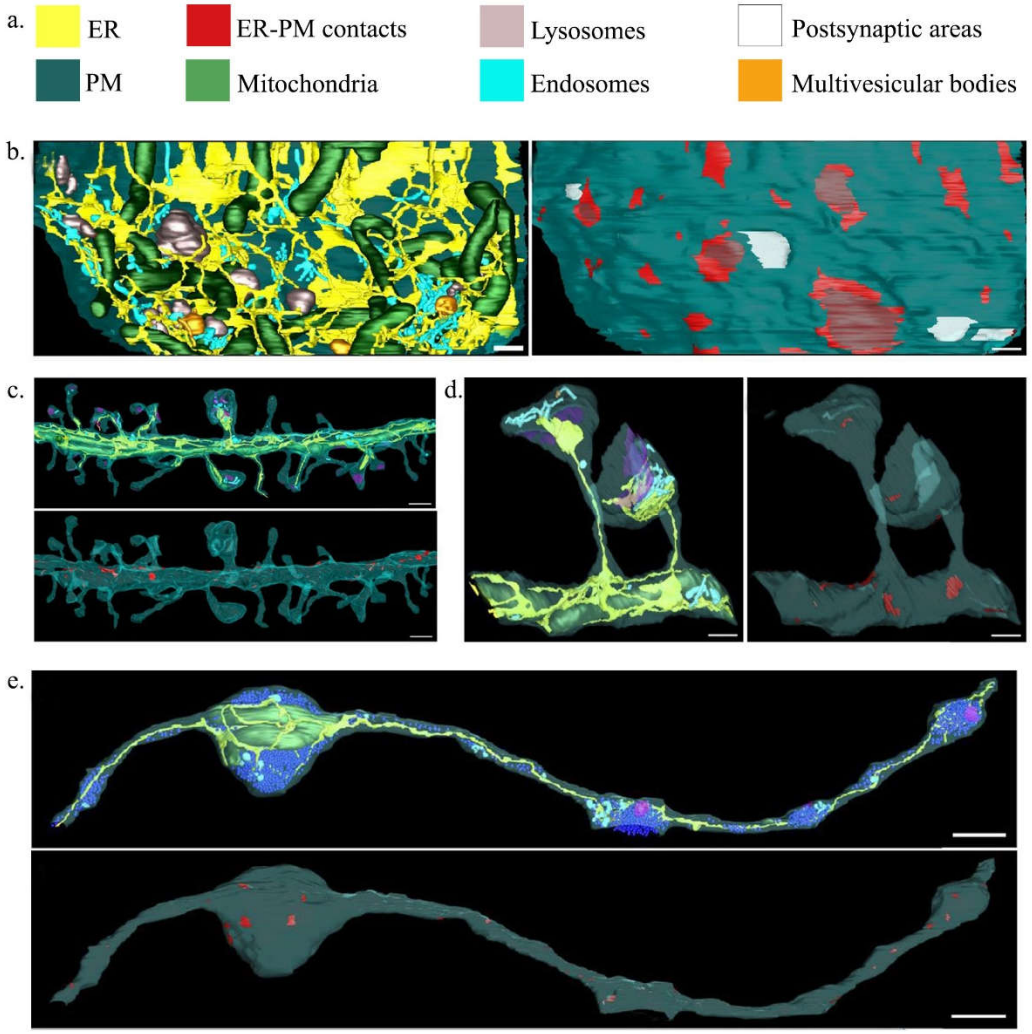

Figure 10. FIB-SEM 3D reconstruction of ER and ER-PM contact sites in neuronal compartments (a) Color-coded legend for membranous organelles present in the images below (b-e). (b) Cell body. (Left image) Portion of the peripheral cytoplasm including all membranous organelles in the region. (Right image) PM areas in contact with the ER are shown in red: bright red for wide ER cisternae and dark red for "thin" ER. (c) Dendrite. (Upper image) Membranous organelles in this dendrite. Note the continuity of the ER and its penetration into a subset of dendritic spines. (Lower image) Areas of contacts between ER and PM. (d) Dendritic spine. (Upper image) Membranous organelles within the spines, with the ER reaching their heads. (Lower image) Areas of contacts between ER and PM. (e) Axonal segment. (Upper image) A single ER tubule travels along the axon and expands into small tubular networks at presynaptic varicosities. (Lower image) Areas of contact between PM and ER. (Images adapted from Wu et al. 2017).

Interestingly enough, this study reveals a high degree of variability in shape and contact area not only within neuronal compartments, but also among different brain regions. As the structure, stability and molecular composition of MCSs might reflect their functions, the regional specializations of cER described above suggest that ER-PM junctions may play

different roles depending on their geographical distribution within the brain (and eventually among different developmental stages), despite their molecular identity is still under investigation. These functions include delivery of newly synthesized lipids from the ER to the PM, and return of lipid metabolites from the PM to the ER for metabolic recycling. That lipid exchange between the ER and the PM can occur also in axons is supported by studies of the giant squid axon, indicating the presence of phospholipid-synthesizing enzymes (Gould et al., 1983) and of numerous ER–PM contact sites along its PM (Metuzals et al., 1987). In developing neurons, lipid delivery to the PM might contribute to membrane expansion required for neurite extension.

1.6.1) Novel ER-PM tethers in the brain

Despite the large amount of literature on the classical ER-PM tethers, the list of proteins involved in bridging ER and PM may still be growing. Particularly, very little is known about the molecular components involved in the establishment, maintenance and function of neuronal ER-PM junctions. Following this direction, two new macromolecular PM complexes have been recently shown to populate ER-PM connections in neurons, where they are believed to play a function unrelated to the typical role assigned to their families. The Sec22b-Stx1 SNARE complex and the Kv2.1 potassium channel clusters represent new unconventional ER-PM tethers (Fox et al. 2015, Petkovic et al. 2014) (Fig. 5).

1.6.1.1) Kv2.1 potassium channels

Based on the well-established association between Kv2.1 clusters and the ER (Antonucci et al. 2001, Mandikian et al. 2014), a study showed, that Kv2.1 channels populate some ER-PM contacts, but also directly induce their formation by remodeling the cER in hippocampal neurons (Fox et al. 2015). It is still unclear whether such channels, able to form clusters at the cell surface, are electrically active. They are, at least so far, believed to act as mere tethers. The proper clustering of Kv2.1 channels depends on the phosphorylation state of a C-terminal 26-amino acid sequence called the proximal restriction and clustering (PRC) domain (Lim et al. 2000) (Fig. 5). Specific serine point mutations in PRC cause a complete abrogation of clustering and, consequently, prevent cER-PM contacts remodeling (Fox et al. 2015). Given the known importance of phosphorylation state in the formation of clusters, it is likely that the critical

factor of Kv2.1-mediated ER-PM junctions is the binding of phosphorylated channels to an unknown ER component, protein or lipid, leading to the stabilization of cER-PM interactions. Interestingly, it has been recently shown that also Kv2.2 channels can operate to remodel cER–PM junctions, indicating that this is a conserved and nonconducting role of mammalian Kv2 ion channels. This function requires an intact PRC domain, indeed, when transferred to another protein, the PRC domain can act autonomously to remodel ER–PM junctions. Moreover, KO mice for Kv2.1 and Kv2.2 display altered ER–PM junctions in neurons (Kirmiz et al., 2017). It is important to note that Kv2.2 and Kv2.1 have distinct patterns of cellular expression. This suggests that the highly similar functions of the two Kv2 channel paralogs, including dynamic phosphorylation-dependent regulation of their clustering (Bishop et al., 2015), might distinctly impact structure, function, and regulation of ER–PM junctions in the classes of neurons in which they are differentially expressed. Overall, these results demonstrated that Kv2 channels are one of the few PM-resident protein to be shown to promote the establishment and remodeling of ER-PM MCSs. This feature explains its unconventional mechanism of action, opposed to the typical behavior of the ER-residing tethers described above.

The exact function the Kv2-induced ER-PM contacts in neurons is still unclear. However, the localization of both store-operated and voltage gated Ca^{2+}channels to Kv2.1-induced ER-PM connections (Fox et al. 2015) and the occurrence of endo and exocytosis in close proximity to these domains (Deutsch et al. 2012) support the idea that such macromolecular complex is involved in both membrane trafficking and Ca^{2+} signaling within the neuronal soma and the axon initial segment. It is also intriguing that several families of ion channels (TMEM16, Kv2.1, VGCC) are found at neuronal ER-PM MCSs, suggesting that MCSs may have evolved to include ion transport in neurons.

1.6.1.2) Sec22b-Stx1 complexes

A recent study from our laboratory showed that a non-fusogenic SNARE complex formed by the ER-localized SNARE Sec22b and the PM-resident SNARE Syntaxin-1 (Stx1) stabilizes ER-PM contacts in neurons. This complex lacked SNAP23, 25, 29 or 47 and *in vitro* experiments showed that in the absence of SNAP25, Sec22b and Stx1 could not mediate membrane fusion (Petkovic et al. 2014). This discovery provides support for a novel role for SNARE proteins, beyond their well-established involvement in membrane fusion, a mechanism that will be extensively discussed in Chapter 2 (Jahn & Fasshauer 2012, Jahn & Scheller 2006).

The formation of a canonical SNARE complex is mediated by the SNARE motif, a characteristic domain of SNARE proteins composed of a stretch of 60-70 amino acids arranged in heptad repeats. The crystal structure of the SNARE synaptic fusion complex revealed that the core complex is represented by elongated coiled coils of four intertwined α-helices oriented in parallel, with each helix being provided by a different SNARE motif (Sutton et al. 1998). SNAREs assembled in a parallel fashion (N-termini at the same end) constitute a mechanical device delivering energy to dock the membranes in close proximity, at less than 10 nm distance, which allows them to fuse (See paragraph 2.3) (Li et al. 2007). However, due to their amphiphilic nature, SNARE motifs can also associate in other combinations, resulting in less stable helical bundles than core complexes. Indeed, *in vitro* experiments have shown that both parallel and antiparallel ternary complexes can be formed in solution (Liu et al. 2011, Weninger et al. 2003). Presumably, the absence of SNAP23, 25, 29 or 47 and possibly the antiparallel configuration would not lead to vesicle–membrane fusion. The Sec22b/Stx1 assembly may thus correspond to a docking and not fusogenic complex.

In agreement with the evidence that tethers account for additional roles besides their structural significance, the Sec22b-mediated bridge between ER and PM contributes to PM expansion during neuronal development (see paragraph 2.4).

Chapter 2

Membrane expansion in neuronal development

From zygote to adult, the development of a multicellular organism is based on cell growth and differentiation. Growth is supported by cell multiplication that is necessary for the formation of different tissues and by the increase in cell size after each division. The process of cellular growth is taken to the extreme in highly polarized cells like neurons, which extend long and elaborate axons and dendrites from the cell body to their final target tissues. Neuronal development represents a unique form of tissue expansion. Considering that the axon of a single neuron can extend to the length of 1 m in humans and up to 30 m in blue whales, growth represents for these cells a highly remarkable task (Smith, 2009).

Neurite elongation is accompanied by dramatic increase in PM surface. For example, a 1 μm-diameter axon growing at a rate of 0.5 mm per day increases its PM surface by 20% every day (Pfenninger, 2009). At physiological temperatures, membrane bilayers can only support a small degree of elastic stretching which is not sufficient to account for such massive increase in surface area. This implies that new membrane material must be inserted into the axonal membrane at a rate that can sustain axonal growth. An additional level of complexity arises from the fact that, being neurons highly polarized cells, the extension of axons and dendrites must be directionally driven in response of guidance cues that enable neurites to reach the correct target. Furthermore, neuronal growth is asymmetric, as axons and dendrites differ not only in their function, morphology and molecular composition, but also in timing, rate, and dynamics of growth (Horton et al., 2005). A number of fascinating questions arise from these considerations: How do neurons coordinate membrane addition in time and space? Where the various membrane components are synthesized and how do they reach the PM? Where on the neurite surface is new membrane inserted? Notwithstanding the last decades of extensive research on membrane expansion in neuronal growth, these questions still lack of exhaustive answers.

I will start the second chapter of my manuscript by giving an overview on the mechanisms by which neurons acquire their polarity during development, trying to summarize the immense body of work done over the years on this complex topic. As membrane expansion during neuronal growth is mainly driven by fusion of secretory vesicle with the PM, I will then discuss

how the conventional secretory pathway mediated by SNARE proteins, contributes to neuronal development. I will present SNARE proteins, their mechanism of action and their known functions in neuronal growth. Finally, I will conclude by presenting novel non-canonical pathways of membrane traffic. During my PhD, I attempted to contribute to this knowledge by focusing on non-vesicular mechanisms of membrane growth at ER-PM contact sites.

2.1) The establishment of neuronal polarity

Typical neurons are composed by one long and thin axon and several shorter dendrites, whose thickness progressively decreases with increased distance from the cell body. Already in 1891, Santiago Ramón y Cajal, the founder of modern neuroscience, argued that the shape of neuronal processes reflects their role in communication: dendrites conduct signals from postsynaptic terminals to the integration site, i.e. the cell body, whereas axons conduct signals from the cell body to presynaptic terminals (Cajal, 1891). After a century of research from the so called "law of dynamic polarization" postulated by Cajal, we now know that the polarized phenotype is equally characteristic of dissociated neurons that develop *in vitro*. This indicates that, independently of functional considerations concerning the flow of information, the morphological distinction between axon and an endogenous program of development may mainly regulate dendrites. Pioneer studies from Dotti and colleagues established dissociated rodent embryonic hippocampal neurons as a basic model system for neuronal development (Dotti et al., 1988). They divided the morphological events into five stages (Fig.11a), based on observations of individual cells in combination with immunolabeling for appropriate marker proteins. First, after being dissociated from embryonic rat brains, hippocampal neurons form several thin filopodia (stage 1, fig. 11b). Several hours after, neurons grow from four to five short neurites, called 'minor processes' (stage 2, fig. 11c). These neurites are morphologically equal, and undergo repeated, random growth and retraction. The major polarity event occurs half a day after plating, when one of these minor processes begins to grow rapidly, becoming much longer than the other neurites (stage 3, fig. 11d). The remaining minor processes continue to undergo brief spurts of growth and retraction, maintaining their net length, for up to a week, when they then become mature dendrites (stage 4, fig. 11e). Stage 5 (Fig. 11f) does not involve a change in polarity, but refers to the continued maturation of both axonal and dendritic compartments, with dendrites becoming thicker and shorter than the axon and establishing

dendritic branching and premature dendritic spines, and axons and dendrites becoming connected by synapses.

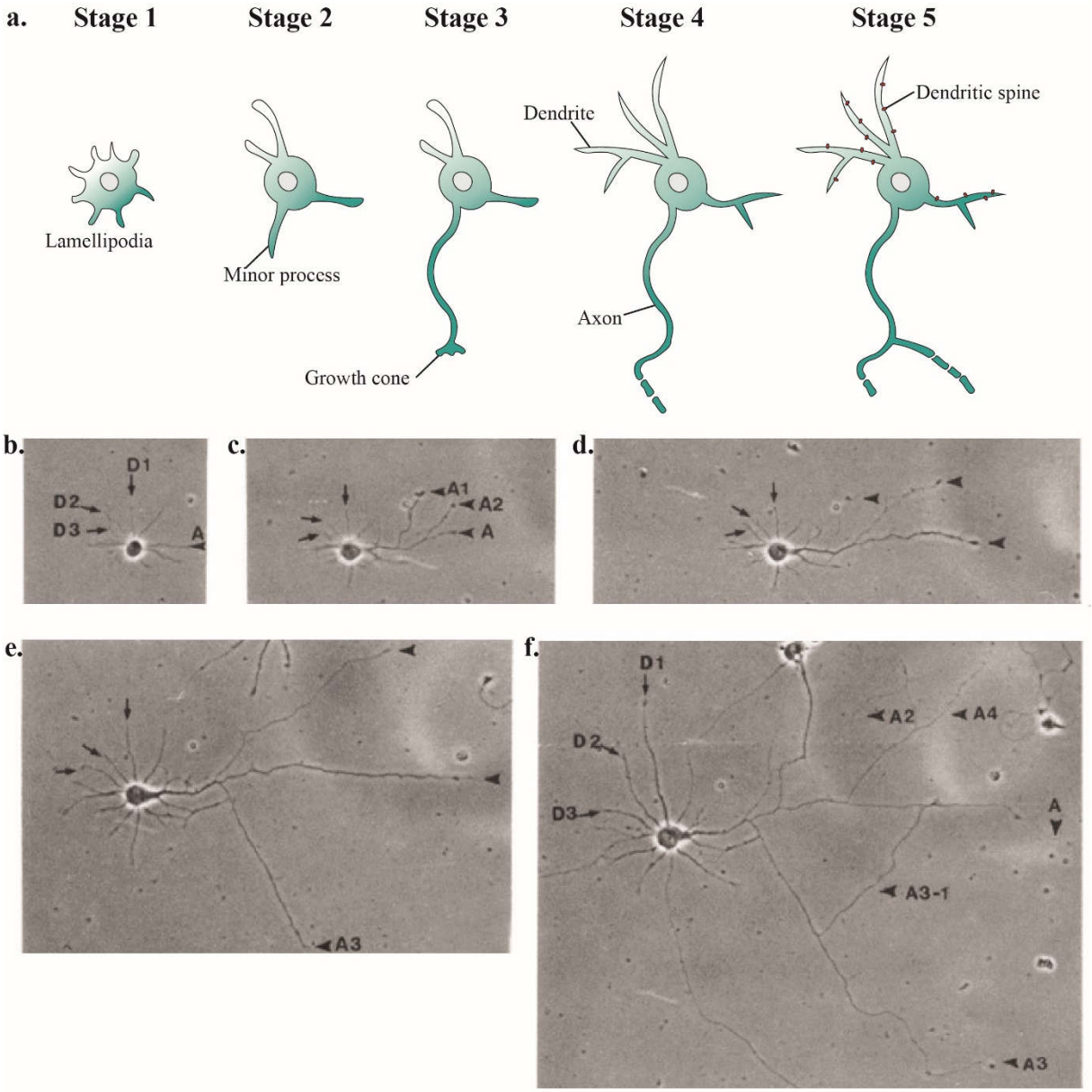

Figure 11. Neuronal polarization of hippocampal neurons in culture. (a) Schematic representation of the stages of development of cultured embryonic hippocampal neurons. (b-f) Series of phase-contrast images illustrating the development of axonal and dendritic arbors in an isolated hippocampal neuron (Images from Dotti et al., 1988). (b) After 1 day in culture, the neuron has developed several short similar processes, named D1-D3 and A. (c) On the second day in culture, the process A, that will be the future axon, elongates considerably more than the others, and branches giving rise to the A1 and A2 processes. (d) After 3 days *in vitro* (DIV3), the major process had elongated still further, while the minor processes remained essentially stationary. (e) At DIV5, the identity of the processes

had become clear: the major process is the axon, while the minor processes are dendrites. The axon collateral (A1) retracted and a new collateral (A3) formed. (f) At DIV7, the axon and its branches had elongated still more, and 2 new branches had formed. The dendrites had also elongated significantly.

Primary cultures make individual living neurons more easily accessible to both manipulation and observation. For instance, neurons can be readily transfected at different developmental stages (Kaech & Banker 2006). By this means, it is possible to overexpress certain proteins or to knock-down (KD) the expression of specific genes to study their function. Moreover, fluorescently tagged proteins can be introduced to explore their subcellular localization and trafficking inside living neurons. However, it should be noted that cells from embryonic day 18 (E18) rat hippocampal culture are post-mitotic neurons upon dissociation. Hence, neuronal polarization using this *in vitro* model corresponds to the re-polarization of previously polarized neurons *in vivo*. Consequently, molecular manipulations can be critical for the interpretation of the results. To overcome this limitation, *in vitro* techniques are often combined with approaches allowing the manipulation of neural progenitors *in situ*, such as *in utero* or *ex utero* cortical electroporation at earlier embryonic stages (E12-16) (Saito & Nakatsuji 2001, Calderon de Anda et al 2008). These approaches allow to visualize the earliest stages of neuronal polarization in a contextual cellular environment, i.e. organotypic slices or intact embryonic brain.

2.1.1) Cytoskeletal dynamics during neuronal polarization

The regulation of the actin and microtubule cytoskeletons is essential for neuronal polarization. During axon specification, one of the identical nascent neurites undergoes drastic microtubules reorganization characterized by the formation of parallel MT bundles with their plus-ends pointing outward (Baas et al. 1989, Baas and Lin 2011). It was also shown that microtubules stabilization in one of the undifferentiated neurites is sufficient to break symmetry and specify axon formation (Witte and Bradke 2008, Schelski and Bradke 2017). Such stabilization probably allows microtubules to protrude with their dynamic ends more distally, thereby promoting axon elongation (Fig. 12). Therefore, stabilization and bundling of parallel

microtubules could be key processes underlying neuronal polarization. This model also includes the presence of specific microtubule-associated proteins, such as TRIM46, which localize to the newly specified axon and regulate the organization of the uniform microtubles bundle (van Beuningen et al., 2015).

The directional transport of microtubule-stabilizing proteins, as well as of other polarization-related factors, is driven by vectorial membrane and cytoplasmic flow into the axon. Intesretingly, many microtubule-based motor proteins, such as KIF5C, are preferentially translocated in the future axon and exhibit a preference to interact with stable microtubules (Bradke and Dotti 1997, Oksdath et al. 2017, Xiao et al. 2016).

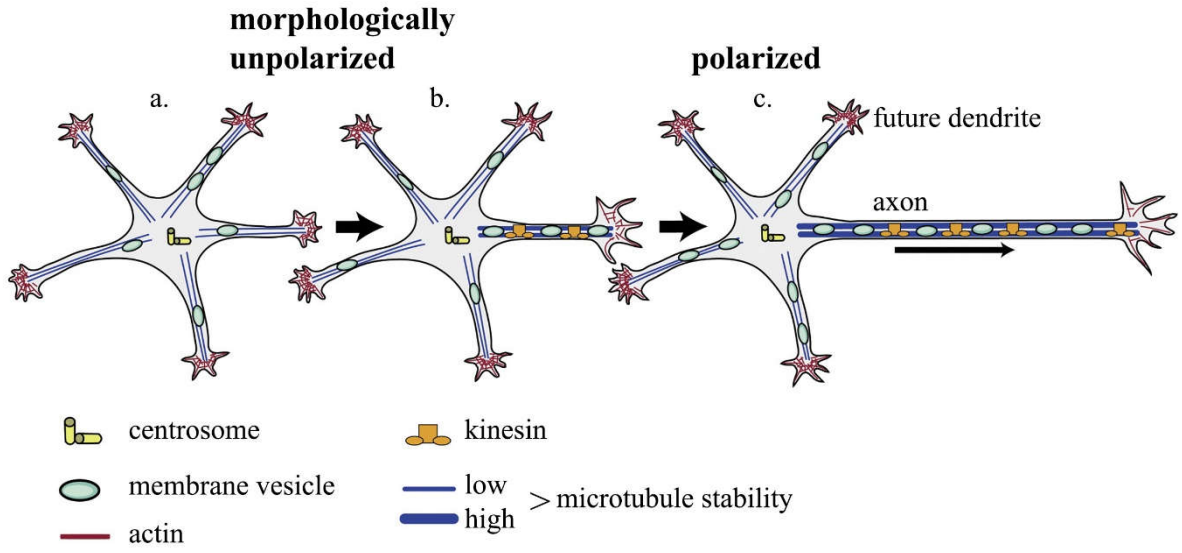

Figure 12. Mechanisms of neuronal polarization. In the course of axon formation, the neuronal cytoskeleton undergoes intense rearrangements. Initially, all neurites are identical (a). The actin cytoskeleton then becomes more dynamic in the growth cone of one neurite (b) and remains dynamic in the axonal growth cone (c). Similarly, polarization of microtubule stability occurs in one neurite before axon formation (b) and is pronounced in the axon of morphologically polarized neurons (c). The motor domain of kinesin preferentially localizes to the future axon (b) and the axon after polarization (c). The preference of motor proteins for microtubules with increased stability or specific posttranslational modifications may mediate directed trafficking into the axon. Possibly, the centrosome is positioned at the basis of the future axon early in development and promotes early polarization of the microtubule cytoskeleton (Image modified from Witte and Bradke 2008).

In addition to microtubules reorganization, Bradke and Dotti (1999) demonstrated in cultured hippocampal neurons that the remodeling of the actin-based cytoskeleton is an important

regulatory step in axon formation. Actin filaments in the putative future axon of stage 2 neurons are more sensitive to the depolymerizing effects of cytochalasin D than the minor neurites. Moreover, global application application of cytochalasin D induces the growth of multiple axon-like processes. These evidences suggest that the actin filaments of future dendrites form a barrier for the protrusion of microtubules, whereas the growing axon contains an actin structure permissive for microtubule protrusion (Bradke and Dotti 1999, 2000, Coles and Bradke 2015).

2.1.2) Intracellular signaling pathways

As polarized growth is also achieved by embryonic neurons in culture, in the absence of a gradient of physiological extracellular cues, cell-autonomous signaling mechanisms are essential to drive asymmetric neurite outgrowth. Several molecular regulators of neuronal polarization have been identified (Arimura and Kaibuchi, 2007). Interestingly, all these different signaling cascades converge on the regulation of cytoskeletal dynamics.

Phosphoinositide 3-kinase (PI3K) is a central player in the establishment of polarized growth of developing neurons (Menager et al., 2004; Shi et al., 2003). In cultured hippocampal neurons, this enzyme accumulates at the tip of the stage 3 axon and its inhibition prevents axon formation (Shi et al. 2003). Active PI3K produces the phospholipid PI(3,4,5)P_3 at the PM which was reported to promote neurite outgrowth and axon specification (Menager et al., 2004). In contrast, the tensin homologue deleted on chromosome 10 (PTEN), represents an antagonist of PI3K which decreases PI(3,4,5)P_3 levels at the leading edge of neurites and disrupts the development of polarity (Shi et al., 2003). These results show that the polarized activation of PI3K is required for axon specification of developing hippocampal neurons in culture. However, in PI3K-deficient mice only the formation of myelinated axons in cortex and striatum is affected, whereas hippocampal neurons develop normally, indicating that the role of PI3K signaling *in vivo* needs to be further investigated (Tohda et al. 2007).

PI3K activation drives two major signaling cascades: the pathway of the glycogen synthase kinase 3 Beta (GSK-3β) and the positive feedback loop composed by members of the Rho family of GTPases Cdc42 and the Par complex (Fig. 13).

Active GSK-3β mainly inhibits its targets, functioning as a negative regulator of polarized axonal outgrowth. Consistent with this idea, the KD of GSK3β or the use of specific inhibitors lead to the formation of multiple axons (Jiang et al., 2005; Yoshimura et al., 2005). Consequently, during neuronal polarization GSK-3β needs to be inactivated and this is achieved *via* its phosphorylation by the protein kinase Akt. Downstream targets inhibited by GSK-3β include the Adenomatous polyposis coli (APC), the collapsin-response mediator protein-2 (CRMP-2), and other microtubule-binding proteins all found enriched in the neurite that will become the axon (Barnes and Polleaux, 2009). Binding of CRMP-2 and APC to microtubules increases microtubule assembly and stability, respectively (Shi et al., 2004; Yoshimura et al. 2005), and their phosphorylation by GSK3β lowers their interaction for microtubules, impairing their function.

A node in the complex network of signaling molecules and cytoskeleton is represented by the Rho family of GTPases. These proteins are bound to GDP and are activated by exchanging GDP for GTP *via* the action of a guanine exchange factor enzyme (GEF). Main members of the Rho GTPases family are Cdc42 and Rac1. They both regulate actin dynamics by modulating filopodia and lamellipodia formation, respectively. Cdc42 and Rac1 form a positive feedback loop together with the Par3/Par6/atypical protein kinase C complex (aPKC). In particular, PI3K-mediated production of PI(3,4,5)P_3 leads to the activation of Cdc42 at the tip of the growing axon. As PAR6 associates with GTP-bound Cdc42, the entire PAR complex becomes activated, and, in turn, PAR3 activates Rac1. Active Rac1 and Cdc42 interact with effector molecules to regulate actin reorganization. Given that Rac1 activates PI3K, the signal initially evoked by this kinase appears to terminate on itself, closing the loop (Yoshimura 2006).

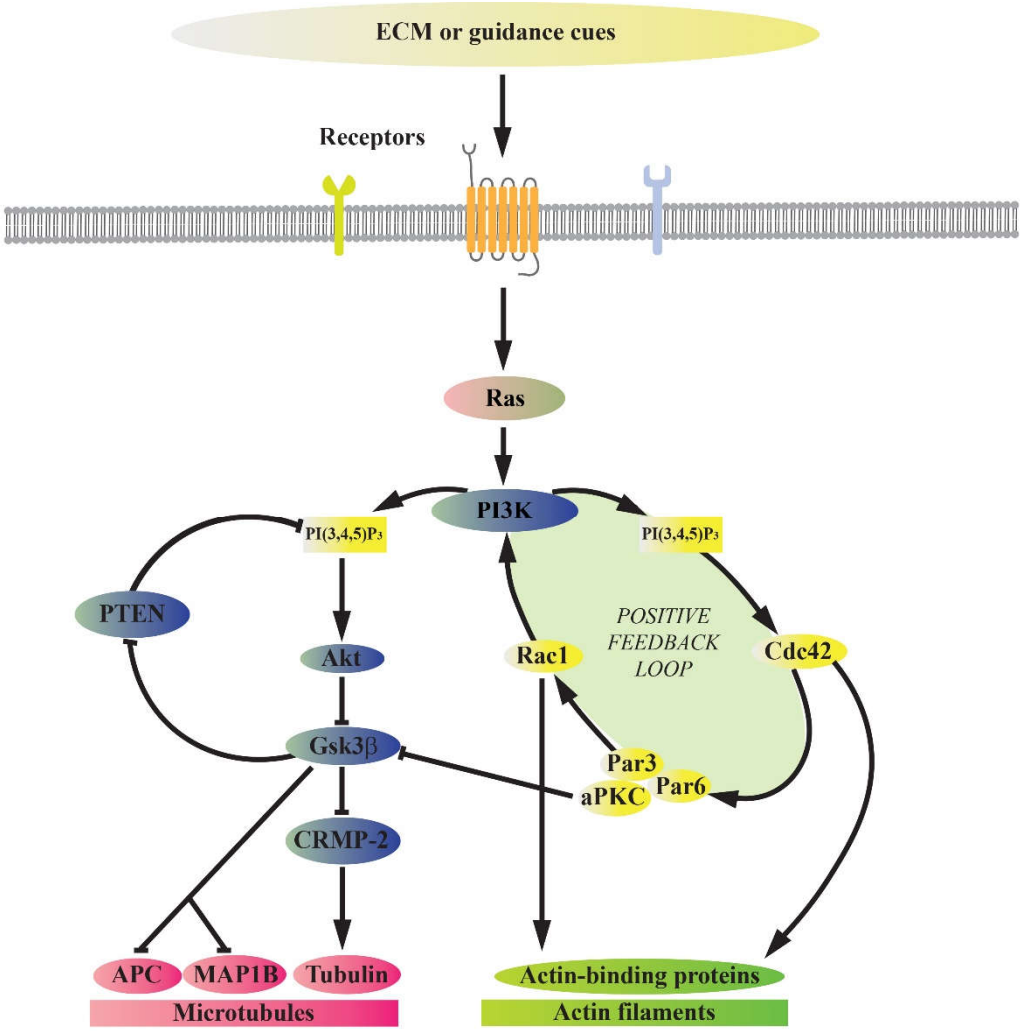

Figure 13. Signaling cascades in axon specification. In one immature neurite (the future axon), the extracellular matrix (ECM) activates PI3-kinase through interaction with adhesion molecules or receptors, thereby producing $PI(3,4,5)P_3$. Accumulated $PI(3,4,5)P_3$ drives two major signaling cascades: the Akt/GSK-3/CRMP-2 pathway and the positive feedback loop composed of Cdc42, the Par complex, and Rac1. These signaling cascades regulate cytoskeleton, endocytosis, protein trafficking, and transcription to promote neurite elongation and to determine axon or dendrite fate. Based on articles cited in the paragraph 2.1.2.

2.1.3) Extracellular cues

Positive and negative regulatory circuits influence microtubule stability and actin dynamics in the future axon, triggering the initial break of symmetry. However, extracellular cues are also essential in orchestrating intracellular signaling during the polarized growth of axon and dendrites, both *in vitro* and *in vivo* (Barnes et Polleux, 2009; Arimura et al. 2007).

Many extracellular matrix and cell adhesion molecules enhance neurite growth and accelerate axon formation in hippocampal cultures. Pioneer experiments from Esch and colleagues (1999)

showed that local presentation of growth-promoting molecules could direct axon specification of hippocampal neurons in culture. Specifically, they grew neurons on coverslips coated with alternating stripes of poly-L-lysine (PLL) and either laminin (LN) or neuron–glia cell adhesion molecule (NgCAM) and they found that the first undifferentiated neurite contacting the boundary between two stripes systematically becomes the axon. If minor process can be positioned on both substrates, axons are always formed on LN or NgCAM. These results represent a direct demonstration that the contact with preferred substrates can govern which neurite will differentiate in axon, thus directing the development of neuronal polarity (Esch et al, 1999).

Neurotrophins have also been proposed as extracellular polarity-regulating cues that accelerate neuronal polarization by enhancing axon growth. *In vitro* experiments using an approach similar to that used by Esch et al. showed that the first neurite contacting a BDNF (Brain Derived Neurotrophic Factor)-striped substrate systematically becomes the axon, indicating that BDNF plays an instructive role in axon specification (Shelly et al 2007). *In vivo* evidence for the role of extracellular signals as potential cues for specifying polarized neuronal growth have also been reported. Among those, an elegant study in C. elegans reported that the secreted UNC-6/netrin proteins, classically involved in axon outgrowth and turning, play also a role in the earlier events, generating, maintaining and orienting asymmetric growth before axon formation (Adler et al., 2006). By using a genetically encoded marker for a single neuron, they were able to visualize the entire process of axon formation and they found that netrin signaling promotes asymmetric neuronal growth and specifies the position at which the axon emerges from the cell.

2.2) The growth cone as the site of membrane insertion

What point along the growing axon is new surface added? In the early 1970s Dennis Bray tried to deduce the site of membrane expansion by monitoring the overall movement of the neuronal cell surface with respect to a stationary object attached to the membrane. Anterograde movement would indicate addition at the cell body, while retrograde movement would indicate addition at the growth cones. By binding glass or carmine particles to the surface of rat sympathetic neurons, Bray observed retrograde movement, consistent with addition of new membrane at the tip of the growing process, namely the growth cone (Bray, 1970). The

approach of following the movement of extracellular particles has been applied to various types of neurons. However, these results did not always confirm Bray's initial observations. The main difficulty of such technique was that some particles might preferentially associate with specific cellular components and they do not accurately reflect the movement of the surface as a whole (Futerman and Banker, 1996). To overcome this problem, alternative approaches, such as the direct labeling of membrane components or the expression of exogenous proteins, have been developed. In chick dorsal root ganglia axons, Dai and Sheetz followed the movement of glycoproteins and lipids labeled with specific antibodies, and they observed retrograde movements, consistent with membrane insertion in growth cones (Dai and Sheetz, 1995). Furthermore, Banker and collaborators expressed the exogenous transmembrane protein CD8a in cultured neurons and they demonstrated that the newly synthesized protein first appeared almost exclusively at the axonal growth cone surface. Preferential addition at the growth cone was also observed in minor processes (immature dendrites), but not in mature dendrites (Craig et al., 1995). Other studies provided further support to this idea (Vogt et al., 1996; Zakharenko & Popov, 1998) raising the possibility that the increase in growth cone size occurring during the transition of a minor neurite into an axon (Bradke & Dotti, 1997) is the consequence of membrane expansion due to preferential membrane addition at this location.

2.2.1) Structure of the growth cone

The neuronal growth cone, the distal tip of growing axons, is a sensory and highly dynamic structure that enables developing neurons to explore the environment and respond to guidance cues, guiding the extension of the neurites towards their final targets.

Under light microscopy, growth cones appear to be composed of two distinct compartments: the peripheral (P) and central (C) regions (Fig. 14a). The P region is a broad and flat area characterized by actin-rich finger-like projections called filopodia and flat sheet-like protrusions called lamellipodia (Fig. 14b). When viewed in time-lapse microscopy, filopodia and lamellipodia are often extremely dynamic, being able to extend, or withdraw within seconds, allowing a continuous probing of the environment. The C region, located behind the P region, is characterized by a dense microtubule array (Fig. 14c), and is enriched in cellular organelles. Although the C region exhibits less PM dynamics than the periphery, a substantial molecular motion occurs within this domain, including the constant shuttling of organelles and vesicles (Dent et al., 2011; Vitriol and Zheng, 2012). High-resolution of the growth cone's

cytoskeleton revealed a third functionally distinct zone located between the P and C regions, called the transitional (T) region (Lowery and Van Vactor, 2009; Rodriguez et al., 2003). The T region is mainly composed by actomyosin contractile structures that play a role in the regulation of both actin and microtubules localization and dynamics. Interestingly, Karl Pfenninger and colleagues have shown that in growth cones of cultured neurons, the T regions contain clusters of large, clear, coat-free vesicles clustered against the PM, sourrounded by plasmalemmal invaginations (Pfenninger et al., 1993; Pfenninger, 2009). These structures, called plasmalemmal precursor vesicles (PPVs), will be discussed in paragraph 2.3 in the context of the conventional secretory pathway driving membrane addition during neuronal development. Remarkably, membrane trafficking at the growth cones involves not only membrane addition but also internalization in the form of endocytosis. Besides the delivering or removing of PM, trafficking enables the internalization of cell adhesion molecules, signaling proteins such as Rho-Family GTPases and lipid mediators, and guidance receptors (Bloom and Morgan, 2011). Localized delivery or removal of these cargos ensures the spatial organization of signaling networks within the growth cone that is needed for growth (Vitriol and Zheng, 2012).

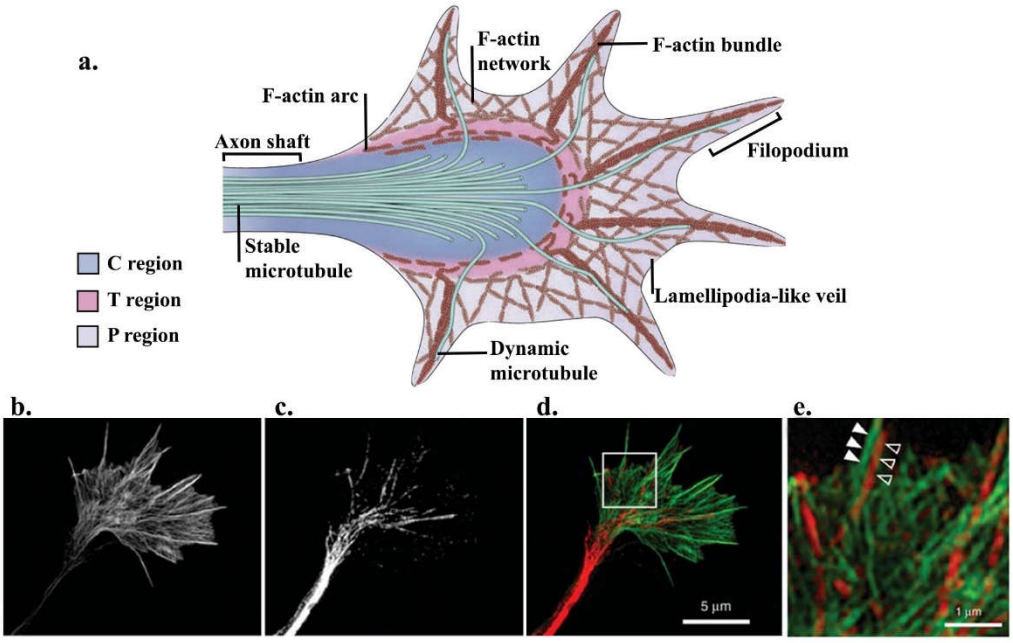

Figure 14. F-actin and microtubule distribution in a hippocampal growth cone. (a) Schematic representation of an axonal growth cone. The growth cone can be separated into three domains based on cytoskeletal distribution. The P region contains long, bundled actin filaments (F-actin bundles), which form the filopodia, as well as mesh-like branched F-actin networks, which give structure to lamellipodia-like veils. The C region encloses stable, bundled MTs that enter the growth cone from

the axon shaft. Finally, the T region sits at the interface between the P and C domains, where actomyosin contractile structures (actin arcs) lie perpendicular to F-actin bundles. (Image adapted from Lowery and Van Vactor, 2009). (b-e) F-actin and microtubule distribution in a hippocampal growth cone, labeled with fluorescent phalloidin (b. green) and an antibody against tyrosinated tubulin (c. red), respectively. (d) Overlay of images in c and d. (e) A close apposition of an F-actin bundle (closed arrowheads) at the base of a filopodium and an individual microtubule (open arrowheads) can be detected in a magnified view of the boxed region in image d. (Images from Dent et al., 2011).

2.2.2) Microtubule-actin interactions driving growth cones protrusion

A traditional description of the axon outgrowth separates the process into three stages: protrusion, engorgement, and consolidation. These stages, first described at the morphological level using differential interference contrast (DIC) microscopy (Goldberg and Burmeister 1986), result from specific cytoskeletal rearrangements driven to microtubule-actin interactions (Fig. 14d-e) within the growth cone in response to chemotropic cues.

Protrusion is the extension of new membrane at the edges of the growth cone, driven by filamentous actin (F-actin) polymerization. In particular, when receptors in the growth cone bind to an adhesive substrate, they activate an intracellular signaling cascade that acts like a molecular link between the receptors and the F-actin. Hence, the retrograde flow of F-actin is prevented and F-actin polymerization continues in the front, allowing lamellipodia and filopodia of the P region to move forward in order to extend the leading edge. Subsequently, F-actin bundles disappear between the adhesion site and the C domain and F-actin arcs reorient from the C domain towards the site of growth, creating a corridor between the two regions. This enables dynamic microtubules to invade the P domain of the growth cone, guided by actin arcs and actin bundles residing in the T and the C regions, respectively. In this way, the growth cone undergoes engorgement, as the C region moves forward. Finally, consolidation of the recently advanced C region occurs when the proximal part of the growth cone compacts and stabilizes to form a new segment of axon shaft, accompanied by the bidirectional movement of organelles and vesicles (Dent et al., 2011; Lowery and Van Vactor 2009).

A structural and functional relationship between microtubules and actin takes place throughout the entire process and it has been the subject of several studies. Live imaging records revealed that actin has a pivotal role in determining microtubules localization in the growth cone, acting both as a barrier to premature microtubules invasion and as a guide to drive grow in the direction of growth cone extension (Schaefer, 2002). Furthermore, Zhou and colleagues have shown that

a local perturbation of actin bundles by drug application on one side of the growth cone results in an inability of microtubules to penetrate into that area, leading to axon bending and growth cone turning (Zhou et al., 2002). This suggests that the spatial distribution of filopodia dictates the direction of microtubule extension. A local stabilization and growth of microtubules can in turn activate the Rho family of GTPases to induce local lamellipodial protrusion and growth cone turning (Buck et al., 2002). Finally, axon branching also depends on microtubule–actin interactions, as treating developing neurons in culture with cytoskeletal depolymerizing drugs affects the number and length of axon branches (Dent and Kalil, 2001).

2.2.3) Local synthesis of membrane components in the distal axon

During development, growing axons have to achieve the difficult task of navigating through a complex molecular environment filled with different guidance cues, which delineate the pathway towards their final targets. Therefore, the possibility for growth cones to synthesize proteins and lipids *in loco* enables a rapid and efficient morphological plasticity in response to extracellular signals. Until the last decade, the prevailing view was that axons lack the protein synthesis machinery, and thus they were not able to synthesize proteins and lipids locally. Nevertheless, a significant body of evidence has now demonstrated that sER, together with a variety of RNA molecules, such as transfer RNA, ribosomal RNA and messenger RNA, are abundant in growth cones of growing processes (Deitch and Banker, 1993; Bassell at al., 1998; Hengst et al., 2007), suggesting the existence of local synthesis in growing axons.

In spite of an active anterograde and retrograde transport of lipid-containing vesicles from the cell body, where they are synthesized, to distal axons, it is now clear that local synthesis of lipids also takes place in growth cones. Some of the first studies supporting this idea used extruded squid axoplasm in which the synthesis of PC, PE, PI and SM was detected (Gould 1983a; Gould 1983b; Tanaka et al., 1987). The invention by Robert B. Campenot of compartmented culture system for neurons, in which distal axons reside in a compartment separated from that containing cell bodies and proximal axons (Campenot, 1977), has opened a new era for studying lipid synthesis in distal axons. For example, Vance et al. demonstrated a local synthesis of PC by combining the compartmented culture system with the use of radiolabeled phospholipid precursors. The authors measured a rapid incorporation of [^{3}H]-Choline in PC and SM when this was added to the distal axon-containing compartment (Vance et al., 1991). Further studies using the same experimental paradigm have shown that PC

synthesis in axons is required for axonal growth. When PC synthesis was inhibited in distal axons alone, axonal growth was strongly impaired. In contrast, when choline was removed from the medium in the cell body-containing compartment, but the distal axons were bathed in choline-containing medium, axonal elongation continued normally (Posse de Chaves et al., 1995). Noticeably, the discovery of SM synthesis in distal axons was surprising at that time, because SM was thought to be synthesized exclusively in the Golgi apparatus, and distal axons do not have Golgi compartment or Golgi outposts. However, after the discovery that the SMS2 enzyme resides both in the Golgi and in the PM (Li et al. 2007, Tafesse et al. 2007), we know nowadays that SM can be also synthesized in the growth cone plasmalemma. In contrast to phospholipids, synthesis of Chol in distal axons was not reported, even though a main enzyme of its synthesis, hydroxymethylglutaryl-CoA reductase, was shown to be present (Vance et al., 1991).

The proteins that are synthesized in axonal growth cones seem to be primarily involved in growth cone guidance (Fig. 15); particularly, they take part in the intracellular signaling mechanisms by which growth cones convert extracellular cues signals into directional decisions. In early experiments, Campbell and Holt (2001) showed that Xenopus retinal growth cones lose their ability to turn in a chemotropic gradient of netrin-1 or Semaphorin3A after a treatment of cultured neurons with protein synthesis inhibitors. These initial then prompted further studies, leading to the identification of various mRNAs whose local translation is required for an appropriate chemotropic response to guidance cues. The attractive guidance cues netrin-1 and nerve growth factor (NGF) trigger local synthesis of proteins including β-actin (Yao et al., 2006), Par3 (Hengst et al., 2009), and TC10, a small GTPase required for exocyst function (Gracias et al., 2014). and MAP1B and Calmodulin (Wang et al, 2015). On the other hand, the repulsive guidance cues Slit2 and Semaphorin3A induce the translation of actin destabilizing proteins, such as RhoA and cofilin (Piper et al., 2006). Besides growth cones guidance, other studies showed how both axonal branching and axonal elongation require intra-axonal synthesis of factors such as β-actin, GAP-43 (Donnelly et al. 2013), MAP1B and Calmodulin (Wang et al 2015).

Local protein translation is also involved in the regulation of growth cone adaptation during chemotaxis (Fig. 15). The process of adaptation is composed of desensitization and resensitization phases, which allow the axon to constantly re-adjust their sensitivity over a wide

range of concentrations of the guidance factor. Ming et al. found that axonal growth cones of cultured Xenopus spinal neurons undergo adaptation during chemotactic migration in the presence of increasing basal concentrations of netrin-1 or BDNF. However, only the resensitization step, during which axons regain their initial sensitivity to the guidance cues, appears to be dependent on protein synthesis (Ming et al., 2002). Protein synthesis-dependent resensitization might be associated either with recovery of functional receptors, or with modulation of downstream cytoplasmic effectors. Finally, local translation within axons and growth cones is crucial for retrograde traffic signals triggered by neurotrophins, which influence neuronal survival or specification through changes of nuclear gene expression (Fig. 15) (Batista and Hengst, 2016).

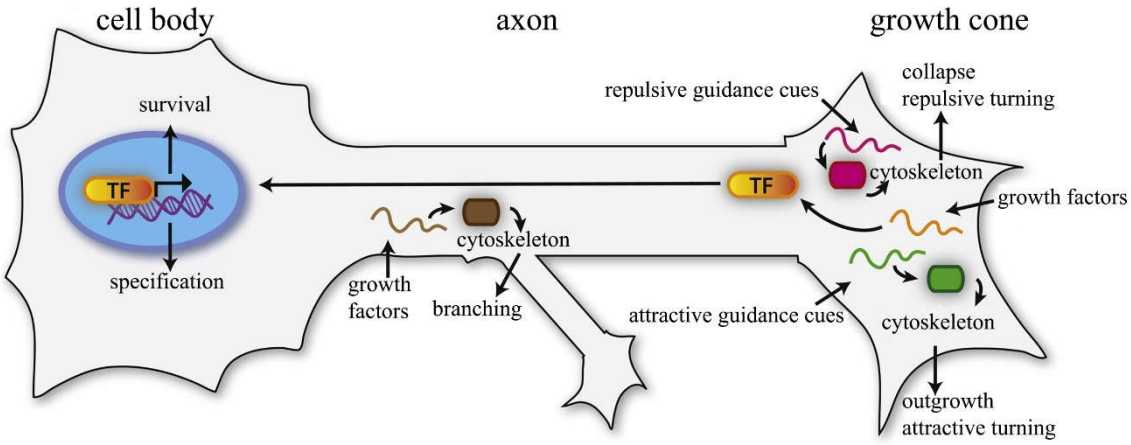

Figure 15. Roles of local protein synthesis in growth cones. Intra-axonal protein synthesis of cytoskeletal regulators supports: axons branching in response to growth factors (brown), axonal elongation and attractive turning triggered by attractive guidance cues (green), and growth cone collapse and axonal retraction induced by repulsive guidance cues (magenta). Local growth factor signalling triggers intra-axonal synthesis of transcription factors that are required for cell survival or specification (yellow). (Image adapted from Batista and Hengst, 2016).

In conclusion, there is convincing evidence for the importance of local synthesis for proper growth and guidance of axons during neuronal development. However, this process remains a minor contributor to membrane biogenesis, and the bulk of production of membrane components occurs in the cell body, following the steps of the secretory pathway. This topic will be discussed in the following paragraph.

2.3) The conventional secretory pathway in neuronal development

The main cellular route governing the addition of membrane at growth cones of developing neurons is represented by the secretory or exocytic pathway. The secretory pathway orchestrates the delivery of newly synthesized membrane components from the ER, through the ERGIC and the Golgi apparatus to the PM (Bentley & Banker, 2016; Wojnacki & Galli, 2016). In neurons, the localization of ER and Golgi compartments, where membrane components are synthesized and processed, is restricted to the cell body and dendrites; therefore, the delivery of proteins from the Golgi to the PM in growing axons involves budding, transport and fusion events, each of them orchestrated by a complex set of trafficking proteins. In addition, due to the functional differences of axons and dendrites, an asymmetric transport of membrane must occur, in order to establish and maintain a differential composition between these two subcellular compartments. In cultured hippocampal neurons, the selective delivery of post-Golgi vesicles to one neurite precedes its specification as the future axon (Bradke and Dotti, 1997) and perturbing the secretory pathways by treating neurons with brefeldin A, a drug that disrupts the Golgi complex within minutes, leads to a complete inhibition of axon elongation within one hour (Jareb and Banker, 1997).

2.3.1) Plasmalemmal precursor vesicles as the source for membrane growth

What is the source of membrane for membrane expansion? It was proposed that the secretory pathway generates large, clear, and polymorphic vesicular structures of approximately 150 nm in diameter called plasmalemmal precursor vesicles (PPVs) (Fig. 16a) (Pfenninger and Friedman, 1993; Pfenninger 2009). PPVs, generated in the cell body, are enriched in lipids and proteins which will reach the PM by microtubule-based transport. Many evidences suggest that different PPV types, carrying diverse sets of membrane proteins, are transported in the axon by different microtubule plus end-directed vesicle motors of the kinesin family, such as KIF2, KIF4 and kinesin-1 (Pfenninger et al., 2003; Wojnacki & Galli, 2016). First indications of the existence of PPVs date 1973, when Mary Bartlett Bunge performed one of the first experiments of electron microscopy on growth cones and found the presence of clusters of large pleomorphic vesicular structures close to the PM (Bunge, 1973). Later studies have been then performed on live growth cones, showing that membrane components move from PPV-like vesicles to the cell surface, where they are inserted. Pulse-chase experiments revealed that, growth cones labeled with ferritin-conjugated lectins (pulse) and then incubated in the absence of label

(chase), exhibited label-free membrane patches above clusters of PPV-like vesicles. (Fig. 16b). In inverse experiments, growth cones were first pulse-labelled with unconjugated (invisible) lectin, then chased and fixed, and finally labelled with ferritin-conjugated lectin (Fig. 16c). In this case, patches of membrane covering vesicles clusters displayed ferritin labeling. Thus, the appearance of label-free areas in the first experiment was caused by the insertion of glycoconjugates from an internal compartment, inaccessible to the label (Pfenninger et al., 1981; 1993).

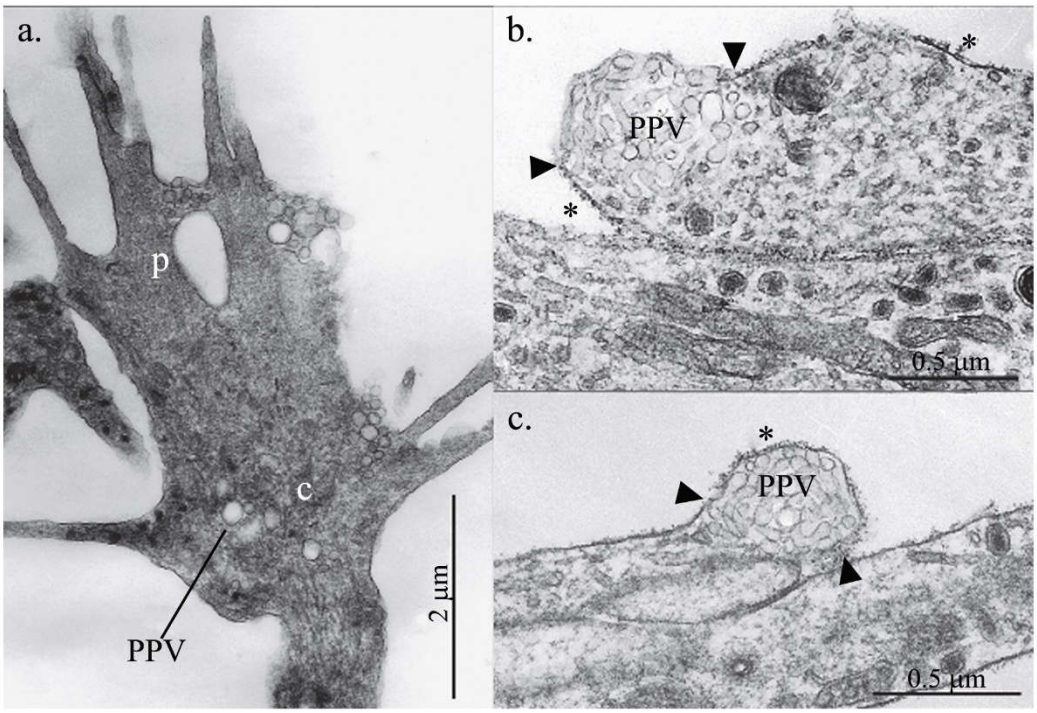

Figure 16. Plasmalemmal precursor vesicles (PPVs) and glycoconjugate externalization in the growth cone. (a) An electron micrograph of a growth cone (from a rat spinal cord neuron) in culture, showing central (c) and peripheral (p) regions. Several clusters of PPVs can be identified. (b,c) Pulse–chase experiments with lectins (wheat germ agglutinin) and lectin–ferritin conjugates show PPV clusters associated with growth cones in culture. After a ferritin–lectin pulse and chase for 15 min in the absence of the label, the plasmalemma covering the vesicle cluster is essentially label-free (b). If the labelling pulse is carried out with unconjugated lectin, followed by ferritin–lectin label after the chase period, the PPV clusters are covered with ferritin particles (c). Asterisks indicate areas of high ferritin label density; arrowheads approximately mark the transition from label-rich to label-poor plasmalemma. These results demonstrate insertion of new glycoconjugates into the plasmalemma at PPV clusters. (Images from Pfenninger, 2009).

Later studies have then demonstrated that PPVs trafficking and exocytosis is mainly regulated by the insulin-like growth factor-1 (IGF-1)-stimulated IRS/PI3K/Akt signaling pathway, indeed inhibition of PI3K blocked IGF-1-stimulated plasmalemmal expansion at the growth cones of cultured neurons (Laurino et al., 2005; Sosa et al., 2006).

The insertion of PPVs at the tip of growing neurites follows the conventional steps of exocytosis, undergoing to docking and fusion. Classically, these two processes are driven by different molecular machineries. The exocyst complex targets and docks vesicles to specific plasmalemmal insertion sites during a variety of cellular processes This is an octameric protein complex, first identified in budding yeast and highly conserved among eukaryotes (Mei et al., 2018). Members of the exocyst, such as Sec6, Sec8 and Sec10, have been shown to localize along the neurites and in growth cones and to be involved in neurite outgrowth (Hazuka 1999; Vega 2001). The exocyst interacts with and is regulated by members of the Rab family of small GTPases. When activated by GTP-binding, Rabs recruit exocyst proteins on the target membrane, which, in turn, act as effector molecules to establish docking. As a general mechanism for regulating trafficking, Rab GTPases recruit various effector proteins involved in all the steps of vesicular trafficking, from vesicles formation to fusion (Zhen and Stenmark, 2015; Wojnacki & Galli, 2016).

The second and final step of exocytosis, i.e. vesicle fusion, is a function of the Soluble N-ethylmaleimide-sensitive-factor (NSF) attachment protein receptors (SNAREs), which are thought to be the force generators bringing the two membranes close enough for fusion. In addition to membrane trafficking, many essential biological processes, such as communication between membrane-enclosed intracellular compartments and neurotransmitter or hormones secretion, rely on membrane fusion. Regardless of the high diversity of the fusing compartments, almost all intracellular fusion reactions require SNAREs, with the notable exception of mitochondrial fusion and fission (Jahn & Scheller 2006; Südhof & Rothman 2009). Although the well-established role and identity of SNAREs involved in fusion of synaptic vesicles (Jahn Fasshauner, 2012; Sudhorf and Rizo, 2012), little is known about the SNAREs involved in PPVs fusion during neuronal development. Nevertheless, an expanding body of evidence is recently showing that the same sets of SNAREs might be required for polarized membrane insertion and initial axonal outgrowth in neurons. SNARE proteins structure, mechanism of action and involvement in neuronal growth will be discussed below

2.3.2) SNAREs: from their discovery to the Nobel prize

Between the 1980s and 1990s, three scientists, James Rothman, Randy Schekman, and Thomas Südhof, have undertaken a set of studies on different aspects of vesicular traffic. Their scientific paths often intertwined, leading to crucial discoveries, which enabled to decipher the molecular events controlling vesicle-based secretory pathway. Schekman's group identified genes for vesicle fusion by using yeast genetics. Particularly, they generated yeast mutants that were deficient in protein secretion and revealed 23 different SEC genes required for exocytosis (Novick et al., 1980). Rothman and collaborators used biochemical approaches. They developed an *in vitro* reconstitution assay based on cells infected by the vesicular stomatitis virus (VSV) to study vesicle budding and fusion, and they purified essential proteins from the cytoplasm of infected cells. The first protein to be purified was the N-ethylmaleimide-sensitive factor (NSF) (Block et al.,1988), which turned out to correspond to SEC18 in yeast (Wilson et al. 1989). In 1993, Rothman proposed the so called "SNARE hypothesis" according to which target and vesicle SNAREs (t-SNAREs and v-SNAREs) interact to mediate vesicle fusion through a sequence of docking, activation and fusion (Sollner et al., 1993a). At the same time, Südhof became interested in how synaptic vesicle fusion machinery was regulated, and he discovered that this process is controlled by the calcium-sensing proteins synaptotagmins to release neurotransmitters at an accurate time in neuronal synapses (Geppert., 1994). In 2013, Rothman, Schekman and Südhof were awarded the Nobel Prize in Physiology or Medicine ''for their discoveries of machinery regulating vesicle traffic, a major transport system in our cells".

2.3.2.1) SNAREs structure

SNAREs form a superfamily of small proteins evolutionarily conserved from yeast to humans (Bock et al., 2001). Common feature of these proteins is the SNARE motif, an evolutionarily conserved stretch of 60–70 amino acids that is arranged in heptad repeats. At their C-terminal ends, Syntaxins and VAMPs, which represent the vast majority of SNAREs, have a single transmembrane domain (TMD) that is connected to the SNARE motif by a short linker (Fig. 17). Others, such as members of the SNAP25 subfamily and the unusual R-SNARE Ykt6, are anchored to the membrane by prenylation and/or palmitoylation (Hong and Lev, 2014) and a few SNAREs are not membrane anchored (SNAP29, 47, amysin, ref). The N-terminal sequences of SNAREs vary substantially between subgroups. In the VAMP subfamily, relatively short N-terminal sequences are found in most VAMPs (1-5, 8). Overall, these proteins

are called “brevins”. Conversely, VAMP7, Ykt6 and Sec22 contain a longer N-terminal domain of ~130 amino acids long called Longin domain (LD) (Fig. 17). LD play important roles not only in regulating the SNAREs fusogenic activity, but also in their subcellular localization and protein interaction. However, not all the LDs behave the same way. It was demonstrated that in Ykt6 and VAMP7 these motifs can fold back on the SNARE domain exerting an auto-inhibitory effect to prevent interactions with t-SNAREs, while the LD of Sec22 does not seem to have such function (Filippini et al., 2001; Gonzalez et al., 2001; Rossi et al., 2004; Burgo et al., 2013; Daste et al., 2015). Interestingly, LDs are not exclusive to SNAREs, but they have been found in a large number of proteins, all related to membranes and their transport (De Franceschi et al., 2014; Rossi et al., 2004). In Syntaxins, the N-terminal region is called Habc domain and is composed of separate antiparallel three-helix bundles. Habc are regulatory domains, which fold back and bind to SNARE domains. This leads to the formation of an inhibitory inactive closed conformation that prevents Syntaxins to associate in SNARE complexes (Misura et al. 2000).

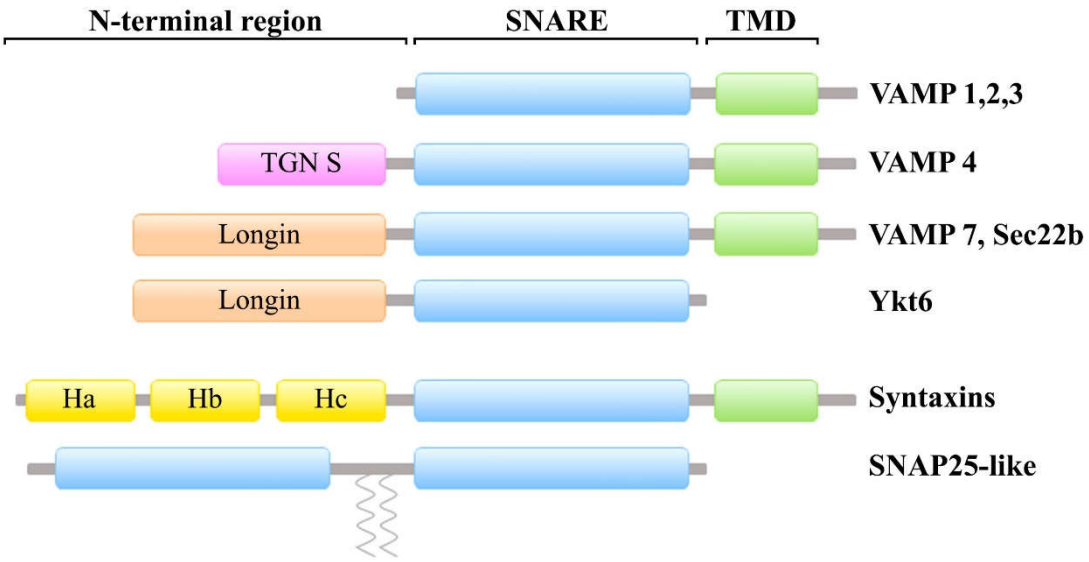

Figure 17. Domain architecture of SNARE proteins. All SNARE proteins have a α-helical coiled-coil domain, called SNARE motif (blue) that is involved in the formation of a parallel four-helix bundle, which brings the membranes into close apposition and triggers their fusion. Syntaxins and VAMPs contribute with one helix to this bundle, and SNAP25-like proteins contribute with two helices. Most SNAREs are connected to their respective membranes by a transmembrane domain (TMD, green), whereas Ykt6 and proteins in the SNAP 25-like subfamily are connected by a linker that is frequently palmitoylated. All syntaxins possess an N-terminal extension, the Habc domain (yellow), while the N-terminal region of VAMPs comprises either a short and variable domain (short VAMPs called ‘brevins’) or a long and conserved longin domain (long VAMPs called ‘longins’). TGN S: TGN-targeting signal.

2.3.2.2) SNAREs classification

Classically, SNARE proteins are classified into two categories depending on the compartment where they localize: vesicular SNAREs (v-SNAREs), localized in the donor vesicle membrane, and target SNAREs (t-SNAREs), localized in the acceptor membrane compartment (Fig. 18a). Given the complexity of intracellular transport, some SNAREs can be both, such as for example the *S. cerevisiae* SNARE Sec22 that functions in both anterograde and retrograde traffic between the ER and the Golgi apparatus. This led to a second more rigorous classification based on the highly conserved molecular structure of the SNARE complexes (Jahn & Scheller 2006; Fasshauer et al. 1998). In their monomeric form, SNAREs have unstructured SNARE motifs. Nevertheless, if a complete set of SNAREs associates, their SNARE motifs spontaneously form a helical core complex of extraordinary stability, the SNARE complex. The SNARE core complex consist of elongated coiled coils out of four intertwined, parallel α-helices, each provided by a different SNARE motif. The center of the bundle is formed by 16 side chain layers interacting with each other, which explains the very high stability of this complex that can resist treatments by strong detergents such as SDS (Hayashi et al. 1994). With the exception of the central layer, internal layers of the bundle remain hydrophobic. The central layer (or 0 layer) is a highly conserved structure that is composed of three glutamine residues (Q) and one arginine residue (R), and the corresponding SNAREs are classified as Q - and R-SNARE, respectively (Fig. 18b-c) (Jahn & Scheller 2006; Fasshauer et al. 1998). Often, R-SNAREs act as v-SNAREs and Q-SNAREs as t-SNAREs. R-SNAREs are represented by synaptobrevin/VAMP subfamily of proteins and their homologues, and Q-SNAREs are represented by Syntaxin and SNAP25 subfamilies of proteins. While VAMPs and Syntaxins have one SNARE domain, proteins of the SNAP25 subfamily have two SNARE motifs. SNARE domains of the Syntaxin subfamily can be further classified in Qa, Qb or Qc (Bock et al., 2001). Most Syntaxins are Qa-SNAREs while Qb and Qc SNAREs are either other Syntaxins (6 and 8) or are found in proteins of the SNAP25 subfamily.

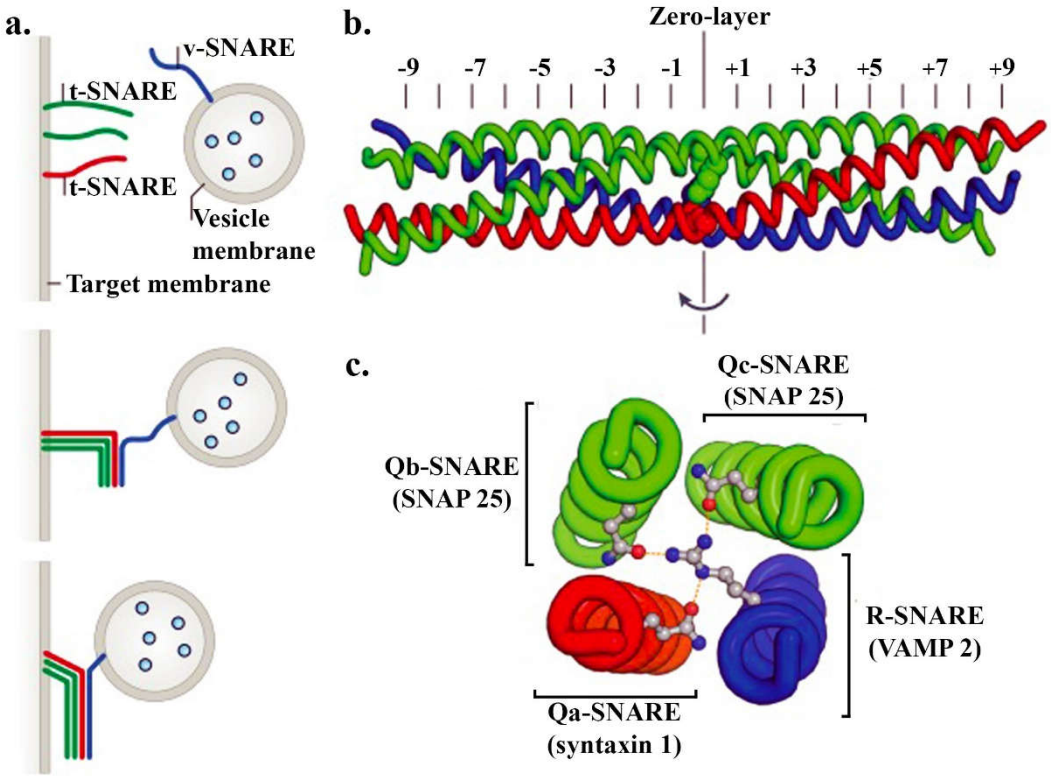

Figure 18. SNAREs classification. (a) SNAREs can be classified as vesicle-associated SNAREs (v-SNAREs) or target-membrane-associated SNAREs (t-SNAREs). (b-c) Alternatively, they can be defined by the residue that contributes to the zero layer and their position within the four-helix bundle: R-SNAREs contribute an Arg residue to the zero layer, whereas Qa-, Qb- and Qc-SNAREs each contribute a Gln residue. Few SNARE proteins, such as SNAP25, contain both Qb- and Qc-SNARE motifs within a single polypeptide chain. (Image adapted from Baker and Hughson, 2016).

2.3.2.3) Mechanism of SNARE-mediated membrane fusion

Current knowledge on the molecular mechanisms underlying the function of SNARE proteins stems from the large body of genetic and biochemical data obtained with SNARE proteins involved in synaptic vesicle fusion. Neuronal communication relies on the Ca^{2+}-regulated release of neurotransmitters in the presynaptic cleft through the fusion of cargo-containing synaptic vesicles with the presynaptic membrane. Synaptic vesicle fusion involves the pairing between VAMP2 (residing in the synaptic vesicle membrane) with Stx1 and SNAP25 (residing in the presynaptic plasma membrane) to form a membrane-bridging *trans*-SNARE complex (or SNAREpin) that allows the synaptic vesicle to dock and fuse with its target membrane. The formation of SNARE complexes during fusion and their dissociation afterwards results in the so-called SNARE cycle (Fig. 19) (Sollner et al., 1993(a); Sollner et al., 1993(b)). The zippering

of the SNARE motifs during the SNAREpin formation proceeds in a parallel orientation, from their N-terminal domains toward the C-terminal domains, proximal to the membranes. Such association generates an inward force that pulls the fusing membrane in close apposition for fusion. After fusion, the TMD regions of SNAREs are present in the same membrane, resulting in the *cis*-complex that needs to be disassembled for reactivation (Südhof and Rothman, 2009). NSF, a specialized adenosine triphosphatase (ATPase) of the AAA family, with the soluble NSF-attachment proteins (SNAPs) as cofactors, catalyzes this reaction (Sollner et al., 1993b). NSF provides the energy needed for the dissociation, since *cis*-SNARE complex configuration has low potential energy. After the dissociation, t-SNAREs are available for a new fusion cycle, while v-SNAREs have to be recycled to the donor membrane in order to engage to a new docking and fusion cycle (Baker & Hughson 2016).

The SNAREpin is under a high-energy state and releases its energy when it zippers up to a low-energy *cis*-SNARE complex. Therefore, the fusion and the completion of zippering are thermodynamically coupled (Südhof and Rothman, 2009). Recent advances demonstrated that SNARE complex formation takes place in multiple steps, each characterized by different energy levels (Lou & Shin 2016). Li and colleagues used a surface forces apparatus (SFA) to determine the energetics and dynamics of SNAREpin formation. SFA allows a direct measurement of the interaction energy between two facing functionalized membranes as a function of their separation distance. This experimental setting enabled the authors to describe the different intermediate structures forming in the course of SNARE complex assembly, each one with characteristic energy levels. They showed that SNAREpin folding is initiated when cognate SNARE membranes are 10 nm apart. Even after very close approach of the bilayers (2–4 nm), the SNAREpins remain partly unstructured in their C-terminal region and the energy accumulated during such partial SNAREpin folding across two membranes is 35 k_BT, where kB is Boltzmann's constant and T is the temperature (Li et al., 2007). Consistent with these measurements, experiments using optical tweezers demonstrated the half-zippered intermediate can release ∼36 k_BT by transitioning to the fully zippered state (Gao et al., 2012). Further structural details on the partially zippered SNARE intermediate have been obtained with using the “nanodisc sandwich” technique, where a single SNARE complex is reconstituted between two separate nanodiscs. Due to the rigid structure of nanodiscs, membrane fusion does not

occur, suggesting that the complete SNAREpin formation could precede membrane fusion, giving strong support for the 'zippering' assembling hypothesis (Shin et al., 2014).

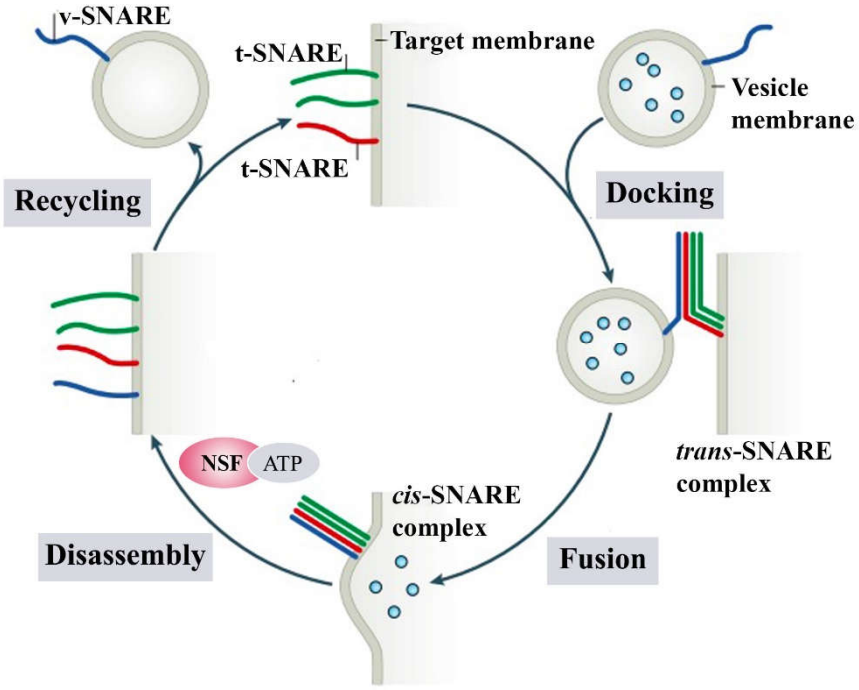

Figure 19. Cycles of SNARE assembly and disassembly. Membrane fusion is thought to begin with a v-SNARE in a vesicle and three t-SNAREs in a target membrane. Assembly into membrane-bridging *trans*-SNARE complexes drives membrane fusion and cargo delivery. The resulting *cis*-SNARE complex is disassembled by the ATPase N-ethylmaleimide-sensitive fusion factor (NSF; working together with the adaptor protein soluble NSF attachment protein (SNAP, not shown), which releases the SNAREs for subsequent cycles of assembly and disassembly (Image adapted from Baker and Hughson, 2016).

Theoretical calculations indicate that the approximation of the two membranes that precedes fusion requires removal of hydration layers, local membrane bending, merging of the two proximal leaflets to yield a so-called stalk intermediate, formation of a fusion pore due to merging of the distal leaflets, and expansion of the fusion (Tareste and Roux, 2018). Each step requires a considerable amount of energy, and the overall free energy necessary for fusion is estimated in the range of 50 to 100 k_BT (Cohen & Melikyan 2004). However, as mentioned above, one SNARE complex delivers ~35-36 k_BT of free energy (Li et al., 2007; Gao et al., 2012). Thus, more than one SNARE complex must be engaged to efficiently mediate membrane fusion. Using the "nanodisc sandwich" containing synaptic SNAREs, Shi et al., (2012) found that, although only one SNAREpin is required to maximize the rate of bilayer fusion, a

minimum requirement for three SNAREpins is necessary to open a fusion pore for efficient neurotransmitter efflux during synaptic transmission.

2.3.2.4) Accessory proteins regulating the SNARE nanomachine

Many proteins collaborate with SNAREs to regulate membrane fusion events spatially and temporally.

SM (Sec1/Munc18-like) proteins are probably the most important partners of SNAREs, which are now even considered as the fifth component of the core membrane fusion nanomachine (Südhof and Rothman, 2009; Rizo and Südhof, 2012). The two major neuronal SM proteins are Munc18-1 and Munc13-1. Munc18-1 is composed by three conserved domains organized into an arch-shaped structure adapted to clasp a four-helix bundle. Munc13-1 contains a C2 domain and a calmodulin-binding (CaMb) module in its N-terminus, and a C1 domain, two C2 domains and a MUN domain, a highly elongated module shared with other tethering factors involved in various forms of membrane traffic, in its C-terminus (Rizo et al., 2018). Together, Munc13-1 and Munc18-1 regulate SNARE complex at synapses, by controlling the docking and priming of vesicles for fusion. During the priming step, that leaves synaptic vesicles ready for neurotransmitter release, Stx1 transitions from a closed conformation to an open conformation within the highly stable SNARE complex. Munc-18-1 stabilizes the closed conformation by binding it very tightly *via* the cavity of its arch-shape (Fig. 20a) (Dulubova et al., 1999; Misura et al., 2000). Munc13-1 opens Stx1, accelerating the transition from the Stx1/Munc18-1 complex to the SNARE complex (Fig. 20b), and its function depends on weak interactions of the MUN domain with the Stx1 SNARE motif, and probably with Munc18-1 (Ma et al., 2011; 2013). At this point, two potential mechanisms can regulate SNARE assembly. The classical view is that open Stx1 may bind SNAP25 to form a Stx1/SNAP25 or a Munc18-1/Stx1/SNAP25 complex (Fig. 20c) (Baker and Hughson, 2016; Rizo and Südhof, 2012; Südhof and Rothman, 2009). An alternative model hypothesizes that open Stx1 may bind VAMP2 to form a Munc18-1/Stx1/VAMP2 template complex which may be further stabilized by Munc13-1 (Fig. 20d) (Jiao et al., 2018). Both complexes, have been proposed to be 'activated' for SNARE assembly (Fig. 20e-f).

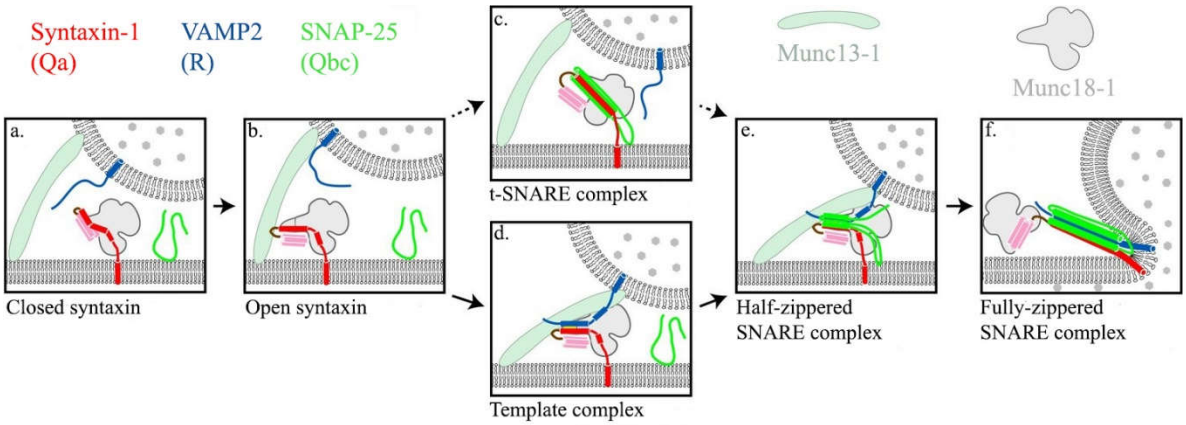

Figure 20. Pathways for Munc18-1 and Munc13-1-regulated neuronal SNARE assembly. (a) Munc18-1 first serves as a Stx1 chaperone and binds Stx1 to inhibit its association with other SNAREs. (b) Closed Stx1 is opened by Munc13-1. (c) Open Stx1 binds SNAP25 forming a Munc18-1/Stx1/SNAP25 complex. (d) Alternatively, open Stx1 binds VAMP2 forming a Munc18-1/Stx1/VAMP2 template complex by Munc13-1. (e-f) Both complexes, (c) and (d), are thought to be 'activated' for SNARE assembly (Image adapted from Jiao et al., 2018).

Proteins from the complexin and synaptotagmin families constitute another class of SNARE regulators that are particularly important in Ca^{2+}-triggered fusion events. These proteins are not necessary for fusion *per se* (Geppert et al., 1994; Reim et al., 2001), but they allow the PM accumulation of a pool of fusion-ready vesicles waiting for the signal (Ca^{2+} entry) that provokes rapid and synchronous release.

Genetic and biophysical studies indicate that complexin traps the SNARE complex in a partially zippered, fusion incompetent state. To exert its clamping activity, it binds to the membrane-proximal region of the t-SNARE, preventing its assembly with the C-terminal residues of the v-SNARE (Giraudo et al., 2009; Li et al., 2011). Later studies depicted the molecular model by which it operates, and showed that the central helix of complexin (CPXcen, the SNARE-binding domain) binds one SNAREpin while the accessory helix (CPXacc, the clamping domain) extends away and bridges to a second SNAREpin. The CPXacc interacts with the t-SNARE in the second SNAREpin, occupying the v-SNARE binding site, thus inhibiting the full assembly of the SNARE complex. This intermolecular *trans* clamping mediated by complexin organizes the SNAREpins into a 'zig-zag' topology that, when interposed between vesicle and PM, is incompatible with fusion (Kummel et al. 2011, Krishnakumar et al. 2011, 2015, Ucheor et al. 2016).

Synaptotagmin-1 is also involved in forming this clamp. Atomic resolution structures of SNARE/complexin/synaptotagmin-1 complexes, revealed that two synaptotagmin-1 molecules simultaneously bind the SNAREpin on opposite surfaces, *via* their C2B domains. One C2B domain ('primary') binds to SNAP-25 within the SNAREpin in a manner compatible with its further assembly into a synaptotagmin-1 ring-oligomer and likely contacts the PM. The second C2B domain ('tripartite') is bound in an incompatible manner, and likely contacts the vesicle surface (Zhou et al. 2017). The ring acts as a spacer to prevent the completion of the SNARE complex assembly, thereby clamping fusion in the absence of calcium.

Based on recent structural and functional insights into SNAREs and accessory proteins assembly and organization, James Rothman and co-workers, formulated the so-called "buttressed-ring hypothesis". Such hypothesis postulates the formation of a three-layered protein structure in which a middle layer of SNAREpins is firmly sandwiched between two 'clamping' layers of C2 domains: a bottom (PM-bound) ring of primary Syt C2Bs; and a top layer of tripartite (vesicle-bound) C2Bs. This arrangement would trap each SNAREpin between the two membranes, held both from above (vesicle) and from below (PM) (Fig. 21). Complexin contributes in strengthening this vice-like clamp by additionally linking the SNAREpin to the vesicle.When the synaptotagmin-1 ring disassembles by binding to Ca^{2+} ions, fusion proceeds (Wang et al. 2014, Zanetti et al. 2016, Li et al. 2019, Ramakrishnan et al. 2018, Rothman et al. 2017). One take-home message from these studies is that SNARE regulators allow for regulation of SNAREpin in ways that v-/t-SNARE interactions do not necessarily lead to fusion *in vivo*.

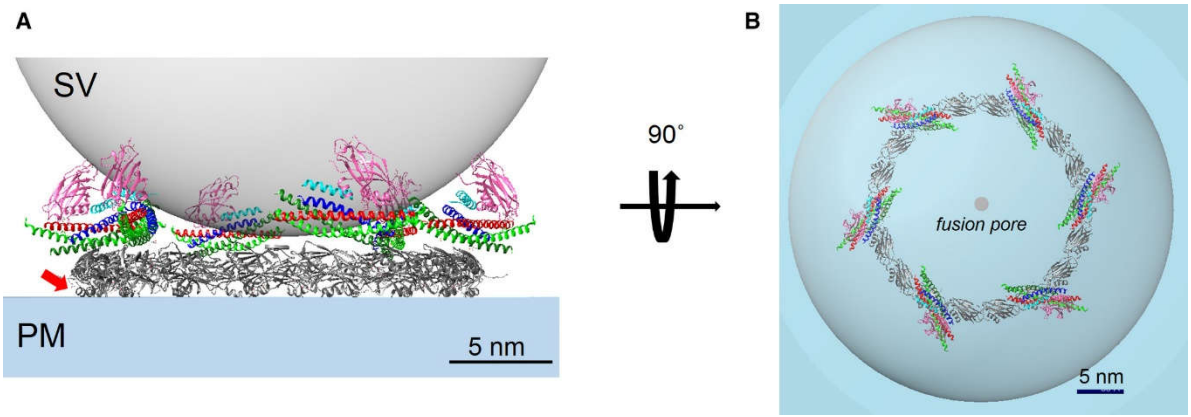

Figure 21. Clamping of SNAREpin terminal zippering according to the buttressed-ring hypothesis. Side view (A) and the top view (B) of the model. The assembling SNAREpins are retained on the inner Synaptotagmin-1 ring via the 'primary' SNARE-C2B domain interaction. In the ring oligomers, the second independent C2B domain (magenta) sits above the SNAREpin bound via

the ‘tripartite’ binding site in conjunction with complexin. Such an arrangement would allow the ‘tripartite’ C2B to bind the vesicle membrane, likely via lipid interaction. As a result, each SNAREpin is held in a vice-like clamp between the two C2B domains, preventing further zippering. Complexin likely strengths this clamp by additionally anchoring its SNAREpin to the vesicle (not shown). (Image from Rothman et a. 2017).

2.3.3) SNAREs involved in neuronal development

In neurons, SNARE-mediated fusion is critical not only at the synapse of mature neurons, but also in early developmental stages for acquisition of neuronal morphology and for membrane expansion during neurite outgrowth. A growing body of research has revealed that several SNARE proteins, belonging to both t- and v-SNARE groups, are involved in axonal and/or dendritic growth.

2.3.3.1) t-SNARES

Among t-SNAREs, both members of the SNAP sub-family, such as SNAP25, and Syntaxins, have been shown to be involved in neurite outgrowth. Early studies on SNAP25 demonstrated that the selective inhibition of this protein prevents neurite elongation in cultured rat cortical neurons, and in developing chicken retina *in vivo* (Osen-Sand et al. 1993). The involvement of Stx1 in neuronal development has been extensively studied by using the botulinum neurotoxin C1 (BoNT⁄C1). Clostridial neurotoxins (tetanus (TeNT) and botulinum (BoNT) neurotoxins) are useful in understanding membrane trafficking events involving SNAREs, because they inhibit neural transmission through their metalloprotease activity specific to each SNARE component (Fig. 22) (Montecucco and Schiavo, 1994; Schiavo et al, 2000). Among them, BoNT⁄C1 cleaves Stx1 and SNAP25 leading to their release from the PM. A series of study have shown that exposing neurons to BoNT⁄C1 impairs neuronal growth both *in vivo,* abolishing Netrin-1-dependent advancement of developing neurons (Cotrufo et al., 2012) and *in vitro* in cultured neurons (Igarashi et al., 1996). Since treatment with BoNTA, which only cleaves SNAP25 leaving Stx1 intact, does not recapitulate these results, Stx1 is likely required for preferential outgrowth toward netrin, whereas another SNAP family member appears to compensate for loss of SNAP25 function (Winkle and Gupton, 2016).

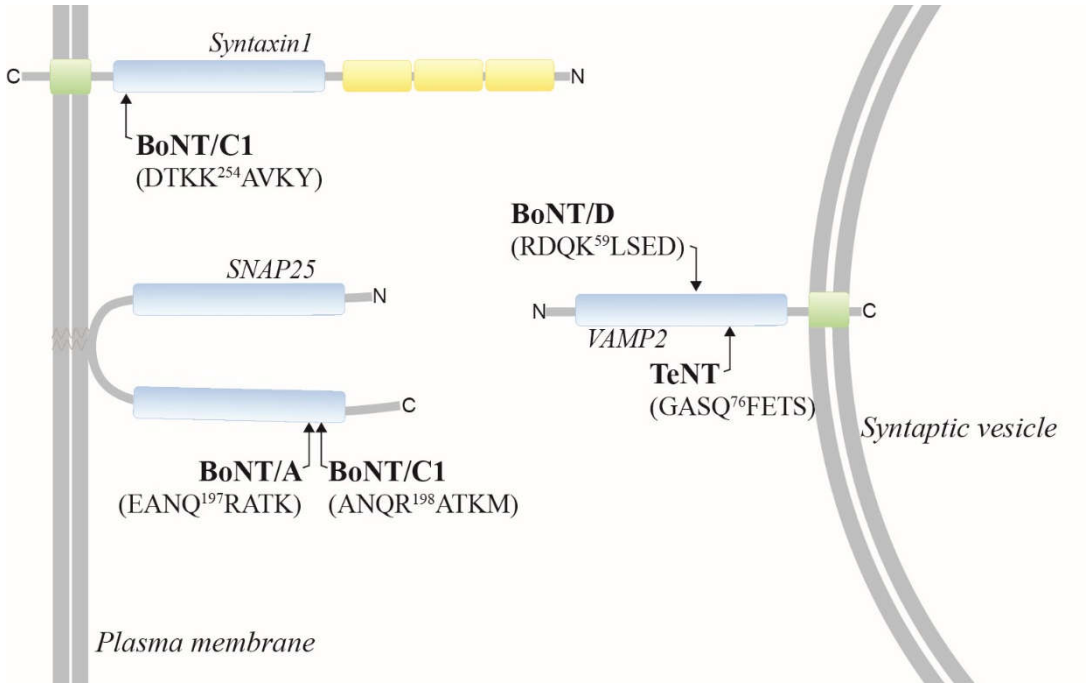

Figure 22. Schematic structure of clostridial neurotoxins cleavage sites on Stx1, SNAP25 and VAMP2. BoNT/A cleaves SNAP25 while BoNT/C1 cleaves both Stx1 and SNAP25. VAMP2 is cleaved by BoNT/D and TeNT. Only neurotoxins relevant for this study have been represented and cleavage sites for other neurotoxins (i.e. BoNT/B, /E, /F, /G) are not shown.

Classically, Stx1 assembles with SNAP25 and VAMP2 to form the synaptic SNARE complex in mature neurons (Söllner et al., 1993b). Stx1 and SNAP25 also interact with VAMP7 in the process of axonal growth (Martinez-Arca et al. 2000; Alberts et al. 2003). In addition to this conventional association, a recent study from our team has shown that Stx1 also localizes in growth cones of developing neurons, where it interacts with the ER-residing R-SNARE Sec22b (Petkovic et al., 2014). Stx1/Sec22b complex does not mediate fusion but it tethers PM and ER membranes in close proximity, forming ER-PM contact sites. Interestingly, this complex is required for neuronal development, and a detailed description of this function will be provided in paragraph 2.4.

2.3.3.2) VAMPs

VAMPs, the widest subfamily of R-SNAREs, includes a series of proteins localizing in the donor compartment. Thus, studying VAMPs would enable to reveal which membrane compartment is engaged during neurite extention, shedding light on the variety of mechanisms participating in neuronal development. Neurons express VAMP4, VAMP2 and VAMP7, with the first localizing predominately to the somatodendritic region, and the last two being enriched

in growth cones. Furthermore, a prerequisite for a protein to be involved in neuronal growth would be to be expressed in early stages of development, and a recent study showed that these three proteins are expressed in hippocampal neurons already after 18 h in culture (Grassi et al., 2015).

The role of VAMP4 in neurite outgrowth has been mainly dissected in the rat pheochromocytoma cell line (PC12). PC12 cells are commonly used as a model for neurobiological and neurochemical studies, as after one week of exposure to nerve growth factor (NGF), they stop to multiply and begin to extend processes similar to those produced by sympathetic neurons in culture (Greene et al., 1976). Various articles from the group of Meldolesi have shown that the activation of Rac1, a downstream step of the neurotrophin signaling cascade, leads to rapid and massive outgrowth of PC12 neurites. This outgrowth takes place only in cells, such as PC12 and embryonic and neonatal neurons, rich in an exocytic organelle called enlargeosome, whose exocytosis is mediated by a SNARE machinery including VAMP4 (Cocucci et al., 2008; Racchetti et al., 2010). A further report confirmed that this observed rapid neurite outgrowth is indeed sustained by VAMP4 exocytosis (Schulte et al., 2010). Interestingly, VAMP4 has been shown to colocalize with IGF-1 in the same PPVs population (Liu et al., 2013). Moreover, together with Stx6 and SNAP23, it forms the first known SNARE complex involved in polarized insertion of IGF-1 receptor and regulation of PPV exocytosis required for initial axonal elongation during the establishment of neuronal polarity (Grassi et al., 2015).

VAMP2, the main v-SNARE in neurotransmission, has been the subject of many *in vivo* and *in vitro* studies on neuronal development. In VAMP2 KO mice, Schoch and colleagues have reported that, even though mice die at birth due to severe impairments in neurotransmission, they develop normally and do not have defects in neurite growth (Schoch et al, 2001). In contrast to *in vivo* data, the specific cleavage of VAMP2 by the neurotoxin TeNT blocks neuritogenesis of neurons cultured on poly-Lysine for DIV2 (Gupton and Gertler, 2010). However, TeNT treatment does not disrupt outgrowth for longer periods or when TeNT is added to the culture subsequent to neuritogenesis (Osen-Sand et al., 1996) and neurons grown on Laminin (Gupton and Gertler, 2010). Taken together, these apparently contrasting results might be explained by the possibility that other v-SNAREs compensate for VAMP2 functions during neuritogenesis. The best candidates for such compensation are the tetanus-toxin resistant

R-SNAREs VAMP7 (Galli et al. 1998) and Sec22b (Petkovic et al., 2014). As hilighted above, Gupton and Getler suggested the existence of redundant pathways mediated by VAMP2 and VAMP7 in neurite outgrowth depending on the substrate where neurons attach and grow (Gupton and Gertler, 2010). Meldolesi and co-workers suggested similar redundancy between VAMP4 and VAMP7 depending on the signaling mechanisms, respectively ROCK inhibition and NGF, inducing neurite growth in PC12 cells (Racchetti et al. 2010). Despite being not an essential requirement for neurite elongation, a study from our team as revealed that VAMP2 is involved in axonal guidance, and particularly in Semaphorin 3A mediated axonal repulsion, both *in vitro* and *in vivo* (Zylbersztejn et al., 2012).

VAMP7 was first identified as SNARE resistant to clostridial neurotoxins (tetanus and botulinum neurotoxins B, D, F, and G) (Galli et al., 1998). For this reason, it was originally called Tetanus neurotoxin-Insensitive Vesicle-Associated Membrane Protein (TI-VAMP). After its discovery within a SNARE complex (also including Stx3 and SNAP23) at the apical membrane of epithelial cells (Galli et al.,1998), later studies showed that VAMP7 is widely expressed in adult rat brain, mainly in somatodendritic compartment, while in a subset of neuronal cell types it is also expressed in axonal terminal (Muzerelle et al., 2003). In developing cultured neurons, VAMP7 localizes to the cell body and neurites where it concentrates into the leading edge of the growth cone (Coco et al., 1999). This enrichment is regulated by the GTPase Cdc42, which coordinates the assembly of the F-actin network in growth cones (Alberts et al., 2006). VAMP7 is broadly expressed within different post-Golgi compartments and its subcellular localization varies depending on the cell type. It localizes to TGN, late endosomes, lysosomes, autophagosomes (Advani et al., 1999; Martinez-Arca et al., 2003), but also in synaptic vesicle (Hua et al., 2011) and secretory granules (Krzewski et al., 2011). A large body of evidences from our and other teams have shown that VAMP7 has a broad pleiotropic function in membrane trafficking. It allows for heterotypic fusion between endosomes and lysosomes (Advani et al., 1999). It is involved in fusion of secretory vesicles with the PM, which is necessary for lysosomal and granule secretion in polarized, migrating and invading cells (Advani et al., 1999; Chaineau et al., 2009; Zylberstein and Galli 2011). Noteworthy, by combining AFM studies, substrate of controlled rigidity and composition, and live imaging of lysosomal exocytosis, a recent study from our laboratory has shown that VAMP7-dependent secretion is controlled by integrin-dependent mechanosensing of substrate rigidity. The

proposed model is a tug-of-war molecular mechanism with LRRK1 and VARP competing for binding to the LD domain of VAMP7. On soft substrates, high activity of LRRK1 and low activity of VARP favors the retrograde transport of VAMP7 vesicles and as a result, depletes the availability of peripheral VAMP7 vesicular pool. Conversely, on rigid substrates, a weaker activity of LRRK1 and stronger activity of VARP increase the amount of VAMP7 vesicles in the periphery, enhancing secretion (Wang et al. 2018). Furthermore, VAMP7 participates in autophagy, from the early steps, mediating the homotypic fusion of autophagosome precursors during phagophore formation (Moreau et al., 2011), to late ones, driving the fusion of ATP-loaded autophagosomes/amphisomes with the PM (Fader et al., 2012). The role of VAMP7 in the secretion of autophagic vesicles suggests that this R-SNARE may mediate both conventional and unconventional secretion.

Regarding its function within the nervous system and, particularly, in neurite growth, our laboratory showed that VAMP7 KO mice displayed increased anxiety and neuroanatomical defects, including decreased brain weight and increased volume of the third ventricle (Danglot et al., 2012). However, axonal growth appeared normal in cultured KO neurons. In previous *in vitro* studies, VAMP7 was shown to mediate axonal and dendritic growth. Indeed, deletion of the VAMP7 N-terminal LD domain strongly stimulated neurite outgrowth in PC12 cells and cultured neurons, and expression of the LD domain alone had an inhibitory effect on growth (Martinez-Arca et al., 2000 and 2001; Alberts et al., 2003). As already mentioned for VAMP2, these contradictory results between *in vivo* and *in vitro* data can be reconciled if one considers that VAMPs compensate for each other. VAMP2 and VAMP4 may be able to fulfil VAMP7 functions during development *in vivo*, allowing KO mice to develop without major brain defect. In line with its involvement in mechanisms of non-canonical secretion, a recent work from our team has shown that VAMP7-dependent autophagic unconventional secretion is involved in axonal elongation in starving condition. Loss of VAMP7 leads to autophagy defects and a deregulation of autophagy-dependent exocytosis. Furthermore, autophagy induction by specific drugs or *via* partial nutrient restriction conditions enhances axonal growth and this process depends on VAMP7. Based on these and further data, the proposed hypothesis is that VAMP7-mediated autophagy secretion participates in resilience mechanisms used by neurons to preserve axonal growth in nutrient restriction conditions (Wojnacki et al. 2019 *in publication*).

2.4) Alternative pathways of membrane trafficking in neuronal development

Alternative membrane trafficking from ER to PM includes a series of mechanisms which bypass COPII based ER to Golgi trafficking and Golgi, generating ER-derived membrane structures. These would directly fuse with the PM, or indirectly through fusion with the lysosomes or late endosomes, involving or not autophagosomes (Nickel and Seedorf, 2008; Rabouille, 2017). In this pathway, proteins are delivered from the ER to the PM in COPII-independent and Golgi-independent manner. In neurons, many examples of non-canonical secretion have been described for a variety of integral membrane proteins. Hanus and colleagues have recently shown that several transmembrane proteins, including neurotransmitter receptors, guidance and adhesion proteins, have immature glycosylation profiles at the cell surface of hippocampal neurons (Hanus et al., 2016). The proposed hypothesis is that these "immature" core-glycosylated proteins might travel to the PM using a non-conventional secretory pathway that bypasses the Golgi apparatus. However, the mechanism is still unknown and further experiments will be necessary to investigate exactly how these proteins are delivered to the surface.

Examples of alternative mechanisms potentially involved in membrane delivery during neurite outgrowth include endosomal membrane trafficking, and non-vesicular delivery of lipids from the ER to the PM.

2.4.1) Endosomal membrane trafficking

In eukaryotes, lipids and proteins from the PM are constantly internalized by different endocytic processes, generating primary endosomes, which then fuse with each other forming early endosomes (EE), also called sorting endosomes (SE). Depending on the cargo, SE can be sorted through two different mechanisms, a "short loop" and a "long loop" pathway. In the ''short-loop'' or fast recycling pathway, endocytosed proteins and lipids are sent back to the PM directly from the SE within 2–3 min. In the ''long loop'' or slow recycling pathway membrane components can be sorted to recycling endosomes (RE), from where they can go back to the cell surface in about 10 min (Li and DiFiglia, 2012; Wojacki and Galli, 2016). Endosomal membrane trafficking is regulated by signaling proteins, SNAREs, and Rab GTPases, many of which have roles in the generation and maintenance of polarity during neuronal development.

Within the "long loop", Rab11, a classical marker of RE, was proposed as an important mediator of axonal growth (Fig. 23). Specifically, by using an innovative approach consisting in the optogenetic control of the positioning of Rab11 recycling endosomes, it has been found that dynein-driven removal or kinesin-driven addition of endosomes, negatively and positively affect growth cone dynamics and axonal growth, respectively (Van Bergeijk et al 2015). In addition, Rab11-positive REs are essential for recycling cell adhesion molecules, such as α9 and β1-integrins, in growth cone of dorsal root ganglion (DRG) neurons and NGF-differentiated PC12 cells, which have been internalized during axon guidance (Eva et al., 2010). Other adhesion molecules also required for axonal growth can be internalized by using different REs. For example, the IgCAM adhesion molecule L1 is endocytosed into VAMP7-positive vesicles in NGF differentiating PC12 cells and developing hippocampal neurons (Alberts et al., 2003).

Rab4 and 5 are implicated in the "short loop" recycling route at growth cone, which is important for fast and bulk membrane recycling (Fig. 23). A recent work from Falk and collaborators (2014) has shown that Rab4 and Rab5 regulate the extension retinal axons in developing Xenopus visual system. Indeed, inhibition of Rab4 function with dominant-negative Rab4, or else constitutive activation of Rab5, decreases the elongation of retinal axons *in vitro* and delays axonal arrival at the tectum *in vivo*.

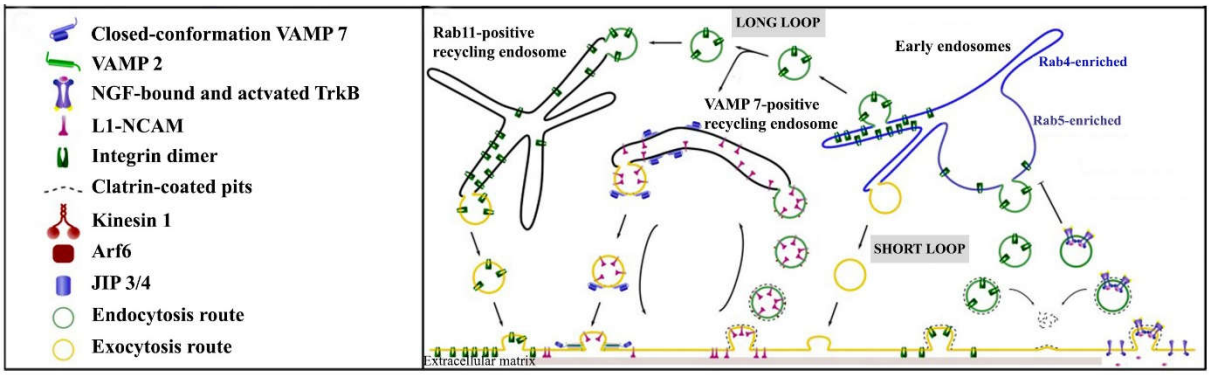

Figure 23. Representation of the recycling pathways present in neuronal growth cones. Three main recycling routes are represented: 1) Bulk membrane recycling through the short loop in retinal ganglion neurons; 2) Integrin recycling in DRG neurons going through the long loop; 3) Local recycling of L1-CAM in PC12 neurites through Vamp7-positive recycling endosomes. (Image adapted from Wojnacki and Galli, 2016).

Overall, the endosomal system constitutes an additional mechanism reservoir regulating membrane trafficking in neuronal development. Its importance in neuronal function is further highlighted by evidences showing that impairing the function of key proteins involved in endocytosis contributes to the pathogenesis of neurological disorders such as Alzheimer's and Huntington's disease (Li and DiFiglia, 2012).

2.4.2) Non-vesicular lipid transfer

As discussed in paragraph 1.5, non-vesicular transport of lipids was demonstrated for glycerophospholipids (Kaplan and Simoni, 1985a), sterols (Baumann et al., 2005) and sphingolipids (Hanada et al., 2003). Lipid transfer from ER to PM can occur through diffusion of lipid monomer or with the use of carrier proteins (LTPs) residing at ER-PM contact sites that would extract a lipid from one membrane and insert it into another. Additionally, phospholipids can move between the two leaflets of one bilayer. This mechanism is catalyzed by lipid translocator proteins, which can be classified in flippases, moving phospholipids from the outer leaflet to the inner leaflet, floppases, moving phospholipids in the opposite direction, and scramblases, which exchange phospholipids in both directions in a calcium activated, ATP-independent process. Below I will discuss two mechanisms by which lipid transport between or within membrane bilayers has been proposed to participate in membrane growth.

2.4.2.1) The SNARE Sec22b at MCSs: lipid transfer replaces fusion?

Sec22 is an ER-localized protein, highly conserved between yeast and mammalian cells. While yeast contains only one Sec22 gene, mammalians contain three Sec22 genes, namely Sec22a, Sec22b and Sec22c. Sec22a and Sec22c code for multi-pass transmembrane proteins, but they lack the SNARE domain and their function is not known. On the other hand, Sec22b is a SNARE protein, as it contains the SNARE domain and it was originally described to be involved in anterograde and retrograde membrane trafficking between the ER and the Golgi apparatus (Burri et al., 2003; Liu and Barlowe, 2002). In anterograde transport, cargo vesicles coated with coat protein–II (COP-II), bud off from the ER and fuse with the *cis*-Golgi compartment leading to exchange of vesicular components. The SNARE complex involved in thiese fusion events include Sec22 and Stx5, Bet1 and membrin. Similarly, in retrograde transport, COP-I vesicles move in the opposite direction from the Golgi towards the ER, and

their fusion is mediated by a SNARE complex composed by Sec22, Use1, Sec20, and Stx18 (Malsam et al., 2011).

Unexpectedly, Sec22b participates in a variety of cellular events, independently to its function in ER-Golgi transport. It is a component of the molecular machinery involved in ER-to-phagosome traffic in macrophages and in antigen cross-presentation by dendritic cells (Becker et al., 2005; Hatsuzawa et al., 2009, Cebrian et al., 2011); however, Sec22b function in these events is still debated. On one hand, studies using shRNA-mediated Sec22b KD assessed Sec22b as a key regulator of antigen cross-presentation (Cebrian et al., 2011). On the other hand, Wu et al. (2017) observed no defect in such process in dendritic cells-specific Sec22b KO mice (CD11c-Cre Sec22b$^{fl/fl}$), In addition, they demonstrated that the Sec22b shRNA sequences used in prior studies impact cross-presentation by off-target effect. Further studies are therefore required to clarify the current controversy.

Additionally, Sec22b is involved in autophagy, where it mediates fusion events driving autophagosome biogenesis (Nair et al., 2011). Moreover, it has been recently shown that Sec22b plays a significant role in the unconventional secretion of leaderless cytosolic proteins by secretory autophagy. Unconventionally secreted cytosolic proteins are characterized by the absence of leader peptides; thus, they do not enter the lumen of the ER and do not follow the conventional secretory pathway, but they are secreted by an autophagy-mediated exocytosis of post-Golgi vesicles. Kimura et al. described that the prototypical secretory autophagy cargo 1L1B/1L-1 is initially recognized by TRIM16 which later interacts with Sec22b. TRIM16 and Sec22b jointly deliver 1L1B cargo to the autophagy-related MAP1LC3B-II-positive membrane carriers. Sec22b together with Syntaxins at the PM finally concludes the cargo secretion (Kimura et al., 2017).

Lastly, a recent study from our laboratory has shown that Sec22b also plays an important role in neurons, where it interacts with the t-SNARE Stx1 to bring the ER and PM into close proximity without mediating their fusion, but rather forming ER-PM contact sites (See paragraph 1.6.1). The SNARE complex that forms between Sec22b and Stx1 does not include any SNAP25-like factors, therefore resulting in a fusion-incompetent association that is unable to mediate vesicle exocytosis in neurons or liposome fusion *in vitro* (Petkovic et al., 2014). Interestingly, we have found that, despite being unable to induce vesicle fusion, Sec22b/Stx1 is

required for PM expansion during neuronal development. Indeed, Sec22b KD impairs neurite growth both in cultured cells *in vitro* and *in vivo* (Fig. 24a,b). Impaired axonal and dendritic growth also occurs when the distance between ER and PM is increased *via* the introduction of a long rigid proline linker between the coiled-coil and transmembrane domains of Sec22b (Fig. 24c).

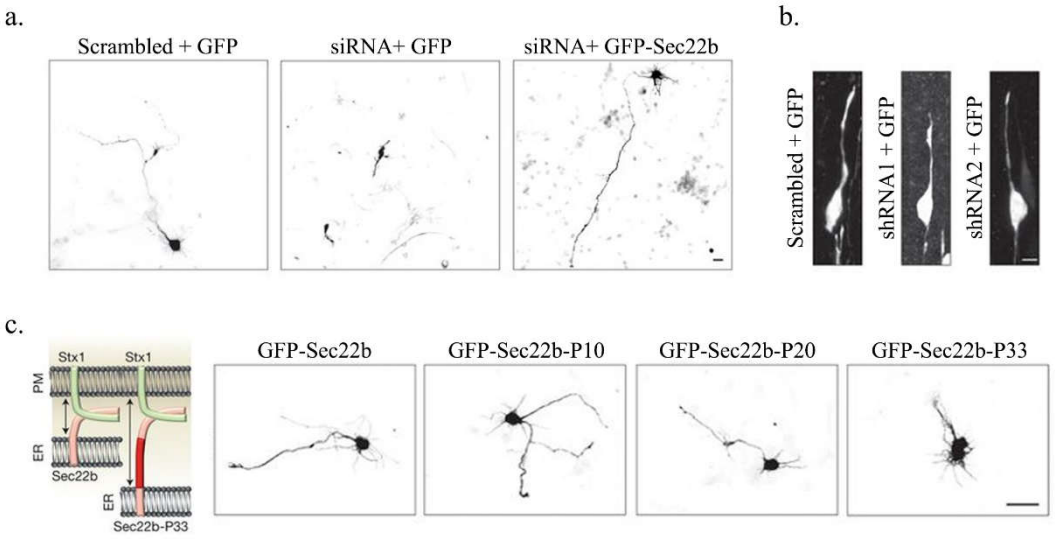

Figure 24. The Sec22b-Stx1 SNARE complex is involved in neuronal development. Impairment of Sec22b by siRNA and shRNA knockdown in culture (a) and *in vivo* (b) inhibits axonal and dendritic growth. (c) Elongating Sec22b by introducing a proline linker of crescent length, progressively increases the distance between the ER and PM, and impairs neurite growth. (Images from Petkovic et al. 2014).

(Petkovic et al. 2014). In yeast, Sec22 also forms a complex with the t-SNARE Sso1, the yeast homologue of Stx1, and we have shown that both proteins interact with the lipid transfer proteins Osh2 and Osh3. Based on these evidences, and on the already established involvement of Sec22b in other mechanisms of unconventional secretion, it is tempting to speculate that the Sec22b-Stx1 complex might account for the addition of membrane in elongating axon, via non-vesicular lipid transfer at ER-PM contacts. It remains to be demonstrated that an LTP protein interacts with Sec22b present in MCSs and my thesis work aimed at addressing this question. In the session "Results" I will provide evidences in support of an association in neurons between Sec22b/Stx1 complex and the LTPs E-Syts, which might promote the extension of developing neurites.

2.4.2.2) The TMEM16F scramblase activity in surface membrane expansion

In addition to the transport between distinct membrane compartments, it has been shown that the shuttle of lipids within a bilayer might also contribute to certain mechanisms of membrane expansion. Two recent works from the group of Donald Hilgemann, reported on a role for the Ca^{2+}-activated TMEM16F in triggering large-scale surface membrane expansion in parallel with lipid scrambling (Bricogne et al., 2018; Fine et al., 2018). The protein TMEM16F, also known as Ano6, is a particular member the mammalian TMEM16 family of Ca2+ activated ion channels (see paragraph 1.4) that functions also as a phospholipid scramblase, transporting PS and other phospholipids between the inner and outer monolayers of the surface membrane in response to Ca2+ (Scudieri et al., 2015; Suzuki et al., 2013). It has been reported that this scramblase activity is required for cell surface PS exposure during platelet aggregation and T cell activation (Suzuki et al., 2010. Yang et al. 2012). Combining patch clamp analysis and confocal imaging, Bricogne and colleagues have shown that cytoplasmic Ca^{2+} elevations cause rapid surface membrane expansion in concert with PS exposure and the opening of TMEM16F channels, in both Jurkat T cells and HEK293 cells. Interestingly, such membrane growth was insensitive to VAMP2 cleavage by TeNT (Bricogne et al., 2018). In a parallel article, the same authors went deeper into the molecular mechanisms by which TMEM16F operates, suggesting that the large-scale PM expansion mediated by TMEM16F reflects the opening of deeply invaginating surface membrane compartments. Normally, these invaginations are closed by proteins that bind anionic phospholipids. Loss of anionic phospholipids from the cytoplasmic leaflet during TMEM16F activity results in constrictions release and opening of these compartments to the extracellular space. They propose a mechanism by which TMEM16F can exist in three activity states: closed, open and inactive. In the absence of cytoplasmic Ca^{2+}, TMEM16F channels are closed and have no scramblase activity. When Ca^{2+} rises, it binds to TMEM16F leading to its opening and allowing anionic phospholipids to permeate the pore together with monovalent cations in an electroneutral fashion. Finally, TMEM16F inactivates when anionic lipids are lost from the cytoplasmic leaflet (Fine et al., 2018). Surprisingly, cells lacking TMEM16F expression not only fail to scramble lipid and expand surface membrane, but they also undergo a rapid membrane internalization known as massive endocytosis (MEND) in response to increase of cytoplasmic Ca^{2+}. Together, these results suggest that TMEM16F plays a fundamental role as a regulator of Ca^{2+}-activated membrane trafficking. However, two main questions still need to be addressed, the first concerning the identity of the proteins

mediating the invaginations' constriction, and the second regarding the biogenesis of such invaginations. Moreover, it is important to note that the TMEM16F-mediated membrane expansion has only been described in non-neuronal cells. Future studies would shed light the still open questions and would determine if this constriction-dependent mechanism of PM expansion also occurs in developing neurons.

Chapter 3

The interaction between non-fusogenic Sec22b-Stx complexes and Extended-Synaptotagmins promotes neurite growth and ramification

During life, cell size and shape are controlled by the rate of PM growth and cytoskeletal rearrangements. Growth is essential for tissue development. Most projection neurons elaborate processes that reach distances several centimeters away, and some can extend up to several meters from the cell body. Membrane expansion occurs through the fusion of secretory vesicles with the PM, a process mediated by the formation of a complex between vesicular and target SNAREs. In addition, non-vesicular mechanisms also contribute to PM growth. The results presented in this study follow previous work of our team showing that a close apposition of the ER and the PM, mediated by the ER-resident Sec22b and the PM-resident Stx1, generated a non-fusogenic SNARE bridge contributing to PM expansion (Petkovic et al. 2014). Such *trans*-SNARE assembly at ER-PM contacts was thought to display a binary configuration, lacking the classical partners of fusogenic SNARE complexes, such as SNAP-23, 25 or 29. Further characterizing potential additional components interacting with the Sec22b-Stx1 tethering complex was therefore a logical perspective of this study, and has been the motivation for my work. Altogether, my results suggest that Sec22b interacts with the ER-resident Extended-Synaptotagmins (E-Syts), known to be lipid transfer proteins (LTPs). In addition, I found that this interaction is a prerequisite for the increase of membrane area required during neurite grow. Figure 1A, B and Figure 3 were contributed by Francesca Giordano to further evaluate the proposed mechanism in non-neuronal cells.

This study is submitted and is attached as the Chapter 3.

In addition, at the end of the Chapter 3, I have added an Appendix containing *in vitro* experiments performed during the course of my PhD that were not included in the submitted paper, but in the context of a thesis manuscript could be interesting for further discussion and future studies.

The interaction between non-fusogenic Sec22b-Stx complexes and Extended-Synaptotagmins promotes neurite growth and ramification

Alessandra Gallo[1,2], Francesca Giordano[3], Lydia Danglot[1], Thomas Binz[4], Christian Vannier[1], Thierry Galli[1]

[1] Université de Paris, Institute of Psychiatry and Neuroscience of Paris (IPNP), INSERM, Membrane Traffic in Healthy & Diseased Brain, Paris, France.

[2] Ecole des Neurosciences de Paris (ENP), Paris, France

[3] Institute for Integrative Biology of the Cell (I2BC), CEA, CNRS, Paris-Sud University, Paris-Saclay University, Gif-sur-Yvette cedex, 91198, France

[4] Medizinische Hochschule Hannover, Institut für Physiologische Chemie OE4310, 30625, Hannover, Germany

* to whom correspondence should be addressed: Thierry Galli, INSERM U1266, 102-108 rue de la Santé, 75014 Paris, France, thierry.galli@inserm.fr

Summary

Axons and dendrites are long and often ramified neurites that need particularly intense plasma membrane expansion during the development of the nervous system. Neurite growth depends on non-fusogenic Sec22b–Stx1 SNARE complexes at endoplasmic reticulum (ER)-plasma membrane (PM) contacts. Here we show that Sec22b interacts with the endoplasmic reticulum lipid transfer proteins Extended-Synaptotagmins (E-Syts) and this interaction depends on the Longin domain of Sec22b. Overexpression of E-Syts stabilizes Sec22b-Stx1 association, whereas silencing of E-Syts has the opposite effect. Overexpression of wild-type E-Syt2, but not mutants unable to transfer lipids or attach to the ER, increase the formation of axonal filopodia and ramification of neurites in developing neurons. This effect is inhibited by a clostridial neurotoxin cleaving Stx1, expression of Sec22b Longin domain and a Sec22b mutant with extended linker between SNARE and transmembrane domains. We conclude that Sec22b-Stx1 ER-PM contact sites contribute to PM expansion by interacting with E-Syts.

Introduction

Cell growth is a universal process supported by cell multiplication and increase in size after each division. The plasma membrane (PM) expands in concert with cell growth. Cell growth is particularly dramatic in highly polarized cells like neurons. During their development, neurons elaborate processes extending hundreds of microns to meters from the cell body, requiring an increase in their PM surface by 20% per day (Pfenninger 2009). Hence, compared to other cell types, developing neurons have to face a formidable challenge of adding new membrane to appropriate locations in a manner that requires both high processivity and fine regulation.

Membrane expansion during neuronal development has been thought to be mediated by soluble N-ethylmalemide-sensitive attachment protein receptor (SNARE)-dependent fusion of secretory vesicles with the PM (Wojnacki & Galli 2016). SNAREs are transmembrane proteins mediating membrane fusion in all the trafficking steps of the secretory pathway. In order for fusion to occur, a *trans*-SNARE complex, composed of three Q-SNAREs (on the acceptor compartment) and one R-SNARE (on the opposing membrane), assemble to bring the opposite lipid bilayers in close proximity and trigger their fusion (Jahn & Scheller 2006, Südhof & Rothman 2009). In mammals, the R-SNAREs Syb2/VAMP2, VAMP4 and TI-VAMP/VAMP7 have been implicated in neurite extension (Alberts et al. 2003, Grassi et al. 2015, Martinez-Arca et al. 2001, Schulte et al. 2010). However, single knockouts (KO) mice for VAMP7 (Danglot et al. 2012) or VAMP2 (Schoch et al. 2001) display no major defects in neuronal development, and redundant pathways of neurite outgrowth, mediated by VAMP2, VAMP4 and VAMP7, have been described (Gupton & Gertler 2010, Racchetti et al. 2010, Schulte et al. 2010). These evidence raised the possibility that several secretory vesicles equipped with different R-SNAREs, as well as complementary non-vesicular mechanisms, could contribute to neurite extension during brain development. Indeed, we previously found that the R-SNARE Sec22b, a conserved endoplasmic reticulum (ER)-localized R-SNARE involved in vesicle fusion within the early secretory pathway, had an additional and unexpected function in promoting PM expansion during polarized growth. Sec22b concentrates in neuronal growth cones, where it interacts with the neuronal Stx1. Sec22b-Stx1 complex does not mediate fusion, but it rather creates a non-fusogenic bridge between ER and PM. In addition, we showed that increasing the distance between ER and PM, by the insertion of a rigid spacer in Sec22b, reduced neuronal growth, and in budding yeast, the orthologue Sec22/Sso1 complexes

contained oxysterol transfer proteins (Petkovic et al. 2014). Based on biophysical experiments with synaptic SNAREs (Li et al. 2007, Zorman et al. 2014), incompletely zippered Sec22b/Stx1 complex would tether ER and PM at distances between 10 and 20 nm, corresponding to the narrowest ER-PM contact sites (Gallo et al. 2016).

The critical role of the ER in PM growth is based on is central role in lipid synthesis. Once synthesized in the ER, lipids travel to the PM along the secretory pathway or they can be directly transferred at ER-PM contact sites. The ER-integral membrane protein Extended-Synaptotagmin (E-Syt) family mediate lipid transfer at ER-PM contact sites. E-Syts are ER-anchored proteins defined by the presence of a cytosolic synaptotagmin-like mitochondrial lipid-binding protein (SMP) domain and multiple Ca^{2+}-binding C2 domains (Giordano et al. 2013, Min et al. 2007). Besides their classical function in tethering ER and PM membranes (Giordano et al. 2013), E-Syts transfer lipids via their SMP domains at ER-PM contact sites (Reinisch & De Camilli 2016, Saheki et al. 2016, Schauder et al. 2014). On one hand, triple KO of E-Syts 1-3 did not show a major morphological phenotype in neurons suggesting that most function associated with these proteins might be redundant with that of other LTPs (Sclip et al. 2016). On the other hand, overexpression of drosophila E-Syt leads to synaptic overgrowth (Kikuma et al. 2017). Therefore, E-Syts may be limiting factors in PM growth associated and their function may be linked to specific features of neuronal differentiation. Based on these data, we hypothesized that E-Syts might interact with Sec22b-Stx1 complexes, which in turn could enable bulk ER to PM transfer of lipids responsible for specific features of neurite growth. Here we found a novel interaction between the Sec22b-Stx1 SNARE complex and members of the E-Syt family. We showed that E-Syts were required to stabilize Sec22b-Stx1 association at ER-PM contact sites and that their overexpression in developing neurons promoted axonal growth and ramification which depended on the presence of the SMP and membrane anchoring domains. Furthermore, this E-Syt-mediated morphogenetic effect was inhibited by botulinum neurotoxin C1, which cleaves Stx1 and the expression of Sec22b Longin domain or a mutant with extended SNARE to transmembrane domain linker. These findings support the conclusion that the ternary association between the LTPs E-Syts, Sec22b and Stx plays an important role in plasma membrane expansion leading to axonal growth and ramification.

Results

1. Sec22b and Stx1, 3 interact with the lipid transfer proteins E-Syt2 and E-Syt3.

First, we asked whether Sec22b and PM Stx could interact with LTPs. We focused on the E-Syt family of ER-resident LTPs because of their well established presence at ER-PM contact sites and role in glycerophospholipid transfer (Saheki et al. 2016, Schauder et al. 2014, Yu et al. 2016) . To test this hypothesis, we performed GFP-trap precipitation experiments on lysates from different cell lines expressing GFP-tagged PM Stx 1 and 3 and Sec22b, and tested the presence of E-Syt family members (Fig. 1).

Firstly, we used HeLa cells, which lacks neuronal Stx1 but express the closely related homologue Stx3 (Bennett et al. 1993). Cells were transfected with the GFP –tagged Stx3 (eGFP-Stx3), together with FLAG-Sec22b and either Myc-E-Syt2 or Myc-E-Syt3. Cell lysates were then subjected to GFP-trap. GFP-Stx3 was able to bring down FLAG-Sec22b, further extending previous results obtained with Stx1 (Petkovic et al. 2014). Furthermore, eGFP-Stx3 also co-immunoprecipitated Myc-E-Syt2 (Fig. 1A) and Myc-E-Syt3 (Fig. 1B). Secondly, we tested whether a Sec22b-Stx-E-Syts association also occurred in a neuronal-like context. PC12 cells were thus chosen because they express neuronal Stx1 and, when treated with NGF, they extend processes similar to those produced by cultured neurons (Greene & Tischler 1976). Lysates of NGF-differentiated PC12 cells transfected with Myc-E-Syt2 and Sec22b-pHLuorin (pHL) were subjected to GFP-trap precipitation. Sec22b-pHL co-immunoprecipitated Myc-E-Syt2 (Fig. 1C, first lane). In addition, Sec22b-pHL precipitated small amounts of endogenous Sec22b, Stx1 and SNAP-25. To assess the extent of the specificity of the interaction between E-Syt2 and Sec22b, we performed GFP-trap in lysates of NGF-differentiated PC12 cells co-expressing Myc-E-Syt2 and various pHL- or GFP-tagged v- and t-SNAREs, i.e. Sec22bΔL-pHL, the mutant Sec22b lacking the N-terminal Longin domain, GFP-SNAP25, Stx1-pHL, VAMP2-pHL, VAMP4-GFP, and GFP alone as indicated (Fig. 1C). A trace amount of E-Syt2 was found to co-precipitate with GFP and reduced amounts were found in the precipitates of GFP-SNAP25, Stx1-pHL, VAMP2-pHL, VAMP4-GFP (Fig. 1D). The amount of co-precipitated E-Syt2 was greatly reduced while the amount of SNAP-25 was increased in the case of Sec22bΔL-pHL mutant, as compared to wild-type Sec22b (Fig. 1E). These data strongly suggest that Sec22b association with E-Syt2 is specific and requires the N-terminal Longin

domain of Sec22b. These results are compatible with Longin domain-dependent presence of Stx1 in Sec22b/E-Syt2 complexes. The fact that Sec22bΔL-pHL precipitated more SNAP-25 than Sec22b-pHL suggests that the Longin domain may prevent SNAP-25 from entering the Stx1/Sec22b complex. It is interesting to note, as positive control, that Stx1-pHL and GFP-SNAP25 co-precipitated large amounts their endogenous synaptic SNARE complex partners (Stx1, SNAP-25, VAMP2).

Taken together GFP-trap experiments support the notion that Sec22b-PM Stx complexes associate with members of the E-Syt family of LTPs and that this interaction occurs both in a non-neuronal and neuronal context. Comparison with the typical synaptic SNARE complex suggests that Stx1 would associate primarily with SNAP-25 and VAMP2 whereas complexes with Sec22b would represent a minor pool of Stx1, in agreement with their restricted occurrence of ER-PM contact sites.

To go further into the characterization of the Sec22bΔL mutant, we used surface staining to detect the presence of wild type or mutant Sec22b at the plasma membrane with ectoplasmic antibodies added to living cells. We used again Sec22b-pHL and Sec22bΔL-pHL chimera in which Sec22b and its mutant version are C-terminally-tagged with pHL, so that anti-GFP antibody present in the medium would bind and reveal only Sec22b that reached the cell surface. N-terminally tagged Sec22b served as a negative control in these experiments, since its GFP tag should never be exposed extracellularly thus be undetectable with anti-GFP antibody without permeabilization. As a positive control for fusion, we used VAMP2-pHL (Figure S1A). In contrast to the strong positive signal given by VAMP2, we found no detectable Sec22b at the plasma membrane, consistent with its non-fusogenic function (Petkovic et al. 2014) (Figure S1B). On the contrary, significant amounts of Sec22bΔL were detected at the cell surface (Figure S1B). Thus, Sec22bΔL was able to mediate fusion to a certain degree with the plasma membrane. In addition, in COS7 cells, Sec22bΔL mutants did not display the ER localization typical of Sec22b wild type, but it was also found in vesicular-like structures (Figure S1C), leading to the hypothesis that it might in part escape into secretory vesicles that eventually fuse with the PM. These data further suggest the involvement of the Longin domain of Sec22b in the formation of the non-fusogenic Sec22b/Stx1 complex.

2. E-Syt2 and Sec22b are in close proximity in neurites and growth cones.

To determine whether the observed association between Sec22b and E-Syts could also be observed in cells *in situ*, we used *in situ* Proximity Ligation Assay (PLA), live cell imaging and and Stimulated Emission Depletion (STED) super-resolution microscopy.

Fixed HeLa cells and hippocampal neurons at 3DIV were reacted with Sec22b and E-Syt2 antibodies and processed for PLA. As specificity control of the PLA signal given by Sec22b and E-Syt2, we also tested the proximity of Sec22b with Calnexin, another ER-resident protein not supposed to interact with Sec22b (Fig. 2). Distinct PLA dots were observed in HeLa cells labeled for endogenous Sec22b and E-Syt2 (7.18 ± 0.60 per cell) (Fig. 2A). The PLA signal decreased to an average of 3.30 ± 0.40 in cells stained for Sec22b and Calnexin and to an average of 1.15 ± 0.14 and 1.20 ± 0.11 in negative controls, performed by incubating cells with only Sec22b and E-Syt2 antibodies, respectively (Fig. 2B). To further confirm these results, we performed live cell imaging in HeLa cells co-expressing Sec22b-mCherry and GFP-E-Syt2. We found co-localization in discrete puncta of Sec22b and E-Syt2, prominently localized in the periphery of the cell. Interestingly, such puncta appeared to be less dynamic compared to corresponding whole protein populations, suggesting that they could represent hot-spots of membrane contact sites populated by Sec22b and E-Syt2 (Movie 1). In neurons, the amount of PLA signal per cell was normalized for the area of neurites or cell body (Fig. 2C). Interestingly, dots revealing Sec22b-E-Syt2 proximity were more numerous in neurites (5.53% ± 0.59%) (Fig. 2D) compared to cell bodies (2.92% ± 0.44%) (Fig. 2E), suggesting a preferential interaction of the two proteins in growing processes. Similarly, the PLA signal between Sec22b and Calnexin and in the negative control was strongly reduced as compared to that of Sec22b-E-Syt2 in neurons.

Close proximity between Sec22b-E-Syt2 was confirmed by STED microcopy visualizing Sec22b-pHL and endogenous E-Syt2 localization in growth cones at high resolution (Fig. 3A, B). Spatial distribution analysis of E-Syt2-and Sec22 was done using “Icy SODA” plugin and Ripley’s function (Lagache et al. 2018) (Fig. 3D). When statistically associated, both Sec22b and E-Syt2 were detected in growth cones at an average distance of 84.33 nm ± 9.64 nm each other (Fig. 3C). Shorter distances between the two proteins were measured in all the analyzed growth cones. Despite a certain degree of variability among the samples, such measured distances displayed a strong statistical power. As an example, in growth cone n°4, 1.59% of E-Syt2 and 3.89 % of Sec22b-pHL were associated together with a high p value (10-14) at a

distance of 29.81 nm (Fig. 3E). Even though those proportions are low, their high statistical power indicates that they are reproducibly associated at the same distance in the growth cone, thus pointing probably a biological association. Furthermore, we measured the distance between these two molecules and the PM. To label the PM, we use Wheat Germ Agglutinin (WGA), which allows the detection of glycoconjugates, i.e., N-acetylglucosamine and N-acetylneuraminic acid (sialic acid) residues, on cell membranes. We found that colocalizing dots of Sec22b-pHL and E-Syt2 were 43.18 nm ± 1.26 distant to the PM (Fig. 3F). These measurements, which would include the lengths of external glycoconiugates labeled by WGA and of immunoglobulins used for the staining, are compatible with a distance to the PM smaller than 30nm, typical of ER-PM contacts distances.

3. E-Syts favor the occurrence of Sec22b-Stx complexes.

As previously reported, E-Syts function as regulated tethers between the ER and the PM and their overexpression stabilizes and increases the density of ER-PM contact sites (Giordano et al. 2013). The question as to whether E-Syts overexpression stabilizes Sec22b-Stx complexes at MCSs was therefore addressed. To do so the PLA technique was used to evaluate Sec22b/Stx3 association in non-transfected or in E-Syt3-overexpressing HeLa cells (Fig. 4A, B). We found that, the number of PLA puncta significantly increased from 4.08 ± 0.67 per cell dots counted in non-transfected cells to 6.66 ± 0.91 in cells where E-Syt3 is overexpressed (Fig. 4C). We then investigated to which extent impairing the formation of ER-PM contact sites would influence the interaction between Sec22b and Stx3. To do this, we inhibited expression of the three E-Syt isoforms (E-Syt1, E-Syt2 and E-Syt3) simultaneously using siRNAs targeting the mRNAs of these proteins (Fig. 4D, E). Interestingly, the total number of PLA dots given by Sec22b and Stx3 was strongly decreased in the E-Syt-deficient HeLa cells as compared to control cells (Fig. 4F).

Taken together, our results indicate that increasing the amount of or abolishing the tethering activity of E-Syts correlates with the probability to observe proximity between Sec22b and Stx3. Thus, E-Syts likely promote the formation of ER-PM contact sites populated by Sec22b-Stx3 complexes.

4. E-Syts overexpression promotes filopodia formation and ramifications in developing neurons

At the neuromuscular junction of Drosophila melanogaster, overexpression of *Esyt* orthologue, enhances synaptic growth (Kikuma et al. 2017). This prompted us to test the effect of E-Syts overexpression in the growth of cultured neurons. Therefore, rat hippocampal neurons were nucleofected with Myc-E-Syt2 and cultured until 3DIV, a time when axonal polarization is achieved and the major axonal process is distinguishable from the minor dendritic neurites (Dotti et al. 1988). eGFP co-transfection was included to appreciate neuronal morphology of transfected neurons. Overexpression of E-Syt2 induced the formation of filopodia and ramifications, particularly in the growing axons (Fig. 5A). Comparison of the phenotype of neurons expressing Myc-E-Syt2, and neurons expressing E-Syt2 mutant versions, lacking either the SMP (Myc-E-Syt2 ΔSMP[119-294]) or the membrane spanning domain (Myc E-Syt2 ΔMSD[1-72]) domains was undertaken using the Myc-Empty vector as negative control (Fig. 5B). Quantification of morphological parameters of transfected cells showed that neurons overexpressing Myc-E-Syt2 displayed a ~1.5- and a ~2-fold increase in the total neurite length and in the number of branching, respectively, as compared to E-Syt2 mutants or negative control (Fig. 5C). Surprisingly, despite a tendency measured as a ~35% increase, the major neurite was not significantly longer in Myc-E-Syt2 overexpressing neurons (Fig. 5C). Noteworthy, E-Syt2 mutants exhibited no significant differences in the parameters analyzed when compared to the negative control. Thus, elevating the expression level of wild type but not mutant E-Syt2 in developing neurons clearly promoted total neurite growth and ramification.

5. E-Syts overexpression stimulates membrane growth in HeLa cells

To assess whether the increase in growth observed in neurons is a general feature resulting from E-Syt2 overexpression, we compared the phenotype elicited by expression of Myc-E-Syt2 and its deleted mutants in non-neuronal HeLa cells, following an experimental paradigm similar to that used in the previous experiment. Briefly, we transfected HeLa with Myc-E-Syt2, Myc-E-Syt2 ΔSMP[119-294], Myc E-Syt2 ΔMSD[1-72] or Myc-Empty vector together with eGFP. Two days after transfection, cell were fixed and the eGFP immunostaining was used to allow a phenotype comparison in the different conditions (Fig. 6A, B). Consistent with the observations in developing neurons, a clear morphogenetic effect was observed. Myc-E-Syt2 overexpressing HeLa cells displayed an enhanced filopodia formation as compared to control and mutants overexpression, as measured by the percentage of the PM spikes area over the total cell surface

(Fig. 6C). Taken together, these results provide additional evidence of the involvement of E-Syts in membrane growth, both in neuronal and non-neuronal contexts.

6. E-Syts-mediated morphogenetic effect depends on Stx1

Next, the role of *the ternary assembly of E-Syt2, Sec22b and Stx1* in the phenotype of enhanced neuronal growth elicited by E-Syt2 was investigated. To this end, we designed experiments aimed at impairing Stx1 in neurons overexpressing Myc-E-Syt2. Enzymatic disruption of the SNARE Sec22b-Stx1 complex was achieved using botulinum (BoNT) neurotoxins, zinc-endoproteases known to cleave SNARE proteins(Binz 2013, Binz et al. 2010, Sikorra et al. 2008). For this study, purified BoNT/A was used to cleave SNAP25, BoNT/C1 to cleave both Stx1 and SNAP25, and BoNT/D to cleave VAMP2 (Fig. 7A). We nucleofected rat hippocampal neurons with Myc-E-Syt2 and, before fixation at 3DIV, we incubated cells with BoNTs (as indicated in figure legend). Cells incubated with the toxins-diluting culture medium were used as negative control. Since exposure to BoNT/C1 at high concentrations and for long incubation periods causes degeneration of neurons in culture (Igarashi et al. 1996, Osen-Sand et al. 1996), various concentrations and incubation times were tested, and a 4-hour treatment of neurons with 1nM BoNTs was chosen to avoid such deleterious effects. This extremely low concentration of toxins, associated with a relatively short incubation period, is sufficient to induce SNARE cleavage, as shown by reduced protein signals detected after Western blotting (Fig. 7B, C). Assuming that Sec22b, Stx1 and E-Syt2 form a complex, only BoNT/C1 was expected to prevent the E-Syt2-induced phenotype of growth, since this would occur following a cleavage of Stx1. BoNT/A and D, acting on SNAP25 and VAMP2 respectively, should have no effect. Noticeably, the cleavage of Stx1, occurring after BoNTC/1 incubation, was found to cause a ~50% decrease in the extent of branching, resulting in a ~20% reduction of the total neurite length, as compared to neurons incubated with the other tested BoNTs and negative control (Fig. 7D, E). No significant decrease in the length of the major neurite was observed in cells after BoNT/C1 incubation.

These results support the conclusion that Stx1 is required for E-Syt2 to promote neuronal growth, as particularly stressed out by ramifications and filopodia formation.

7. E-Syts-mediated morphogenetic effects depend on the close apposition of ER to PM mediated by Sec22b-Stx1 complexes

In view of the data reported above, it was necessary to investigate whether the distance between ER and PM of contact sites formed by Sec22b and Stx1 was a determining factor for the acquisition of the E-Syt2-mediated morphological phenotype. To this end, the GFP-Sec22b-P33 mutant was used as previously described (Petkovic et al. 2014). In GFP-Sec22b-P33 the SNARE and transmembrane domains of Sec22b are linked by a stretch of 33 prolines (Fig. 8A). Electron tomography analysis showed that GFP-Sec22b-P33 expression resulted in a 6-nm increase of of the ER to PM distance at contact sites, without changing Sec22b localization and its interaction with Stx1 (Petkovic et al. 2014). Co-expression of the GFP-Sec22b-P33 mutant with Myc-E-Syt2 was found to prevent the increase in branching observed in neurons overexpressing E-Syt2 (Fig. 8B, C). This data confirmed and extended results obtained by impairing Stx1 via BoNT/C1. They support the notion that, for E-Syt2 to perform its function in membrane growth, the strict structure of the Sec22b-Stx1 complex is required at ER-PM contact sites.

To gain further insight in the requirement of Sec22b in E-Syts mediated neurite growth, the effect of co-expressing the Sec22b Longin domain with E-Syt2 was tested because we showed previously (Fig. 1) that the Longin domain was important for Sec22b/E-Syt2 interaction. Similarly to what was previously reported for the Sec22b-P33 mutant, the expression of the Sec22b Longin domain was found to reduce branching and the overall neurite length in Myc-E-Syt2 overexpressing hippocampal neurons (Fig. 8B, C).

Discussion

In the present study, we report on a novel interaction between two ER-resident membrane proteins, the R-SNARE Sec22b and members of the Extended-Synaptotagmin (E-Syts) family and show the functional relevance of this interaction in neuronal differentiation. Indeed we found 1/ an interaction between Sec22b and E-Syt2 which required the Longin domain of Sec22b, 2/ this interaction occurred at ER-PM contact sites particularly in neurites, 3/overexpression of wild type E-Syt2 but not mutants devoid of lipid transfer or membrane anchoring domains increased filopodia formation, neurite growth and ramification, and 4/ this morphological effect of E-Syt2 overexpression required functional Stx1 and Sec22b.

LTPs as novel partners of SNARE complexes at MCSs

GFP-trap pull down experiments using Sec22b as a bait systematically captured E-Syts. The N-terminal Longin domain of Sec22b had a prominent role in this interaction because the Longin deletion mutant of Sec22b had a reduced ability to capture E-Syts. PM Stx1 and Stx3 also precipitated Sec22b and E-Syts suggesting a ternary complex. This complex however likely corresponded to a small pool of Stx1 in PC12 cells, when compared to the synaptic SNARE complex. Notably, SNAP25 coprecipitated with Sec22b at a very low level and deletion of the Longin domain increased the amount of coprecipitated SNAP25. This is consistent with the lack of SNAP proteins in Stx1/Sec22b complexes (Petkovic et al. 2014) and the notion that the Longin domain may play a role to exclude SNAP25. Moreover, the 1:1 complex Stx1 and SNAP25 is very abundant and it precedes the recruitment of VAMP2 leading to the formation of the ternary synaptic SNARE complex essential for neurotransmitter release (Fasshauer & Margittai 2004, Weninger et al. 2008). Hence, we are led to propose a model whereby the binding of a pre-assembled, ER-resident, Sec22b/E-Syts complex to a PM-resident Stx1/SNAP25 complex might displace SNAP25 from Stx1 leading to the formation of a non-fusogenic ternary assembly of Sec22b, Stx1 and E-Syts and this sequence of event would depend on the presence of the Longin domain (Fig. 9). Because small amounts of E-Syt2 were precipitated by GFP-SNAP25, it is also possible that E-Syts interact first with the Stx1/SNAP25 complex and then Sec22b binding to E-Syts would compete out SNAP-25. This displacement would depend on Sec22b's Longin domain (Fig. 9). Additional experiments using *in vitro* reconstitution assay will be required to further test this hypothesis. Other LTPs are expected to

interact with Sec22b and PM Stx as already in yeast we previously found Osh2/3 associated with Sso1 (Petkovic et al. 2014). Furthermore, in mammalian cells, both Sec22b and Stx1 were shown to interact with the ER-resident VAMP-associated protein VAP-A. (Weir et al. 2001). VAP-A mediates stable ER-PM tethering (Loewen et al. 2003) and binds a wide number of LTPs, such as oxysterol-binding protein (OSBP)-related proteins (ORPs) and ceramide transfer protein (CERT). Identifying the full catalogue of LTP associated with PM Stx and Sec22b will thus be an important future direction to understand in greater details the molecular mechanisms occurring at ER-PM contact sites.

Interdependence of E-Syts and Sec22b-Stx complexes for the establishment of ER-PM junctions operating in membrane expansion

The association of Sec22b to PM Syntaxins was dependent upon E-Syts expression because it was increased upon E-Syts overexpression and reduced in the absence of the three E-Syts isoforms. By promoting Sec22b/PM Stx interaction, E-Syts may promote closer contact sites between ER and PM because SNARE complexes mediate a ~10nm distance. This shortening of the distance between the ER and the PM may further enhance the LTP activity of E-Syts. In addition, E-Syts interaction may take Sec22b away from its main function of mediating fusion events within the anterograde and retrograde membrane trafficking between ER and Golgi, in association with SNARE partners such as Stx5 or Stx18 (Burri et al. 2003, Liu & Barlowe 2002). As an ER-resident protein, Sec22b can diffuse over the entire ER network, and thus is expected to visit areas of cortical ER where it can be trapped by E-Syts eventually engaged in an ER-PM tethering (Fig. 9). This in turn increases the probability to bind the PM-residing Syntaxins and form a complex in *trans*-configuration. In this view, E-Syts would have a dual function. Firstly, they would be responsible for promoting activity by Sec22b in the formation of a non-fusogenic membrane-tethering complex with PM Syntaxins. Secondly, the lipid transfer activity E-Syts would be enhanced by the formation of the minimal ternary complex E-Syts-Sec22b-Stx because the distance between the ER and the PM would be smaller at these interaction sites. This dual activity of E-Syts could be viewed as the generation of a MCS specialized for lipid transfer functioning in membrane growth.

Morphogenetic effect of E-Syt overexpression

Our data showed that the elicited membrane expansion promoted by elevated E-Syt2 expression was abolished in cells expressing deleted non-functional versions of E-Syt2, i.e. E-Syt2 ΔSMP and E-Syt2 ΔMSD. The increased neurite growth and filopodia formation induced by E-Syt2 overexpression depended on the presence of a functional Stx1 in neurons because it was prevented by treatment with BoNTC1 but not BoNTs A or D. This morphological phenotype also depended on Sec22b since expression of 33P mutant and the Longin domain alone both reversed the effect of E-Syt2 overexpression. It is thus very clear that E-Syts, Stx1 and Sec22b interact both biochemically and functionally. Interestingly, growth was not impaired in cells expressing E-Syt2 mutants, as we could not detect significant differences in membrane expansion as compared to control cells. Therefore, expression of these mutants did not act in a dominant negative manner. These results suggest that other LTPs share redundant function with E-Syts. Similar results were obtained at the neuromuscular junction of Drosophila melanogaster, where overexpression of *Esyt* orthologue enhanced synaptic growth, whereas *Esyt* mutant flies exhibited no difference in synaptic membrane surface area as compared to wild-type animals (Kikuma et al. 2017). Furthemore, *Esyt* triple knockout mice display no major defects in neuronal development and morphology (Sclip et al. 2016). Taken together, these evidence suggest that a functional redundancy exists among LTPs in promoting membrane growth, as the removal of one class of such proteins can be compensated by the activity of the others. The precise contribution of each class LTPs, as well as their mutual interplay, will require further studies. The effect of E-Syt overexpression suggest that LTP may be limiting factors and that fine tuning of their expression level may be critical for their function.

In conclusion the protein complex between E-Syts and Sec22b unraveled here appears as an important model for further studies aimed at understanding how lipid transfer at MCS between the ER and PM could participate to the development of the neuronal cell shape. As exemplified in the case of other SNAREs like VAMP7, our results point to central regulatory function of the Longin domain of Sec22b.

Materials and Methods

Antibodies

Primary antibodies used in this study were: mouse monoclonal anti-Sec22b 29-F7 (Santa Cruz, sc-101267); rabbit polyclonal anti-ESYT2 (Sigma-Aldrich, HPA002132); rabbit polyclonal anti-Calnexin (Cell Signaling, 2433S); mouse monoclonal anti-GFP (Roche, 11814460001); mouse monoclonal anti-c-myc 9E10 (Roche, 11667203001); mouse monoclonal anti-FLAG M2 (Sigma-Aldrich); mouse monoclonal anti-Stx1 HPC-1 (Abcam, (ab3265); mouse monoclonal anti-SNAP25 (Synaptic Systems, 111011); rabbit polyclonal anti-VAMP2 (Synaptic Systems, 104 202); rabbit polyclonal anti-β3 tubulin (Synaptic Systems, 302 302); chicken polyclonal anti-MAP2 (AbCam, ab5392); goat polyclonal anti-GFP (AbCam, ab6673). Rabbit polyclonal anti-Sec22b (Clone TG51) and rabbit polyclonal anti-Syntaxin3 (Clone TG0) were produced in the laboratory.

Plasmids and cDNA clones

Plasmids encoding EGFP-ESyt2, EGFP-ESyt3, myc-ESyt2 and myc-ESyt3 were obtained from P. De Camilli (Giordano et al, 2013). mCherry-Sec22b, the pHluorin-tagged forms of Syntaxin1, Sec22b, and VAMP2 and GFP-tagged forms of Sec22b-P33 mutant, of Sec22b-Longin (Ribrault et al., 2011. Petkovic et al., 2014), of VAMP4 and of SNAP25 (Mallard et al., 2002, Martinez Arca et al. 2000) were previously described. cDNA clones of human Sec22b and Syntaxin2 and Syntaxin3 were obtained from Dharmacon (GE Healthcare) (Sec22b: Clone3051087, Accession BC001364; Syntaxin2: Clone 5296500, Accession BC047496; Syntaxin3: Clone 3010338, Accession BC007405).

Construction of ΔLonginSec22b -pHluorin:

ΔLonginSec22b-pHluorin was generated from ERS24-pQ9 construct and cloned into pEGFPC1-pHluorin using the following primers:

Forward NheI Sec22deltaLongin,
5’-CGCGCTAGCATGCAGAAGACCAAGAAACTCTACATTGAT
Reverse EcoRI Sec22deltaLongin,
5’-CGGGAATTCCAGCCACCAAAACCGCACATACA

Construction of 3XFLAG-Secc22b, EGFP-Syntaxin2 and EGFP-Syntaxin3:

cDNAs of human Sec22b, Syntaxin2 and Syntaxin3 ORFs were amplified by PCR using the following primers:

Forward EcoRI-Sec22b,
5'-CAAGCTTC GAATTC ATGGTGTTGCTAACAATGATC
Reverse BamHI-Sec22b,
5'- TCCGATTCTGGTGGCTGTGAGGATCCACCGGTCG
Forward SalI-Syntaxin2,
5'- ACCG GTCGAC ATGCGGGACCGGCTGCCAGA
Reverse SacII- Syntaxin2,
5'- ATCCTAGCAACAACATTGTCCTAGCCGCGGCGGT
Forward SalI-Syntaxin2,
5'- ACCG GTCGAC ATGAAGGACCGTCTGGAGCAG
Reverse SacII- Syntaxin2,
5'- GACTTTCCGTTGGGCTGAATTAACCGCGGCGGT

PCR products were ligated into the p3XFLAGCMV10 (Sigma-Aldrich) and pEGFP-C1 (Clontech) vectors, respectively to generate 3XFLAG-Sec22b, EGFP-Syntaxin2 or EGFP-Syntaxin3.

Construction of ΔSMP myc-ESyt2 and ΔMSD myc-ESyt2:

ΔSMP myc-ESyt2 and ΔMSD myc-ESyt2 mutants were generated by site-directed mutagenesis by deleting respectively fragment [119-294] and [1-72] using the following primers:

Forward DeltaSMP,
5'-CTGGGTTCATTTTCCAGACACTGAAAGTGAAGTTCAAATAGCTCAGTTGC

Reverse DeltaSMP,
5'-CCAACTGAGCTATTTGAACTTCACTTTCAGTGTCTGGAAAATGAACCCAG

Forward DeltaMSD,
5'-AGATCTCGAGCTCAAGCTTCGAATTCTCGCAGCCGCGGCCTCAAG

Reverse DeltaMSD,

5’-CTTGAGGCCGCGGCTGCGAGAATTCGAAGCTTGAGCTCGAGATCT

Cell culture, siRNA and transfection

HeLa cells were cultured in DMEM containing GlutaMax (ThermoFisher 35050038) and supplemented with 10% (v/v) Bovine Fetal Calf Serum (Biosera 017BS346).) and 1% (v/v) penicillin/streptomycin (ThermoFisher 15140122) at 37°C and 5% CO_2. Transfections were carried out with Lipofectamine 2000 transfection reagent (ThermoFisher 11668027) according to manufacturer’s instructions. For knockdowns, HeLa cells were transfected with control or E-Syts siRNA oligos by using Oligofectamine transfection reagent (ThermoFisher 12252011) according to manufacturer’s instructions. Double-stranded siRNAs targeting the three human E-Syts and control siRNAs were as described (Giordano et al. 2013). Routinely, transfected cells were cultured for 24 or 48 hours on coverslips prior to analysis.

PC12 cells were grown at 37°C and 5% CO_2 in RPMI containing and 10% (v/v) horse serum (ThermoFisher 26050088), 5% (v/v) Bovine Fetal Calf Serum (Biosera 017BS346) and 1% (v/v) penicillin/streptomycin. Cells were coated on plastic dishes with a 1 µg/ml collagen (Sigma C7661) solution. Then, cells were differentiated with hNGF-β (Sigma-Aldrich N1408) at 50 ng/ml for 3–4 days. PC12 transfections were carried out with Amaxa Nucleofection Kit V (Lonza VCA-1003) according to manufacturer’s instructions.

Hippocampal neurons from embryonic rats (E18) were prepared as described previously (Danglot et al.2012). Cells were grown on onto poly-L-lysine-coated 18-mm coverslips (1 mg/ml) or 30-mm plastic dishes (0.1 mg/ml) at a density of 25,000-28,000 cells/cm^2 in Neurobasal-B27 medium previously conditioned by a confluent glial feeder layer [Neurobasal medium (ThermoFisher 21103049) containing 2% B27 supplement (ThermoFisher A3582801), and 500 µM L-Glutamine (ThermoFisher 25030024)]. Neurons were transfected before plating by using Amaxa Rat Neuron Nucleofection Kit (Lonza VPG-1003) following manufacturer’s instructions. After 3 days *in vitro* (3DIV), neurons were processed for immunofluorescence or lysed for immunoblot assays.

Botulinum Neurotoxins (BoNTs) treatment

BoNT/A and BoNT/C were a kind gift from Dr Thomas Binz (Hannover Medical School, Germany), BoNT/D (described in Schiavo et al., 2000). Toxins working concentration at 1 nM in culture media were prepared from 4 µM stock solutions.

Hippocampal neurons overexpressing Myc-E-Syt2 were treated with BoNT/A, BoNT/C, BoNT/D or naïve culture media at 3DIV and maintainedfor 4 hours at 37°C and 5% CO_2. After extensive washing with culture media, cells were processed for immunofluorescence or lysed for immunoblot assays.

Immunofluorescence

HeLa cells and hippocampal neurons at 3DIV were fixed on coverslips in 4% paraformaldehyde in PBS for 15 minutes and quenched in 50 mM NH_4Cl in PBS for 20 min. Cells were then permeabilized in 0.1% (w/v) Triton X-100 in PBS for 5 min and blocked in 0.25% (w/v) fish gelatin in PBS for 30 min. Primary antibodies were diluted in 0.125% fish gelatin in PBS and incubated overnight at 4°C. After washing, secondary antibodies conjµgated with Alexa 488, 568, 594 or 647 were incubated for 45 min at room temperature before mounting in Prolong medium (ThermoFisher P36930).

Surface staining

Hippocampal neurons at 3DIV were placed on an ice-chilled metallic plate. Neurobasal medium was replaced with ice cold DMEM with 20 mM Hepes containing primary antibody (mouse GFP). Cells were incubated for 5-10 min on ice. Cells where then washed with PBS at 4°C and fixed with 4% para-formaldehyde sucrose for 15 min at room temperature. Following fixation, cells were subjected to the already described whole cell staining protocol. The total pool of tagged proteins was detected with anti-goat GFP antibody. Images were acquired on the epifluorescent microscope with the same exposure in all conditions. Presence at the plasma membrane was expressed as ratio between total and surface signal.

In situ proximity ligation assays (PLA)

In situ proximity ligation assays (PLA) to quantify protein vicinity in HeLa cells and in neurons on coverslips as indicated in figures were performed using the Duolink In Situ Detection Reagents Orange kit (Sigma-Aldrich, DUO92007). Cells were fixed, permeabilized as described above, blocked in Duolink Blocking solution (supplied with the kit) for 30 min at 37°C in a humidified chamber. This was followed by incubation with the primary antibodies rabbit Stx3 (4µg/ml), or rabbit E-Syt2 (2µg/ml) or rabbit Calnexin (2µg/ml) and mouse Sec22b (2µg/ml). For the rest of the protocol the manufacturer's instructions were followed. Briefly,

cells were washed in kit Buffer A 3 times for 15 minutes and incubated with the PLA probes Duolink In Situ PLA Probe Anti-Mouse PLUS (Sigma-Aldrich, DUO92001) and Duolink In Situ PLA Probe Anti-Rabbit MINUS (Sigma-Aldrich, DUO92005) for 1 hour at 37°C in a humid chamber followed by two washes of 5 min in Buffer A. The ligation reaction was carried out at 37°C for 30 min in a humid chamber followed by two washes of 5 min in Buffer A. Cells were then incubated with the amplification-polymerase solution for 100 min at 37°C in a dark humidified chamber. After two washings with kit Buffer B for 10 minutes followed by a 1 minute wash with 0.01x Buffer B, cells were mounted using the Duolink In Situ Mounting Medium with DAPI (Sigma-Aldrich, DUO92040).

Microscopy and image analysis (missing STED)

Confocal imaging: Z-stacked confocal images of neurons and HeLa cells were acquired in a Leica TCS SP8 confocal microscope (Leica Microsystems CMS GmbH), using a 63x/1.4 Oil immersion objective.

HeLa cells live imaging: HeLa co-expressing mCherry-Sec22b and GFP-E-Syt2 were transferred to an imaging chamber (Chamlide EC) and maintained in Krebs-Ringer buffer (140mM NaCl, 2.8mM KCl, 1mM MgCl2, 2mM CaCl2, 20mM HEPES, 11.1mM glucose, pH 7.4). Time-lapse videos were recorded at 5s intervals for 2min using an inverted DMI6000B microscope (Leica Microsystems) equipped with a 63X/1.4-0.6 NA Plan-Apochromat oil immersion objective, an EMCCD digital camera (ImageEMX2, Hamamatsu) and controlled by Metamorph software (Roper Scientific, Trenton, NJ). To virtually abrogate latency between two channels acquisition, illumination was sequentially provided by a 488nm- and a 561nm-diode acousto-optically shuttered lasers (iLas system; Roper Scientific) and a dualband filter cube optimized for 488/561nm laser sources (BrightLine; Semrock) was used. Environmental temperatures during experimental acquisitions averaged 37°C. FIJI software was used for bleaching correction and for movies montage. Binary mask of particles was generated by applying the wavelet-based spot detector plugin of Icy imaging software (http://icy.bioimageanalysis.org) to each channel sequence.

STED imaging: Neuronal membrane was labeled on live neurons using the lectin Wheat Germ Agglutinin (WGA) coupled to Alexa 488 nm for 10 min. Neurons were washed and fixed with a 4% PFA /0,2% Glutaraldehyde mixture and then processed for immunochemistry. Growth

cone were imaged with 3D STED microscopy using the 775 nm pulsed depletion laser. Depletions were realised on primary antibody to endogeneous E-Syt2 labelled with secondary antibodies coupled to Alexa 594. Sec22b-pHL were labelled with primary anti-GFP and ATTO647N secondary antibodies. Acquisitions were done in 3D STED so that the voxel size were isotropic (22 nm in XYZ). Typically, we imaged a matrix of 1400x1400 pixels over 20 to 25 z planes to include all the growth cone volume. Growth cone was segmented using Icy "HK means" plugin (Dufour et al. 2008). Spatial distribution analysis of E-Syt2-and Sec22 was done using "Icy SODA" plugin (Lagache et al. 2008) and a dedicated LD protocol automation. Briefly, E-Syt2 and Sec22b distribution were analysed through the Ripley function. Statistical coupling between the two molecules was assessed in a 22 nm radius (size of the voxel) concentric target. Over 13784 E-Syt2 clusters analysed in 4 different growth cone, 20 percent were statistically associated with Sec22b. When associated, the 2 molecules were at 84nm ±9nm, which corresponds to 34% of Secc22b clusters. This coupling is of very high significance since the p value was ranging between 10-5 and 10-24. Distance to the plasma membrane was measured using the Icy ROI inclusion analysis plugin (Publication ID: ICY-B3M8X7).

PLA signal: Maximum intensity projections of a confocal z-stack including a whole cell were performed to observe the maximum amount of PLA puncta. The number of puncta per cell was counted using the Cell Counter plugin in Fiji/ImageJ. In neurons, the PLA puncta were separately counted in cell body and neurites and the PLA signals were divided by the area of the two compartments.

Neurite length. For the analysis of neurite length of cultured neurons, images were analyzed using the NeuronJ plugin in Fiji/ImageJ on the maximal intensity projections of z-stacks of the eGFP channel. Main process and branches were measured for each neuron. We could not detect any association among individual cells thereby we considered each cell a sampling unit.

Area of spikes: in Myc-E-Syt2 overxpressing HeLa cells, the spikes area was measured on the maximal intensity projections of z-stacks of the eGFP channel. The measurement was carried by subtracting the Region on Interest (ROI) of the cell without spikes, obtained with the tool Filters/Median on Fiji/ImageJ by applying a radius of ~80 pixels, from the ROI of the entire cell.

GFP-Trap pull-down and Immunoblotting

Transfected HeLa or PC12 cells were lysed in TBS (20mM Tris-HCl, pH7.5, 150mM NaCl), containing 2mM EDTA, 1% Triton-X100 and protease inhibitors (Roche Diagnostics). of Clarified lysate was obtained by centrifugation at 16,000xg 15 min, and 1 mg protein was submitted to GFP-Trap pull-down for 1 hour at 4 °C under head-to-head agitation.using 10µl of Sepharose-coupled GFP-binding protein (Rothbauer et al., 2008) prepared in the lab After four washes with lysis buffer, beads were heathed at 95°C for 5 min in reducing Laemmli sample buffer. Soluble material was processed for SDS-PAGE using 10 % acrylamide gels and electrotransferred on nitrocellulose membranes (GE-healthcare). The membranes were blocked with 2.5% (w/v) skimmed milk, 0.1% (w/v) Tween-20 in PBS. Membrane areas of interest were incubated with primary antibodies as indicated in figure legends. After washing, the membranes were blotted with HRP-coupled secondary antibodies. Revelation was carried out by using a ChemiDoc luminescence imager (BioRad).

Statistical analysis

Calculations were performed in Microsoft Excel. GraphPad Prism software were used for statistical analyses. For each dataset, at least three independent experiments were considered and all data are shown as mean ± SEM. Data were analyzed using one-way ANOVA followed by Dunn's, Tukey or Dunnet post-hoc tests were applied as indicated in figure legends.

Figure Legends

Figure 1. Sec22b and Stx interact with the lipid transfer proteins E-Syt2 and E-Syt3.

(A-B) Immunoblots of material recovered after GFP-Trap pull-down from HeLa cell lysates. Cells were transfected for the co-expression of FLAG-Sec22b and Myc-E-Syt2 (A) or FLAG-Sec22b and Myc-E-Syt3 (B) in the presence of either eGFP-Stx3, or eGFP (negative control). Cell lysates were subjected to GFP-Trap pull-down. Total cells lysate (Input) and trapped material (Bound) were processed for SDS-PAGE and Western blotting. Blots were probed with antibodies directed against the tags (GFP, FLAG and Myc) as indicated. Both Myc-E-Syt2 and Myc-E-Syt3 were selectively recruited by eGFP-Stx3. (C) Immunoblots of material recovered after GFP-Trap pull-down from NGF-treated PC12 cell lysates. Cells were transfected for co-expression of Myc-E-Syt2 and the indicated GFP-tagged SNAREs, and processed as in A, B. Blots were revealed with antibodies against the indicated six target proteins. Only Sec22b-pHL, but not its longin-deleted version Sec22bΔL-pHL or the other tested SNAREs, could recruit Myc-E-Syt2. GFP-Trap pull-down of eGFP was used as control for nonspecific binding. (D) Quantification of the ratio between Myc-E-Syt2 signal and the GFP signal given by the immunoprecipitated GFP-tagged vSNAREs (upper graph) and tSNAREs (lower graph). (E) Quantification of the ratio between Myc-E-Syt2 signal and the GFP signal (left graph) and between endogenous SNAP25 signal and the GFP signal (right graph) given by the immunoprecipitated Sec22b-pHL vs Sec22bΔL-pHL. One-way ANOVA followed by Dunnett's multiple comparison post-test, P<0,05*, P<0,001***,. n= 3 independent experiments. Error bars represent the SEM.

Figure 2. E-Syt2 and Sec22b are abundantly in close proximity in neurites and growth cones.

Duolink proximity ligation assay (PLA) for protein interactions ***in situ*** **was performed** in HeLa cells (A) and 3DIV hippocampal neurons (C). Representative confocal images are shown for the indicated antibody combinations using mouse anti-Sec22b, rabbit anti-E-Syt2, or rabbit anti-Calnexin. Negative controls consisted in using anti-Sec22b or anti-E-Syt2 antibody only. In each field, maximum intensity projection of a confocal z-stacks including a whole cell were performed to observe the maximum amount of PLA dots (red). Nuclei were stained by DAPI (blue). A1-4, PLA dots. Lower panel is a higher magnification of region outlined in A1. C1-3, PLA dots. C4-6, MAP2 immunofluorescence staining superimposed to fields shown in C1-3. Lower panels are a higher magnifications of region outlined in C1 and C4. Scale bar, 10 μm. (B, D, E) Quantification of PLA is expressed as dots per HeLa cell (B), and in 3DIV hippocampal neurons as dots per μm^2 of surface area in neurites (D), or in cell body (E). The number of individual fluorescent dots is higher in the Sec22b-E-Syt2 pair as compared to Sec22b-Calnexin pair or negative controls both in HeLa and in neurons. It is higher in neurites as compared to cell bodies in neurons. One-way ANOVA followed by Dunn's multiple comparison post-test, P<0,05*, P < 0.001***. n=3 independent experiments. Error bars represent the SEM.

Figure 3. Analysis of E-Syt2 / Sec22b colocalization using super-resolution microscopy.

(A) Representative confocal images of a 3DIV hippocampal neuron labeled for endogenous E-Syt2 (green) and Sec22b-pHL (red). Wheat Germ Agglutinin (WGA) conjugated to Alexa Fluor® 488 has been used to label the plasma membrane (grey). Scale bar, 10 µm. (B) Super-resolution (STED) 3D reconstruction of the inset in (A) showing localization of endogenous E-Syt2 and Sec22b-pHL in the growth cone. (C) Table showing the average percentages of E-Syt2 colocalizing with Sec22b-pHL (and viceversa) at an average distance of 84.3329 nm ± 9.6427 nm. (D) Image representing the principle of spatial distribution analysis using SODA software (Lagache et al. 2008). (E) Summarizing table showing percentages of E-Syt2 and Sec22b-pHL colocalization with their relative distances, for each analyzed growth cone. Despite a certain degree of variability between cells, the statistical power of the analysis is relevant. (E) Table showing the average distance measured between E-Syt2 / Sec22b-pHL colocalizing puncta and the plasma membrane.

Figure 4. E-Syts favor the occurrence of Sec22b-Stx complexes.

Duolink proximity ligation assay (PLA) for protein interactions *in situ* **was performed** in HeLa cells non transfected or overexpressing eGFP-E-Syt3 (A) and in HeLa cells expressing siRNAs targeting E-Syt1, E-Syt2 and E-Syt3 simultaneously (E). Representative confocal images are shown for PLA between Sec22b (Mouse anti-Sec22b) and Stx3 (Rabbit anti-Stx3) Negative controls combined IgG2A and IgGR. In each field, maximum intensity projection of a confocal z-stacks including a whole cell were performed to observe the maximum amount of PLA dots (red). Nuclei were stained by DAPI (blue). Scale bar, 10 µm. (B) Confocal maximal projection image showing co-localization of Sec22-Stx3 PLA signal and E-Syt3-positive cortical ER. Scale bar, 10 µm. (C, F) Quantification of PLA is expressed as dots per HeLa cell. The number of individual fluorescent dots is higher in cells overexpressing eGFP-E-Syt3 as compared to non-transfected cells or negative control (C). It is lower in cells expressing siRNAs targeting the three E-Sys isoforms as as compared to cells expressing siCtrl (F). Data are expressed as means ± SEM. Student t-test P<0,05*, P<0,001***. n= 3 independent experiments. (D) Representative immunoblots from lysates of HeLa cells expressing siRNAs targeting the three E-Sys isoforms. Tubulin was used as a loading control.

Figure 5. E-Syts overexpression promotes filopodia formation and ramifications in developing neurons

(A) Myc-E-Syt2 expression in 3DIV hippocampal neurons. A2, representative morphology of a nucleofected neuron expressing Myc-E-Syt2. eGFP co-expression was used to view cell shape. A2, higher-magnification of inset in A1 showing high density of filopodia in a segment of the axonal shaft. Scale bar, 10 µm. (B) Expression of Myc-E-Syt2 mutated forms. 3DIV neurons co-expressing eGFP and Myc-E-Syt2 or one of the deletion mutants Myc-E-Syt2ΔSMP and Myc-E-Syt2ΔMSD, lacking the SMP domain [119-294] and the membrane spanning region [1-72], respectively. The empty Myc vector was used as negative control. Scale bar, 10 µm. (C)

Quantification of morphological parameters in transfected neurons shown in B. Plots were acquired on maximal intensity projections of z-stacks of the eGFP channel. Note that in comparison with the longest neurite length (C2), the number of branching per neuron (C1) and the total neurite length (C3) are increased in neurons upon Myc-E-Syt2 expression, whereas expression mutants had no effect. Data are expressed as means ± SEM. Oneway ANOVA P<0,001***, Dunn's multiple comparison post-test labeled on graph. n= 3 independent experiments.

Figure 6. E-Syts overexpression stimulates membrane growth in HeLa cells

(A) HeLa cells were transfected for co-expression of Myc-E-Syt2 and eGFP (the latter to delineate cell shape). Shown is a representative image of two cells (A1). A2, 3, higher magnifications of regions outlined in A1, showing high density of filopodia at the cell periphery. Scale bar, 10 µm. (B) HeLa cells co-expressing eGFP and Myc-E-Syt2 or one of the deletion mutants Myc-E-Syt2ΔSMP and Myc-E-Syt2ΔMSD as in figure 2. The empty Myc vector was used as control. Scale bar, 10 µm. (C) Quantification of spike area in transfected cells shown in B, acquired from maximal intensity projections of z-stacks of the eGFP channel. It is expressed as percentage of the total cell surface area. Filopodia formation was enhanced in cells expressing Myc-E-Syt2 as compared to cells expressing the mutant proteins. Data are expressed as means ± SEM. Oneway ANOVA P<0,01**, Dunn's multiple comparison post-test labeled on graph. n= 3 independent experiments.

Figure 7. E-Syts-mediated morphogenetic effect depends on Stx1

(A) Schematic of cleavage sites on neuronal SNARE targets of BoNTs. Cleavage can occur on SNAP25 (BoNT/A), on both SNAP25 and Stx1 (BoNT/C1), or specifically on VAMP2 (BoNT/D). (B1, 2) Cleavage activity of BoNTs. (B1) Representative immunoblots from lysates of neurons exposed for 4 h to 1 nM BoNTs. (B2) Quantification of ECL signals from B1. Ratios of SNAREs to tubulin are plotted. Oneway ANOVA P<0,05*, followed by post-hoc Tukey HSD test. n=3 independent experiments. Data are expressed as means ± SEM. (D) 3DIV hippocampal neurons co-expressing Myc-E-Syt2 and eGFP and treated with BoNTs (1 nM, 4h). Scale bar, 10 µm. (E) Quantification of morphometric parameters on treated neurons, measured on maximal intensity projections of z-stacks of the eGFP channel. The specific cleavage of Stx1 by BoNT/C1 reduces the number of ramifications and the total neurite length of Myc-E-Syt2 expressing neurons. Data are expressed as means ± SEM. Oneway ANOVA P<0,01** P<0,001 ***, Dunn's multiple comparison post-test labeled on graph. n= 3 independent experiments.

Figure 8. E-Syts-mediated morphogenetic effects depend on ER to PM distance

(A) Scheme showing the predicted effect of a polyproline stretch insertion in Sec22b on the ER-PM distance (see text). (B) Hippocampal neurons co-expressing Myc-E-Syt2 and either GFP-Sec22b, GFP-Sec22b-P33 mutant or Sec22b GFP-Longin domain , observed at 3DIV.

Scale bar, 10 µm. (D) Quantification of morphological parameters on treated neurons, measured on maximal intensity projections of z-stacks of the GFP channel. Effect of overexpressed Myc-Esyt2 on number of ramifications and on the sum of neurite lengths is reduced in neurons expressing the GFP-Sec22b-P33 mutant or the GFP-Longin domain. Data are expressed as means ± SEM. Oneway ANOVA P<0,01** P<0,001 ***, Dunn's multiple comparison post-test labeled on graph. n= 3 independent experiments.

Figure 9. Proposed model for the formation of a SNARE-mediated ER-PM contact site

Sec22b diffuses within the ER membrane (A) and is stabilized in the cortical ER after binding to E-Syts (B1). Sec22b association to the PM-resident Stx1-SNAP25 complex causes SNAP25 displacement from Stx1 and potentially E-Syt, leading to the formation of a non-fusogenic assembly of Sec22b, Stx1 and E-Syts (C). Alternatively, E-Syt first interacts with the PM-resident Stx1-SNAP25 complex (B2), then Sec22b binds to E-Syts, possibly via its Longin domain, chasing out SNAP25 from the complex.

Figure S1. The Sec22bΔLongin mutant reaches the cell surface

(A-B) Hippocampal neurons at 3DIV were transfected with Sec22b or Sec22bΔL mutant tagged with pHluorin at the C-terminal, so that if the Sec22b compartment fuses with the PM, it would be detected by anti-GFP antibody in the medium. N-terminally tagged Sec22b (GFP-Sec22b) has been used as a negative control since its GFP tag should never be exposed extracellularly and detected with anti-GFP antibody, even in the event of membrane fusion. VAMP2-pHL was used as positive control for fusion. For surface staining anti-GFP antibody was allowed to bind for 10 min at 4°C, neurons were fixed and processed for immunochemistry. (A) Scheme of the topology of constructs in the PM if fusion is assumed to occur. (B, left) Representative images. Scale bar, 10 µm (B, right) Quantitative analysis of surface staining versus total staining expressed as normalized ratio to GFP-Sec22b. Oneway ANOVA P<0,0001 ***, Dunn's multiple comparison post-test labeled on graph. (C) Representative images of COS7 cells expressing Sec22b-HA (left) or Sec22bΔL-HA (right) and labeled with an anti-HA antibody. Note that the typical reticular localization of Sec22b is partially lost for the Sec22bΔL mutant.

Figure 1. Sec22b and Stx interact with the lipid transfer proteins E-Syt2 and E-Syt3.

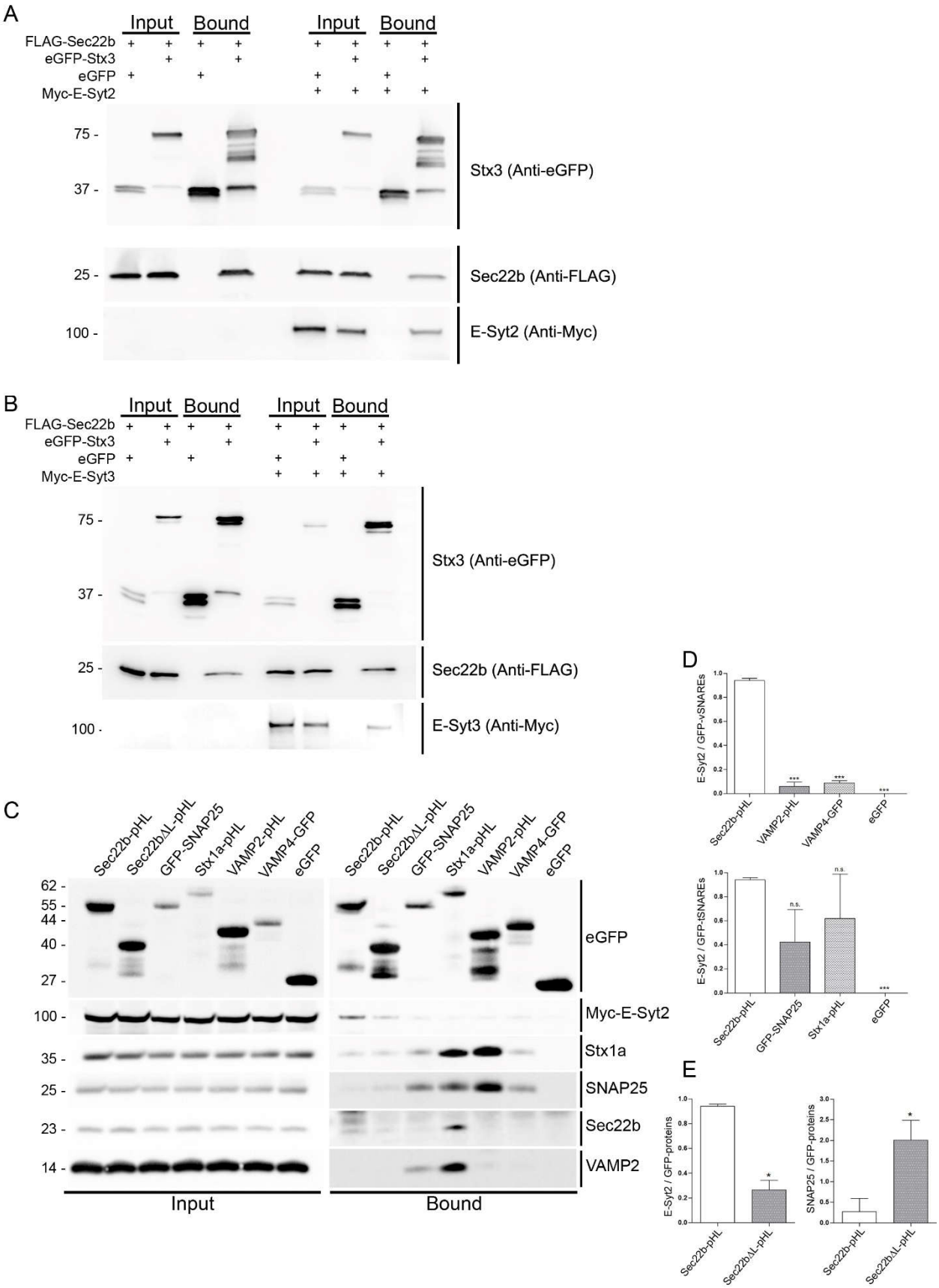

Figure 2. E-Syt2 and Sec22b are abundantly in close proximity in neurites and growth cones.

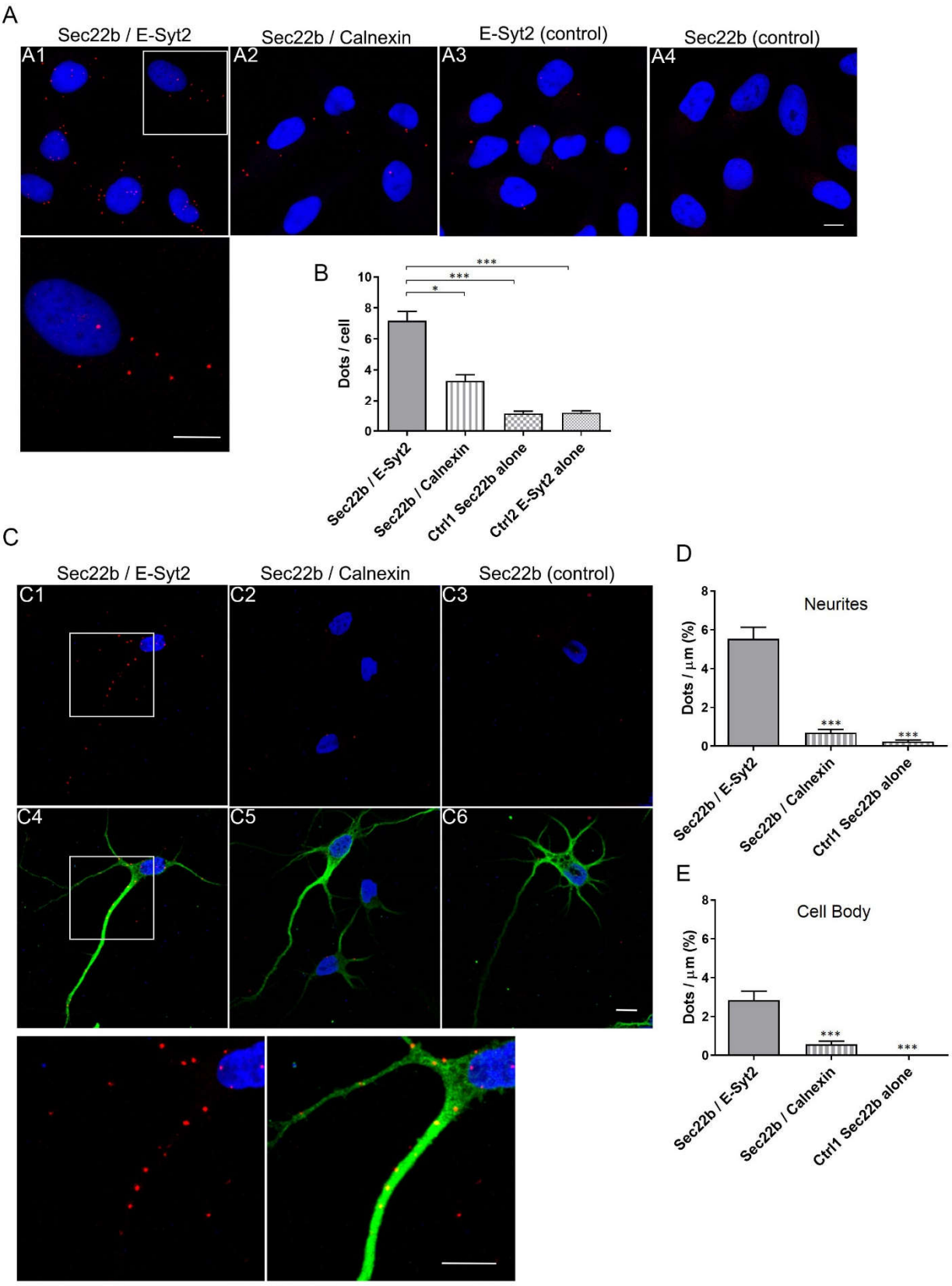

Figure 3. Analysis of E-Syt2 / Sec22b colocalization using super-resolution microscopy

A

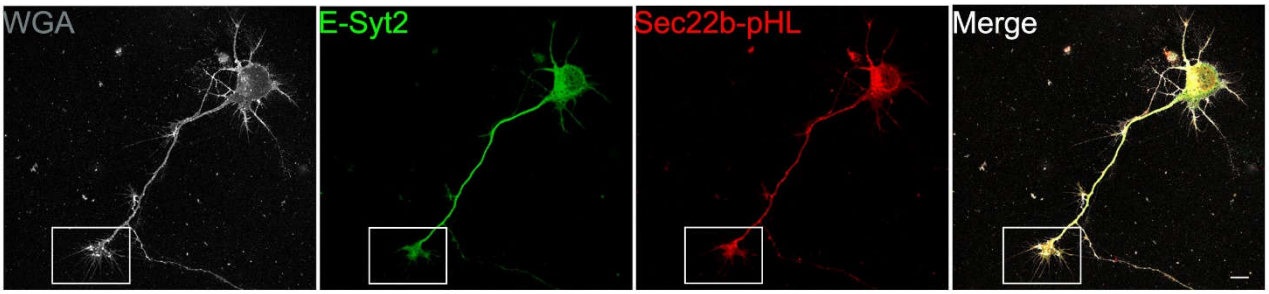

B

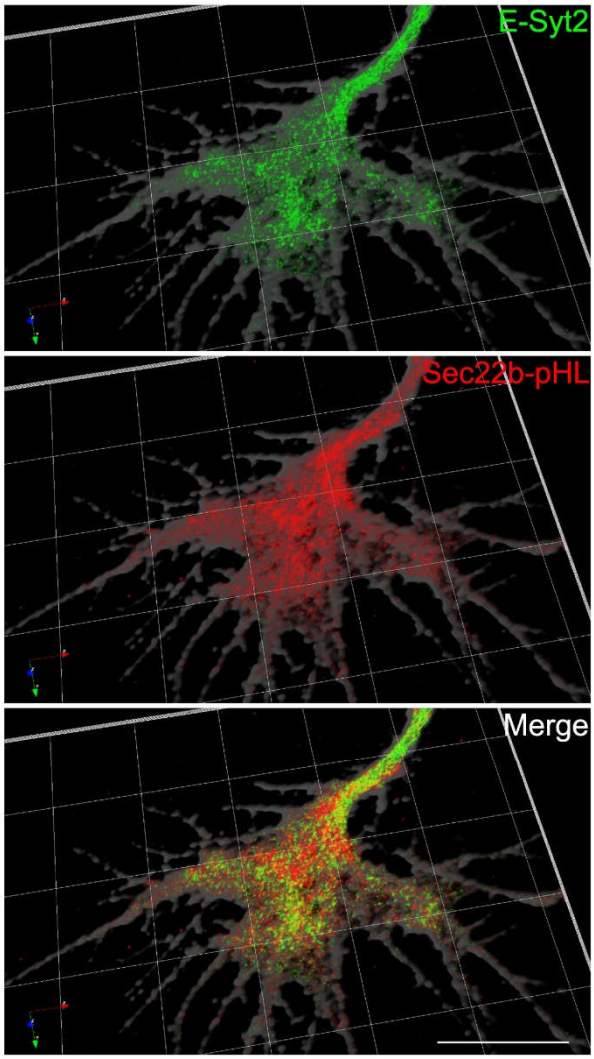

C

E-Syt2 colocalizing with Sec22-pHL (%)	Sec22-pHL colocalizing with E-Syt2 (%)	E-Syt2 / Sec22b-pHL distance (nm)
20.5357 ± 9.1501	34.9916 ± 8.8064	84.3329 ± 9.6427

Average measurements for four growth cones.
Total E-Syt2 dots: 13784
Total Sec22b dots: 6307

D

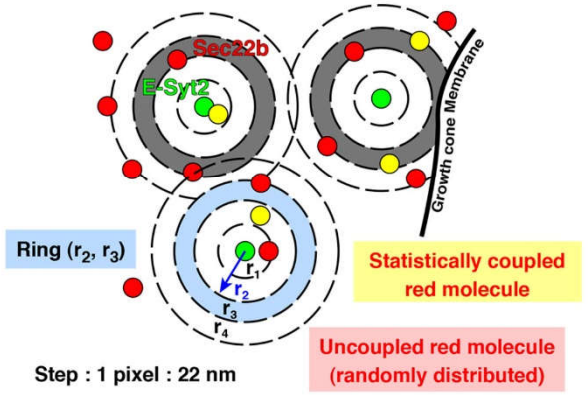

E

		r max (r = 22 nm)	E-Syt2 colocalizing with Sec22-pHL (%)	Sec22-pHL colocalizing with E-Syt2 (%)	Distance (nm)	Log_10 (p value)
Growth cone n°1	n° Syt2 dots: 3517 n°Sec22b dots: 1110	1	0.2024	0.3373	14.3029	-1.0547
		2	2.1503	3.5835	29.5776	-7.9500
		3	6.9820	11.4671	46.0646	-9.4662
		4	14.7483	23.1029	61.7353	-9.4662
		5	23.8806	34.8651	76.4124	-9.4662
		6	36.9087	49.7049	94.2992	-9.4662
		7	47.6600	59.7386	108.7222	-9.4662
		8	47.6600	59.7386	108.7222	-9.4662
		9	47.6600	59.7386	108.7222	-9.4662
Growth cone n°2	n° Syt2 dots: 3953 n°Sec22b dots: 2372	1	0.0000	0.0000	> 22 nm	-2.5843
		2	1.2226	3.8739	32.9621	-2.5526
		3	3.6679	11.7117	46.9123	-24.4212
		4	8.3310	25.7658	63.3365	-24.4212
		5	8.3310	25.7658	63.3365	-24.4212
		6	8.3310	25.7658	63.3365	-24.4212
		7	8.3310	25.7658	63.3365	-24.4212
		8	8.3310	25.7658	63.3365	-24.4212
		9	8.3310	25.7658	63.3365	-24.4212
Growth cone n°3	n° Syt2 dots: 1711 n°Sec22b dots: 948	1	0.0000	0.0000	> 22 nm	-1.9932
		2	1.1105	2.0042	31.1446	-3.6765
		3	2.7469	4.9578	43.7017	-5.6271
		4	6.1368	10.8650	61.3209	-5.6271
		5	6.1368	10.8650	61.3209	-5.6271
		6	10.9877	19.7257	88.7335	-5.6271
		7	10.9877	19.7257	88.7335	-5.6271
		8	10.9877	19.7257	88.7335	-5.6271
		9	10.9877	19.7257	88.7335	-5.6271
Growth cone n°4	n° Syt2 dots: 4603 n°Sec22b dots: 1877	1	0.2607	0.6393	13.8607	-14.8450
		2	1.5859	3.8892	29.8154	-14.8450
		3	4.7795	11.7208	46.0161	-14.8450
		4	9.2766	21.6303	60.6486	-14.8450
		5	15.1640	34.7363	76.5395	-14.8450
		6	15.1640	34.7363	76.5395	-14.8450
		7	15.1640	34.7363	76.5395	-14.8450
		8	15.1640	34.7363	76.5395	-14.8450
		9	15.1640	34.7363	76.5395	-14.8450

F

E-Syt2 / Sec22b-pHL distance to the membrane (nm)	43.1820 ± 1.2665	Average measurements for two growth cones. Total E-Syt2 dots: 7470 Total Sec22b dots: 3482

Figure 4. E-Syts favor the occurrence of Sec22b-Stx complexes.

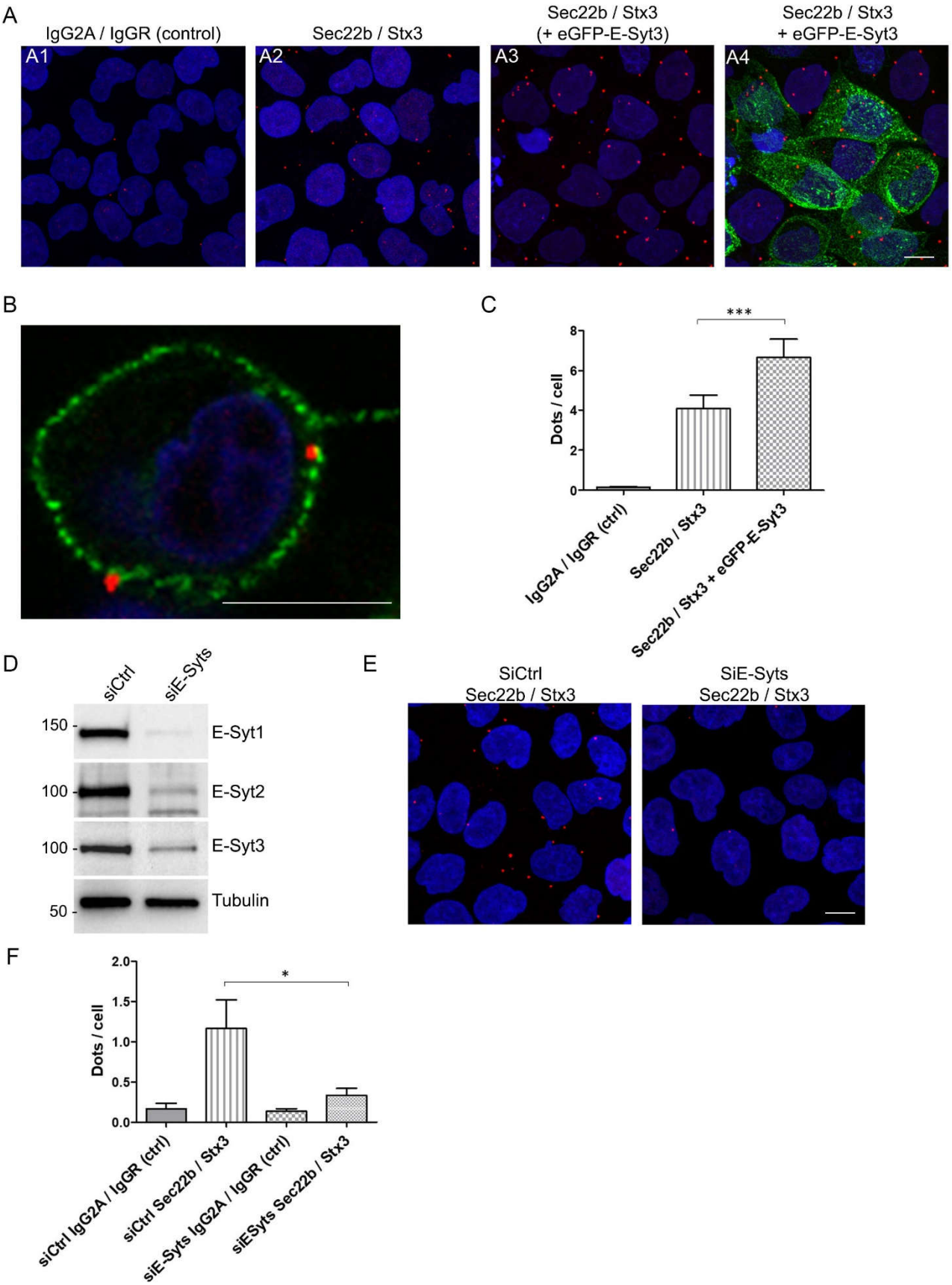

Figure 5. E-Syts overexpression promotes filipodia formation and ramification in developing neurons

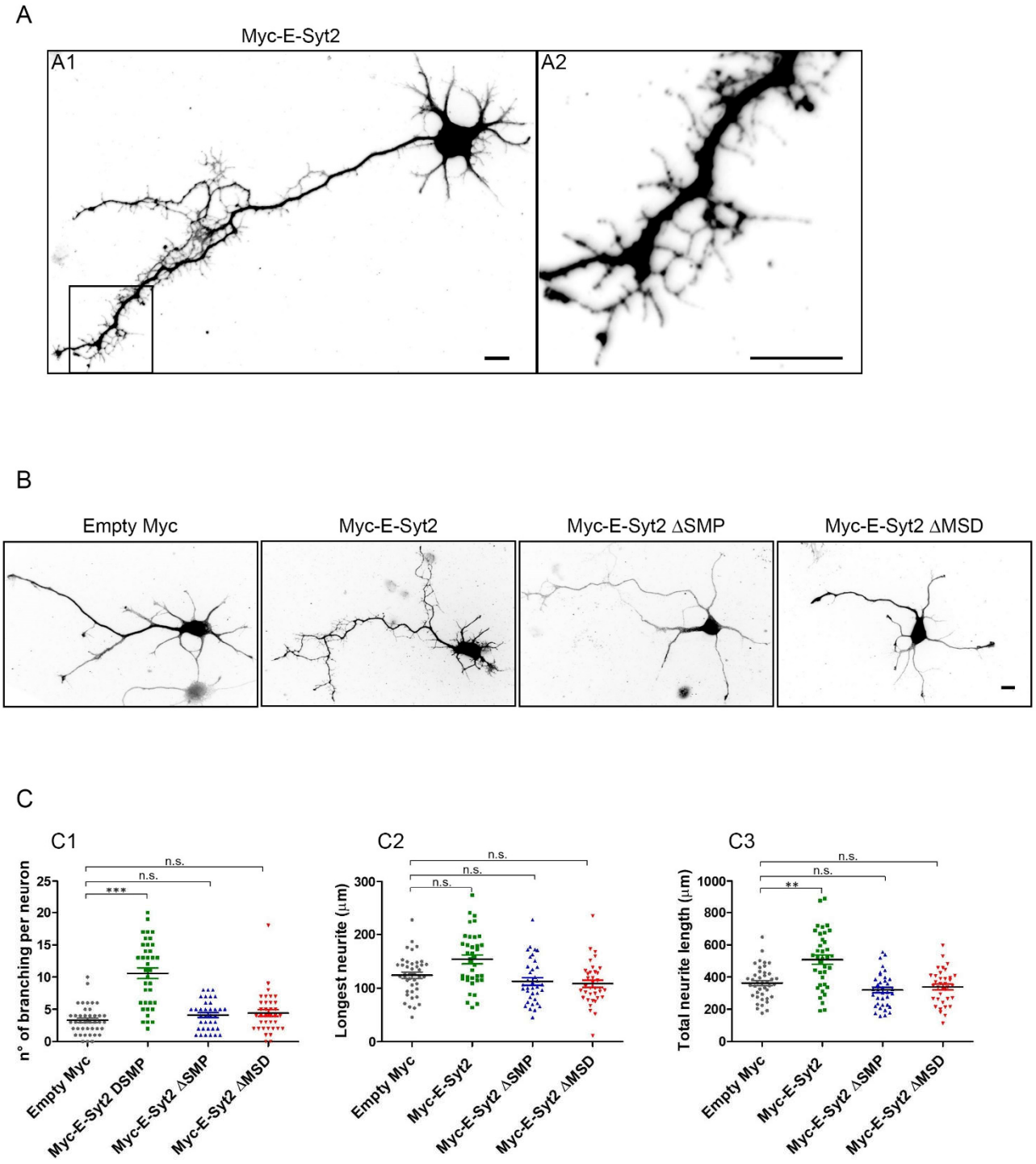

Figure 6. E-Syts overexpression promotes membrane growth in HeLa cells

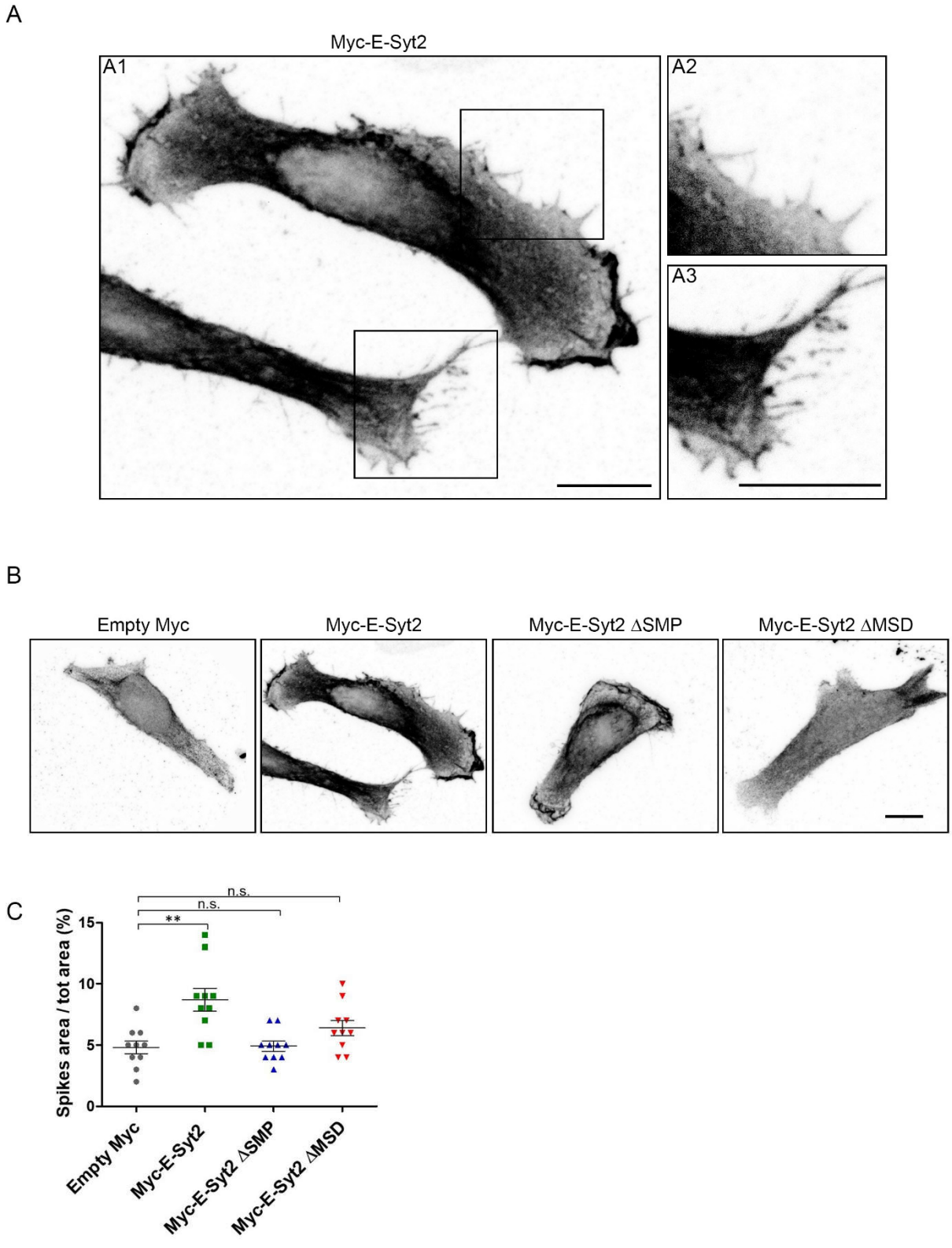

Figure 7. E-Syts-mediated morphogenetic effect depends on Stx1

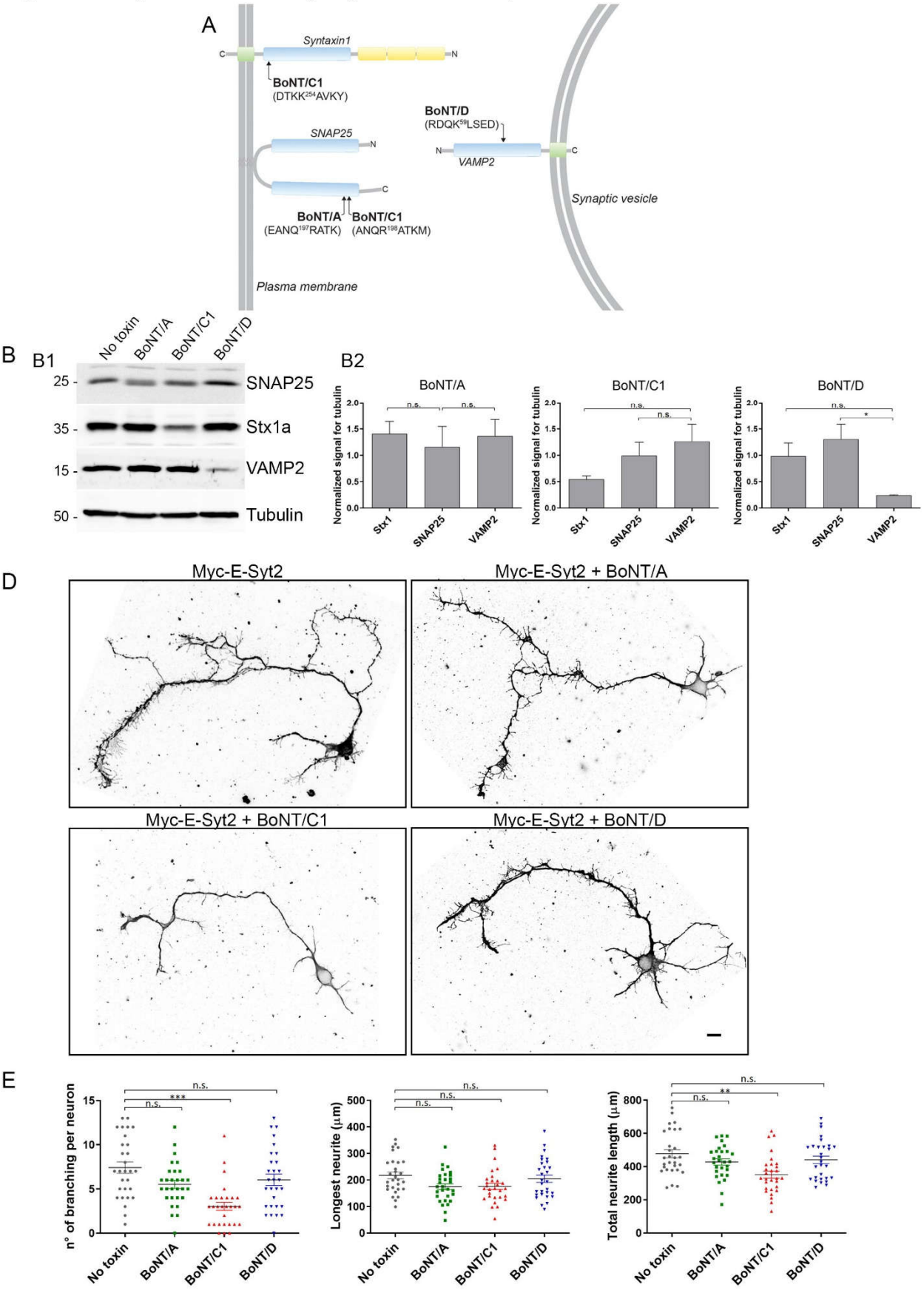

Figure 8. E-Syts-mediated morphogenetic effects depend on the close apposition of ER to PM mediated by Sec22b-Stx1 complexes

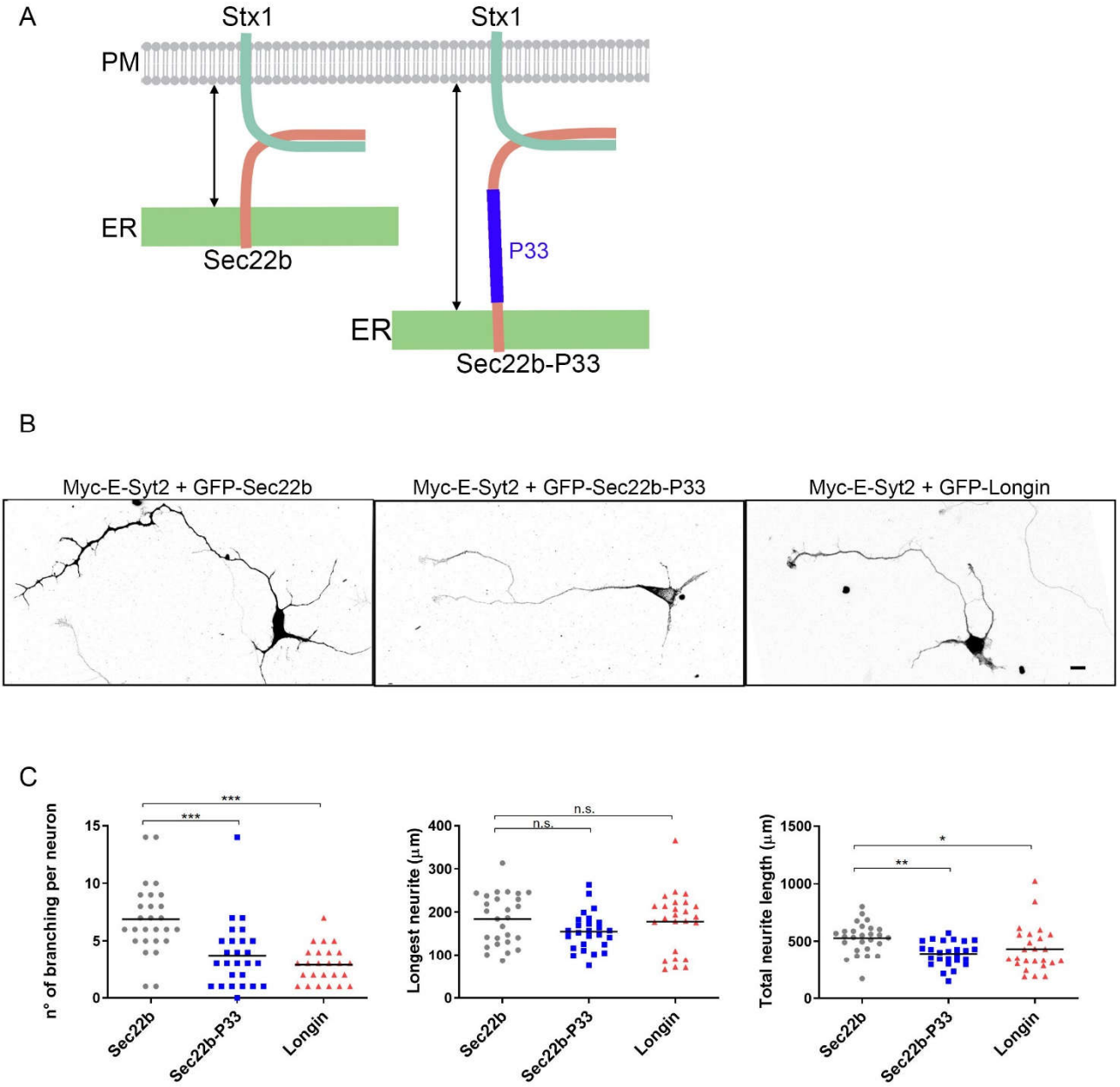

Figure 9. Proposed model for the formation of a SNARE-mediated ER-PM contact site

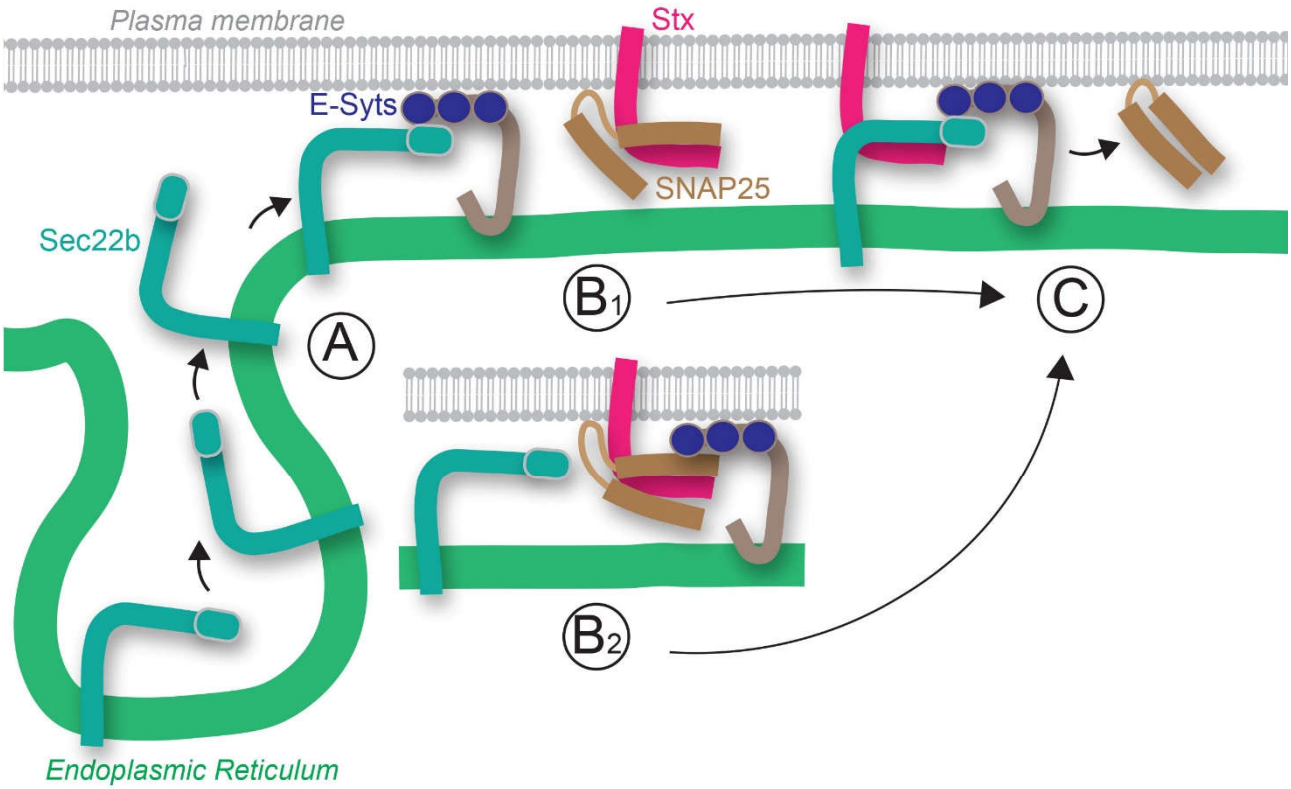

Figure S1. The Sec22bΔLongin mutant reaches the cell surface

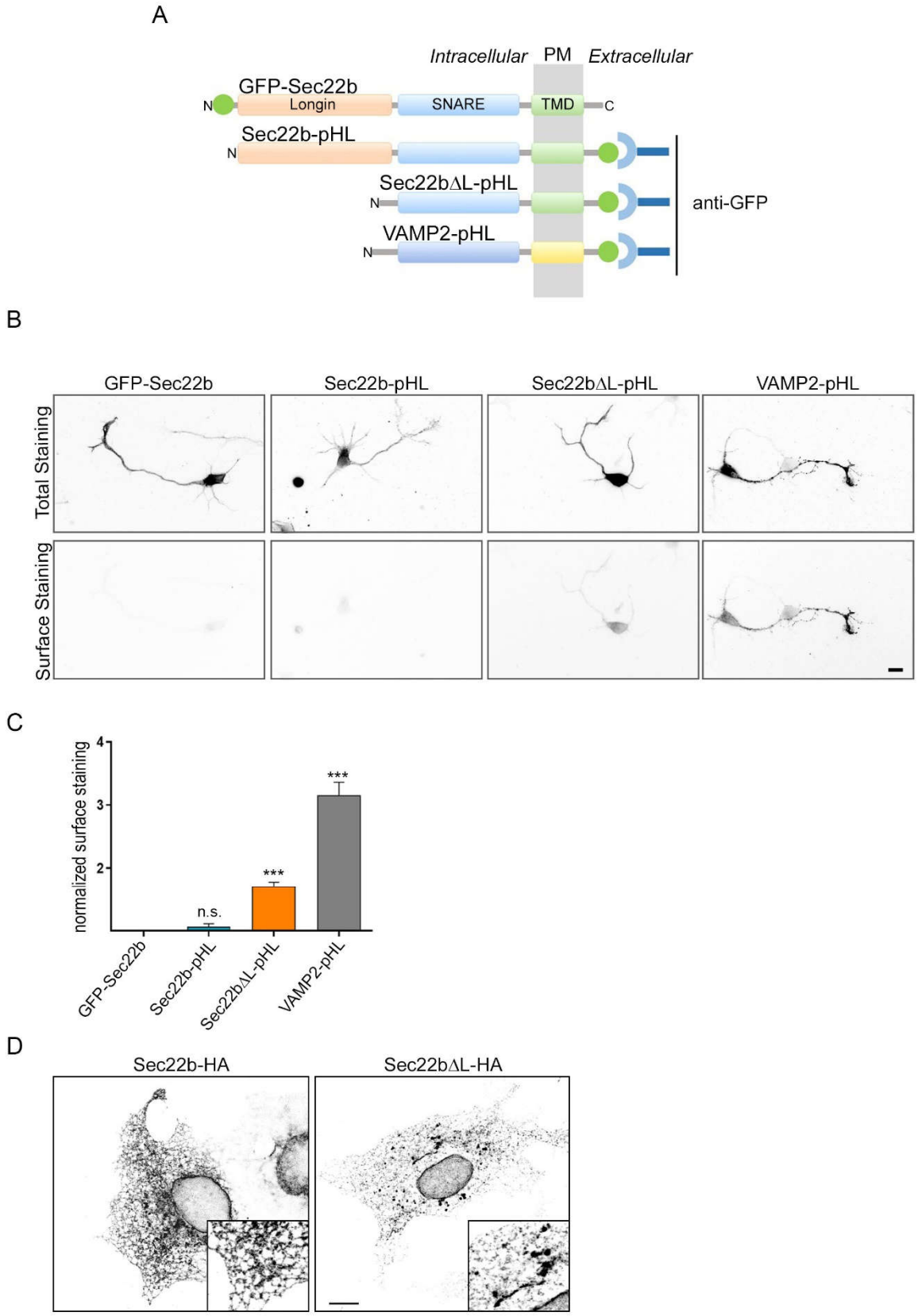

Bibliography

Alberts P, Rudge R, Hinners I, Muzerelle A, Martinez-Arca S, et al. 2003. Cross talk between tetanus neurotoxin-insensitive vesicle-associated membrane protein-mediated transport and L1-mediated adhesion. Mol. Biol. Cell. 14(10):4207–4220

Bennett MK, García-Arrarás JE, Elferink LA, Peterson K, Fleming AM, et al. 1993. The syntaxin family of vesicular transport receptors. Cell. 74(5):863–873

Binz T. 2013. Clostridial neurotoxin light chains: devices for SNARE cleavage mediated blockade of neurotransmission. Curr. Top. Microbiol. Immunol. 364:139–157

Binz T, Sikorra S, Mahrhold S. 2010. Clostridial neurotoxins: mechanism of SNARE cleavage and outlook on potential substrate specificity reengineering. Toxins (Basel). 2(4):665–682

Burri L, Varlamov O, Doege CA, Hofmann K, Beilharz T, et al. 2003. A SNARE required for retrograde transport to the endoplasmic reticulum. Proc. Natl. Acad. Sci. USA. 100(17):9873–9877

Danglot L, Zylbersztejn K, Petkovic M, Gauberti M, Meziane H, et al. 2012. Absence of TI-VAMP/Vamp7 leads to increased anxiety in mice. J. Neurosci. 32(6):1962–1968

Dotti CG, Sullivan CA, Banker GA. 1988. The establishment of polarity by hippocampal neurons in culture. J. Neurosci. 8(4):1454–1468

Fasshauer D, Margittai M. 2004. A transient N-terminal interaction of SNAP-25 and syntaxin nucleates SNARE assembly. J. Biol. Chem. 279(9):7613–7621

Gallo A, Vannier C, Galli T. 2016. Endoplasmic Reticulum-Plasma Membrane Associations:Structures and Functions. Annu. Rev. Cell Dev. Biol. 32:279–301

Giordano F, Saheki Y, Idevall-Hagren O, Colombo SF, Pirruccello M, et al. 2013. PI(4,5)P(2)-dependent and Ca(2+)-regulated ER-PM interactions mediated by the extended synaptotagmins. Cell. 153(7):1494–1509

Grassi D, Plonka FB, Oksdath M, Guil AN, Sosa LJ, Quiroga S. 2015. Selected SNARE proteins are essential for the polarized membrane insertion of igf-1 receptor and the regulation of initial axonal outgrowth in neurons. Cell Discov. 1:15023

Greene LA, Tischler AS. 1976. Establishment of a noradrenergic clonal line of rat adrenal pheochromocytoma cells which respond to nerve growth factor. Proc. Natl. Acad. Sci. USA. 73(7):2424–2428

Gupton SL, Gertler FB. 2010. Integrin signaling switches the cytoskeletal and exocytic machinery that drives neuritogenesis. Dev. Cell. 18(5):725–736

Igarashi M, Kozaki S, Terakawa S, Kawano S, Ide C, Komiya Y. 1996. Growth cone collapse and inhibition of neurite growth by Botulinum neurotoxin C1: a t-SNARE is involved in axonal growth. J. Cell Biol. 134(1):205–215

Jahn R, Scheller RH. 2006. SNAREs--engines for membrane fusion. Nat. Rev. Mol. Cell Biol. 7(9):631–643

Kikuma K, Li X, Kim D, Sutter D, Dickman DK. 2017. Extended synaptotagmin localizes to presynaptic ER and promotes neurotransmission and synaptic growth in drosophila. Genetics. 207(3):993–1006

Lagache T, Grassart A, Dallongeville S, faklaris O, Sauvonnet N et al. 2018. Mapping molecular assemblies with fluorescence microscopy and object-based spatial statistics. Nat. Commun. 9(1):698

Li F, Pincet F, Perez E, Eng WS, Melia TJ, et al. 2007. Energetics and dynamics of SNAREpin folding across lipid bilayers. Nat. Struct. Mol. Biol. 14(10):890–896

Liu Y, Barlowe C. 2002. Analysis of Sec22p in endoplasmic reticulum/Golgi transport reveals cellular redundancy in SNARE protein function. Mol. Biol. Cell. 13(9):3314–3324

Loewen CJR, Roy A, Levine TP. 2003. A conserved ER targeting motif in three families of lipid binding proteins and in Opi1p binds VAP. EMBO J. 22(9):2025–2035

Martinez-Arca S, Coco S, Mainguy G, Schenk U, Alberts P, et al. 2001. A common exocytotic mechanism mediates axonal and dendritic outgrowth. J. Neurosci. 21(11):3830–3838

Min S-W, Chang W-P, Sudhof T. 2007. E-Syts, a family of membranous Ca2+-sensor proteins with multiple C2domains. Proc. Natl. Acad. Sci. USA. 104:3823–28

Osen-Sand A, Staple JK, Naldi E, Schiavo G, Rossetto O, et al. 1996. Common and distinct fusion proteins in axonal growth and transmitter release. J. Comp. Neurol. 367(2):222–234

Petkovic M, Jemaiel A, Daste F, Specht CG, Izeddin I, et al. 2014. The SNARE Sec22b has a non-fusogenic function in plasma membrane expansion. Nat. Cell Biol. 16(5):434–444

Pfenninger KH. 2009. Plasma membrane expansion: a neuron's Herculean task. Nat. Rev. Neurosci. 10(4):251–261

Racchetti G, Lorusso A, Schulte C, Gavello D, Carabelli V, et al. 2010. Rapid neurite outgrowth in neurosecretory cells and neurons is sustained by the exocytosis of a cytoplasmic organelle, the enlargeosome. J. Cell Sci. 123(Pt 2):165–170

Reinisch KM, De Camilli P. 2016. SMP-domain proteins at membrane contact sites: Structure and function. Biochim. Biophys. Acta. 1861(8 Pt B):924–927

Saheki Y, Bian X, Schauder CM, Sawaki Y, Surma MA, et al. 2016. Control of plasma membrane lipid homeostasis by the extended synaptotagmins. Nat. Cell Biol. 18(5):504–515

Schauder CM, Wu X, Saheki Y, Narayanaswamy P, Torta F, et al. 2014. Structure of a lipid-bound extended synaptotagmin indicates a role in lipid transfer. Nature. 510(7506):552–555

Schoch S, Deák F, Königstorfer A, Mozhayeva M, Sara Y, et al. 2001. SNARE function analyzed in synaptobrevin/VAMP knockout mice. Science. 294(5544):1117–1122

Schulte C, Racchetti G, D'Alessandro R, Meldolesi J. 2010. A new form of neurite outgrowth sustained by the exocytosis of enlargeosomes expressed under the control of REST. Traffic. 11(10):1304–1314

Sclip A, Bacaj T, Giam LR, Südhof TC. 2016. Extended Synaptotagmin (ESyt) Triple Knock-Out Mice Are Viable and Fertile without Obvious Endoplasmic Reticulum Dysfunction. PLoS One. 11(6):e0158295

Sikorra S, Henke T, Galli T, Binz T. 2008. Substrate recognition mechanism of VAMP/synaptobrevin-cleaving clostridial neurotoxins. J. Biol. Chem. 283(30):21145–21152

Südhof TC, Rothman JE. 2009. Membrane fusion: grappling with SNARE and SM proteins. Science. 323(5913):474–477

Weir ML, Xie H, Klip A, Trimble WS. 2001. VAP-A binds promiscuously to both v- and tSNAREs. Biochem. Biophys. Res. Commun. 286(3):616–621

Weninger K, Bowen ME, Choi UB, Chu S, Brunger AT. 2008. Accessory proteins stabilize the acceptor complex for synaptobrevin, the 1:1 syntaxin/SNAP-25 complex. Structure. 16(2):308–320

Wojnacki J, Galli T. 2016. Membrane traffic during axon development. Dev. Neurobiol. 76(11):1185–1200

Yu H, Liu Y, Gulbranson DR, Paine A, Rathore SS, Shen J. 2016. Extended synaptotagmins are Ca2+-dependent lipid transfer proteins at membrane contact sites. Proc. Natl. Acad. Sci. USA. 113(16):4362–4367

Zorman S, Rebane AA, Ma L, Yang G, Molski MA, et al. 2014. Common intermediates and kinetics, but different energetics, in the assembly of SNARE proteins. Elife. 3:e03348

Chapter 4

APPENDIX A: Setting up tools for *in vitro* experiments

The fusogenic activity of Sec22b has been observed *in vitro* using FRET-based liposome fusion assays when ER-like liposomes bearing Sec22b underwent fusion with PM-like liposomes containing Stx1/SNAP-25. In contrast, no fusion was measured with liposomes containing only Stx1 (Petkovic et al. 2014). These evidences led us to hypothesize that the default status of Sec22b and Stx1 would be to form canonical SNARE complexes only in the presence of SNAP-25 or SNAP-like molecules. The results presented so far suggest that the Sec22b-Stx1 SNARE complex at ER-PM contact sites is not engaged in a classical fusogenic assembly because of the lack of SNAP-like partners. Instead, our results rather favor an interaction with LTPs belonging to the family of the ER-resident E-Syts.

One of the goals of my PhD project was therefore to address the question of the hierarchy of the assembly of Sec22b-containing complexes in order to shed light on the mechanism whereby Sec22b and Stx1 at ER-PM contacts could generate a non-fusogenic complex lacking SNAP25-like partners.

We have designed a set of *in vitro* assays using recombinant purified proteins. Such assays give access to competition and displacement methods delineating causal relationships in complex assembly. The rational is toimmobilize purified Stx1 onto a solid matrix and measure the binding and/or retention of various sequences and amounts of either SNAP25, Sec22b (or VAMP2 as control) and E-Syt2 (see paragraph A5). A displacement of SNAP25 from a pre-formed ternary complex (containing Sec22b and Stx1) upon E-Syt2 exposure should be accompanied by the formation of a putative non-fusogenic Sec22b-Stx1-E-Syt2 complex. Such result would be consistent with an apparent competition for binding to Stx1 upon exposure to the three free Sec22b, SNAP25, E-Syt2 proteins (Fig. A1). In mirror experiments, Sec22b would be immobilized onto the solid matrix. A prerequisite to perform all these possible combinations is to have access to purified proteins carrying different purification tags, i.e. GST, 6xHis, or Intein.

Herein, I will first report on the different methods used to purify the proteins dedicated to the planned assays and then present preliminary experiments.

A long-term perspective for this study is to perform *in vitro* lipid transfer assays aimed at studying the transfer of lipids mediated by purified E-Syts between liposomes bearing Sec22b and Stx1. For this purpose, we will again use the purified proteins described below.

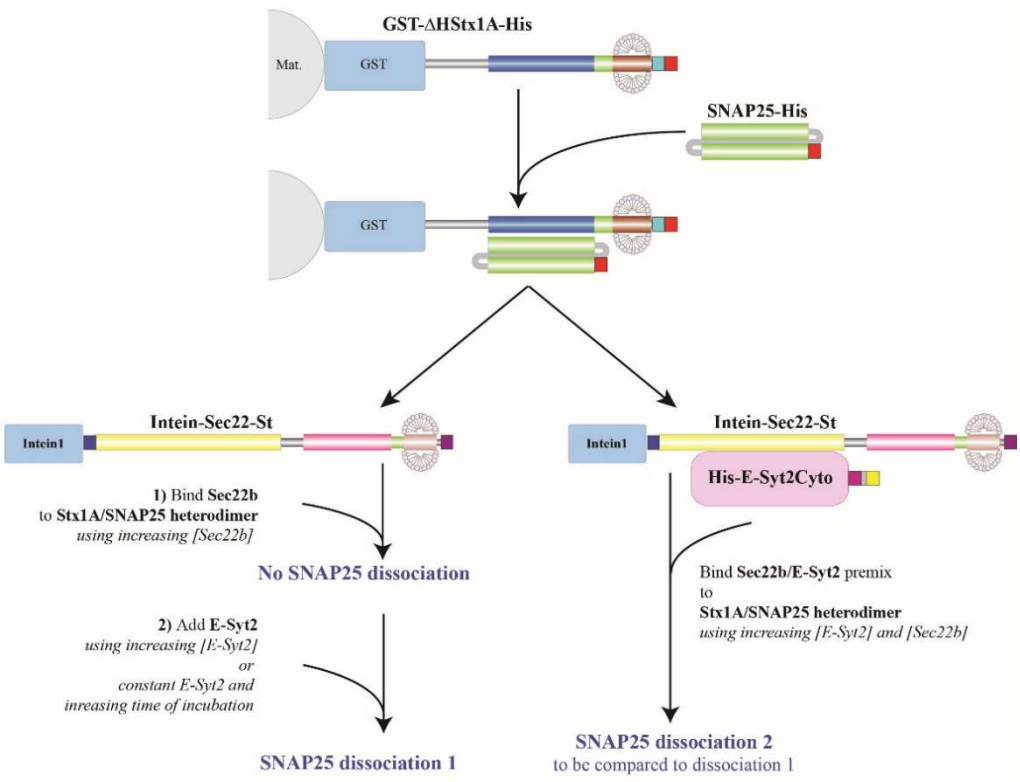

Figure A1. Example of *in vitro* displacement experiments. Immobilized Stx1 will be pre-incubated with soluble SNAP25. This pre-mix will then be sequentially incubated with Sec22b and E-Syt2 (left) or with a Sec22b-E-Syt2 pre-mix. SNAP25 dissociation from Stx1 will be measured by chemiluminescence after SDS-PAGE and Western Blotting. Note that each protein carries distinct purification tags (His, GST or Intein).

A1. Purification of 6xHis-tagged proteins

Sec22b, Stx1ΔHabc, SNAP25 and E-Syt2 carrying a C- or N-terminal 6xHistidine-tag (Fig. A2a) have been purified by Immobilized Metal Affinity Chromatography using Ni-NTA (nickel-nitrilotriacetic acid)-coupled sepharose, following standard procedures (Chapman et al. 1994, Kweon et al. 2003, McMahon and Südhof 1995, Walch Solimena et al. 1995). Briefly, cDNAs of interest were sub-cloned into pET28a vector and 6xHis-fusion proteins were expressed in *E. coli* Bl21(DE)pLysS cells, in the presence of 1 mM isopropyl-P-D-thiogalactopyranoside (IPTG). Purification was routinely obtained using a 50mM to 300mM imidazole gradient. Eluted proteins were stored at -80°C. Homogeneity was estimated after SDS-PAGE and Coomassie Blue staining (Fig. A2b). Note that the pattern displayed by SNAREs and E-Syt2 is characterized by several bands, in addition to the proteins of interest (red rectangles). Such patterns are common in protocols in which short purification tags, such as 6xHis, are used for SNAREs purification. . Monomeric SNAREs, being highly unstructured proteins, very likely these contaminants are *E. coli*-derived factors, such as chaperonins, which bind to SNAREs to help maintaining a native protein conformation (Bolanos-Garcias and Davies, 2006). The material banding

at the size of the corresponding the expected proteins was therefore submitted to mass spectrometry (MALDI) in order to confirm their identity.

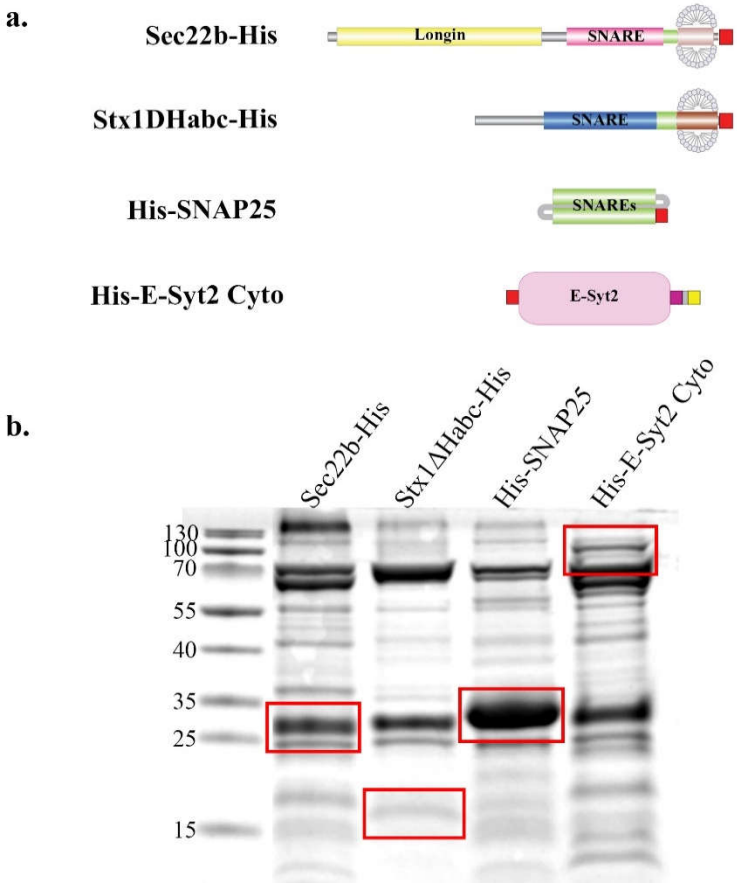

Figure A2. Affinity chromatography of 6xHis-fusion proteins. (A) Domain architecture of the 6xHis-tagged proteins used in this study. The 6xHis tag, represented in red, is located at the C terminus of Sec22b and Stx1ΔHabc and at the N terminus of SNAP25 and E-Syt2 Cyto. (B) Coomassie Blue staining of eluate material after SDS-PAGE. The red rectangles indicate the bands corresponding to the proteins of interest, the identity of which was confirmed by mass spectrometry (MALDI).

A2. Purification of GST-tagged proteins

For the production of glutathione S-transferase (GST)-fusion proteins, Sec22b, Stx1ΔHabc and VAMP2 cDNAs (Fig. A3a) were sub-cloned into pGEX-6p vector. Procedures for expression and induction were similar to those described for 6xHis-tagged proteins. Protein purification was achieved by affinity chromatography on immobilized glutathione resin and elution with 20mM of reduced L-Glutathione (GSH), according to procedures mentioned above. When needed, GST was cleaved from the N terminus of purified proteins with PreScission protease (3U/100 µg of fusion protein). Aliquots were subjected to SDS-PAGE and visualized by Coomassie Blue staining (Fig. A3 b-d). In spite of an apparent easy purification of GST-SNARE chimera, we routinely encountered difficulties in using the PreScission

protease cleavage with an efficiency allowing pure and concentrated preparations of active proteins. These difficulties were exacerbated in the case of Sec22b, almost precluding the use of GST-Sec22b chimera for our purposes.

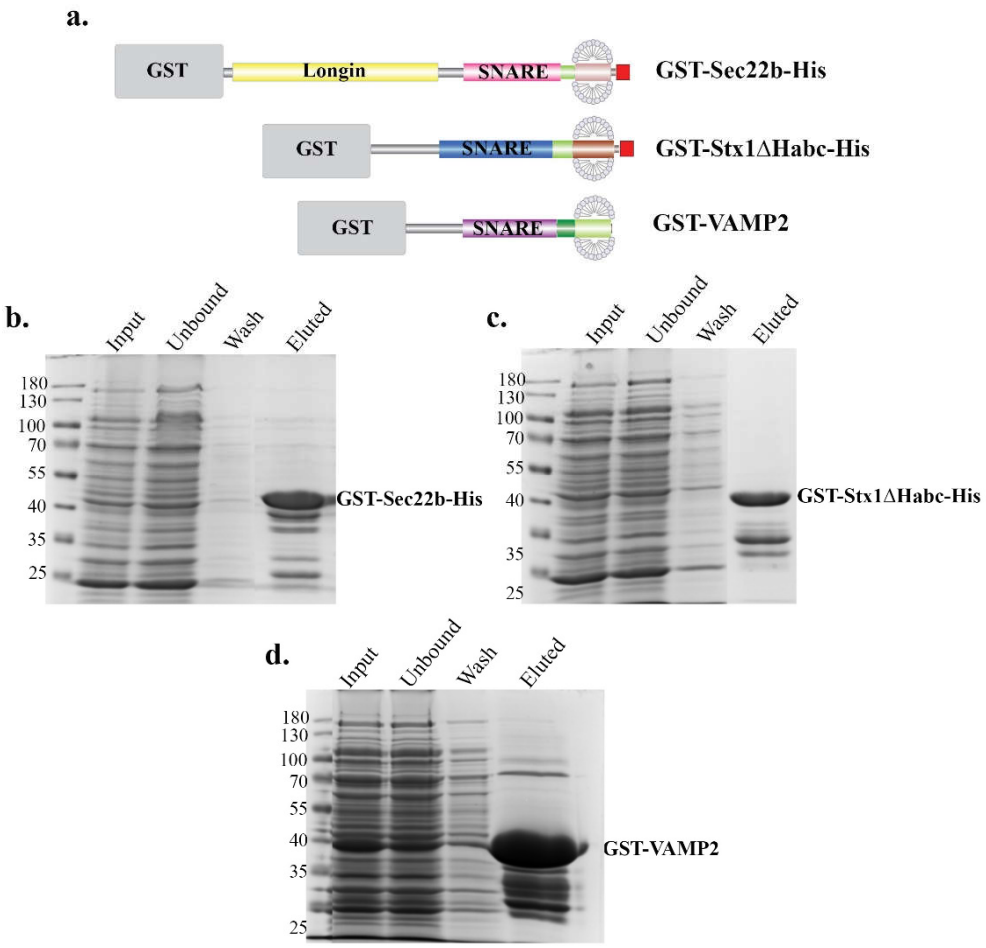

Figure A3. Purification of GST-fusion proteins. (A) Domain architecture of the GST-fusion proteins purified in this study. (B) SDS-PAGE followed by Coomassie Blue staining of purified GST-Sec22b-His (B), GST-Stx1ΔHabc-His (C) and GST-VAMP2 (D) proteins. Note the limited presence of degradation products.

A3. Identification of SDS-resistant SNARE complexes

The association of SNARE domains in a four-helix bundle is known to give rise to a SDS-resistant complex that can easily be identified by SDS-PAGE due to its 1:1:1 stoichiometry. This property was exploited to test whether the purified 6xHis- and GST-fusion proteins were functional and able to assemble in a SDS-resistant SNARE complex (Hayashi et al. 1994). An *in vitro* assay for complex reconstitution in solution was first set up with either His-tagged (Fig. A4) or GST-tagged (Fig. A5) SNAREs equimolar amounts of Sec22b (or VAMP2), Stx1ΔHabc and His-SNAP25 (4 μM final) were incubated at 37°C for the indicated times. Then, samples of the protein mixtures were supplemented with Laemmli sample buffer and either kept at room temperature (R.T.) or heated at 95°C for 5 min.

The samples were processed for SDS-PAGE and Western Blotting. The formation of a SDS-resistant complex was demonstrated by the presence of high MW bands corresponding to assembled SNARE complex in non-heated samples only (Fig. A4 and Fig. A5). There are two limitations in using this test. First, the identification of a specific protein in a blotted resistant complex (transferred as quasi-native protein) relies on the accessibility of antigenic sites targeted by the used antibodies. Therefore, this assay is not adapted to characterize the exact composition of the SDS-resistant entities. Second, complexes formed with SNARE proteins can exist that will not be detected with this approach because of an SDS-sensitive association.

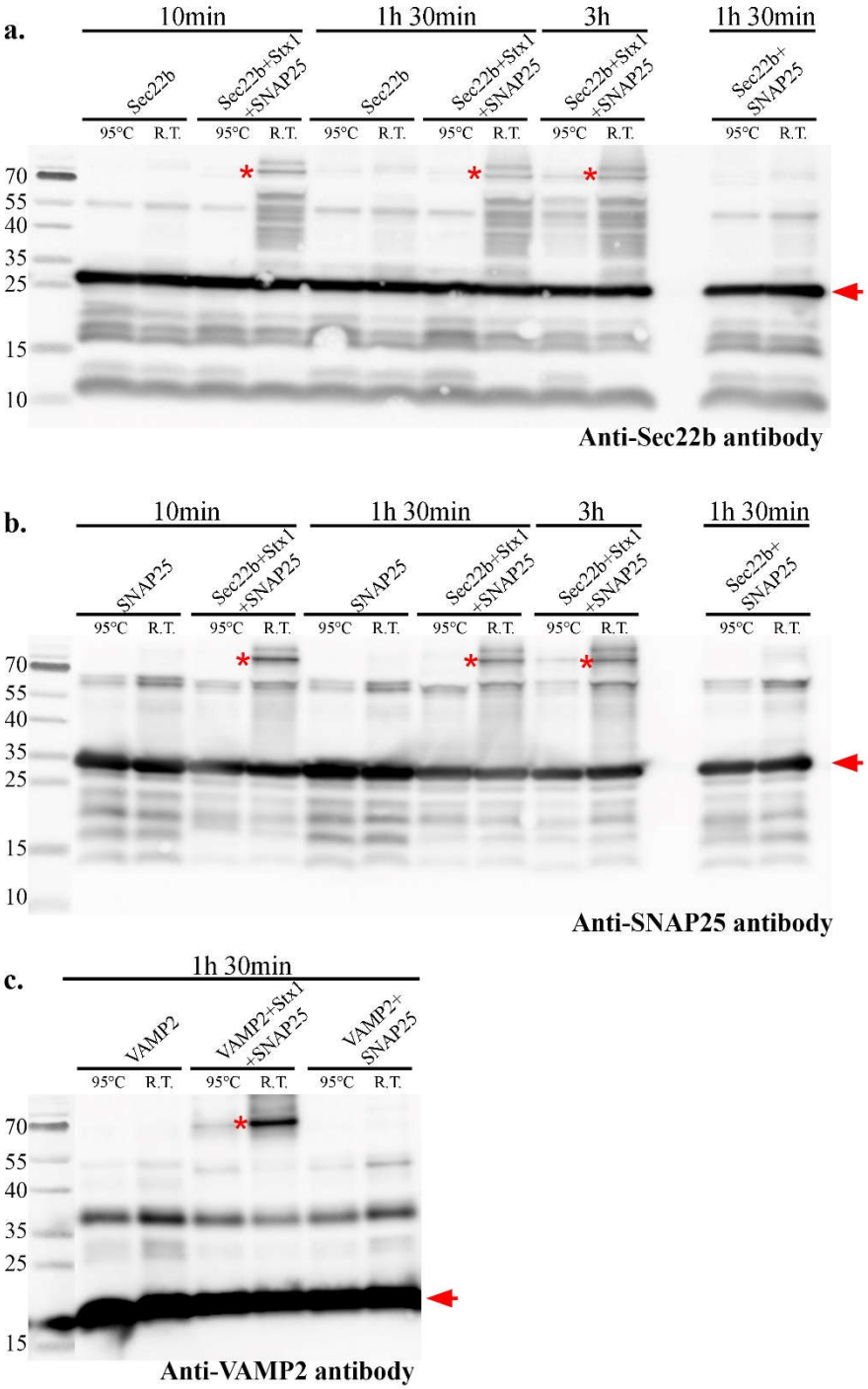

Figure A4. ***In vitro*** **SNARE complex reconstitution with 6xHis-tagged SNARE proteins**. (A, B) Sec22b-based complexes. Equimolar amounts of Sec22b (or VAMP2), Stx1ΔHabc and His-SNAP25 (4 mM final each) were combined as indicated and incubated for 10 min, 1h 30 min or 3h at 37°C. Samples were then supplemented with Laemmli sample buffer and heated at 95 °C for 5 min or kept at room temperature (R.T.) before being processed for SDS-PAGE and Western Blotting (A) Sec22b immunodetection. Sec22b-His monomer is visible at m ~25kDa (arrowhead). (B) SNAP25 immunodetection. His-SNAP25 monomer is visible at m ~35kDa (arrowhead). The asterisk indicates the high molecular weight material (m ~ 70 kDa) corresponding to a SDS-resistant SNARE complex absent from heated samples and reactive toward anti-Sec22b and anti-SNAP25 antibodies. (C)

VAMP2-based complexes. VAMP2, Stx1ΔHabc and SNAP25 combinations processed as in A and B after a 90-min incubation, with VAMP2 immunodetection. The asterisk indicates the high molecular material (m ~ 70 kDa) corresponding to a SDS-resistant SNARE complex. VAMP2 monomer is visible at m ~18 kDa (arrowhead). Note that in (A-C) the complex (*) was obtained only in the presence of the three SNAREs.

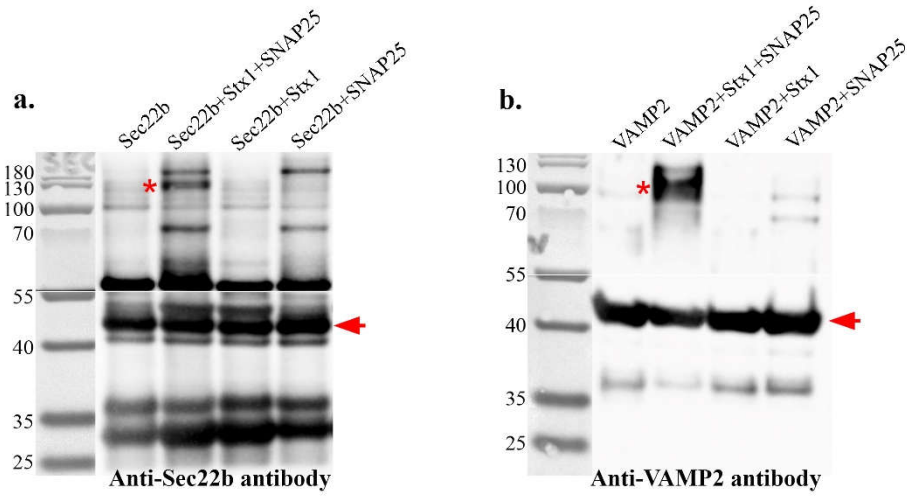

Figure A5. *In vitro* SNARE complex reconstitution with GST-fused SNARE proteins. Various combinations of GST-Sec22b, GST-Stx1ΔHabc and His-SNAP25were incubated at 37°C for 90 min. Samples were kept at room temperature before being processed for Western Blotting as in Figure 4. (A) Sec22b-based complex immunodetected using an anti-Sec22b antibody. (B) VAMP2-based complex immunodetected using an anti- VAMP2 antibody. Asterisks indicate the high molecular material corresponding to a SDS-resistant Sec22b-based complex (m ~ 130 kDa, A) and of VAMP2 -based complex (m ~ 100 kDa, B). Monomers of GST-Sec22b GST-VAMP2 are visible at m ~ 50kDa and at m ~ 40kDa respectively (arrowheads). SDS resistant complexes having the expected mass were obtained only in the presence of the three SNAREs.

A4. Purification of Intein-tagged proteins

The purification and cleavage problems occurring with GST-chimera, as mentioned above (paragraph A2), prompted us to test an Intein-driven production of the SNARE proteins. This was expected to provide an additional purification tag along with the possibility to use the proteins either in the chimeric or in the cleaved form. A third set of recombinant proteins were therefore constructed (See Fig. A7a) and dedicated for solid phase binding assays, i.e. binding assays involving an immobilized SNARE protein as a bait (affinity ligand). They are currently used in displacement and competition approaches aimed at dissecting causal relationships in SNARE complex assembly in the presence of E-Syts. To do so, Intein-SNAREs chimera were designed according to the IMPACT engineering and purification strategy (Wood et al. 2005). Inteins (INTervening protEINS) are internal protein elements that self-excise from their host protein and catalyse ligation of the flanking sequences (exteins) with a peptide

bond. They are found in eubacteria, archaea, some lower eukaryotes, as well as in viruses and phages. An intein is a genetic element similar to an intron and this self-excision process is called protein splicing, by analogy to the splicing of RNA introns from pre-mRNA (Perler et al. 1994). IMPACT uses the inducible autoprocessing activity of an engineered intein-target protein chimera. Since the intein moiety harbors a chitin binding domain (CBD) allowing binding to chitin resin, the target protein is spontaneously eluted after cleavage as a pure protein with no additional sequence. Inteins can be fused either at the C or at the N terminus of the protein of interest, and autoprocessing is then triggered in an on-column way respectively under mild reducing conditions (for example with thiols) or by lowering pH and increasing temperature (Fig. A6). The main advantage of this system is that a single column is used to purify and cleave the protein of interest, with no additional step to remove the affinity tag. Furthermore, the self-excision process avoids the use of proteases, reducing time and cost of the experiment.

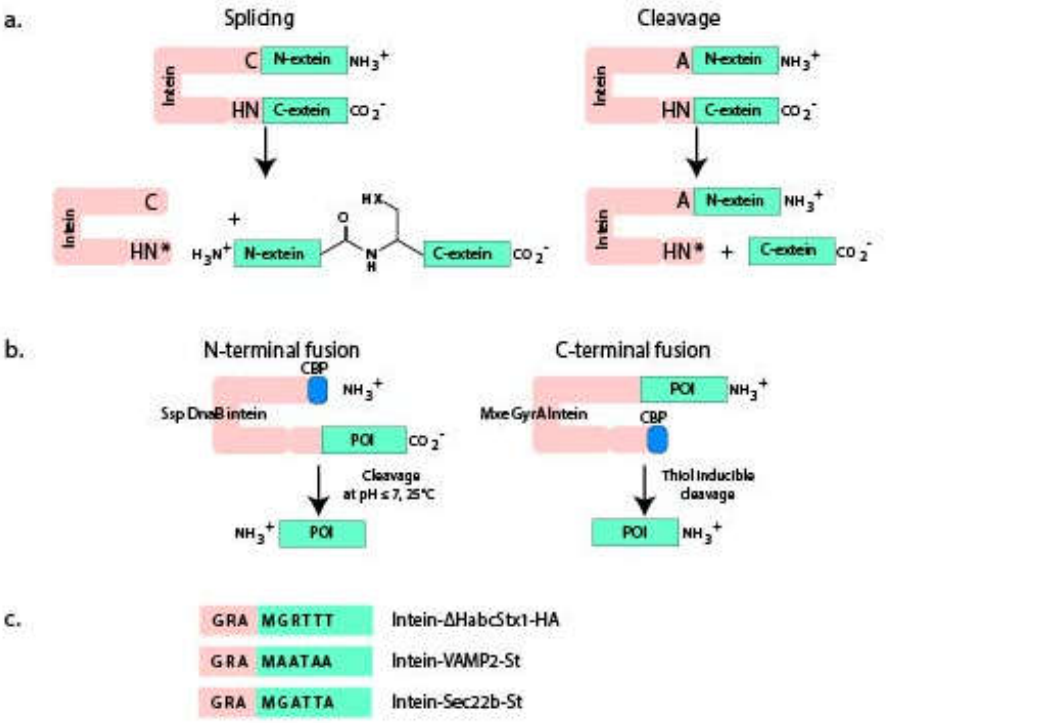

Figure A6. Protein splicing with inteins. (A) Main reactions of autoprocessing involving a simple intein (mini-intein). Left: Splicing. A sequence of reactions involving key aminoacid residues at the intein termini results in intein excision and formation of a peptidic bond fusing the intein-flanking sequences (exteins). Right: Cleavage. Modification of residues at one intein extremity can impose a single cleavage, as examplified with the release of the C-extein after a C1A mutation in the intein. (B) Intein chimera generated from the pTWIN1 expression vector in the IMPACT™ system from New England Biolabs. Using two distinct inteins, two types of chimera can be produced, allowing two type of cleavage triggered by pH, temperature, or reducing factors as shown. The chitin binding peptide (CBP) harbored by the intein is an affinity tag for chromatography on chitin resin. SNARE

proteins of interest (POI) were produced as N-terminal fusion chimera using Ssp DnaB intein. (C) Primary structure of chimera at the intein SNARE junction. N-terminal sequences in Stx1 and VAMP2 are natural, whereas that of Sec22b is was added to improve cleavage efficiency by Ssp DnaB intein.

In our study we sub-cloned Sec22b, Stx1ΔHabc and VAMP2 into the pTWIN1 vector to obtain an N-terminally tagged intein-fusion protein (Fig. A7a). Procedures for expression and induction were similar to those described for 6xHis-tagged proteins. Induced proteins were purified on chitin columns and eluted by incubation at 23-25°C and pH 6.8-6.9, which induces self-cleavage of the chimera. Efficiency of isolation and cleavage as estimated by SDS-PAGE and Western blotting were confirmed for Stx1 and VAMP2 (Fig. A7b). Regarding Intein-Sec22b, a modification of the hinge sequence between intein and Sec22b was required to improve autoprocessing. Unfortunately, in this case release of free Sec22b was accompanied by the generation of several additional anti-Sec22b reactive molecular species. We have chosen to avoid the cleavage step. In a first step, the complete purification/cleavage procedure being unnecessary for the purpose of our study, we followed a protocol of phase partitioning in Triton X-114, as described elsewhere (Bordier, 1981). This allows the separation of hydrophilic proteins (which are recovered exclusively in the aqueous phase), from integral, amphipathic, membrane proteins, which partition in the detergent phase, as illustrated for Intein-Sec22b (Fig. A7c).

-

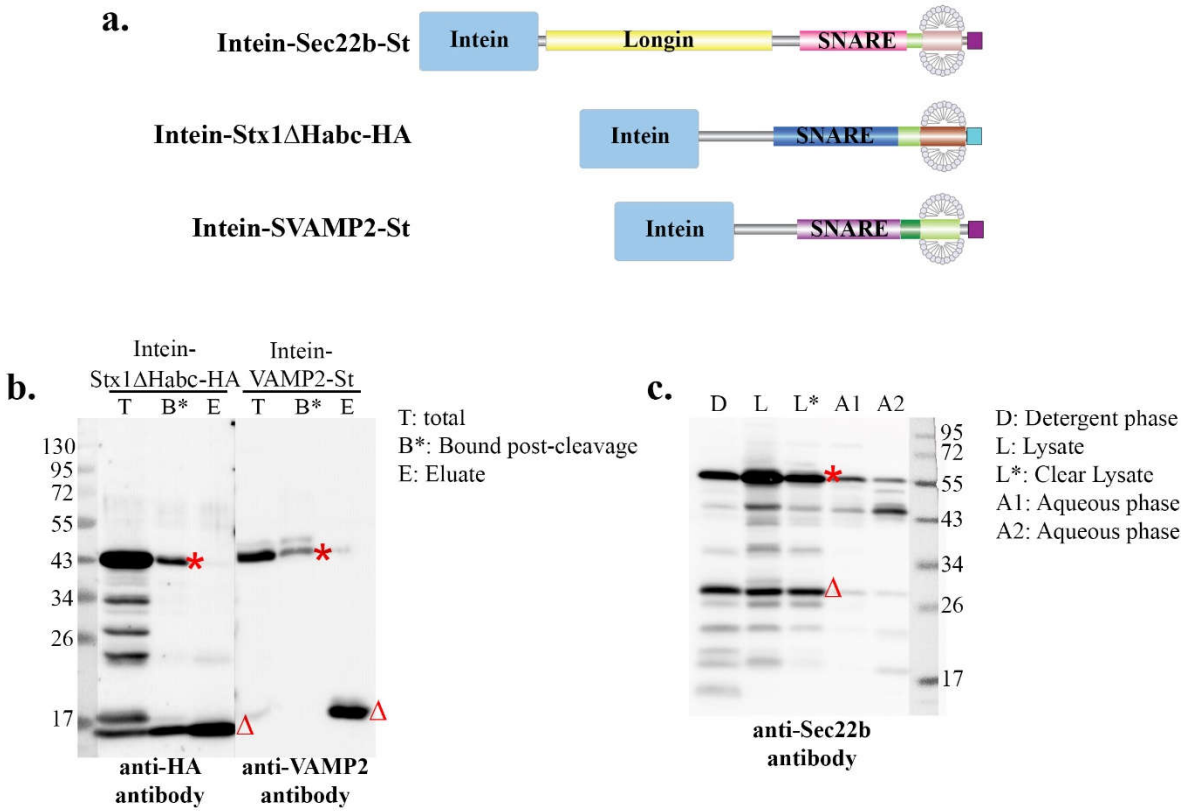

Figure A7. Intein-SNARE fusion proteins used in vitro assays. (A) Diagram of the domain structure of the Intein chimera. SNAREs are N-terminally fused to the intein and harbor an affinity (StrepTag, St reddish) or antigenic (HA, green) tag fused at the transmembrane anchor C-terminus. (B) Autoprocessing of expressed InteinStx1ΔHabc-HA and Intein-VAMP2-St revealed after Western blotting and reaction with anti-HA tag and anti-VAMP2 antibodies, respectively. The prominent chimera band (*) in cell extract (T) gives rise to a soluble extein (Δ) recovered in eluate (E). Note that some cleaved and uncleaved SNARE molecular forms can remain bound to chitin matrix after processing (B*). (C) Partition of expressed Intein-Sec22b. Uncleaved (*) and cleaved (Δ) forms are present in cell (L) and clarified (L*) lysates obtained in Triton X-114 after expression. Aqueous (A) and detergent (D) phases were obtained as described by Bordier (1981) in two rounds giving A1/D1 and A2/D. Autoprocessing was allowed to take place after solubilization of D1 in phosphate buffer at pH 6.8 for 16h at 23°C. Phase D containing Intein-Sec22b (*) and Sec22b (Δ) is to be used *in vitro* assays**.**

A5. Sec22b and SNAP25 binding to immobilized Stx1

A first set of *in vitro* experiments using the above expressed proteins concerned the SNAP25-dependence of Sec22b binding to Stx1 (Fig A8a). Glutathione matrix-bound GST-Stx1ΔHabc, used as bait, was incubated with a mixture of its potential molecular partners. In the experiment reported here,

His-SNAP25 at increasing concentration was present in a ternary mixture with a constant Sec22b:Stx1 ratio (Fig A8b-c) and this was then incubated for 90 min at 4°C. Western blotting analysis of the bound material (Fig A8b-d) confirmed the capability of Stx, SNAP25 and Sec22b to form a complex as shown in Figure A4 (See also Petkovic et al., 2013). Stx-binding of Sec22b was clearly SNAP25-dependent and occurred in an apparently saturable manner (Fig A8c-d), without altering the extent of SNAP25 association to Stx1 (Fig A8b).

These results now constitute a necessary basis to further investigate, as proposed in the introduction of this chapter, the formation of a SNARE complex in the presence of proteins such as E-Syts. As illustrated in Figure A8a, current experiments correspond to studying E-Syts or Sec22b concentration effects on Stx1 interactions in the presence of a quaternary mixture.

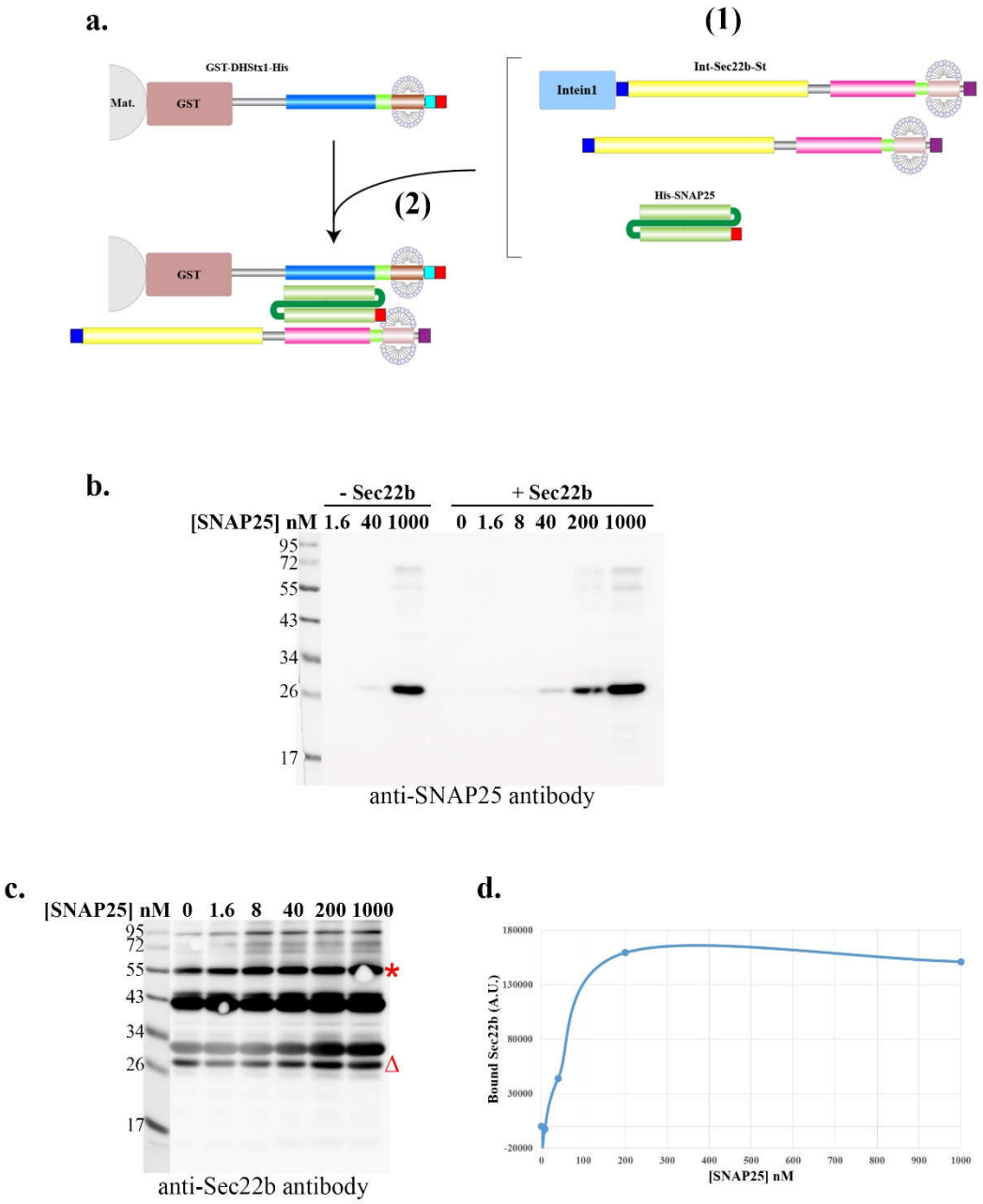

Figure A8. Sec22b binding to Stx1/SNAP25 heterodimers (A) Principle of the solid phase assay e followed in this experience. (1) Mixture His-SNAP25 (increasing concentration) and Sec22b (constant concentrations) obtained after purification (Fig. A2b) and in the lysate detergent phase (Fig. A7c). This mixture was then incubated with constant amount of immobilized GST-Stx1ΔHabc (2). SNAP25 was used at concentration ranging from 0 to 1000 nM as shown, in the presence or absence of Sec22b. Incubation of the proteins was allowed for 90 min at 4°C. After washing of the GST-Stx1ΔHabc matrix, bound proteins were revealed following SDS-PAGE and Western blotting using SNARE specific antibodies. Quantification of ECL signals performed using ImageJ. (B) SNAP25 associated with GST-Stx1ΔHabc matrix after incubation in the absence or presence of Sec22b. Note that the increasing binding of SNAP25 according to its own concentration is not dependent on Sec22b

presence. (C) Sec22b associated with GST-Stx1ΔHabc. SNAP25-dependent binding seems to be observed for both the Intein-Sec22b chimera (*) and the free Sec22b protein (Δ). The origin of reactive additional bands is unknown (compare with Fig. A7c) (D) Binding curve of Sec22b to Stx1 as function of SNAP25 concentration. Only signals obtained for free Sec22b protein (Δ) in (C) were plotted. Under the experimental conditions chosen, half of Sec22b binding could thus be estimated to be reached at 50 nM SNAP25.

Chapter 5

Discussion of the main results of the thesis

During my PhD, I have tried to address the mechanisms whereby the Sec22b-Stx complexes residing at MCSs between ER and PM participate to plasma membrane expansion during cell growth and neuronal development. I have found that these non-fusogenic SNARE complexes interact with LTPs at ER-PM contact sites, which in turn might drive lipid transfer, rather than classical vesicular fusion, to mediate the expansion of membrane required for growth. These results could potentially open new questions regarding the intertwined function of vesicular and non-vesicular routes for membrane growth, as well as how both pathways are regulated not only in physiological conditions, but also in pathologies such as cancer, in which cell growth represents one of the main hallmarks of its pathogenesis.

5.1) LTPs as alternative partners of SNARE complexes at MCSs

In a first set of GFP-trap pull down experiments in neuronal-like PC12 and HeLa cells, we found that Sec22b-Stx interact with E-Syt2 and E-Syt3, members of the ER-resident LTPs Extended-Synaptotagmins (E-Syts). In PC12 cells, the pull down of E-Syt2 by Sec22b was highly reduced after deletion of Sec22b Longin domain (Sec22bΔL mutant), suggesting that this N-terminal module could play a role in mediating the association with E-Syt2. Longins share a unique topology characterized by five antiparallel β-strands sandwiched by two α-helices on one side, and one α-helix on the other. Three binding regions have been identified within its structure (Fig. 25). Among them, the region A is involved in both intramolecular interactions with the SNARE coiled-coil domain (to regulate its activity) and intermolecular binding to other trafficking proteins in order to target Longin SNAREs to their site of action (De Franceschi et al. 2014). It is likely *via* this region that the association with E-Syt2 occurs, however this hypothesis requires further investigation.

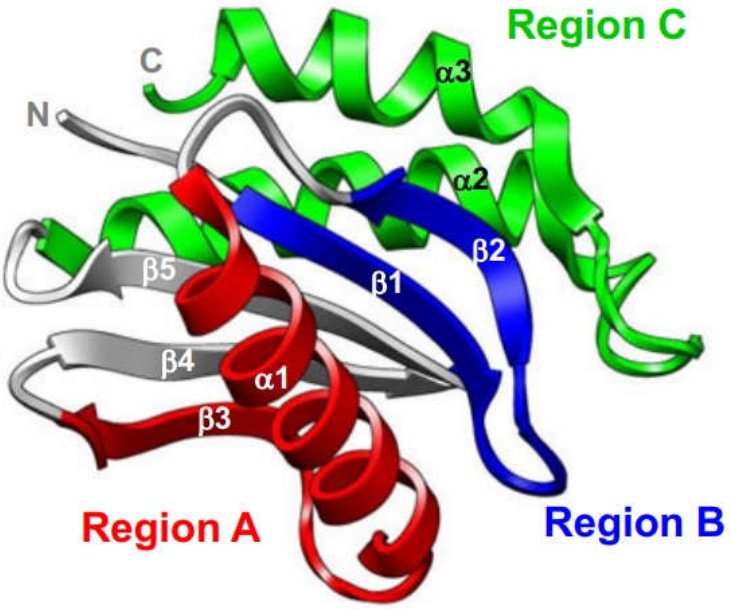

Figure 25. Architecture of a canonical Longin domain. The Longin domains display a globular fold of 120-140 amino acids, arranged as an α–β–α sandwich architecture (five antiparallel β-strands sandwiched by two α-helices on one side and one α-helix on the other). Three binding regions (regions A, B and C) have been identified within Longins: region A (red in the figure), involved in intra- and inter-molecular interactions; region B (blue), implicated in interactions with small GTPases; and region C (green), involved in conformational interactions with bulky protein complexes. (Image adapted from Daste et al. 2015).

The Longin domain is present not only in Sec22b but also in two other SNAREs, i.e. VAMP7 and in Ykt6, where it folds back onto the SNARE coiled-coil domain, thereby inhibiting membrane fusion (Filippini et al. 2001, Gonzalez et al. 2001, Rossi et al. 2004, Burgo et al. 2013, Daste et al. 2015). Overexpression of the Longin domain of Sec22b in developing neurons reduces neurite outgrowth (Petkovic et al. 2014), in agreement with the known inhibitory function of Longins with regard to SNARE-complex assembly. However, the exact role of the Longin domain of Sec22b in this process remains to be determined, as well as its general functions. Interestingly, its removal has been shown to augment the fusogenicity of VAMP7 (Martinez-Arca et al., 2000; Martinez-Arca et al., 2003). Hence, it is likely that mutating Sec22b to a more fusogenic form, by deleting its N-terminal Longin, might impair the Sec22-Stx1 tethering function at ER-PM contacts, leading to fusion of the two apposed compartments. To test this, we have performed experiments of surface staining in developing neurons and we

found that, contrary to Sec22b wild-type, the Sec22bΔL mutant can be detected at the cell surface of neurons, indicating that it may mediate a certain degree of membrane fusion between ER and PM . These findings are consistent with our hypothesis, and open the way for further research on the possible mechanisms involving the Longin domain by which fusion between ER and PM is prevented. An explanation might be that the Sec22bΔL mutant appeared at the cell surface by escaping into secretory vesicles. This is supported by data in COS7 cells showing that this mutant did not display a reticular localization typical of Sec22b, but it was mainly found concentrated in vesicular-like structures. Taken together, these results suggest that the Longin domain plays a key role in the localization of Sec22b, as well as in the establishment of interactions with specific partners, such as LTPs, allowing this protein to exert its function at MCSs. Additional studies are required to clarify this assumption.

Besides the discovery of a novel interaction between Sec22b and E-Syt2, three other conclusions can be inferred from the GFP-trap experiments. First, the association between E-Syt2 and Sec22b observed in PC12 cells is highly specific; indeed, a similar interaction with other v- or t-SNAREs could not be detected. Second, consistent with the lack of SNAP partners in Sec22b-Stx1 complexes (Petkovic et al. 2014), endogenous SNAP25 could not be detected in significant amounts in association with Sec22b-pHL, whereas deletion of the Longin domain increased the amount of coprecipitated SNAP25, leading to the hypothesis that the Longin domain may play a role to exclude SNAP25. Lastly, in HeLa cells Sec22b interacts with Stx3, indicating that, in non-neuronal cell types which do not express Stx1, it can also generate ER-PM tethering complexes with other Q-SNAREs.

The above described biochemical results have been further supported by experiments of PLA and super-resolution microscopy, demonstrating an association between endogenous Sec22b and E-Syt2, both in non-neuronal and neuronal contexts. Particularly, using STED super-resolution microscopy we showed that the average distances of Sec22b and E-Syt2 to the PM in growth cones of developing neurons is consistent with the association of these proteins at MCSs.

5.2) The mutual dependence of E-Syts and Sec22b-Stx complexes for the establishment of ER-PM junctions operating in membrane growth

5.2.1) A model for the assembly of a SNARE-mediated ER-PM junction

What is the functional relevance of Sec22b-Stx-E-Syts assembly? By using the Proximity Ligation Assay (PLA) technique, we have demonstrated in HeLa cells that the overexpression of E-Syt3 promoted the occurrence of Sec22b-Stx3 association, whereas inhibiting the expression of the three E-Syt isoforms strongly reduced their assembly. Sec22b has the main function of mediating fusion events within the anterograde and retrograde membrane trafficking between ER and Golgi, in association with SNARE partners such as Stx5 or Stx18 (Burri et al., 2003; Liu and Barlowe, 2002). As all the ER-resident proteins, Sec22b diffuses within the entire ER network, and, in doing so, it is expected to visit areas of close apposition between ER and PM. Thus, it can be trapped there under conditions that enhance their binding in *trans*-configuration to the PM. This is likely what happens upon E-Syts overexpression. The resulting increased ER tethering to the PM, may favor the possibility for Sec22b to come closer to the PM, where it is stabilized by its association with E-Syts molecules (Fig. 26a, b_1). This might facilitate its assembly with Syntaxins residing in the apposed PM, leading to the formation SNARE-mediated ER-PM contact sites. In addition, it is well established that a 1:1 assembly between Stx1 and SNAP25 (acceptor complex) precedes the recruitment of VAMP2 leading to the ternary synaptic SNARE complex essential for neurotransmitter release (Weninger et al. 2008). We have shown that purified Sec22b and Stx1 can form SDS resistant complexes with SNAP25 (See Appendix A, Fig. A4 and A5). Furthermore, this *in vitro* association is able to mediate fusion of liposomes (Petkovic et al. 2014). However, no Sec22b could be co-immunoprecipitated with SNAP25 from brain homogenates (Petkovic et al. 2014). Reversely, we could not detect endogenous SNAP25 associated with Sec22b-GFP in pull down experiments using PC12 cells. Hence, we are led to propose a model whereby the binding of assembled, ER-resident, Sec22b and E-Syts to the PM-resident Stx1-SNAP25 complex might compete SNAP25 out, leading to the formation of a non-fusogenic ternary assembly of Sec22b, Stx1 and E-Syts (Fig. 26c). Because small amounts of E-Syt2 were precipitated by GFP-SNAP25, it is also possible that E-Syts interact first with the Stx1/SNAP25 complex (Fig. $26b_2$)

and then Sec22b binding to E-Syts would compete out SNAP-25. This displacement would depend on Sec22b's Longin domain. This sequence of events would depend on the presence of the Longin domain of Sec22b, as described above. Experiments using *in vitro* reconstitution assay will be required to test this hypothesis.

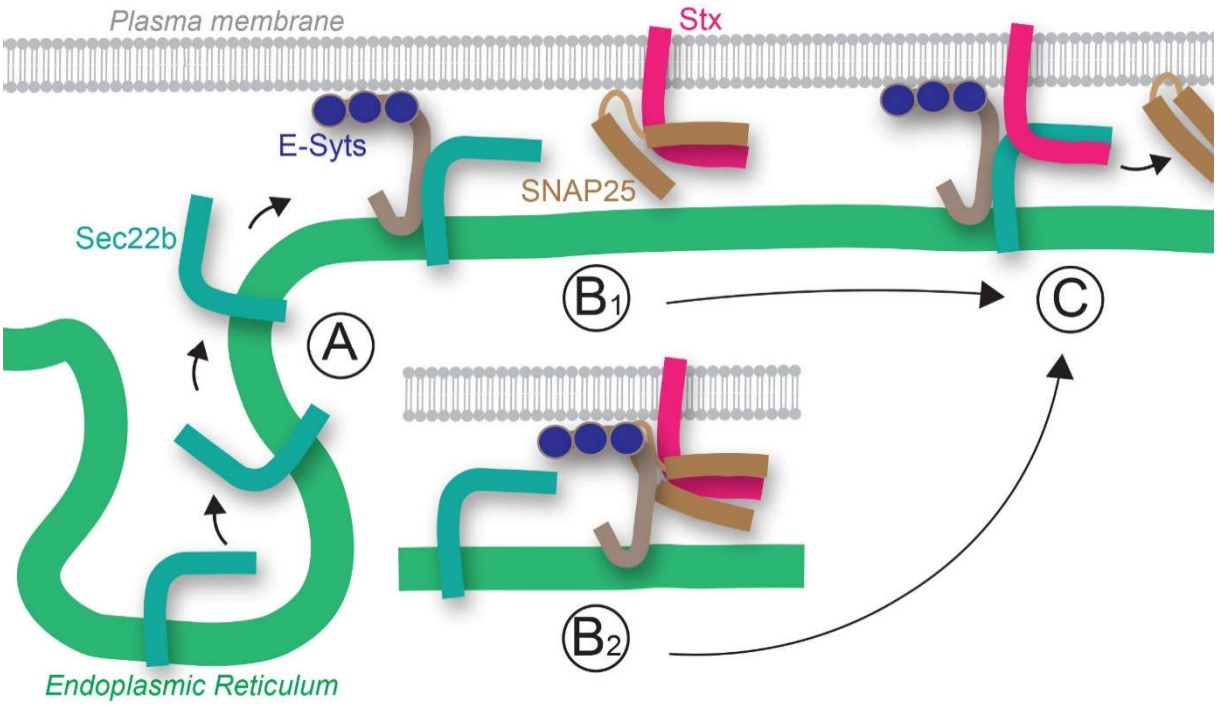

Figure 26. Proposed model for the formation of a SNARE-mediated ER-PM contact site. Sec22b diffuses within the ER membrane (A) and is stabilized in the cortical ER after binding to E-Syts (B1). Sec22b association to the PM-resident Stx1-SNAP25 complex causes SNAP25 displacement from Stx1, leading to the formation of a non-fusogenic assembly of Sec22b, Stx1 and E-Syts (C). Alternatively, E-Syt first interacts with the PM-resident Stx1-SNAP25 complex (B2), then Sec22b binds to E-Syts, possibly via its Longin domain, chasing out SNAP25 from the complex.

5.2.2) Morphogenetic effect of E-Syt overexpression

E-Syts belong to the heterogeneous category of ER-PM tethering proteins, promoting to formation of ER-PM junctions. However, like the vast majority of tethers, their role at ER-PM contacts cannot be solely reduced to tethering the two membranes (Gallo et al. 2016). Recent

studies have shown that dimers of E-Syts are functional in transferring lipids between ER and PM *via* their SMP lipid-transfer module, which accommodates lipids creating a hydrophobic bridge between the two bilayers or operating as a shuttle (Schauder et al. 2014). In line with their double function as tethers and LTPs, we found that E-Syts not only favor the occurrence of ER-PM contact sites populated by Sec22b-Stx complexes, but the overexpression of the E-Syt2 isoform in developing hippocampal neurons and in HeLa cells stimulated membrane expansion, likely as consequence of their lipid transfer activity. Like other LTPs, E-Syts transfer lipid passively from one compartment to another because the SMP domain acts as a hydrophobic bridge (Schauder et al. 2014). This process may result in net lipid transfer if metabolic or thermodynamic lipid trapping in the two participating membranes impact the free concentration of the lipid (See paragraph 1.5.4) (Lahiri et al. 2015). E-Syts might therefore function in membrane expansion or contraction, carrying glycerophospholipids unidirectionally either to the PM from the ER or back. This mechanism of membrane growth (or retraction) would allow to respond to signals much more quickly than it would be possible *via* vesicular transport.

In developing hippocampal neurons, we found that E-Syt2 overexpression increased the formation of neurite branching and axonal filopodia. Filopodia are highly dynamic, narrow, cylindrical extensions emerging from neurites, which play pivotal roles in the initial stages of synaptogenesis. In addition to bundles of filamentous actin, axonal filopodia also contain motile clusters of synaptic vesicles which move bidirectionally along the axonal shaft and the filopodia axis, and are recruited at the site of contact with the appropriate target cell to generate mature presynaptic sites (Kraszewski et al. 1995, Matteoli et al. 2004). Thus, filopodia emerging from axons are essential for the formation of future presynaptic sites. Hence, it is likely that the increased E-Syt expression not only enhances neurite growth during the early stages of neuronal development, but also promotes synaptogenesis and synaptic transmission, by incrementing the number of axonal filopodia. Evidences in this direction come from studies in the neuromuscular junction of Drosophila melanogaster, where the presynaptic overexpression of the *Esyt* orthologue increased the number of synaptic boutons and facilitated the presynaptic neurotransmitter release (Kikuma et al. 2017). Future studies are necessary to assess whether this also occurs in mammalian neurons.

Interestingly, the E-Syt2-mediated morphogenetic effect observed in developing neurons appears to depend on the proximity between ER and PM established by Sec22b-Stx1 complexes. Two sets of data support this assumption. The enzymatic disruption of Sec22b-Stx1 SNARE assembly, achieved by treating neurons with BoNT/C1 that cleaves Stx1, and the co-expression of E-Syt2 with the Se22b-P33 mutant, who has been shown to provoke a 6-nm increase of the ER to PM distance at contact sites (Petkovic et al. 2014), both prevented the enhanced neurite growth resulting from E-Syt2 overexpression.

Taken together, the results described above support the hypothesis that a mutual dependence of functional E-Syts and Sec22b-Stx complexes at ER-PM contact sites is required to promote membrane growth during neuronal development. E-Syts, acting as tethers, are required to stabilize the Sec22b-Stx association at MCSs. In doing so, they may promote closer contact sites between ER and PM because SNARE complexes mediate a ~10nm distance. In turn, this shortening of the distance between the ER and the PM may further enhance the LTP activity of E-Syts, allowing the net transfer of lipids to the PM, which contributes to membrane expansion. This paradigm opens the way to further dissect the mechanisms by which these ER-PM MCSs-residing proteins co-operate during growth.

It is important to note that other factors may contribute to the stabilization of ER-PM contact sites during membrane growth. These might include ER shaping proteins, such as Reticulon 4 (Jozsef et al., 2014), and the cortical cytoskeleton (Dingsdale et al., 2013; van Vliet et al., 2017) already known to control stabilization and dynamics of ER-PM junctions. Particularly, it has been recently shown that the architecture of the cortical actin meshwork contributes to stability and spatial organization of ER–PM junctions. Given the structure-function coupling in biological system, this results in modulation of functional activities mediated by such contacts (Hsieh et al. 2017).

5.3) Functional redundancy of LTPs at ER-PM junctions?

We have assessed the formation of a ternary Sec22b-Stx-E-Syt assembly at ER-PM contact, as well as how such association modulates membrane growth. It cannot be excluded that additional ER-residing LTPs partners could be involved. Evidences in this direction come from experiments in yeast showing a physical association between the SNAREs Sec22p and Sso1, yeast homologues of Sec22b and Stx1, and Osh2 and Osh3, another class of ER-PM MCS-

localized LTPs (Petkovic et al. 2014). Furthermore, in mammalian cells, both Sec22b and Stx1 have been shown to interact with the ER-resident VAMP-associated protein VAP-A. (Weir et al. 2001). VAP-A mediates stable ER-PM tethering (Loewen et al. 2003) and binds a wide number of LTPs, such as oxysterol-binding protein (OSBP)-related proteins (ORPs) and ceramide transfer protein (CERT). This raises the possibility that a structural and functional link between various lipid transfer machineries and the SNARE tethering complex at ER-PM contact sites is necessary to promote membrane expansion.

Our data showed that the elicited membrane expansion promoted by elevated E-Syt2 expression was abolished in developing neurons and HeLa cells expressing deleted non-functional versions of E-Syt2, i.e. E-Syt2 ΔSMP and E-Syt2 ΔMSD. Interestingly, these cells expressing E-Syt2 mutants grew normally, as we observed no significant differences in membrane extension as compared to control cells. Therefore, expression of these mutants did not act in a dominant negative manner. Similar results were described in Drosophila melanogaster, where overexpression of *Esyt* orthologue at the presynaptic terminal of the neuromuscular junction not only increased neurostrasmitter release, as previously mentioned, but also enhanced synaptic growth, whereas *Esyt* mutant flies exhibited no difference in synaptic membrane surface area as compared to wild-type animals (Kikuma et al. 2017). Furthemore, *Esyt* triple knock-out mice display no major defects in neuronal development and morphology (Sclip et al. 2016). Taken together, these evidences, coming from our and other works, strongly imply that a functional redundancy exists among LTPs in promoting membrane growth, as the removal of one class of such proteins might be compensated by the activity of the others. The precise contribution of each class of LTPs, as well as their mutual interplay, will require further studies.

Besides the functional redundancy between LTPs, other classes of proteins interacting with SNAREs and / or residing at ER-PM MCSs, may converge in the similar function of promoting membrane expansion and neurite growth. The overexpression of Munc18a, a Stx1 binding protein involved in the regulation of SNARE complex formation during synaptic vesicle membrane fusion, also induce a phenotype similar to the one elicited by E-Syt2 overexpression. Indeed, it led to an increase of the total length of primary neurites and their branching, whereas the average lengths of primary neurites was not affected (Steiner et al. 2002). Furthermore, different types of actin-binding proteins differentially modulate the formation of filopodia in developing neurons. For instance, the BDNF-stimulated filopodia formation in developing

hippocampal neurons was inhibited by the actin-capping protein Eps8 and its removal increased the number of neurite branches and filopodia (Menna et al. 2009). Conversely, actin nucleating proteins such as Ena/VASP and Arp2/3 positively regulate axon filopodia formation and their overexpression results in increased neurite length and ramification (Ahuja et al. 2007, Lebrand et al. 2004, Spillane et al. 2012). Such actin-binding factors might act on the pool of cortical actin residing at contact sites, contributing to the formation of functional ER-PM junctions operating in neuronal development.

5.4) A scaffold model for non-vesicular membrane expansion at ER-PM MCSs

Altogether, the data presented here led us to propose a working model for membrane growth at ER-PM contact sites whereby a scaffold of proteins needs to be assembled to allow the formation of a stable platform for transferring lipids towards the PM. This platform is composed by the SNARE Sec22b-Stx complex interacting with the LTPs E-Syts and, possibly, with other factors, such as cytoskeleton, ER-shaping proteins and other classes of LTPs, which contribute to both stabilization and function of the ER-PM junctions (Fig. 27). The identification of the full catalog of proteins composing such scaffold, along with the functional contribution of each component, is an interesting question that paves the way for additional investigations. We have shown that the enhanced growth mediated by E-Syts is a general phenotype, occurring both in neuronal and non-neuronal contexts. Hence, additional open questions concern the different molecular composition of the platform depending on the cell type, as well as how such combination of molecules can vary in pathological conditions like cancer, or in mechanisms of membrane retrieval leading to axonal retraction and neurodegeneration.

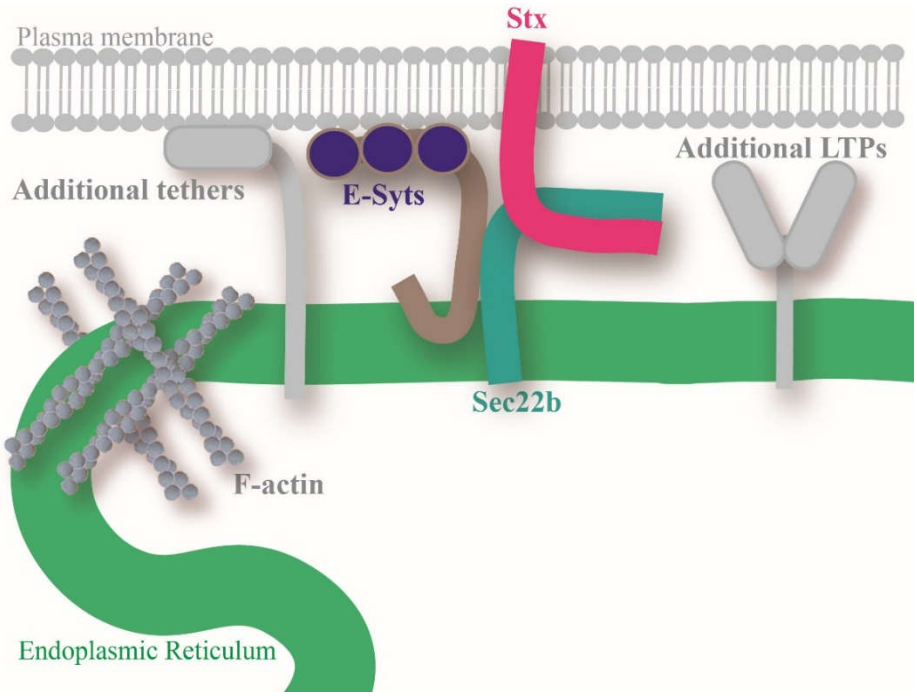

Figure 27. The scaffold hypothesis for membrane expansion. During membrane growth, a scaffold of proteins must be organized at ER-PM contact sites to allow an efficient transfer of lipids towards PM. These proteins include stabilizing factors (tethers like Sec22b-Stx complex, ER-shaping proteins (not shown), cytoskeleton and various classes of LTPs including E-Syts.

5.5) Fusion and tethering: different processes, similar actors, converging functions

Despite substantially different, fusion and tethering can be considered like distant relatives, as structural and sometimes functional similarities exist between proteins operating at fusion sites and at MCSs. The ER-PM MCSs-resident E-Syts studied here, and the closely related proteins Synaptotagmins, essential players in membrane fusion, provide the most striking example for such correlation. Synaptotagmins and E-Syts share an analogous domain organization, as they both contain cytoplasmic Ca^{2+}-binding C2 domains, which confer to these proteins a dependence for similar intracellular Ca^{2+} concentrations (low micromolar range) in order to exert their functions in fusion and tethering, respectively. Surprisingly, it has been shown that at physiological ion concentrations Synaptotagmin-1 does not bind to SNAREs, but just to $PI(4,5)P_2$ acting as a Ca^{2+}-dependent membrane tether, rather than a fusion-mediating protein, further empathizing its similarly to E-Syts (Park et al., 2015). In line with this, the "buttressed-

ring hypothesis" (See paragraph 2.3) postulates that Synaptotagmin-1, together with Complexin and other accessory proteins, forms a ring, which acts as a spacer between the apposed vesicle and PM, preventing fusion in the absence of Ca^{2+}.

In turn, E-Syts have been shown to be required for rapid clathrin-dependent endocytosis of activated Fibroblast Growth Factor (FGF) receptor (Jean et al. 2010), indicating that, in specific conditions, these tethers might reach the cell surface. Furthermore, we found that, similarly to Synaptotagmins, E-Syts can interact with SNARE proteins residing at ER-PM contacts.

As the name indicates, E-Syts contain an extra cytosolic SMP domain, which is absent in Synaptotagmins, that confers to these proteins the additional function of harboring and transferring lipids. As a matter of fact, we discovered that the overexpression of E-Syts promote filopodia formation and membrane expansion. An analogous phenotype of increased branching and filopodia has been also observed after the overexpression of Synaptotagmins (Feany and Buckley 1993). However, these two proteins take advantage of different mechanisms to converge on a similar phenotype: if E-Syts use their own property of transferring lipids at ER-PM contact sites, Synaptotagmins might simultaneously interact with acidic phospholipids in the PM, *via* their C2 domains, and with SNARE proteins helping the merging of membranes required for vesicle fusion. Thus, the involvement of both E-Syts and Synaptotagmins in cell growth constitutes a further example of how fusion and tethering are functionally connected. It is important to mention that, in addition to lipids, growth of the PM requires proteins, particularly receptors necessary for cell adhesion, guidance and sensing the environment. Mechanisms of vesicular fusion mediated by R-SNAREs like VAMP2 and VAMP7, already known to be implicated in neuronal growth (Gupton and Gertler 2010, Martinez-Arca et al., 2000 and 2001; Alberts et al., 2003), would operate in both lipid and protein delivery. Non-vesicular lipid transfer, which only shuttles lipids between the membranes, not only would significantly contribute to the bulk lipid addition, but it may also act in refining the lipid composition of the expanding membrane. This intertwined action of vesicular and non-vesicular molecular machineries in cell growth generates a more complex scenario for membrane expansion, raising a number of new questions regarding how the two mechanisms are balanced and regulated to efficiently respond to cell needs.

Further analysis of similarities between fusion and tethering could contribute to a better understanding of contact formation and function as well as how these two processes are connected in other cellular functions.

5.6) Perspectives for future research

The work presented in this PhD manuscript has provided key notions on the physiological meaning of ER-PM contact sites. Furthermore, it fits into a new field of research aimed at revisiting the biology of SNAREs, looking for additional functions of these proteins besides their well-established role within the secretory pathway. However, as new scientific discoveries always demand further explanations, this study raises a number of open questions.

What is the topology of the Sec22b-Stx SNARE complexes at MCSs? Classically, fusogenic SNAREs assemble in a parallel configuration (Sutton et al. 1998). Even though the parallel configuration is the most stable, SNARE complex *in vitro* can also acquire an antiparallel topology. Parallel configurations begin to form when the membrane bilayers are 20 nm apart, and full zippering then occurs when the membranes contact each other. In contrast, the antiparallel assembly can form completely when membranes are separated by 10 nm. Hence, it is likely that it would not lead to fusion, but it would only tether the two apposed bilayers (Weninger et al. 2003). The evidence that Sec22b and Stx do not mediate fusion but they rather form a bridge between ER and PM, leads to the hypothesis that they may assemble in an antiparallel manner. To test this we have designed an experimental paradigm based on the strategy termed bipartite tetracysteine display (Griffin et al. 1998, Adams et al. 2001, Luedtke et al. 2007). This assay is based on the use of profluorescent biarsenical dyes, called FlAsh or ReAsh, that are cell-permeable and selectively label recombinant proteins containing a tetracysteine motif. The bound forms of FlAsH and ReAsH are highly fluorescent. The advantage of this technique is that the tetracysteine motif could function as a reporter of protein conformation or protein-protein binding if displayed in a bipartite mode, with two Cys-Cys pairs located on separated proteins that become proximal when these two proteins assemble together (Fig. 28a). Following this principle, mutant versions of Sec22b and Stx, in which a Cys-Cys pair has been inserted in different positions within their SNARE domain, will be expressed in cells. The analysis of cell fluorescence after the addition FlAsH will give us information concerning the topology of their interactions, and will help deciphering the mechanism by which fusion is prevented when these SNARE proteins assemble at MCSs (Fig. 28b).

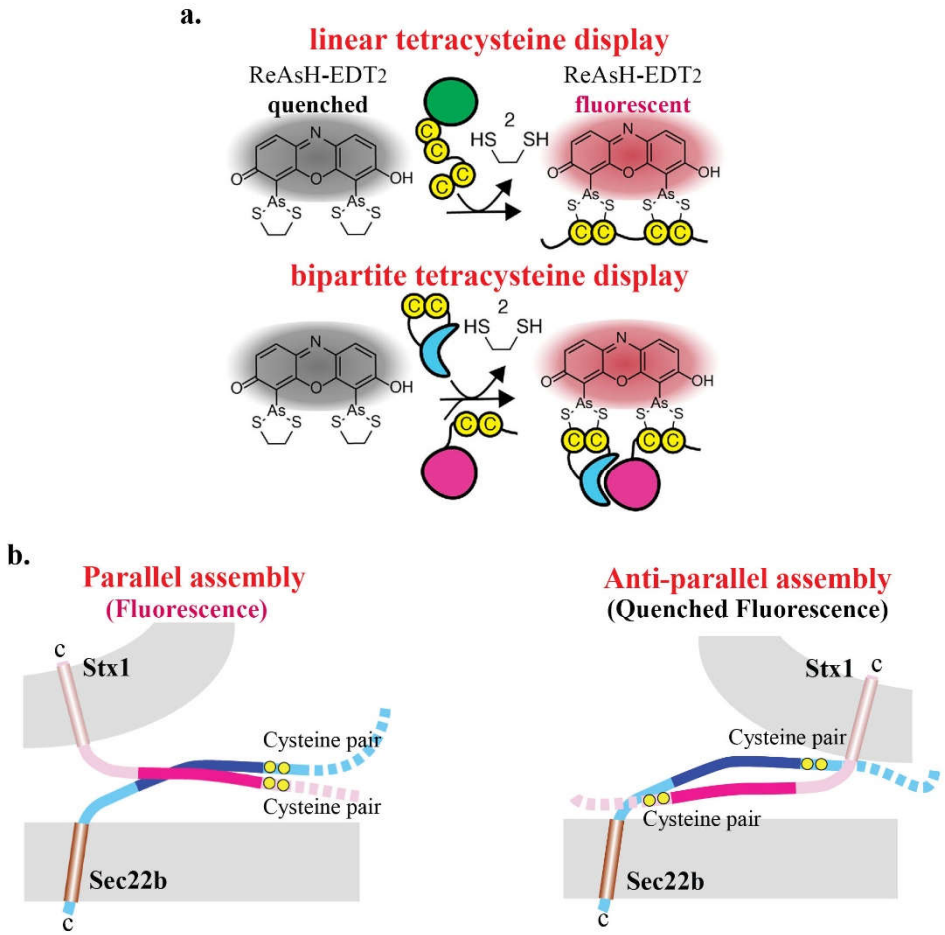

Figure 28. The tetracysteine display. (a) Bis-arsenical dyes such as ReAsH are quenched when coordinated to ethanedithiol (EDT) but become fluorescent upon ligand exchange with a single protein carrying a linear Cys4 motif (Linear tetracysteine display) or a protein assembly in which the Cys4 motif is recapitulated upon folding or association (Bipartite tetracysteine display). Image modified from Walker et al. 2016. (b) Schematic representation of the bipartite tetracysteine display applied to the SNARE Sec22b-Stx1 complex. If the two proteins assemble in a parallel manner, the Cys4 motif is reconstructed, leading to fluorescence dequenching; if they assemble in an anti-parallel orientation, the Cys-Cys pairs are too far away from each other, therefore the Cys4 motif is not formed and fluorescence is not dequenched.

What are the additional partners of the Sec22b-Stx-E-Syts complexes at ER-PM contact sites? To elucidate the composition of the scaffold operating during membrane growth we will perform proteomic analysis on sample enriched in Sec22b-Stx1 complexes at MCSs. This will be achieved through sequential immunoprecipitations from PC12 cells expressing tagged versions of Stx1 and Sec22b. A first GFP-Trap for cell surface Stx1-GFP on living cells will be followed by a Sec22b immunoprecipitation on the Stx1 eluate, therefore allowing the selective isolation of the complex from ER-PM contacts.

If non-vesicular lipid transfer mediated by E-Syts contributes to PM expansion, a naturally consequent investigation concerns the measurement of such transfer, as well as the analysis of its selectivity for specific lipid species. This would provide information on the rate of the E-Syts-mediated lipid flow at contacts formed by Sec22b-Stx, and on how these LTPs can modulate the lipid composition of membranes during their expansion. On the basis of already published data (Saheki et al. 2016, Less et al. 2017, Yu et al. 2016), we have designed an *in vitro* lipid transfer assay in which fluorescence-labeled donor liposomes are anchored to streptavidin beads and bear Sec22b through a cleavable phospholipid. The lipid transfer reactions would be carried out by incubation with unlabeled acceptor liposomes bearing Stx1 together with soluble E-Syt2. After Sec22b cleavage, fluorescence in the soluble liposomes would be measured as an indication of an E-Syt2-mediated lipid transfer (Fig. 29).

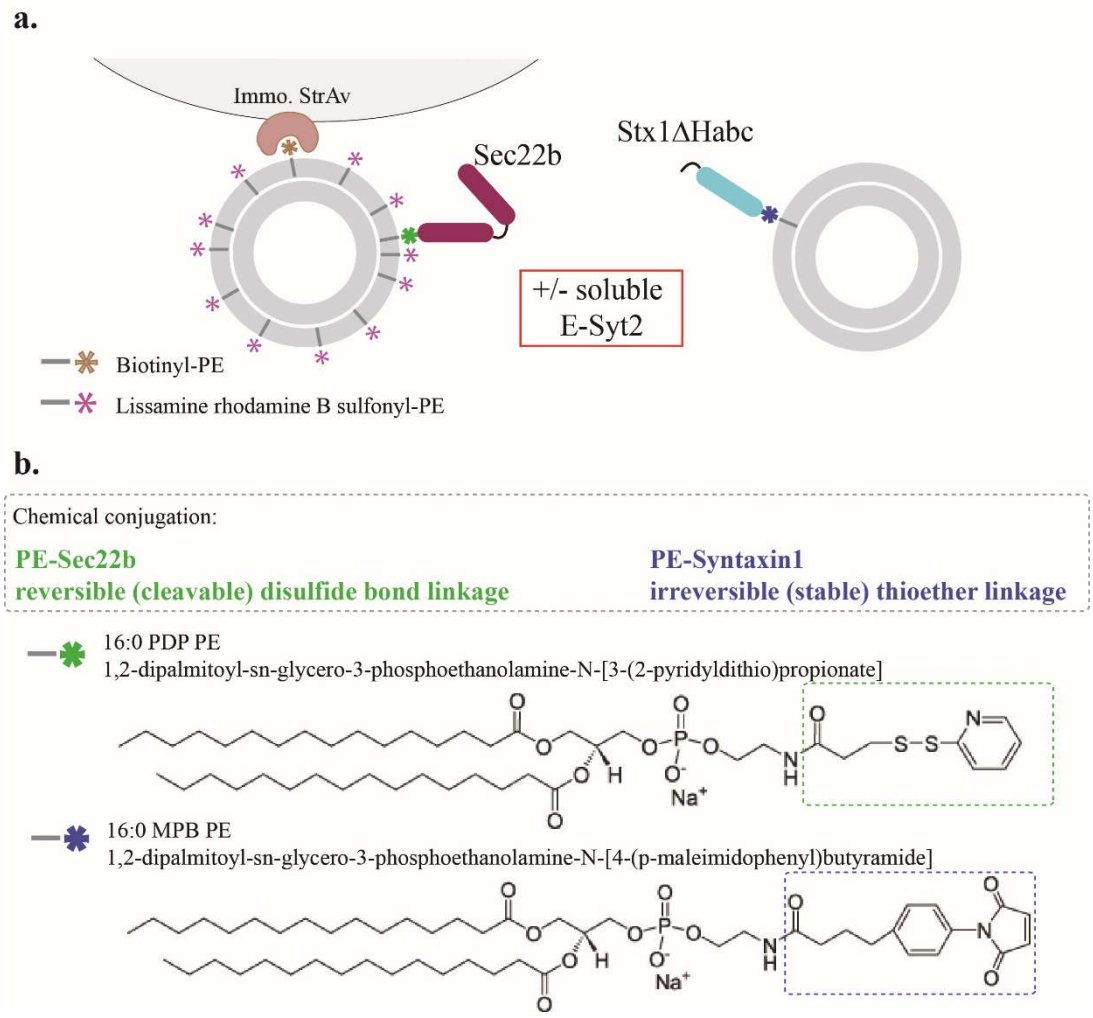

Figure 29. The *in vitro* phospholipid transfer assay. (a) Schematic representation of the assay. Immobilized fluorescent donor proteoliposomes bearing cleavable Sec22b are mixed with unlabeled

Stx1-containing acceptor proteoliposomes. Soluble E-Syt2 is added or not to the mix. The formation of Sec22b/Stx1/E-Syt2 complex would facilitate E-Syt2 lipid transfer activity. This would lead to the transfer of fluorescent lipids from donor to acceptor liposomes. The measurement of fluorescence in the soluble liposome fraction obtained after cleavage of Sec22b would be an indication of the E-Syt2-mediated lipid transfer. (b) Structure of phospholipids conjugated to soluble Sec22b and Stx1. 16:0 PDP-PE [1,2-dipalmitoyl-sn-glycero-3-phosphoethanolamine-N-3-(2-pyridyldithio)propionate] is conjugated to Sec22b and contains a cleavable disulfide bond linkage. 16:0 MPB-PE [1,2-dipalmitoyl-sn-glycero-3-phosphoethanolamine-N-4-(p-maleimidophenyl)butyramide] is conjugated to Stx1 and contains stable uncleavable thioether linkage.

We have highlighted how specific tethers residing at ER-PM contact sites could be involved in growth of mammalian cells, including neurons. In this context, a further point that should be more precisely delineated concerns the control of PM expansion and withdrawal. In the context of growth and retraction events that modulate membrane area in cell growth and axon guidance and collapse, deciphering the contributions of MCSs to membrane delivery and retrieval, as well as the relative weights of vesicular and non-vesicular trafficking, will represent a crucial challenge of MCS biology. I plan to continue my scientific career trying to address this exciting question.

In conclusion, this work on a small subset of proteins, SNAREs and E-Syts, has opened several important perspectives in the fields of lipid transfer and neuronal cell growth and differentiation.

Chapter 6

APPENDIX B: F1000 Recommendations

Complementary to the scientific research, during my PhD I have been nominated Associate Faculty Member of F1000 by the Faculty Member Thierry Galli, with the aim of recommending scientific literature in the field of neuroscience. Particularly, I have been writing F1000 recommendations, which consist in brief comments on the best articles I have read in the chosen field, highlighting the key findings and putting the work into context. These recommendations are published in the website of the F1000 Scientific Community (https://f1000.com/prime/recommendations).

In Appendix B I will include citations and full texts of the published F1000 recommendation I have composed.

Control of plasma membrane lipid homeostasis by the extended synaptotagmins.

Saheki Y, Bian X, Schauder CM, Sawaki Y ... Klose C, Pincet F, Reinisch KM, De Camilli P.
Nat Cell Biol 2016 05; 18(5):504-515
PMID: 27065097 DOI: 10.1038/ncb3339

How to cite this recommendation
Galli T and Gallo A: F1000Prime Recommendation of [Saheki Y et al., Nat Cell Biol 2016 18(5):504-515]. In F1000Prime, 22 Apr 2016; 10.3410/f.726277237.793517163

22 Apr 2016 | New Finding

Efficient communication between the endoplasmic reticulum (ER) and the plasma membrane (PM) has recently appeared important for PM lipid homeostasis; however, little is known about the molecular mechanisms involved. In this article, Saheki and colleagues provide evidence for the ability of the Ca2+-regulated ER-resident extended-synaptotagmin proteins (E-Syts), classically known as membrane tethers at ER-PM contact sites {1}, to transfer lipids between bilayers. Combining in vitro lipid transfer assays, genome editing using the TALEN and the CRISPR/Cas9 systems and lipidomic analysis, they demonstrated that E-Syts transfer glycerolipids between bilayers. This mechanism is bidirectional and dependent on cytosolic Ca2+ levels and, as already predicted by crystallography {2}; it requires the lipid-harbouring property of SMP domains present in E-Syt proteins. These findings have been instrumental in identifying E-Syts as a new class of lipid transfer proteins (LTPs) that operate in trans at ER-PM contact sites, contributing to the maintenance of PM lipid composition in response to acute metabolic changes, such as those provoked by the activation of signaling pathways. It is now necessary to gain further insight into the role of non-vesicular lipid transfer mediated by E-Syts, as well as by other LTPs located at membrane contact sites, in cell growth and maintenance, particularly in the context of a mild developmental phenotype of E-Syts 2/3 knockout in the mouse {3}.

References

1.
PI(4,5)P(2)-dependent and Ca(2+)-regulated ER-PM interactions mediated by the extended synaptotagmins.
Giordano F, Saheki Y, Idevall-Hagren O, Colombo SF, Pirruccello M, Milosevic I, Gracheva EO, Bagriantsev SN, Borgese N, De Camilli P. Cell. 2013 Jun 20; 153(7):1494-509
PMID: 23791178 DOI: 10.1016/j.cell.2013.05.026

2.
Structure of a lipid-bound extended synaptotagmin indicates a role in lipid transfer.
Schauder CM, Wu X, Saheki Y, Narayanaswamy P, Torta F, Wenk MR, De Camilli P, Reinisch KM. Nature. 2014 Jun 26; 510(7506):552-5
PMID: 24847877 DOI: 10.1038/nature13269

3.
Loss of Extended Synaptotagmins ESyt2 and ESyt3 does not affect mouse development or viability, but in vitro cell migration and survival under stress are affected.
Herdman C, Tremblay MG, Mishra PK, Moss T. Cell Cycle. 2014; 13(16):2616-25
PMID: 25486202 DOI: 10.4161/15384101.2014.943573

Diffusional spread and confinement of newly exocytosed synaptic vesicle proteins.

Gimber N, Tadeus G, Maritzen T, Schmoranzer J, Haucke V.
Nat Commun 2015 Sep 24; 6:8392
PMID: 26399746 DOI: 10.1038/ncomms9392

How to cite this recommendation
Galli T and Gallo A: F1000Prime Recommendation of [Gimber N et al., Nat Commun 2015 6:8392]. In F1000Prime, 31 May 2016; 10.3410/f.725807187.793518738

31 May 2016 | New Finding, Technical Advance

Communication within the nervous system mainly occurs at chemical synapses, specialized contacts where electrical signals are transmitted through the release of neurotransmitters by a calcium-dependent fusion of synaptic vesicles (SVs) with the presynaptic membrane. Exocytosis is a fast process that occurs in a millisecond timescale and it is immediately followed by a compensatory recycling of SV membranes in order to maintain the presynaptic membrane homeostasis {1}. Hitherto, the velocity of the exocytic process has created challenges to the study of the diffusional behavior of newly exocytosed SV proteins, mainly because of a lack of techniques to follow SV recycling in the way of ultra-fast and -sensitive imaging techniques. This problem has been partially overcome by Gimber and colleagues. They monitored the diffusional fate of the newly exocytosed pHluorin-tagged Synaptobrevin2, Synaptophysin and Synaptotagmin I, three main SV proteins, by combining high-resolution time-lapse imaging in hippocampal neurons and Gaussian fit analysis. Rapid free diffusion was observed, followed by confinement within a limited area of the bouton, and by slow reclustering. These last two processes are essential to prevent proteins' escape into the axon and to allow the proper reformation of SVs by endocytosis. The authors further found that diffusional spread of SV proteins was limited by their association with endocytic adaptors (i.e. AP180 and CALM) of clathrin-mediated endocytosis. Altogether, these results led to the proposal of a model whereby SV proteins spread through the presynaptic bouton within the first few seconds after exocytosis. This article thus supports the notion of diffusional behavior of newly exocytosed membrane proteins in neurons, a mechanism so far investigated only in cells, such as the neuroendocrine PC12 {2}, which lack the typical exocytosis-endocytosis coupling occurring during neurotransmission. Further studies are now necessary to uncover the additional factors that may contribute to SV proteins spread, confinement and reclustering after exocytosis, which may include membrane lipids and actin filaments, already known to participate in the clathrin-mediated endocytosis {3,4}.

References

1.
Molecular mechanisms of presynaptic membrane retrieval and synaptic vesicle reformation.
Kononenko NL, Haucke V. Neuron. 2015 Feb 4; 85(3):484-96
PMID: 25654254 DOI: 10.1016/j.neuron.2014.12.016

2.
Imaging the post-fusion release and capture of a vesicle membrane protein.

Sochacki KA, Larson BT, Sengupta DC, Daniels MP, Shtengel G, Hess HF, Taraska JW. Nat Commun. 2012; 3:1154
PMID: 23093191 DOI: 10.1038/ncomms2158

3.
A modular design for the clathrin- and actin-mediated endocytosis machinery.
Kaksonen M, Toret CP, Drubin DG. Cell. 2005 Oct 21; 123(2):305-20
PMID: 16239147 DOI: 10.1016/j.cell.2005.09.024

4.
Cholesterol and F-actin are required for clustering of recycling synaptic vesicle proteins in the presynaptic plasma membrane.
Dason JS, Smith AJ, Marin L, Charlton MP. J Physiol (Lond). 2014 Feb 15; 592(4):621-33
PMID: 24297851 DOI: 10.1113/jphysiol.2013.265447

v-SNARE transmembrane domains function as catalysts for vesicle fusion.

Dhara M, Yarzagaray A, Makke M, Schindeldecker B ... Böckmann RA, Lindau M,Mohrmann R, Bruns D.
elife 2016 06 25; 5
PMID: 27343350 DOI: 10.7554/eLife.17571

How to cite this recommendation
Galli T and Gallo A: F1000Prime Recommendation of [Dhara M et al., elife 20165]. In F1000Prime, 19 Jul 2016; 10.3410/f.726465373.793520853

19 Jul 2016 | New Finding

Membrane fusion mediating neurotransmitter and hormone release is driven by the formation of a SNARE complex between proteins anchored in the lipid bilayers of the vesicle and the plasma membrane. While much is known about the mechanism whereby SNARE proteins act as force generators pulling the two membranes together, the importance of the transmembrane domains (TMD) particularly in membrane merge and fusion pore dynamics is still unclear. By using membrane capacitance measurements and amperometry recordings, the authors studied the impact of Syb2 TMD structural flexibility on Ca2+ dependent exocytosis in secretory granule v-SNARE deficient chromaffin cells. They demonstrated that increasing the frequency of β-branched amino acid residues (i.e. valine and isoleucine) within Syb2 TMD enhances its flexibility. Such modified Syb2 proteins restore normal secretion in mutant cells and accelerate fusion pore expansion with a higher rate than the wildtype protein. Based on their observations, they propose a model by which conformational flexibility of Syb2 TMD, and particularly within its N-terminal half, enhances lipid splay in the cytoplasmic leaflet to facilitate the first contact between the two opposing membranes, and lowers the high membrane curvature of the outer leaflet to enhance pore expansion. The hypothesis that TMDs may affect surrounding phospholipids thereby facilitating trans-membrane contacts and subsequent fusion pore expansion is particularly appealing. In essence, the present report provides important evidence in support of the involvement of SNARE TMDs in membrane fusion via a protein-lipid link, which will now need to be further explored in the context of other SNARE-mediated fusion reactions.

The Vici Syndrome Protein EPG5 Is a Rab7 Effector that Determines the Fusion Specificity of Autophagosomes with Late Endosomes/Lysosomes.

Wang Z, Miao G, Xue X, Guo X ... Chen Y, Feng D, Hu J, Zhang H.
*Mol Cell*2016 09 01; 63(5):781-795
PMID: 27588602 DOI: 10.1016/j.molcel.2016.08.021

How to cite this recommendation
Galli T and Gallo A: F1000Prime Recommendation of [Wang Z et al., Mol Cell 2016 63(5):781-795]. In F1000Prime, 20 Oct 2016; 10.3410/f.726706034.793524166

20 Oct 2016 | New Finding

Autophagy, a dynamic intracellular catabolic process for turnover of cytoplasmic elements, involves the formation of double-membrane autophagosomes and their direct fusion with lysosomes for degradation. Intracellular trafficking and membrane fusion are required along the pathway of autophagosome maturation, from their early biogenesis to their later degradation in lysosomes, and each step involves different sets of Rab GTPases, tethers, and SNARE proteins {1}.

In this elegant article, Wang and colleagues discovered that the protein product of the metazoan-specific autophagy gene *EPG5* is a novel molecular player in the process of autophagosomes' maturation. The authors used *Caenorhabditis elegans* and/or HeLa cells as experimental models and performed confocal and electron microscopy, together with *in vitro* pull-down assay, to show that EPG5 localizes on Rab7-positive late endosomes, where it functions as Rab7 effector. In autophagy conditions, EPG5 determines the specific recognition of lysosomes and autophagosomes, by simultaneously binding Rab7 and VAMP7/8 on lysosomal membrane and LC3 on autophagosomal membrane. Finally, EPG5 coordinates the docking and fusion of the two

compartments, by promoting the assembly of the *C-elegans* Stx17-SNAP29-VAMP7 *trans*-SNARE complex, as demonstrated by *in vitro* lipid mixing assay. However, the *c.elegans* VAMP protein does not possess the typical longin domain of VAMP7; therefore, further studies are necessary to go into the details of the influence of the longin module in this process. Overall, the data shown in this study allow us to classify EPG5 protein as a tethering factor, which promotes the fusion specificity of autophagosomes with late endosomes/lysosomes.

Mutations in human *EPG5* gene cause the multisystem disorder Vici syndrome, the most typical example of a novel group of inherited neurometabolic conditions, called *congenital disorders of autophagy* {2}. However, the molecular mechanisms by which the absence of EPG5 induces the pathogenesis of Vici syndrome is still unclear. The present report contributes to extending this knowledge by shedding light on the role of EPG5 in autophagic and endocytic trafficking.

References

1.
SNARE-mediated membrane fusion in autophagy.
Wang Y, Li L, Hou C, Lai Y, Long J, Liu J, Zhong Q, Diao J. Semin Cell Dev Biol. 2016 Jul 12;
PMID: 27422330 DOI: 10.1016/j.semcdb.2016.07.009

2.
Recessive mutations in EPG5 cause Vici syndrome, a multisystem disorder with defective autophagy.
Cullup T, Kho AL, Dionisi-Vici C, Brandmeier B, Smith F, Urry Z, Simpson MA, Yau S, Bertini E, McClelland V, Al-Owain M, Koelker S, Koerner C, Hoffmann GF, Wijburg FA, ten Hoedt AE, Rogers RC, Manchester D, Miyata R, Hayashi M, Said E, Soler D, Kroisel PM, Windpassinger C, Filloux FM, Al-Kaabi S, Hertecant J, Del Campo M, Buk S, Bodi I, Goebel HH, Sewry CA, Abbs S, Mohammed S, Josifova D, Gautel M, Jungbluth H. Nat Genet. 2013 Jan; 45(1):83-7
PMID: 23222957 DOI: 10.1038/ng.2497

SNARE-mediated membrane fusion trajectories derived from force-clamp experiments.

Oelkers M, Witt H, Halder P, Jahn R, Janshoff A.
Proc Natl Acad Sci USA 2016 11 15; 113(46):13051-13056
PMID: 27807132 DOI: 10.1073/pnas.1615885113

How to cite this recommendation
Galli T and Gallo A: F1000Prime Recommendation of [Oelkers M et al., Proc Natl Acad Sci USA 2016 113(46):13051-13056]. In F1000Prime, 06 Dec 2016; 10.3410/f.726917584.793525808

6 Dec 2016 | Confirmation, Technical Advance

Fusion of membranes, a crucial event in cell physiology, is catalyzed by SNARE proteins. SNAREs overcome the energetic fusion barrier through the formation of a tetrameric coiled-coil complex that releases enough free energy to lower such barriers.

Here, the authors developed a sophisticated method based on membrane-coated colloidal probes equipped with SNARE proteins and attached to an atomic force microscope (AFM), to measure the free energy barriers and force-dependent lifetimes of fusion intermediates as a function of an externally applied load. Analysis of the step

heights distribution after time traces obtained in force clamp experiments, allowed the identification of three main intermediate events during SNARE-mediated fusion, which correspond to stalk formation, hemifusion and full fusion. Furthermore, these measurements allowed definition of the removal of the hydration shell as the main free energy barrier that has to be reached in order to achieve membrane fusion.

Although computational and experimental data on the energy associated with transition barriers during membrane fusion was clearly available {1,2}, the innovation here is the estimation of the energy of the hydration barrier in the presence of SNAREs.

Of further interest is the observation that, besides the typical fusion pore opening, a second reaction pathway can exist, where the hemifusion state can be stabilized and not followed by full fusion. Also, the authors found that calcium positively regulates complete fusion, for both SNARE-free and SNARE-containing membranes. They demonstrate that, in the absence of calcium, SNARE zippering is incomplete, probably due to the hydrostatic repulsion between the two opposing membranes. Calcium allows the neutralization of the negatively charged headgroups of the two opposing lipids bilayers, therefore facilitating their approach. This process might help the full SNARE zippering, and consequently, increase the fusion rate.

Overall, by using their innovative technique based on AFM, Oelkers and colleagues have characterized the energy landscape of membrane fusion and how SNARE proteins shape such a landscape by lowering the energy barriers associated with merging of lipid bilayers.

References

1.
Calculating Transition Energy Barriers and Characterizing Activation States for Steps of Fusion.
Ryham RJ, Klotz TS, Yao L, Cohen FS. Biophys J. 2016 Mar 8; 110(5):1110-24
PMID: 26958888 DOI: 10.1016/j.bpj.2016.01.013

2.
How SNARE molecules mediate membrane fusion: recent insights from molecular simulations.
Risselada HJ, Grubmüller H. Curr Opin Struct Biol. 2012 Apr; 22(2):187-96
PMID: 22365575 DOI: 10.1016/j.sbi.2012.01.007

Activity-Dependent Exocytosis of Lysosomes Regulates the Structural Plasticity of Dendritic Spines.

Padamsey Z, McGuinness L, Bardo SJ, Reinhart M, Tong R, Hedegaard A, Hart ML, Emptage NJ.
Neuron 2017 Jan 04; 93(1):132-146
PMID: 27989455 DOI: 10.1016/j.neuron.2016.11.013

How to cite this recommendation

Galli T and Gallo A: F1000Prime Recommendation of [Padamsey Z et al., Neuron 2017 93(1):132-146]. In F1000Prime, 19 Jan 2017; 10.3410/f.727118680.793527370

19 Jan 2017 | New Finding

Lysosomes, classically viewed as the intracellular digestive system of the cell, are also emerging as important intracellular calcium stores, distinct from the ER and mitochondria. Calcium release from lysosomes, driven by a stimulus-dependent production of the second messenger nicotinic acid adenine dinucleotide phosphate (NAADP)

{1} plays a role in neuronal development and differentiation. However, little is known about its involvement in neuronal maintenance and plasticity. Here, the authors found that the activity-dependent cytosolic release of calcium from lysosomes is necessary for long-term plasticity of dendritic spines in hippocampal pyramidal neurons.

Back propagating action potentials (bp-AP) evoke calcium influx in dendrites. Interestingly, lysosomes contribute to this activity-dependent calcium signaling. Indeed the addition of GPN, a drug that transiently disrupts lysosomal compartments, reduces the calcium rise evoked by a bp-AP. Similar results have been obtained by pharmacological agents that specifically inhibit lysosomal calcium storage or release. By imaging lysosomal fusion events in neurons expressing a pH-sensitive version of the lysosomal protein LAMP-2, the authors further demonstrate that lysosomal calcium signaling drives the fusion of lysosomes with the plasma membrane. This results in the release of Cathepsin B. In turn, this leads to ECM remodeling, by eliciting the activity of matrix metalloproteinases, particularly MMP-9, known to be involved in the structural changes occurring during LTP. However, the molecular mechanisms by which these secretion events occur are still unclear. In glial and epithelial cells, the vesicular SNARE VAMP7 mediates lysosome exocytosis and controls the release of Cathepsin B {2} and membrane type 1-matrix metalloproteinase {3}. Further studies are thus required to decipher the molecular mechanisms of neuronal lysosome secretion.

The involvement of lysosomes in the maintenance of long-lasting structural plasticity has been finally confirmed by the inhibition of lysosomal calcium signaling, which abolished the structural enlargement of dendritic spines, typically induced by Hebbian pairing.

The innovation in this elegant study lies in the finding of a role for lysosomal calcium signaling in bp-AP evoked calcium influx in neurons, which regulates the long-term structural plasticity of dendritic spines. This is an exclusive feature of lysosomes, since ER and mitochondrial calcium stores do not contribute to this process.

References

1.
A primer of NAADP-mediated Ca(2+) signalling: From sea urchin eggs to mammalian cells.
Galione A. Cell Calcium. 2015 Jul; 58(1):27-47
PMID: 25449298 DOI: 10.1016/j.ceca.2014.09.010

2.
TI-VAMP/VAMP7 is the SNARE of secretory lysosomes contributing to ATP secretion from astrocytes.
Verderio C, Cagnoli C, Bergami M, Francolini M, Schenk U, Colombo A, Riganti L, Frassoni C, Zuccaro E, Danglot L, Wilhelm C, Galli T, Canossa M, Matteoli M. Biol Cell. 2012 Apr; 104(4):213-28
PMID: 22188132 DOI: 10.1111/boc.201100070

3.
MT1-MMP-dependent invasion is regulated by TI-VAMP/VAMP7.
Steffen A, Le Dez G, Poincloux R, Recchi C, Nassoy P, Rottner K, Galli T, Chavrier P. Curr Biol. 2008 Jun 24; 18(12):926-31
PMID: 18571410 DOI: 10.1016/j.cub.2008.05.044

Lipid transport by TMEM24 at ER-plasma membrane contacts regulates pulsatile insulin secretion.

Lees JA, Messa M, Sun EW, Wheeler H, Torta F, Wenk MR, De Camilli P,Reinisch KM.
Science 2017 02 17; 355(6326)
PMID: 28209843 DOI: 10.1126/science.aah6171

How to cite this recommendation

Galli T and Gallo A: F1000Prime Recommendation of [Lees JA et al., Science 2017 355(6326)]. In F1000Prime, 15 Mar 2017; 10.3410/f.727310557.793529501

15 Mar 2017 | New Finding

The coupling between Ca^{2+} and phosphoinositide signaling drives insulin secretion after glucose stimulation of pancreatic β-cells. This is a two-phase process, taking place with a first rapid exocytosis of granules already docked and primed at the plasma membrane (PM), followed by a second slow phase, where a series of small exocytic bursts occurs in response to pulsatile spikes in Ca^{2+} levels.

Lees and colleagues reported on a role for the ER-resident protein TMEM24 in the coordination of Ca^{2+} pulsatility and phosphoinositide dynamics during insulin secretion. TMEM24 is localized at ER-PM contact sites. Pharmacological experiments based on the inhibition of Ca^{2+} dynamics and Ca^{2+}-mediated signaling showed that such localization is reversible and regulated by Ca^{2+}-dependent phosphorylation and dephosphorylation of its C terminus, the protein detaching from the PM when it is phosphorylated. Interestingly, the pulsatile PM localization of TMEM24 is strictly linked to Ca^{2+} variations after glucose stimulation in insulin-secreting cells: the peak of Ca^{2+} oscillations preceded that of TMEM24 dissociation from the PM, supporting the notion that TMEM24 localization at ER-PM contact sites is Ca^{2+}-dependent. Furthermore Ca^{2+} oscillations were abolished in TMEM24 KO cells, indicating that TMEM24 might contribute to their sustainment.

TMEM24 operates as a lipid transfer protein (LTP) at ER-PM contact sites. Indeed, it harbors a lipid-binding SMP module (shared with other classes of LTPs at ER-PM contact sites, such as the extended-synaptotagmins {1}) known to transport glycerolipids with a preference for phosphatidylinositol (PI). Here, the authors demonstrated the function of TMEM24 as LTP by using a classic *in vitro* lipid transfer assay and a more sophisticated optogenetic approach in living cells. The LTP activity of TMEM24 plays an essential role in maintaining the pool of PM phosphoinositides during insulin secretion. It translocates PI lipids to the PM, where they are converted to phosphatidylinositol-4,5-bisphosphate (PI(4,5)P2) to restore the pool of this lipid, which is depleted from the PM during glucose-stimulated signaling.

This elegant work thus shows how, in the context of ER-PM contact sites, Ca^{2+} and lipid dynamics in the ER are essential in sustaining PM functions. Along the same line, de Juan-Sanz *et al.* recently showed how, during synaptic transmission in neurons, the level of Ca^{2+} in the presynaptic ER, monitored by the ER Ca^{2+} sensing protein STIM1 residing at ER-PM contacts, modulates neurotransmitter release {2}. Altogether these studies suggest that ER-PM contacts regulate conventional secretory mechanisms via both Ca^{2+} and phosphoinositides regulation in endocrine and neuronal cells.

References

1.
Structure of a lipid-bound extended synaptotagmin indicates a role in lipid transfer.
Schauder CM, Wu X, Saheki Y, Narayanaswamy P, Torta F, Wenk MR, De Camilli P, Reinisch KM. Nature. 2014 Jun 26; 510(7506):552-5
PMID: 24847877 DOI: 10.1038/nature13269

2.
Axonal endoplasmic reticulum ca(2+) content controls release probability in CNS nerve terminals.
de Juan-Sanz J, Holt GT, Schreiter ER, de Juan F, Kim DS, Ryan TA. Neuron. 2017 Feb 22; 93(4):867-881.e6
PMID: 28162809 DOI: 10.1016/j.neuron.2017.01.010

Dilation of fusion pores by crowding of SNARE proteins.

Wu Z, Bello OD, Thiyagarajan S, Auclair SM, Vennekate W, Krishnakumar SS,O'Shaughnessy B, Karatekin E.

elife 2017 03 27; 6
PMID: 28346138 DOI: 10.7554/eLife.22964

How to cite this recommendation
Galli T and Gallo A: F1000Prime Recommendation of [Wu Z et al., elife 2017 6]. In F1000Prime, 11 May 2017; 10.3410/f.727446608.793531537

11 May 2017 | New Finding

Membrane fusion during vesicle exocytosis begins with the formation of an initial narrow connection between the two fusing compartments, called the fusion pore. Fusion pore is initiated by the assembly of v-SNARE proteins on the vesicle with their cognate t-SNAREs on the target membrane. This newly formed structure is metastable, indeed it flickers repeatedly and then expands or reseals during the release of hormones and neurotransmitters.

Methods combining electrophysiology and high-resolution optical systems have been used to study fusion pore dynamics. However, these approaches do not allow deduction of quantitative information about the molecular mechanism of fusion pore nucleation and dilation. This limit has been overcome by Wu and colleagues. In a previous paper, they developed an assay to probe single fusion pore dynamics based on a nanodisc-cell fusion system {1}. Such a system uses nanometer-sized lipid particles (NLPs), bearing V-SNAREs and large enough to allow the expansion of a fusion pore, and “tCells” expressing engineered cognate “flipped” t-SNAREs, with the active SNARE domains facing the extracellular space rather than the cytosol. The “open” configuration of NLPs allows a direct measurement of currents between cytosol and extracellular space after fusion between NLPs and voltage-clumped tCell membranes, providing information about some properties of single pore geometry.

Here, the authors have measured the currents through voltage-clamped pores using NLPs bearing a varying copy number of v-SNARE, and they have found that only two SNARE complexes are required to reach the maximal nucleation rate. On the other hand, pore dilation requires a much higher number of proteins, as demonstrated by a dramatic increase in pore conductance and radius when the number of v-SNAREs per NLP face reaches fifteen.

Through the analysis of free energy profiles associated to fusion pores generated by an increasing number of SNAREs, they propose a model to explain how fusion pore dilation is driven by SNARE proteins. In protein-free pores a net force of 22pN generated by membrane bending and tension resists to pore expansion. In SNARE-populated pores, the crowding effect of SNAREs produces an entropic force that lowers the resisting force from 22pN to a minimum of 5pN (when 15 SNARE complexes are present), thus driving pore expansion.

Overall, by using a sophisticated experimental approach combined with computational analysis, Wu *et al.* quantitatively demonstrated how SNARE availability is essential in the regulation of the balance between transient versus full fusion. The notion that SNARE crowding may underlie transient *vs* full fusion will certainly require further experiments.

References

1.
Nanodisc-cell fusion: control of fusion pore nucleation and lifetimes by SNARE protein transmembrane domains.
Wu Z, Auclair SM, Bello O, Vennekate W, Dudzinski NR, Krishnakumar SS, Karatekin E. Sci Rep. 2016 Jun 06; 6:27287
PMID: 27264104 DOI: 10.1038/srep27287

ER-plasma membrane contact sites contribute to autophagosome biogenesis by regulation of local PI3P synthesis.

Nascimbeni AC, Giordano F, Dupont N, Grasso D, Vaccaro MI, Codogno P, Morel E.
EMBO J 2017 07 14; 36(14):2018-2033
PMID: 28550152 DOI: 10.15252/embj.201797006

How to cite this recommendation
Galli T and Gallo A: F1000Prime Recommendation of [Nascimbeni AC et al.,EMBO J 2017 36(14):2018-2033]. In F1000Prime, 11 Jul 2017; 10.3410/f.727658081.793533982

11 Jul 2017 | New Finding

Autophagy, a catabolic process of cytoplasmic material, occurs through the formation of a double-membrane organelle, called autophagosome, and its subsequent fusion with lysosomes for degradation. Autophagosomes biogenesis requires phosphatidylinositol 3-phosphate [PI(3)P], and begins from sites on the endoplasmic reticulum (ER) positive for PI3P and PI3P-binding proteins, termed omegasomes {1}.

The implication for autophagy of the ER is well established; indeed, it provides a platform for expansion of autophagosomal membranes, and its connections with other intracellular membrane bound compartments might play a role in the mechanism by which the ER, together with its partner organelle, participates in autophagosome formation.

In this article, Nascimbeni and colleagues reported on a role for ER-plasma membrane (PM) contact sites in the early steps of autophagosome biogenesis.

By using a combination of high resolution imaging, electron microscopy and biochemical experiments, the authors observed that HeLa cells under starvation, a condition that induces autophagy, show an increase in the number of ER-PM contact sites. These sites are positive for the extended synaptotagmins (E-Syts), a family of proteins which play a central role in the formation of ER-PM tethering zones, and for LC3, an early autophagy marker, indicating that phagophores and/or autophagosomes could be associated to these contacts. In E-Syts-overexpressing cells, a higher number of LC3 positive puncta at the PM, as well as an increase of protein degradation, was found. These data suggest that the autophagic structures arising from E-Syt-induced ER-PM contact sites are likely to be functional.

The first signature of autophagosomal membrane emergence is the synthesis of PI3P by the class 3 PI3Kinase complex (PI3KC3), which includes VPS34, Beclin-1, and ATG14L. Interestingly, PI3P puncta were observed in ER regions positive for E-Syts and LC3, and the number of such puncta was reduced in E-Syt triple knock-down cells. Furthermore, after autophagy induction, E-Syts co-localized and co-immunoprecipitated with Beclin1 and VMP1, a regulating adaptor that participates in PI3P synthesis by recruiting Beclin1. This last set of data proposes a role for E-Syts in PI3P synthesis required for autophagosome biogenesis by acting as a scaffold for the PI3KC3 complex at ER-PM contact sites.

Previously, ER-mitochondria contact sites had been found to be implicated in the regulation of autophagosome biogenesis {2}; here, the authors demonstrated the involvement of a second class of contacts, the ER-PM contact sites, in such a process, opening a new field of research on the role of interconnections between ER and other membrane compartments in autophagy.

References

1.
Autophagosome formation from membrane compartments enriched in phosphatidylinositol 3-phosphate and dynamically connected to the endoplasmic reticulum.
Axe EL, Walker SA, Manifava M, Chandra P, Roderick HL, Habermann A, Griffiths G, Ktistakis NT. J Cell Biol. 2008 Aug 25; 182(4):685-701
PMID: 18725538 DOI: 10.1083/jcb.200803137

2.
Autophagosomes form at ER-mitochondria contact sites.

Hamasaki M, Furuta N, Matsuda A, Nezu A, Yamamoto A, Fujita N, Oomori H, Noda T, Haraguchi T, Hiraoka Y, Amano A, Yoshimori T. Nature. 2013 Mar 21; 495(7441):389-93
PMID: 23455425 DOI: 10.1038/nature11910

Golgi-Resident Gαo Promotes Protrusive Membrane Dynamics.

Solis GP, Bilousov O, Koval A, Lüchtenborg AM, Lin C, Katanaev VL.
Cell 2017 Aug 24; 170(5):939-955.e24
PMID: 28803726 DOI: 10.1016/j.cell.2017.07.015

How to cite this recommendation
Galli T and Gallo A: F1000Prime Recommendation of [Solis GP et al., Cell 2017170(5):939-955.e24]. In F1000Prime, 13 Sep 2017; 10.3410/f.728639728.793536390

13 Sep 2017 | New Finding

Heterotrimeric G proteins, composed of three subunits, α β and γ, are the major signaling switches that turn on intracellular signaling cascades in eukaryotic cells. G proteins are activated by G protein-coupled receptors (GPCRs). GPCRs act as guanine nucleotide exchange factors, which induce an exchange of guanosine diphosphate (GDP) to guanosine triphosphate (GTP) on the Gα and its subsequent dissociation from Gβγ subunits. Gα-GTP then modulates the activity of downstream effectors, and the specificity of this signal depends on the different Gα targets.

Gαo is the major G protein in the nervous system, and it controls a variety of evolutionarily conserved programs in both development and adulthood. However, despite its crucial roles, only few molecular targets of Gαo were known. In this study, Solis and colleagues have significantly enriched the list of Gαo partners by performing a combination of different screens (yeast two-hybrid, proteomics, fly genetics, and RNAi) and bioinformatic analysis. The Gαo interactome identified is composed of more than 250 proteins, in different functional modules.

Among these modules, the authors focused on the vesicular trafficking subset of Gαo targets and on neuritogenesis and protrusion formation, two processes that require vesicle-mediated transport. They found that expression of Gαo induced massive neurite and protrusion outgrowth, in mouse neuroblastoma N2a cells and in Drosophila S2 cells, respectively. In both Drosophila and mammalian systems, Gαo displayed a dual localization: at the plasma membrane (PM) and in the Golgi apparatus. The Golgi pool of Gαo was found to be activated by KDELR, a Golgi-resident GPCR receptor, and the active form of Gαo to interact and activate the small GTPases Rab1 and Rab3, as demonstrated by pull-down and co-localization experiments. The overexpression of these small GTPases strongly potentiated the Gαo-induced protrusion formation, but not the proportion of neurite-forming cells or the number of neurites per cells, indicating that the functional interaction between Gαo and these proteins is important for the elongation, but not for the initiation of protrusions.

Based on their findings, as well as previous studies, the authors propose a model in which the PM and the Golgi pools of Gαo cooperate in outgrowth and protrusion. The PM pool of protein would initiate protrusion formation through cytoskeleton regulation {1}, and the Golgi-resident Gαo would contribute to elongation and maintenance of cell protrusions by stimulating the vesicular trafficking from Golgi to PM via KDELR-Gαo-Rab1/3 signaling. Future studies should certainly address the quest for potential molecular mechanisms coordinating the two pools of Gαo.

References

1.
Heterotrimeric Go protein links Wnt-Frizzled signaling with ankyrins to regulate the neuronal microtubule cytoskeleton.
Lüchtenborg AM, Solis GP, Egger-Adam D, Koval A, Lin C, Blanchard MG, Kellenberger S, Katanaev VL. Development. 2014 Sep; 141(17):3399-409
PMID: 25139856 DOI: 10.1242/dev.106773

Control of Cell Shape, Neurite Outgrowth, and Migration by a Nogo-A/HSPG Interaction.

Kempf A, Boda E, Kwok JCF, Fritz R ... Fawcett JW, Pertz O, Buffo A, Schwab ME.
Dev Cell 2017 10 09; 43(1):24-34.e5
PMID: 28943240 DOI: 10.1016/j.devcel.2017.08.014

How to cite this recommendation
Galli T and Gallo A: F1000Prime Recommendation of [Kempf A et al., Dev Cell 2017 43(1):24-34.e5]. In F1000Prime, 01 Nov 2017; 10.3410/f.731255319.793538314

1 Nov 2017 | New Finding

Nogo-A is one of the most potent anti-adhesive and neurite growth inhibiting factors in the central nervous system. It is enriched in oligodendrocytes and mostly associated with the endoplasmic reticulum (ER), but is also found at the cell surface in several types of neurons and glial cells, where it is involved in a variety of functions, both in development and the adult brain {1}. Despite its well documented activity and function, little is known about the mechanisms by which the Nogo-A-induced downstream signals are activated.

In this work, Kempf and colleagues identified the cell-surface heparan sulfate proteoglycans (HSPGs) as functional receptors of the extracellular active domain of Nogo-A, namely Nogo-A-Δ20. HSPGs consist of a protein module that determines whether the proteoglycans are localized on the cell surface or in the extracellular matrix (ECM), and one or more covalently attached heparan sulfate chains (HS) that generally act as co-receptors for extracellular ligands, such as growth factors and adhesion molecules, modulating cell adhesion, migration, proliferation and differentiation processes during development {2}.

The role of cell surface HS in Nogo-A-Δ20 function has been determined by monitoring cell spreading inhibition in Swiss 3T3 cells treated with heparinase III (HepIII), which cleaves HS. In these conditions, cell spreading on Nogo-A-Δ20-coated culture dishes increased compared to control conditions. Similar experiments have been performed in a variety of neuronal cell types, i.e. cerebellar granule cells, dorsal root ganglion neurons and embryonic cortical neurons, where the Nogo-A-Δ20-mediated inhibition of neurite outgrowth was abolished after HS cleavage by HepIII. Overall, these results suggest that HS not only bind Nogo-A-Δ20, but are also required for its function.

Nogo-A inhibits neurite outgrowth and cell spreading through the activation of the RhoA/ROCK signaling, which leads to destabilization of the actin cytoskeleton {3}. Here, the authors found that HSPGs also mediate this step of Nogo-A-Δ20 inhibition. Indeed, as expected, they observed an increase in RhoA activation after application of Nogo-A-Δ20 in wild-type CHO cells, but no increase was detected in pgsD-677 cells, an HS-deficient mutant CHO cell line. Finally, they identified Syndecan-4 and Syndecan-3, which are members of the transmembrane HSPCs, as cell-specific mediators of Nogo-A-Δ20 inhibition of cell spreading and neurite outgrowth, respectively.

Based on their observations, Kempf et al. propose a mechanism by which Nogo-A-Δ20 exerts its inhibitory effects by affecting cytoskeletal dynamics through a cell-specific interaction with members of the transmembrane HSPG family. Future studies are necessary to further characterize the Nogo-A-Δ20-activated transduction upon extracellular binding to the HS chains, which might involve the cytoplasmic tails of syndecans.

References

1.
Functions of Nogo proteins and their receptors in the nervous system.
Schwab ME. Nat Rev Neurosci. 2010 12; 11(12):799-811
PMID: 21045861 DOI: 10.1038/nrn2936

2.
Heparan sulfate proteoglycans.
Sarrazin S, Lamanna WC, Esko JD. Cold Spring Harb Perspect Biol. 2011 Jul 01; 3(7)
PMID: 21690215 DOI: 10.1101/cshperspect.a004952

3.
Nogo-A and myelin-associated glycoprotein mediate neurite growth inhibition by antagonistic regulation of RhoA and Rac1.
Niederöst B, Oertle T, Fritsche J, McKinney RA, Bandtlow CE. J Neurosci. 2002 Dec 01; 22(23):10368-76
PMID: 12451136

The Neuronal Gene Arc Encodes a Repurposed Retrotransposon Gag Protein that Mediates Intercellular RNA Transfer.

Pastuzyn ED, Day CE, Kearns RB, Kyrke-Smith M ... Morado DR, Briggs JAG,Feschotte C, Shepherd JD.
Cell 2018 01 11; 172(1-2):275-288.e18
PMID: 29328916 DOI: 10.1016/j.cell.2017.12.024

How to cite this recommendation

Galli T and Gallo A: F1000Prime Recommendation of [Pastuzyn ED et al., Cell 2018 172(1-2):275-288.e18]. In F1000Prime, 02 Feb 2018; 10.3410/f.732441824.793542062

2 Feb 2018 | New Finding

Communication within the nervous system and between the nervous system and other organs relies on classical communication systems via chemical and electrical synapses. In addition, recent studies have identified novel *trans*-cellular communication routes mediated by extracellular vesicles (EVs), such as exosomes and microvesicles {1}. However, the molecular machinery that governs these mechanisms of intercellular transport still needs to be uncovered.

Here the authors found a striking link between neuronal communication and retrovirus. Indeed, interspersed sequences of viral and retrotransposon origin compose the 50% of animal genomes. In many cases, these transposable elements generate protein-coding genes, many of which are expressed in the brain, but their molecular functions is still unclear. The present report shows that the mammalian activity-regulated cytoskeleton-associated protein (Arc) belongs to the retroviral group-specific antigen (Gag) polyproteins. Their finding starts with the observation that ARC forms retroviral capsid-like structures when expressed in bacteria. Phylogenetic reconstructions show that Arc genes originated from the Ty3/gypsy retrotransposon, which shares high homology with Gag proteins. By using a multi-technical approach, the authors then propose a novel mechanism of Arc-mediated intercellular trafficking of RNAs, in which Arc, similarly to Gag proteins, is self-assembled into capsids, which encapsulate RNAs, and it is released in EVs, which allow the transfer of mRNAs into target cells. *In vitro* approaches, such as negative stain- and cryo-EM on purified Arc and qRT-PCR on Arc mRNAs from bacteria lysates, show the ability of this protein to assemble into virus-like capsids and to encapsulate RNAs. *In vivo* studies in cells lines and neurons show that Arc mRNA and protein can be released by donor cells via EVs and taken up by recipient cells by endocytosis. Finally, they found that the transferred Arc mRNA is accessible for activity-dependent translation (a key process for synaptic plasticity), as demonstrated by the increase in the levels

of dendritic Arc protein in neurons treated with DHPG, a drug that induces translation by activating the group 1 metabotropic glutamate receptors (mGluR1/5).

Arc is a master regulator of synapse maturation, synaptic plasticity and memory consolidation. Its mRNA is rapidly transcribed and targeted to active dendritic spines, where it is locally translated during synaptic plasticity {2}. Mutations in Arc are associated with various neurological disorders, including Alzheimer's disease {3} and schizophrenia {4}. Thus, understanding the molecular mechanisms of its function is essential to better determine how brains work in both physiological and pathological conditions. Overall, this elegant study by Pastuzyn and colleagues proposes a ground-breaking mechanism of Arc EV-mediated *trans*-synaptic signaling during synaptic plasticity, changing current vision on the role of Arc within the nervous system.

References

1.
Extracellular vesicles round off communication in the nervous system.
Budnik V, Ruiz-Cañada C, Wendler F. Nat Rev Neurosci. 2016 Mar; 17(3):160-72
PMID: 26891626 DOI: 10.1038/nrn.2015.29

2.
Selective localization of arc mRNA in dendrites involves activity- and translation-dependent mRNA degradation.
Farris S, Lewandowski G, Cox CD, Steward O. J Neurosci. 2014 Mar 26; 34(13):4481-93
PMID: 24671994 DOI: 10.1523/JNEUROSCI.4944-13.2014

3.
Arc/Arg3.1 regulates an endosomal pathway essential for activity-dependent β-amyloid generation.
Wu J, Petralia RS, Kurushima H, Patel H, Jung MY, Volk L, Chowdhury S, Shepherd JD, Dehoff M, Li Y, Kuhl D, Huganir RL, Price DL, Scannevin R, Troncoso JC, Wong PC, Worley PF. Cell. 2011 Oct 28; 147(3):615-28
PMID: 22036569 DOI: 10.1016/j.cell.2011.09.036

4.
De novo mutations in schizophrenia implicate synaptic networks.
Fromer M, Pocklington AJ, Kavanagh DH, Williams HJ, Dwyer S, Gormley P, Georgieva L, Rees E, Palta P, Ruderfer DM, Carrera N, Humphreys I, Johnson JS, Roussos P, Barker DD, Banks E, Milanova V, Grant SG, Hannon E, Rose SA, Chambert K, Mahajan M, Scolnick EM, Moran JL, Kirov G, Palotie A, McCarroll SA, Holmans P, Sklar P, Owen MJ, Purcell SM, O'Donovan MC. Nature. 2014 Feb 13; 506(7487):179-84
PMID: 24463507 DOI: 10.1038/nature12929

Impairment of Release Site Clearance within the Active Zone by Reduced SCAMP5 Expression Causes Short-Term Depression of Synaptic Release.

Park D, Lee U, Cho E, Zhao H ... Regan P, Ho WK, Cho K, Chang S.

*Cell Rep*2018 Mar 20; 22(12):3339-3350
PMID: 29562188 DOI: 10.1016/j.celrep.2018.02.088

How to cite this recommendation

Galli T and Gallo A: F1000Prime Recommendation of [Park D et al., Cell Rep 201822(12):3339-3350]. In F1000Prime, 12 Apr 2018; 10.3410/f.732882871.793544509

12 Apr 2018 | New Finding

Secretory carrier membrane proteins (SCAMPs) represent a family of highly conserved membrane proteins present in transport vesicles. Some SCAMP members, such as SCAMPs 1 and 5, are highly enriched in brain and synaptic vesicles (SVs). However, the relatively mild phenotype of the SCAMP1 knockout mice {1}, particularly in the brain, raises the possibility that the second dominant isoform within the brain, SCAMP5, may also play a role in synaptic function.

Here, Park and colleagues show that SCAMP5 is involved in release site clearance at active zones during intense neuronal activity, assessing for the first time a specialized function for SCAMP5 in synaptic transmission.

By using immunoprecipitation assays, they show that SCAMP5 interacts with the µ2 subunit of adaptor protein 2 (AP2-µ2), an endocytic protein involved in the clearance of SV components from release sites whose silencing causes short-term depression (STD) of synaptic transmission {2}. Interestingly, whole-cell voltage-patch clamp recordings of SCAMP5 knockdown neurons showed a phenotype of fast STD similar to that observed when AP2-

μ2 is silenced. Such STD is followed by a slower recovery of the recycling SV pool. Finally, combining electrophysiological experiments and super-resolution microscopy, the authors show that the stimulation frequency-dependent STD observed in SCAMP5 knockdown neurons is the result of an inefficient release site clearance within the active zone. Overall, these data suggest that SCAMP5 plays a critical role in SV endocytosis and in release site clearance, a function that is accomplished together with its partner AP-μ2.

SCAMP5 has been identified, together with NBEA and AMYSIN, as a candidate gene for autism, and its expression is reduced to 40% in a patient with idiopathic sporadic autism {3}. In essence, the present report provides important evidence in support of a link between a reduced expression of SCAMP5 and synaptic dysfunction observed in patients with autism.

References

1.
Analysis of SCAMP1 function in secretory vesicle exocytosis by means of gene targeting in mice.
Fernández-Chacón R, Alvarez de Toledo G, Hammer RE, Südhof TC. J Biol Chem. 1999 Nov 12; 274(46):32551-4
PMID: 10551807

2.
Disruption of adaptor protein 2μ (AP-2μ) in cochlear hair cells impairs vesicle reloading of synaptic release sites and hearing.
Jung S, Maritzen T, Wichmann C, Jing Z, Neef A, Revelo NH, Al-Moyed H, Meese S, Wojcik SM, Panou I, Bulut H, Schu P, Ficner R, Reisinger E, Rizzoli SO, Neef J, Strenzke N, Haucke V, Moser T. EMBO J. 2015 Nov 03; 34(21):2686-702
PMID: 26446278 DOI: 10.15252/embj.201591885

3.
SCAMP5, NBEA and AMISYN: three candidate genes for autism involved in secretion of large dense-core vesicles.
Castermans D, Volders K, Crepel A, Backx L, De Vos R, Freson K, Meulemans S, Vermeesch JR, Schrander-Stumpel CT, De Rijk P, Del-Favero J, Van Geet C, Van De Ven WJ, Steyaert JG, Devriendt K, Creemers JW. Hum Mol Genet. 2010 Apr 1; 19(7):1368-78
PMID: 20071347 DOI: 10.1093/hmg/ddq013

Cytochrome c is an oxidative stress-activated plasmalogenase that cleaves plasmenylcholine and plasmenylethanolamine at the sn-1 vinyl ether linkage.

Jenkins CM, Yang K, Liu G, Moon SH, Dilthey BG, Gross RW.
J Biol Chem 2018 Jun 01; 293(22):8693-8709
PMID: 29530984 DOI: 10.1074/jbc.RA117.001629

How to cite this recommendation

Galli T and Gallo A: F1000Prime Recommendation of [Jenkins CM et al., J Biol Chem 2018 293(22):8693-8709]. In F1000Prime, 21 Jun 2018; 10.3410/f.732838273.793547101

21 Jun 2018 | New Finding, Novel Drug Target

Plasmalogens represent a major subclass of glycerophospholipids, the synthesis of which is initiated in peroxisomes and completed in the endoplasmic reticulum.

Although plasmalogens are constituents of all mammalian tissues, they are particularly enriched in heart and brain. These organs are sensitive to plasmalogen concentrations, as indeed a reduction in their levels is

associated with phenotypes ranging from augmented sensitivity to oxidative stress {1} to neurological disorders, such as Alzheimer's disease (AD) {2}.

The unique molecular structure of plasmalogens, namely a vinyl ether linkage at the sn-1 position and polyunsaturated fatty acids at the sn-2 position of the glycerol backbone, has intrigued researchers for decades. However, hitherto it has been difficult to assess their biophysical roles in cell membrane functioning, mainly due to the lack of suitable methodologies.

In this work, Jenkins and colleagues have identified the cytochrome C (cyt C) as the first protein able to cleave plasmalogens, paving the way for a better understanding of the pathophysiological roles of this class of phospholipids in cells.

Cyt *C* is a heme protein localized in the compartment between the inner and outer mitochondrial membranes, where it transfers electrons between complex III and complex IV of the respiratory chain. During oxidative stress, cyt C binds to the mitochondrion-specific phospholipid cardiolipin (CL), undergoing a conformational change that confers a novel peroxidase activity on the protein {3}.

By using a combination of stable isotope experiments and mass spectrometric analysis, the authors demonstrated that, in the presence of CL and H_2O_2, the conformationally altered cyt C catalyzes the oxidation of the vinyl ether linkage of plasmalogens, promoting its hydrolytic cleavage. This results in the generation of two lipid molecules that act as novel signaling messengers generated from plasmalogen-rich membranes.

The plasmalogenase activity of cyt C is also triggered by other negatively charged phospholipids (i.e. phosphatidylinositol phosphates), indicating that, besides the inner mitochondrial bilayer, when released from mitochondria during oxidative stress, cyt C can also target other membrane compartments, such as the plasma membrane.

Furthermore, they showed that also the cyt C released by myocardial mitochondria mediates a plasmalogenase activity that generates lipid signaling molecules acting during ischemia-induced oxidative stress.

Overall, the present report identifies cyt C as a key regulator of novel plasmalogen-mediated lipid signaling pathways that participates in physiological and pathological cellular functions. This opens up new frontiers for the development of novel potential therapeutic targets in diseases such as stroke and neurological disorders, where oxidative stress leads to massive amounts of plasmalogen breakdown.

References

1.
Plasmalogen degradation by oxidative stress: production and disappearance of specific fatty aldehydes and fatty alpha-hydroxyaldehydes.
Stadelmann-Ingrand S, Favreliere S, Fauconneau B, Mauco G, Tallineau C. Free Radic Biol Med. 2001 Nov 15; 31(10):1263-71
PMID: 11705705

2.
Disease and anatomic specificity of ethanolamine plasmalogen deficiency in Alzheimer's disease brain.
Ginsberg L, Rafique S, Xuereb JH, Rapoport SI, Gershfeld NL. Brain Res. 1995 Nov 06; 698(1-2):223-6
PMID: 8581486

3.
Cardiolipin drives cytochrome c proapoptotic and antiapoptotic actions.
Ascenzi P, Polticelli F, Marino M, Santucci R, Coletta M. IUBMB Life. 2011 Mar; 63(3):160-5
PMID: 21445846 DOI: 10.1002/iub.440

Aspirin induces lysosomal biogenesis and attenuates amyloid plaque pathology in a mouse model of alzheimer's disease via pparα.

Chandra S, Jana M, Pahan K.
J Neurosci 2018 Jul 25; 38(30):6682-6699
PMID: 29967008 DOI: 10.1523/JNEUROSCI.0054-18.2018

How to cite this recommendation

Galli T and Gallo A: F1000Prime Recommendation of [Chandra S et al., J Neurosci 2018 38(30):6682-6699]. In F1000Prime, 17 Jul 2018; 10.3410/f.733575200.793548126

17 Jul 2018 | Controversial, Interesting Hypothesis, New Finding, Novel Drug Target

Aberrant accumulation of endogenous, misfolded, toxic proteins, leading to the formation of cytotoxic aggregates, is a frequent feature of neurodegenerative diseases, which, for this reason, often correspond to proteinopathies. The most common of such disorders, Alzheimer's disease (AD), is characterized by the formation of extracellular plaques, consisting of insoluble aggregated amyloid-β (Aβ) peptides and intracellular neurofibrillary tangles (NFTs) containing aggregated microtubule-associated protein tau.
A large number of studies have reported on a link between dysfunctional autophagy–lysosomal intracellular degradation system and AD. Accumulation of autophagic vacuoles containing Aβ peptides in affected neurons {1}, as well as impaired Aβ clearance {2}, are indeed two of the main hallmarks of AD pathogenesis. Therefore, promoting autophagic degradation, either by inducing autophagosome formation or enhancing lysosomal function, might provide potential therapeutic strategies to rescue the amyloid pathogenesis in AD. Along this line of research is the work of Chandra and colleagues, who discovered a non-canonical role for aspirin, the most widespread anti-inflammatory drug, in decreasing the amyloid plaque pathology in AD by stimulating lysosomal biogenesis and function.
By integrating multiple experimental approaches, including electron microscopy, immunocytochemistry, quantitative real-time PCR and *in vitro*assays, the authors showed that a low dose of aspirin can stimulate lysosomal biogenesis in mouse primary astrocytes through the activation of peroxisome proliferator-activated receptor α (PPARα), which in turn stimulates the expression of the central regulator of the lysosomal machinery, TFEB. TFEB is a transcription factor previously shown to master the expression of lysosomal-related genes {3}. Furthermore, the aspirin-mediated lysosomal biogenesis enhances the uptake and the subsequent degradation of Aβ by astrocytes. Finally, the authors further confirmed this novel effect of aspirin, *in vivo,* by showing that oral administration of low dose of aspirin enhanced lysosomal biogenesis and decreased amyloid plaque pathology in the 5XFAD mouse model of AD.
Previous works had already highlighted a potential connection between aspirin consumption and reduced risk of Alzheimer's dementia {4}. On the contrary, other studies found no evidence that low dose aspirin decreases the risk of cognitive decline {5}. Despite this ongoing controversy, the present report provides important evidence in support of a protective role of aspirin in AD pathogenesis, proposing a novel mechanism of action for this drug that favors its therapeutic use in AD treatment.

References

1.
Macroautophagy--a novel Beta-amyloid peptide-generating pathway activated in Alzheimer's disease.
Yu WH, Cuervo AM, Kumar A, Peterhoff CM, Schmidt SD, Lee JH, Mohan PS, Mercken M, Farmery MR, Tjernberg LO, Jiang Y, Duff K, Uchiyama Y, Näslund J, Mathews PM, Cataldo AM, Nixon RA. J Cell Biol. 2005 Oct 10; 171(1):87-98
PMID: 16203860 DOI: 10.1083/jcb.200505082

2.
Decreased clearance of CNS beta-amyloid in Alzheimer's disease.
Mawuenyega KG, Sigurdson W, Ovod V, Munsell L, Kasten T, Morris JC, Yarasheski KE, Bateman RJ. Science. 2010 Dec 24; 330(6012):1774
PMID: 21148344 DOI: 10.1126/science.1197623

3.
A gene network regulating lysosomal biogenesis and function.
Sardiello M, Palmieri M, di Ronza A, Medina DL, Valenza M, Gennarino VA, Di Malta C, Donaudy F, Embrione V, Polishchuk RS, Banfi S, Parenti G, Cattaneo E, Ballabio A. Science. 2009 Jul 24; 325(5939):473-7
PMID: 19556463 DOI: 10.1126/science.1174447

4.
Does aspirin protect against Alzheimer's dementia? A study in a Swedish population-based sample aged > or =80 years.
Nilsson SE, Johansson B, Takkinen S, Berg S, Zarit S, McClearn G, Melander A. Eur J Clin Pharmacol. 2003 Aug; 59(4):313-9
PMID: 12827329 DOI: 10.1007/s00228-003-0618-y

5.
Low-Dose Aspirin Use and Cognitive Function in Older Age: A Systematic Review and Meta-analysis.
Veronese N, Stubbs B, Maggi S, Thompson T, Schofield P, Muller C, Tseng PT, Lin PY, Carvalho AF, Solmi M. J Am Geriatr Soc. 2017 Aug; 65(8):1763-1768
PMID: 28425093 DOI: 10.1111/jgs.14883

Precisely measured protein lifetimes in the mouse brain reveal differences across tissues and subcellular fractions.

Fornasiero EF, Mandad S, Wildhagen H, Alevra M ... Bonn S, Simons M, Urlaub H, Rizzoli SO.
Nat Commun 2018 10 12; 9(1):4230
PMID: 30315172 DOI: 10.1038/s41467-018-06519-0

How to cite this recommendation
Galli T and Gallo A: F1000Prime Recommendation of [Fornasiero EF et al., Nat Commun 2018 9(1):4230]. In F1000Prime, 05 Nov 2018; 10.3410/f.734222062.793552310

5 Nov 2018 | New Finding, Technical Advance

Protein turnover, the result of protein synthesis and degradation which sets their relative abundance, is a fundamental process in cellular homeostasis. In the last few decades, advances in mass spectrometry-based technologies combined with pulse-chase SILAC (Stable Isotope Labeling in Cell Culture) techniques have efficiently improved protein turnover measurements *in vitro* {1,2}. However, the application of similar pulse-chase protocols in living animals is still challenging, due to technical difficulties related to the initially non-labeled pool of amino acids that can be reused after the degradation of pre-existing proteins. To overcome this problem, Fornasiero and colleagues have developed an elaborate *in vivo* pulse strategy workflow that allows to measure with high accuracy the lifetime of more than 3500 proteins in the mouse brain.

With this method, mice were pulsed with a conventional SILAC diet containing C6-lysine for three times (5, 14 or 21 days). Then the researchers dissected the cortices and carried out mass spectrometry analyses to detect the C6-lysine-containing newly synthesized proteins. Mass spectrometry results were then interpreted to provide protein lifetimes. The main improvements in the determination of protein turnover *in vivo*include the development of a mathematical model to take into account the inclusion of non-labeled lysines deriving from protein degradation into the newly synthesized proteins. To experimentally verify this theoretical model, the authors conducted several independent controls, some of which were performed for the first time *in vivo*, using techniques such as gas chromatography mass spectrometry (GC-MS), to measure the soluble C6-lysine pool in the mouse blood plasma, or tamoxifen-inducible systems, and determine whether or not the C6-lysine incorporation in exogenous proteins reflects the one predicted by the model.

The large dataset obtained in this study not only increases the knowledge of brain protein lifetimes, but it also provides an efficient tool to study a set of molecular events occurring for instance in learning, under drug treatments and in neurodegeneration.

References

1.
Systematic analysis of protein turnover in primary cells.
Mathieson T, Franken H, Kosinski J, Kurzawa N, Zinn N, Sweetman G, Poeckel D, Ratnu VS, Schramm M, Becher I, Steidel M, Noh KM, Bergamini G, Beck M, Bantscheff M, Savitski MM. Nat Commun. 2018 02 15; 9(1):689
PMID: 29449567 DOI: 10.1038/s41467-018-03106-1

2.
Metabolic turnover of synaptic proteins: kinetics, interdependencies and implications for synaptic maintenance.
Cohen LD, Zuchman R, Sorokina O, Müller A, Dieterich DC, Armstrong JD, Ziv T, Ziv NE. PLoS ONE. 2013; 8(5):e63191
PMID: 23658807 DOI: 10.1371/journal.pone.0063191

Altered distribution of ATG9A and accumulation of axonal aggregates in neurons from a mouse model of AP-4 deficiency syndrome.

De Pace R, Skirzewski M, Damme M, Mattera R ... Han TU, Mancini GMS,Buonanno A, Bonifacino JS.
PLoS Genet 2018 04; 14(4):e1007363
PMID: 29698489 DOI: 10.1371/journal.pgen.1007363

How to cite this recommendation
Galli T and Gallo A: F1000Prime Recommendation of [De Pace R et al., PLoS Genet 2018 14(4):e1007363]. In F1000Prime, 19 Dec 2018; 10.3410/f.733111608.793554272

19 Dec 2018 | New Finding

Autophagy has been linked to neurodegeneration but how it precisely contributes at molecular and cellular levels is still largely unknown.

In this paper, De Pace and colleagues have described a knockout (KO) mouse for the expression of the e subunit of the human adaptor protein 4 (AP-4) as a suitable animal model for AP-4 deficiency syndrome, providing a novel tool to investigate the pathogenesis of this disease. AP-4 deficiency syndrome is indeed a subset of hereditary spastic paraplegia (HSP) caused by mutations in four loci encoding the subunits of AP-4, a heterotetrameric adaptor protein complex located in the *trans*-Golgi network (TGN) and involved in the sorting of transmembrane cargos in post-Golgi compartments of the endomembrane system {1}.

AP-4 e deficient mice exhibit a set of pathological characteristics that are consistent with several clinical features observed in patients, such as motor and behavioral defects, a thin corpus callosum and axonal spheroid and swelling, as observed by behavioral tests in combination with MRI and histological analysis. Immunostaining of sections from different brain regions revealed an accumulation at the TGN of the transmembrane autophagy protein ATG9A in AP-4 e KO neurons. This mislocalization, also observed in fibroblast of AP-4 deficient patients, reveals a failure in the delivering of ATG9A from the Golgi complex to the cell periphery. In axons, autophagy is essential for the degradation of protein aggregates, the accumulation of which leads to neuronal degeneration. Interestingly, the authors found that the redistribution of ATG9A was associated with an increased accumulation of mutant huntingtin aggregates in axons of AP-4 e KO neurons. Autophagic defects and impaired aggregate clearance might thus contribute to the axonal dystrophy observed in AP-4 ε KO mice and, eventually, to the neurological symptoms of AP-4 deficiency in humans.

Overall, the new mouse model of AP-4 deficiency syndrome characterized in this report not only reflects the typical neurological phenotype and motor deficits consistent with those observed in patients, but it also provides further insight into AP-4 deficiency syndrome, paving the way towards the development of more effective and cell-targeted therapeutic strategies to target autophagy to treat neurodegenerative diseases. Furthermore, it adds yet another line to the stronger and stronger connection between neurodegeneration and neuronal membrane dynamics.

References

1.
Neuronal functions of adaptor complexes involved in protein sorting.
Guardia CM, De Pace R, Mattera R, Bonifacino JS. Curr Opin Neurobiol. 2018 08; 51:103-110
PMID: 29558740 DOI: 10.1016/j.conb.2018.02.021

A genetic model of CEDNIK syndrome in zebrafish highlights the role of the SNARE protein Snap29 in neuromotor and epidermal development.

Mastrodonato V, Beznoussenko G, Mironov A, Ferrari L, Deflorian G, Vaccari T.
Sci Rep 2019 Feb 04; 9(1):1211
PMID: 30718891 DOI: 10.1038/s41598-018-37780-4

How to cite this recommendation
Galli T and Gallo A: F1000Prime Recommendation of [Mastrodonato V et al., Sci Rep 2019 9(1):1211]. In F1000Prime, 28 Feb 2019; 10.3410/f.735011435.793556904

28 Feb 2019 | New Finding

Synaptosomal-associated protein 29 (Snap29) belongs to the Snap25 sub-family of SNAREs (Soluble N-ethylmaleimide-Sensitive Factor Attachment Protein REceptor), which are characterized by the presence of two SNARE motifs {1}. Recent studies have highlighted its key role in macroautophagy, where it operates in concert with syntaxin-17 and VAMP8 or VAMP7 to mediate fusion of autophagosomes with lysosomes, leading to the formation of degradative autolysosomes {2,3}.

Despite its multiple functions within the cell, complete loss of Snap29 does not lead to embryonic lethality, but rather results in CEDNIK (cerebral dysgenesis, neuropathy, ichthyosis and keratoderma) syndrome, a rare, inherited, congenital condition affecting skin and nervous system development and causing short life span {4}. In the present report, the authors describe the first genetic model of CEDNIK in zebrafish, providing new information on unexplored aspects of this disease, mainly related to the nervous system.

First, they compared two different mutants of the *snap29* gene, *snap29*^{N171sf} and *snap29*^{K164*}, generated by CRISPR/Cas9 and ENU treatment, respectively. They found a reduction in the level of expression of *snap29* mRNA, similar to that observed in CEDNIK patient-derived fibroblasts in the *snap29*^{K164*} homozygous larvae, but not in *snap29*^{N171sf} mutant. Moreover, no increase in *snap29* paralogs have been found, suggesting that compensatory mechanisms do not occur. These observations establish the *snap29*^{K164*} mutant as a solid genetic model to study CEDNIK syndrome in zebrafish.

The *snap29*^{K164*} mutant larvae display many aspects of loss of Snap29 function as in CEDNIK patients, such as impaired autophagy, revealed by increased levels of the autophagy markers LC3II and p62 and accumulation of aberrant multilamellar organelles, skin defects and short life expectancy (mutant larvae die at 9 days post-fertilization [dpf]).

In a second step, the authors focused on the less characterized neurological defects of CEDNIK pathology. They found that the prominent microcephaly of *snap29*^{K164*} mutant larvae, also observed in patients, is caused by high levels of apoptotic cell death not compensated by an increase in cell proliferation. Furthermore, mutant larvae lack of trigeminal motorneurons controlling mandibular arch muscles and mouth opening, which might explain the feeding defects also observed in CEDNIK infants. Finally, neurons lacking Snap29 exhibit an increased motor neuron arborization, whereas Snap25 mutants are reported to show an opposite effect. Such a phenotype suggests that Snap29 could act as a negative modulator of motor neuron development, by acting in opposition with Snap25 activity. This observation is of particular interest in the context of SNAP-29 inhibiting VAMP7 exocytosis {5}, a mechanism known to promote axonal growth {6}.

Overall, the *snap29*^{K164*} zebrafish mutant characterized in this study increases the knowledge of CEDNIK pathogenesis due to the loss of Snap29 function, providing further insight into the less investigated neurological

symptoms. The data presented here assess this mutant as a valid model of CEDNIK syndrome, that can be used to screen new pharmacological compounds aimed at ameliorating some traits of this severe disease.

References

1.
The SNAP-25 Protein Family.
Kádková A, Radecke J, Sørensen JB. Neuroscience. 2018 Sep 27;
PMID: 30267828 DOI: 10.1016/j.neuroscience.2018.09.020

2.
Multiple functions of the SNARE protein Snap29 in autophagy, endocytic, and exocytic trafficking during epithelial formation in Drosophila.
Morelli E, Ginefra P, Mastrodonato V, Beznoussenko GV, Rusten TE, Bilder D, Stenmark H, Mironov AA, Vaccari T. Autophagy. 2014; 10(12):2251-2268
PMID: 25551675 DOI: 10.4161/15548627.2014.981913

3.
Autophagosomal Syntaxin17-dependent lysosomal degradation maintains neuronal function in Drosophila.
Takáts S, Nagy P, Varga Á, Pircs K, Kárpáti M, Varga K, Kovács AL, Hegedűs K, Juhász G. J Cell Biol. 2013 May 13; 201(4):531-539
PMID: 23671310 DOI: 10.1083/jcb.201211160

4.
A mutation in SNAP29, coding for a SNARE protein involved in intracellular trafficking, causes a novel neurocutaneous syndrome characterized by cerebral dysgenesis, neuropathy, ichthyosis, and palmoplantar keratoderma.
Sprecher E, Ishida-Yamamoto A, Mizrahi-Koren M, Rapaport D, Goldsher D, Indelman M, Topaz O, Chefetz I, Keren H, O'brien TJ, Bercovich D, Shalev S, Geiger D, Bergman R, Horowitz M, Mandel H. Am J Hum Genet. 2005 Aug; 77(2):242-251
PMID: 15968592 DOI: 10.1086/432556

5.
The Q-soluble N-Ethylmaleimide-sensitive Factor Attachment Protein Receptor (Q-SNARE) SNAP-47 Regulates Trafficking of Selected Vesicle-associated Membrane Proteins (VAMPs).
Kuster A, Nola S, Dingli F, Vacca B, Gauchy C, Beaujouan JC, Nunez M, Moncion T, Loew D, Formstecher E, Galli T, Proux-Gillardeaux V. J Biol Chem. 2015 Nov 20; 290(47):28056-28069
PMID: 26359495 DOI: 10.1074/jbc.M115.666362

6.
Membrane traffic during axon development.
Wojnacki J, Galli T. Dev Neurobiol. 2016 11; 76(11):1185-1200
PMID: 26945675 DOI: 10.1002/dneu.22390

Bibliography

Adams SR, Campbell RE, Gross LA, Martin BR, Walkup GK, et al. 2002. New biarsenical ligands and tetracysteine motifs for protein labeling in vitro and in vivo: synthesis and biological applications. J. Am. Chem. Soc. 124(21):6063–6076

Adler CE, Fetter RD, Bargmann CI. 2006. UNC-6/Netrin induces neuronal asymmetry and defines the site of axon formation. Nat. Neurosci. 9(4):511–518

Advani RJ, Yang B, Prekeris R, Lee KC, Klumperman J, Scheller RH. 1999. VAMP-7 mediates vesicular transport from endosomes to lysosomes. J. Cell Biol. 146(4):765–776

Ahuja R, Pinyol R, Reichenbach N, Custer L, Klingensmith J, et al. 2007. Cordon-bleu is an actin nucleation factor and controls neuronal morphology. Cell. 131(2):337–350

Alberts P, Rudge R, Hinners I, Muzerelle A, Martinez-Arca S, et al. 2003. Cross talk between tetanus neurotoxin-insensitive vesicle-associated membrane protein-mediated transport and L1-mediated adhesion. Mol. Biol. Cell. 14(10):4207–4220

Antonucci DE, Lim ST, Vassanelli S, Trimmer JS. 2001. Dynamic localization and clustering of dendritic Kv2.1 voltage-dependent potassium channels in developing hippocampal neurons. *Neuroscience*. 108(1):69–81

Arimura N, Kaibuchi K. 2007. Neuronal polarity: from extracellular signals to intracellular mechanisms. Nat. Rev. Neurosci. 8(3):194–205

Baas PW, Lin S. 2011. Hooks and comets: The story of microtubule polarity orientation in the neuron. Dev. Neurobiol. 71(6):403–418

Baker RW, Hughson FM. 2016. Chaperoning SNARE assembly and disassembly. Nat. Rev. Mol. Cell Biol. 17(8):465–479

Bankaitis VA, Garcia-Mata R, Mousley CJ. 2012. Golgi membrane dynamics and lipid metabolism. *Curr. Biol.* 22(10):R414–24

Barnes AP, Polleux F. 2009. Establishment of axon-dendrite polarity in developing neurons. Annu. Rev. Neurosci. 32:347–381

Bassell GJ, Zhang H, Byrd AL, Femino AM, Singer RH, et al. 1998. Sorting of beta-actin mRNA and protein to neurites and growth cones in culture. J. Neurosci. 18(1):251–265

Batista AFR, Hengst U. 2016. Intra-axonal protein synthesis in development and beyond. Int. J. Dev. Neurosci. 55:140–149

Baumann NA, Sullivan DP, Ohvo-Rekilä H, Simonot C, Pottekat A, et al. 2005. Transport of newly synthesized sterol to the sterol-enriched plasma membrane occurs via nonvesicular equilibration. *Biochemistry*. 44(15):5816–5826

Becker T, Volchuk A, Rothman JE. 2005. Differential use of endoplasmic reticulum membrane for phagocytosis in J774 macrophages. Proc. Natl. Acad. Sci. USA. 102(11):4022–4026

Bentley M, Banker G. 2016. The cellular mechanisms that maintain neuronal polarity. Nat. Rev. Neurosci. 17(10):611–622

Bian X, Saheki Y, De Camilli P. 2018. calcium Syt1 auto...embrane tethering with lipid transport. *EMBO J.* 37:219–234

Bian X, Zhang Z, Xiong Q, De Camilli P, Lin C. 2019a. A programmable DNA-origami ...ed lipid transfer between bilayers. In revision

Bian X. 2019b. In Vitro Assays to Measure the Membrane...ivities of the Extended Synaptotagmins. *Methods Mol. Biol.* 1949:201–212

Bishop HI, Guan D, Bocksteins E, Parajuli LK, Murray KD, et al. 2015. Distinct Cell- and Layer-Specific Expression Patterns and Independent Regulation of Kv2 Channel Subtypes in Cortical Pyramidal Neurons. *J. Neurosci.* 35(44):14922–14942

Block MR, Glick BS, Wilcox CA, Wieland FT, Rothman JE. 1988. Purification of an N-ethylmaleimide-sensitive protein catalyzing vesicular transport. Proc. Natl. Acad. Sci. USA. 85(21):7852–7856

Blom T, Somerharju P, Ikonen E. 2011. Synthesis and biosynthetic trafficking of membrane lipids. *Cold Spring Harb. Perspect. Biol.* 3(8):a004713

Bloom OE, Morgan JR. 2011. Membrane trafficking events underlying axon repair, growth, and regeneration. Mol. Cell. Neurosci. 48(4):339–348

Bock JB, Matern HT, Peden AA, Scheller RH. 2001. A genomic perspective on membrane compartment organization. Nature. 409(6822):839–841

Bolanos-Garcia VM, Davies OR. 2006. Structural analysis and classification of native proteins from E. coli commonly co-purified by immobilised metal affinity chromatography. Biochim. Biophys. Acta. 1760(9):1304–1313

Bordier C. 1981. Phase separation of integral membrane proteins in Triton X-114 solution. J. Biol. Chem. 256(4):1604–1607

Bradke F, Dotti CG. 1997. Neuronal polarity: vectorial cytoplasmic flow precedes axon formation. Neuron. 19(6):1175–1186

Bradke F, Dotti CG. 1999. The role of local actin instability in axon formation. Science. 283(5409):1931–1934

Bradke F, Dotti CG. 2000. Establishment of neuronal polarity: lessons from cultured hippocampal neurons. Curr. Opin. Neurobiol. 10(5):574–581

Brandsma J, Bailey AP, Koster G, Gould AP, Postle AD. 2017. Stable isotope analysis of dynamic lipidomics. *Biochimica et Biophysica Acta - Molecular and Cell Biology of Lipids*. 1862(8):792–796

Bray D. 1970. Surface movements during the growth of single explanted neurons. Proc. Natl. Acad. Sci. USA. 65(4):905–910

Brennan PJ, Griffin PFS, Losel DM, Tyrrell D. 1974. The lipids of fungi. *Prog. Chem. Fats Other Lipids*. 14:49–89

Bricogne C, Fine M, Pereira PM, Wang Y, Sung J, et al. 2018. TMEM16F activation by Ca2+ triggers plasmalemma expansion and directs PD-1 trafficking. *BioRxiv*

Brown DA, London E. 1997. Structure of detergent-resistant membrane domains: does phase separation occur in biological membranes? *Biochem. Biophys. Res. Commun.* 240(1):1–7

Brown DA, Rose JK. 1992. Sorting of GPI-anchored proteins to glycolipid-enriched membrane subdomains during transport to the apical cell surface. *Cell*. 68(3):533–544

Buck KB, Zheng JQ. 2002. Growth cone turning induced by direct local modification of microtubule dynamics. J. Neurosci. 22(21):9358–9367

Bunge MB. 1973. Fine structure of nerve fibers and growth cones of isolated sympathetic neurons in culture. J. Cell Biol. 56(3):713–735

Burgo A, Casano AM, Kuster A, Arold ST, Wang G, et al. 2013. Increased activity of the vesicular soluble N-ethylmaleimide-sensitive factor attachment protein receptor TI-VAMP/VAMP7 by tyrosine phosphorylation in the Longin domain. J. Biol. Chem. 288(17):11960–11972

Burri L, Varlamov O, Doege CA, Hofmann K, Beilharz T, et al. 2003. A SNARE required for retrograde transport to the endoplasmic reticulum. Proc. Natl. Acad. Sci. USA. 100(17):9873–9877

Cajal SR y. 1891. Significación fisiológica de las expansiones protoplásmicas y nerviosas de las células de la sustancia gris. Memoria leída en el Congreso Médico de Valencia

Calderon de Anda F, Gärtner A, Tsai L-H, Dotti CG. 2008. Pyramidal neuron polarity axis is defined at the bipolar stage. J. Cell Sci. 121(Pt 2):178–185

Campbell DS, Holt CE. 2001. Chemotropic responses of retinal growth cones mediated by rapid local protein synthesis and degradation. Neuron. 32(6):1013–1026

Campenot RB. 1977. Local control of neurite development by nerve growth factor. Proc. Natl. Acad. Sci. USA. 74(10):4516–4519

Carrasco S, Meyer T. 2011. STIM proteins and the endoplasmic reticulum-plasma membrane junctions. *Annu. Rev. Biochem.* 80:973–1000

Cebrian I, Visentin G, Blanchard N, Jouve M, Bobard A, et al. 2011. Sec22b regulates phagosomal maturation and antigen crosspresentation by dendritic cells. Cell. 147(6):1355–1368

Chaineau M, Danglot L, Proux-Gillardeaux V, Galli T. 2008. Role of HRB in clathrin-dependent endocytosis. J. Biol. Chem. 283(49):34365–34373

Chang CL, Hsieh TS, Yang TT, Rothberg KG, Azizoglu DB, et al. 2013. Feedback regulation of receptor-induced Ca2+ signaling mediated by E-Syt1 and Nir2 at endoplasmic reticulum-plasma membrane junctions. *Cell Rep.* 5(3):813–825

Chapman ER, An S, Barton N, Jahn R. 1994. SNAP-25, a t-SNARE which binds to both syntaxin and synaptobrevin via domains that may form coiled coils. J. Biol. Chem. 269(44):27427–27432

Choi JY, Wu WI, Voelker DR. 2005. Phosphatidylserine decarboxylases as genetic and biochemical tools for studying phospholipid traffic. *Anal. Biochem.* 347(2):165–175

Choi UB, Zhao M, Zhang Y, Lai Y, Brunger AT. 2016. Complexin induces a conformational change at the membrane-proximal C-terminal end of the SNARE complex. Elife. 5:

Chung J, Torta F, Masai K, Lucast L, Czapla H, et al. 2015. INTRACELLULAR TRANSPORT. PI4P/phosphatidylserine countertransport at ORP5- and ORP8-mediated ER-plasma membrane contacts. *Science*. 349(6246):428–432

Cocucci E, Racchetti G, Rupnik M, Meldolesi J. 2008. The regulated exocytosis of enlargeosomes is mediated by a SNARE machinery that includes VAMP4. J. Cell Sci. 121(Pt 18):2983–2991

Cohen FS, Melikyan GB. 2004. The energetics of membrane fusion from binding, through hemifusion, pore formation, and pore enlargement. J. Membr. Biol. 199(1):1–14

Coles CH, Bradke F. 2015. Coordinating neuronal actin-microtubule dynamics. Curr. Biol. 25(15):R677–91

Cotrufo T, Andrés RM, Ros O, Pérez-Brangulí F, Muhaisen A, et al. 2012. Syntaxin 1 is required for DCC/Netrin-1-dependent chemoattraction of migrating neurons from the lower rhombic lip. Eur. J. Neurosci. 36(9):3152–3164

Craig AM, Wyborski RJ, Banker G. 1995. Preferential addition of newly synthesized membrane protein at axonal growth cones. Nature. 375(6532):592–594

Creutz CE, Snyder SL, Schulz TA. 2004. Characterization of the yeast tricalbins: membrane-bound multi-C2-domain proteins that form complexes involved in membrane trafficking. *Cell Mol. Life Sci.* 61(10):1208–1220

D'Angelo G, Vicinanza M, De Matteis MA. 2008. Lipid-transfer proteins in biosynthetic pathways. *Curr. Opin. Cell Biol.* 20(4):360–370

Dai J, Sheetz MP. 1995. Regulation of endocytosis, exocytosis, and shape by membrane tension. Cold Spring Harb. Symp. Quant. Biol. 60:567–571

Danglot L, Zylbersztejn K, Petkovic M, Gauberti M, Meziane H, et al. 2012. Absence of TI-VAMP/Vamp7 leads to increased anxiety in mice. J. Neurosci. 32(6):1962–1968

Danielli JF, Davson H. 1935. A contribution to the theory of permeability of thin films. . *J Cell Comp Physiol*. 5:495–508

Daste F, Galli T, Tareste D. 2015. Structure and function of longin SNAREs. J. Cell Sci. 128(23):4263–4272

Daum G. 1985. Lipids of mitochondria. *Biochim. Biophys. Acta*. 882:1–42

De Franceschi N, Wild K, Schlacht A, Dacks JB, Sinning I, Filippini F. 2014. Longin and GAF domains: structural evolution and adaptation to the subcellular trafficking machinery. Traffic. 15(1):104–121

de Saint-Jean M, Delfosse V, Douguet D, Chicanne G, Payrastre B, et al. 2011. Osh4p exchanges sterols for phosphatidylinositol 4-phosphate between lipid bilayers. *J. Cell Biol.* 195(6):965–978

Deitch JS, Banker GA. 1993. An electron microscopic analysis of hippocampal neurons developing in culture: early stages in the emergence of polarity. J. Neurosci. 13(10):4301–4315

Dent EW, Gupton SL, Gertler FB. 2011. The growth cone cytoskeleton in axon outgrowth and guidance. Cold Spring Harb. Perspect. Biol. 3(3):

Dent EW, Kalil K. 2001. Axon branching requires interactions between dynamic microtubules and actin filaments. J. Neurosci. 21(24):9757–9769

Deutsch E, Weigel AV, Akin EJ, Fox P, Hansen G, et al. 2012. Kv2.1 cell surface clusters are insertion platforms for ion channel delivery to the plasma membrane. *Mol. Biol. Cell*. 23(15):2917–2929

Di Paolo G, De Camilli P. 2006. Phosphoinositides in cell regulation and membrane dynamics. *Nature*. 443(7112):651–657

Dingsdale H, Okeke E, Awais M, Haynes L, Criddle DN, et al. 2013. Saltatory formation, sliding and dissolution of ER-PM junctions in migrating cancer cells. Biochem. J. 451(1):25–32

Donnelly CJ, Park M, Spillane M, Yoo S, Pacheco A, et al. 2013. Axonally synthesized β-actin and GAP-43 proteins support distinct modes of axonal growth. J. Neurosci. 33(8):3311–3322

Dotti CG, Sullivan CA, Banker GA. 1988. The establishment of polarity by hippocampal neurons in culture. J. Neurosci. 8(4):1454–1468

Douglas SM, Dietz H, Liedl T, Högberg B, Graf F, Shih WM. 2009. Self-assembly of DNA into nanoscale three-dimensional shapes. *Nature*. 459(7245):414–418

Dulubova I, Sugita S, Hill S, Hosaka M, Fernandez I, et al. 1999. A conformational switch in syntaxin during exocytosis: role of munc18. EMBO J. 18(16):4372–4382

Endo M. 2009. Calcium-induced calcium release in skeletal muscle. *Physiol. Rev.* 89(4):1153–1176

Ercan E, Momburg F, Engel U, Temmerman K, Nickel W, Seedorf M. 2009. A conserved, lipid-mediated sorting mechanism of yeast Ist2 and mammalian STIM proteins to the peripheral ER. *Traffic*. 10(12):1802–1818

Esch T, Lemmon V, Banker G. 1999. Local presentation of substrate molecules directs axon specification by cultured hippocampal neurons. J. Neurosci. 19(15):6417–6426

Escribá PV, González-Ros JM, Goñi FM, Kinnunen PK, Vigh L, et al. 2008. Membranes: a meeting point for lipids, proteins and therapies. *J. Cell Mol. Med.* 12(3):829–875

Eva R, Dassie E, Caswell PT, Dick G, ffrench-Constant C, et al. 2010. Rab11 and its effector Rab coupling protein contribute to the trafficking of beta 1 integrins during axon growth in adult dorsal root ganglion neurons and PC12 cells. J. Neurosci. 30(35):11654–11669

Fader CM, Aguilera MO, Colombo MI. 2012. ATP is released from autophagic vesicles to the extracellular space in a VAMP7-dependent manner. Autophagy. 8(12):1741–1756

Falk J, Konopacki FA, Zivraj KH, Holt CE. 2014. Rab5 and Rab4 regulate axon elongation in the Xenopus visual system. J. Neurosci. 34(2):373–391

Farquhar MG, Palade GE. 1981. The Golgi Apparatus (Complex)-(1954-1981) from Artifact to Center Stage. *J. Cell Biol.* 91(1):77–103

Fasshauer D, Sutton RB, Brunger AT, Jahn R. 1998. Conserved structural features of the synaptic fusion complex: SNARE proteins reclassified as Q- and R-SNAREs. Proc. Natl. Acad. Sci. USA. 95(26):15781–15786

Feany MB, Buckley KM. 1993. The synaptic vesicle protein synaptotagmin promotes formation of filopodia in fibroblasts. Nature. 364(6437):537–540

Fernández-Busnadiego R, Saheki Y, De Camilli P. 2015. Three-dimensional architecture of extended synaptotagmin-mediated endoplasmic reticulum-plasma membrane contact sites. *Proc. Natl. Acad. Sci. USA*. 112(16):E2004–13

Filippini F, Rossi V, Galli T, Budillon A, D'Urso M, D'Esposito M. 2001. Longins: a new evolutionary conserved VAMP family sharing a novel SNARE domain. Trends Biochem. Sci. 26(7):407–409

Fine M, Bricogne C, Hilgemann DW. 2018. Massive surface membrane expansion without involvement of classical exocytic mechanisms. *BioRxiv*

Fischer MA, Temmerman K, Ercan E, Nickel W, Seedorf M. 2009. Binding of plasma membrane lipids recruits the yeast integral membrane protein Ist2 to the cortical ER. *Traffic*. 10(8):1084–1097

Fox PD, Haberkorn CJ, Akin EJ, Seel PJ, Krapf D, Tamkun MM. 2015. Induction of stable ER-plasma-membrane junctions by Kv2.1 potassium channels. *J. Cell Sci.* 128(11):2096–2105

Futerman AH, Banker GA. 1996. The economics of neurite outgrowth--the addition of new membrane to growing axons. Trends Neurosci. 19(4):144–149

Galli T, Zahraoui A, Vaidyanathan VV, Raposo G, Tian JM, et al. 1998. A novel tetanus neurotoxin-insensitive vesicle-associated membrane protein in SNARE complexes of the apical plasma membrane of epithelial cells. Mol. Biol. Cell. 9(6):1437–1448

Gallo A, Vannier C, Galli T. 2016. Endoplasmic Reticulum-Plasma Membrane Associations:Structures and Functions. *Annu. Rev. Cell Dev. Biol.* 32:279–301

Gao Y, Zorman S, Gundersen G, Xi Z, Ma L, et al. 2012. Single reconstituted neuronal SNARE complexes zipper in three distinct stages. Science. 337(6100):1340–1343

Garbino A, van Oort RJ, Dixit SS, Landstrom AP, Ackerman MJ, Wehrens XH. 2009. Molecular evolution of the junctophilin gene family. *Physiol. Genomics*. 37(3):175–186

Geppert M, Goda Y, Hammer RE, Li C, Rosahl TW, et al. 1994. Synaptotagmin I: a major Ca2+ sensor for transmitter release at a central synapse. Cell. 79(4):717–727

Giordano F, Saheki Y, Idevall-Hagren O, Colombo SF, Pirruccello M, et al. 2013. PI(4,5)P(2)-dependent and Ca(2+)-regulated ER-PM interactions mediated by the extended synaptotagmins. *Cell*. 153(7):1494–1509

Giraudo CG, Garcia-Diaz A, Eng WS, Chen Y, Hendrickson WA, et al. 2009. Alternative zippering as an on-off switch for SNARE-mediated fusion. Science. 323(5913):512–516

Goldberg DJ, Burmeister DW. 1986. Stages in axon formation: observations of growth of Aplysia axons in culture using video-enhanced contrast-differential interference contrast microscopy. J. Cell Biol. 103(5):1921–1931

Golovina VA. 2005. Visualization of localized store-operated calcium entry in mouse astrocytes. Close proximity to the endoplasmic reticulum. *J. Physiol. (Lond.)*. 564(Pt 3):737–749

Goñi FM. 2014. The basic structure and dynamics of cell membranes: an update of the Singer-Nicolson model. *Biochim. Biophys. Acta*. 1838(6):1467–1476

Gonzalez LC, Weis WI, Scheller RH. 2001. A novel snare N-terminal domain revealed by the crystal structure of Sec22b. J. Biol. Chem. 276(26):24203–24211

Gorter E, Grendel F. 1925. On Bimolecular Layers of Lipoids on the Chromocytes of the Blood. . *J. Exp. Med.* 41:439–443

Gould RM, Pant H, Gainer H, Tytell M. 1983. Phospholipid synthesis in the squid giant axon: incorporation of lipid precursors. *J. Neurochem.* 40(5):1293–1299

Gould RM, Spivack WD, Robertson D, Poznansky MJ. 1983b. Phospholipid synthesis in the squid giant axon: enzymes of phosphatidylinositol metabolism. J. Neurochem. 40(5):1300–1306

Gracias NG, Shirkey-Son NJ, Hengst U. 2014. Local translation of TC10 is required for membrane expansion during axon outgrowth. Nat. Commun. 5:3506

Grassi D, Plonka FB, Oksdath M, Guil AN, Sosa LJ, Quiroga S. 2015. Selected SNARE proteins are essential for the polarized membrane insertion of igf-1 receptor and the regulation of initial axonal outgrowth in neurons. Cell Discov. 1:15023

Greene LA, Tischler AS. 1976. Establishment of a noradrenergic clonal line of rat adrenal pheochromocytoma cells which respond to nerve growth factor. Proc. Natl. Acad. Sci. USA. 73(7):2424–2428

Griffin BA, Adams SR, Tsien RY. 1998. Specific covalent labeling of recombinant protein molecules inside live cells. Science. 281(5374):269–272

Gupton SL, Gertler FB. 2010. Integrin signaling switches the cytoskeletal and exocytic machinery that drives neuritogenesis. Dev. Cell. 18(5):725–736

Gurtovenko AA, Vattulainen I. 2007. Lipid transmembrane asymmetry and intrinsic membrane potential: two sides of the same coin. *J. Am. Chem. Soc.* 129(17):5358–5359

Haj FG, Sabet O, Kinkhabwala A, Wimmer-Kleikamp S, Roukos V, et al. 2012. Regulation of signaling at regions of cell-cell contact by endoplasmic reticulum-bound protein-tyrosine phosphatase 1B. *PLoS One*. 7(5):e36633

Hanada K, Kumagai K, Yasuda S, Miura Y, Kawano M, et al. 2003. Molecular machinery for non-vesicular trafficking of ceramide. *Nature*. 426(6968):803–809

Hankin JA, Farias SE, Barkley RM, Heidenreich K, Frey LC, et al. 2011. MALDI mass spectrometric imaging of lipids in rat brain injury models. *J Am Soc Mass Spectrom*. 22(6):1014–1021

Hannun YA, Obeid LM. 2018. Sphingolipids and their metabolism in physiology and disease. *Nat. Rev. Mol. Cell Biol.* 19(3):175–191

Hanus C, Geptin H, Tushev G, Garg S, Alvarez-Castelao B, et al. 2016. Unconventional secretory processing diversifies neuronal ion channel properties. Elife. 5:

Harayama T, Riezman H. 2018. Understanding the diversity of membrane lipid composition. *Nat. Rev. Mol. Cell Biol.* 19(5):281–296

Hartzell HC, Yu K, Xiao Q, Chien LT, Qu Z. 2009. Anoctamin/TMEM16 family members are Ca2+-activated Cl- channels. *J. Physiol. (Lond.)*. 587(Pt 10):2127–2139

Hatsuzawa K, Hashimoto H, Hashimoto H, Arai S, Tamura T, et al. 2009. Sec22b is a negative regulator of phagocytosis in macrophages. Mol. Biol. Cell. 20(20):4435–4443

Hayashi M, Raimondi A, O'Toole E, Paradise S, Collesi C, et al. 2008. Cell- and stimulus-dependent heterogeneity of synaptic vesicle endocytic recycling mechanisms revealed by studies of dynamin 1-null neurons. *Proc. Natl. Acad. Sci. USA*. 105(6):2175–2180

Hayashi T, McMahon H, Yamasaki S, Binz T, Hata Y, et al. 1994. Synaptic vesicle membrane fusion complex: action of clostridial neurotoxins on assembly. EMBO J. 13(21):5051–5061

Hazuka CD, Foletti DL, Hsu SC, Kee Y, Hopf FW, Scheller RH. 1999. The sec6/8 complex is located at neurite outgrowth and axonal synapse-assembly domains. J. Neurosci. 19(4):1324–1334

Helle SC, Kanfer G, Kolar K, Lang A, Michel AH, Kornmann B. 2013. Organization and function of membrane contact sites. *Biochim. Biophys. Acta*. 1833(11):2526–2541

Hengst U, Deglincerti A, Kim HJ, Jeon NL, Jaffrey SR. 2009. Axonal elongation triggered by stimulus-induced local translation of a polarity complex protein. Nat. Cell Biol. 11(8):1024–1030

Hengst U, Jaffrey SR. 2007. Function and translational regulation of mRNA in developing axons. Semin. Cell Dev. Biol. 18(2):209–215

Henn FA, Decker GL, Greenawalt JV, Thompson TE. 1967. Properties of lipid bilayer membranes separating two aqueous phases: Electron microscope studies. . *J. Mol. Biol.* 24:51–58

Henne WM, Liou J, Emr SD. 2015. Molecular mechanisms of inter-organelle ER-PM contact sites. *Curr. Opin. Cell Biol.* 35:123–130

Henriksen J, Rowat AC, Brief E, Hsueh YW, Thewalt JL, et al. 2006. Universal behavior of membranes with sterols. *Biophys. J.* 90(5):1639–1649

Herdman C, Moss T. 2016. Extended-Synaptotagmins (E-Syts); the extended story. *Pharmacol. Res.* 107:48–56

Herdman C, Tremblay MG, Mishra PK, Moss T. 2014. Loss of Extended Synaptotagmins ESyt2 and ESyt3 does not affect mouse development or viability, but in vitro cell migration and survival under stress are affected. *Cell Cycle*. 13(16):2616–2625

Holthuis JC, Levine TP. 2005. Lipid traffic: floppy drives and a superhighway. *Nat. Rev. Mol. Cell Biol.* 6(3):209–220

Holthuis JC, Menon AK. 2014. Lipid landscapes and pipelines in membrane homeostasis. *Nature*. 510(7503):48–57

Horton AC, Rácz B, Monson EE, Lin AL, Weinberg RJ, Ehlers MD. 2005. Polarized secretory trafficking directs cargo for asymmetric dendrite growth and morphogenesis. Neuron. 48(5):757–771

Hsieh T-S, Chen Y-J, Chang C-L, Lee W-R, Liou J. 2017. Cortical actin contributes to spatial organization of ER-PM junctions. Mol. Biol. Cell. 28(23):3171–3180

Hua Z, Leal-Ortiz S, Foss SM, Waites CL, Garner CC, et al. 2011. v-SNARE composition distinguishes synaptic vesicle pools. Neuron. 71(3):474–487

Idevall-Hagren O, Lü A, Xie B, De Camilli P. 2015. Triggered Ca2+ influx is required for extended synaptotagmin 1-induced ER-plasma membrane tethering. *EMBO J.* 34(17):2291–2305

Igarashi M, Kozaki S, Terakawa S, Kawano S, Ide C, Komiya Y. 1996. Growth cone collapse and inhibition of neurite growth by Botulinum neurotoxin C1: a t-SNARE is involved in axonal growth. J. Cell Biol. 134(1):205–215

Im YJ, Raychaudhuri S, Prinz WA, Hurley JH. 2005. Structural mechanism for sterol sensing and transport by OSBP-related proteins. *Nature*. 437(7055):154–158

Ito K, Komazaki S, Sasamoto K, Yoshida M, Nishi M, et al. 2001. Deficiency of triad junction and contraction in mutant skeletal muscle lacking junctophilin type 1. *J. Cell Biol.* 154(5):1059–1067

Izquierdo E, Delgado A. 2018. Click chemistry in sphingolipid research. *Chem Phys Lipids*. 215:71–83

Jackson CL, Walch L, Verbavatz JM. 2016. Lipids and their trafficking: an integral part of cellular organization. *Dev. Cell*. 39(2):139–153

Jacquemyn J, Cascalho A, Goodchild RE. 2017. The ins and outs of endoplasmic reticulum-controlled lipid biosynthesis. *EMBO Rep.* 18(11):1905–1921

Jahn R, Fasshauer D. 2012. Molecular machines governing exocytosis of synaptic vesicles. Nature. 490(7419):201–207

Jahn R, Scheller RH. 2006. SNAREs--engines for membrane fusion. Nat. Rev. Mol. Cell Biol. 7(9):631–643

Jareb M, Banker G. 1997. Inhibition of axonal growth by brefeldin A in hippocampal neurons in culture. J. Neurosci. 17(23):8955–8963

Jean S, Mikryukov A, Tremblay MG, Baril J, Guillou F, et al. 2010. Extended-synaptotagmin-2 mediates FGF receptor endocytosis and ERK activation in vivo. Dev. Cell. 19(3):426–439

Jeckel D, Karrenbauer A, Burger KN, van Meer G, Wieland F. 1992. Glucosylceramide is synthesized at the cytosolic surface of various Golgi subfractions. *J. Cell Biol.* 117(2):259–267

Jiang H, Guo W, Liang X, Rao Y. 2005. Both the establishment and the maintenance of neuronal polarity require active mechanisms: critical roles of GSK-3beta and its upstream regulators. Cell. 120(1):123–135

Jiang X, Zhang Z, Cheng K, Wu Q, Jiang L, et al. 2019. Membrane-mediated disorder-to-order transition of SNAP25 flexible linker facilitates its interaction with syntaxin-1 and SNARE-complex assembly. FASEB J. 33(7):7985–7994

Jiao J, He M, Port SA, Baker RW, Xu Y, et al. 2018. Munc18-1 catalyzes neuronal SNARE assembly by templating SNARE association. Elife. 7:

Jozsef L, Tashiro K, Kuo A, Park EJ, Skoura A, et al. 2014. Reticulon 4 is necessary for endoplasmic reticulum tubulation, STIM1-Orai1 coupling, and store-operated calcium entry. J. Biol. Chem. 289(13):9380–9395

Kaech S, Banker G. 2006. Culturing hippocampal neurons. Nat. Protoc. 1(5):2406–2415

Kagiwada S, Hashimoto M. 2007. The yeast VAP homolog Scs2p has a phosphoinositide-binding ability that is correlated with its activity. *Biochem. Biophys. Res. Commun.* 364(4):870–876

Kaiser SE, Brickner JH, Reilein AR, Fenn TD, Walter P, Brunger AT. 2005. Structural basis of FFAT motif-mediated ER targeting. *Structure*. 13(7):1035–1045

Kannan M, Riekhof WR, Voelker DR. 2015. Transport of phosphatidylserine from the endoplasmic reticulum to the site of phosphatidylserine decarboxylase2 in yeast. *Traffic*. 16(2):123–134

Kaplan MR, Simoni RD. 1985. Intracellular transport of phosphatidylcholine to the plasma membrane. J. Cell Biol. 101(2):441–445

Kaplan MR, Simoni RD. 1985b. Transport of cholesterol from the endoplasmic reticulum to the plasma membrane. *J. Cell Biol.* 101(2):446–453

Kawano M, Kumagai K, Nishijima M, Hanada K. 2006. Efficient trafficking of ceramide from the endoplasmic reticulum to the Golgi apparatus requires a VAMP-associated protein-interacting FFAT motif of CERT. *J. Biol. Chem.* 281(40):30279–30288

Kikuma K, Li X, Kim D, Sutter D, Dickman DK. 2017. Extended synaptotagmin localizes to presynaptic ER and promotes neurotransmission and synaptic growth in drosophila. Genetics. 207(3):993–1006

Kim YJ, Guzman-Hernandez ML, Balla T. 2011. A highly dynamic ER-derived phosphatidylinositol-synthesizing organelle supplies phosphoinositides to cellular membranes. *Dev. Cell*. 21(5):813–824

Kimura T, Jia J, Claude-Taupin A, Kumar S, Choi SW, et al. 2017. Cellular and molecular mechanism for secretory autophagy. Autophagy. 13(6):1084–1085

Kirmiz M, Palacio S, Thapa P, King AN, Sack JT, Trimmer JS. 2018. Remodeling neuronal ER-PM junctions is a conserved nonconducting function of Kv2 plasma membrane ion channels. *Mol. Biol. Cell*. 29(20):2410–2432

Klose C, Surma MA, Simons K. 2013. Organellar lipidomics--background and perspectives. *Curr. Opin. Cell Biol.* 25(4):406–413

Kopec KO, Alva V, Lupas AN. 2010. Homology of SMP domains to the TULIP superfamily of lipid-binding proteins provides a structural basis for lipid exchange between ER and mitochondria. *Bioinformatics*. 26(16):1927–1931

Kopec KO, Alva V, Lupas AN. 2011. Bioinformatics of the TULIP domain superfamily. *Biochem. Soc. Trans.* 39(4):1033–1038

Kralt A, Carretta M, Mari M, Reggiori F, Steen A, et al. 2015. Intrinsically disordered linker and plasma membrane-binding motif sort Ist2 and Ssy1 to junctions. *Traffic*. 16(2):135–147

Kraszewski K, Mundigl O, Daniell L, Verderio C, Matteoli M, De Camilli P. 1995. Synaptic vesicle dynamics in living cultured hippocampal neurons visualized with CY3-conjugated antibodies directed against the lumenal domain of synaptotagmin. J. Neurosci. 15(6):4328–4342

Krishnakumar SS, Li F, Coleman J, Schauder CM, Kümmel D, et al. 2015. Re-visiting the trans insertion model for complexin clamping. Elife. 4:

Krishnakumar SS, Radoff DT, Kümmel D, Giraudo CG, Li F, et al. 2011. A conformational switch in complexin is required for synaptotagmin to trigger synaptic fusion. Nat. Struct. Mol. Biol. 18(8):934–940

Kudo N, Kumagai K, Tomishige N, Yamaji T, Wakatsuki S, et al. 2008. Structural basis for specific lipid recognition by CERT responsible for nonvesicular trafficking of ceramide. *Proc. Natl. Acad. Sci. USA*. 105(2):488–493

Kuerschner L, Moessinger C, Thiele C. 2008. Imaging of lipid biosynthesis: how a neutral lipid enters lipid droplets. *Traffic*. 9(3):338–352

Kümmel D, Krishnakumar SS, Radoff DT, Li F, Giraudo CG, et al. 2011. Complexin cross-links prefusion SNAREs into a zigzag array. Nat. Struct. Mol. Biol. 18(8):927–933

Kweon D-H, Kim CS, Shin Y-K. 2003. Regulation of neuronal SNARE assembly by the membrane. Nat. Struct. Biol. 10(6):440–447

Lahiri S, Toulmay A, Prinz WA. 2015. Membrane contact sites, gateways for lipid homeostasis. *Curr. Opin. Cell Biol.* 33:82–87

Lalanne F, Ponsin G. 2000. Mechanism of the phospholipid transfer protein-mediated transfer of phospholipids from model lipid vesicles to high density lipoproteins. *Biochim. Biophys. Acta*. 1487(1):82–91

Lamari F, Mochel F, Sedel F, Saudubray JM. 2013. Disorders of phospholipids, sphingolipids and fatty acids biosynthesis: toward a new category of inherited metabolic diseases. *J. Inherit. Metab. Dis.* 36(3):411–425

Landstrom AP, Beavers DL, Wehrens XH. 2014. The junctophilin family of proteins: from bench to bedside. *Trends Mol. Med.* 20(6):353–362

Laurino L, Wang XX, de la Houssaye BA, Sosa L, Dupraz S, et al. 2005. PI3K activation by IGF-1 is essential for the regulation of membrane expansion at the nerve growth cone. J. Cell Sci. 118(Pt 16):3653–3662

Lebrand C, Dent EW, Strasser GA, Lanier LM, Krause M, et al. 2004. Critical role of Ena/VASP proteins for filopodia formation in neurons and in function downstream of netrin-1. Neuron. 42(1):37–49

Lee I, Hong W. 2006. Diverse membrane-associated proteins contain a novel SMP domain. *FASEB J.* 20(2):202–206

Lees JA, Messa M, Sun EW, Wheeler H, Torta F, et al. 2017. Lipid transport by TMEM24 at ER-plasma membrane contacts regulates pulsatile insulin secretion. Science. 355(6326):

Lek A, Evesson FJ, Sutton RB, North KN, Cooper ST. 2012. Ferlins: regulators of vesicle fusion for auditory neurotransmission, receptor trafficking and membrane repair. *Traffic*. 13(2):185–194

Lev S, Ben Halevy D, Peretti D, Dahan N. 2008. The VAP protein family: from cellular functions to motor neuron disease. *Trends Cell Biol.* 18(6):282–290

Lev S. 2010. Non-vesicular lipid transport by lipid-transfer proteins and beyond. *Nat. Rev. Mol. Cell Biol.* 11(10):739–750

Levine T. 2004. Short-range intracellular trafficking of small molecules across endoplasmic reticulum junctions. *Trends Cell Biol.* 14(9):483–490

Levy A, Zheng JY, Lazarowitz SG. 2015. Synaptotagmin SYTA forms ER-plasma membrane junctions that are recruited to plasmodesmata for plant virus movement. *Curr. Biol.* 25(15):2018–2025

Li F, Pincet F, Perez E, Eng WS, Melia TJ, et al. 2007a. Energetics and dynamics of SNAREpin folding across lipid bilayers. Nat. Struct. Mol. Biol. 14(10):890–896

Li F, Pincet F, Perez E, Giraudo CG, Tareste D, Rothman JE. 2011. Complexin activates and clamps SNAREpins by a common mechanism involving an intermediate energetic state. Nat. Struct. Mol. Biol. 18(8):941–946

Li X, DiFiglia M. 2012. The recycling endosome and its role in neurological disorders. Prog. Neurobiol. 97(2):127–141

Li X, Radhakrishnan A, Grushin K, Kasula R, Chaudhuri A, et al. 2019. Symmetrical organization of proteins under docked synaptic vesicles. FEBS Lett. 593(2):144–153

Li Z, Hailemariam TK, Zhou H, Li Y, Duckworth DC, et al. 2007. Inhibition of sphingomyelin synthase (SMS) affects intracellular sphingomyelin accumulation and plasma membrane lipid organization. *Biochim. Biophys. Acta*. 1771(9):1186–1194

Lim ST, Antonucci DE, Scannevin RH, Trimmer JS. 2000. A novel targeting signal for proximal clustering of the Kv2.1 K+ channel in hippocampal neurons. *Neuron*. 25(2):385–397

Lindsey J, Ellisman M. 1985. The Neuronal Endomembrane System. *J. Neurosci.* 5:3133–3145

Liou J, Fivaz M, Inoue T, Meyer T. 2007. Live-cell imaging reveals sequential oligomerization and local plasma membrane targeting of stromal interaction molecule 1 after Ca2+ store depletion. *Proc. Natl. Acad. Sci. USA*. 104(22):9301–9306

Liu W, Montana V, Parpura V, Mohideen U. 2011. Single-molecule measurements of dissociation rates and energy landscapes of binary trans snare complexes in parallel versus antiparallel orientation. *Biophys. J.* 101(8):1854–1862

Liu Y, Barlowe C. 2002. Analysis of Sec22p in endoplasmic reticulum/Golgi transport reveals cellular redundancy in SNARE protein function. Mol. Biol. Cell. 13(9):3314–3324

Liu Y, Xu X-H, Chen Q, Wang T, Deng C-Y, et al. 2013. Myosin Vb controls biogenesis of post-Golgi Rab10 carriers during axon development. Nat. Commun. 4:2005

Lockerbie RO, Miller VE, Pfenninger KH. 1991. Regulated plasmalemmal expansion in nerve growth cones. J. Cell Biol. 112(6):1215–1227

Loewen CJ, Levine TP. 2005. A highly conserved binding site in vesicle-associated membrane protein-associated protein (VAP) for the FFAT motif of lipid-binding proteins. *J. Biol. Chem.* 280(14):14097–14104

Loewen CJ, Roy A, Levine TP. 2003. A conserved ER targeting motif in three families of lipid binding proteins and in Opi1p binds VAP. *EMBO J.* 22(9):2025–2035

Loewen CJ, Young BP, Tavassoli S, Levine TP. 2007. Inheritance of cortical ER in yeast is required for normal septin organization. *J. Cell Biol.* 179(3):467–483

Loewen CJR, Roy A, Levine TP. 2003. A conserved ER targeting motif in three families of lipid binding proteins and in Opi1p binds VAP. EMBO J. 22(9):2025–2035

Lou X, Shin Y-K. 2016. SNARE zippering. Biosci. Rep. 36(3):

Lowery LA, Van Vactor D. 2009. The trip of the tip: understanding the growth cone machinery. Nat. Rev. Mol. Cell Biol. 10(5):332–343

Luedtke NW, Dexter RJ, Fried DB, Schepartz A. 2007. Surveying polypeptide and protein domain conformation and association with FlAsH and ReAsH. Nat. Chem. Biol. 3(12):779–784

Lynes EM, Simmen T. 2011. Urban planning of the endoplasmic reticulum (ER): how diverse mechanisms segregate the many functions of the ER. *Biochim. Biophys. Acta*. 1813(10):1893–1905

Ma C, Li W, Xu Y, Rizo J. 2011. Munc13 mediates the transition from the closed syntaxin-Munc18 complex to the SNARE complex. Nat. Struct. Mol. Biol. 18(5):542–549

Ma C, Su L, Seven AB, Xu Y, Rizo J. 2013. Reconstitution of the vital functions of Munc18 and Munc13 in neurotransmitter release. Science. 339(6118):421–425

Maeda K, Anand K, Chiapparino A, Kumar A, Poletto M, et al. 2013. Interactome map uncovers phosphatidylserine transport by oxysterol-binding proteins. *Nature*. 501(7466):257–261

Malsam J, Söllner TH. 2011. Organization of SNAREs within the Golgi stack. Cold Spring Harb. Perspect. Biol. 3(10):a005249

Mandikian D, Bocksteins E, Parajuli LK, Bishop HI, Cerda O, et al. 2014. Cell type-specific spatial and functional coupling between mammalian brain Kv2.1 K+ channels and ryanodine receptors. *J. Comp. Neurol.* 522(15):3555–3574

Manford AG, Stefan CJ, Yuan HL, Macgurn JA, Emr SD. 2012. ER-to-plasma membrane tethering proteins regulate cell signaling and ER morphology. *Dev. Cell*. 23(6):1129–1140

Mannella CA, Buttle K, Rath B, Marko M. 1998. Electron microscopic tomography of rat-livermitochondria and their interactions withthe endoplasmic reticulum. *Biofactors*. 8:225–228

Martinez-Arca S, Alberts P, Zahraoui A, Louvard D, Galli T. 2000. Role of tetanus neurotoxin insensitive vesicle-associated membrane protein (TI-VAMP) in vesicular transport mediating neurite outgrowth. J. Cell Biol. 149(4):889–900

Martinez-Arca S, Coco S, Mainguy G, Schenk U, Alberts P, et al. 2001. A common exocytotic mechanism mediates axonal and dendritic outgrowth. J. Neurosci. 21(11):3830–3838

Martinez-Arca S, Rudge R, Vacca M, Raposo G, Camonis J, et al. 2003. A dual mechanism controlling the localization and function of exocytic v-SNAREs. Proc. Natl. Acad. Sci. USA. 100(15):9011–9016

Martone ME, Zhang Y, Simpliciano VM, Carragher BO, Ellisman MH. 1993. Three-dimensional visualization of the smooth endoplasmic reticulum in Purkinje cell dendrites. *J. Neurosci.* 13(11):4636–46

Matteoli M, Coco S, Schenk U, Verderio C. 2004. Vesicle turnover in developing neurons: how to build a presynaptic terminal. Trends Cell Biol. 14(3):133–140

McMahon HT, Südhof TC. 1995. Synaptic core complex of synaptobrevin, syntaxin, and SNAP25 forms high affinity alpha-SNAP binding site. J. Biol. Chem. 270(5):2213–2217

Mei K, Guo W. 2018. The exocyst complex. Curr. Biol. 28(17):R922–R925

Ménager C, Arimura N, Fukata Y, Kaibuchi K. 2004. PIP3 is involved in neuronal polarization and axon formation. J. Neurochem. 89(1):109–118

Menna E, Disanza A, Cagnoli C, Schenk U, Gelsomino G, et al. 2009. Eps8 regulates axonal filopodia in hippocampal neurons in response to brain-derived neurotrophic factor (BDNF). PLoS Biol. 7(6):e1000138

Mesmin B, Bigay J, Moser von Filseck J, Lacas-Gervais S, Drin G, Antonny B. 2013. A four-step cycle driven by PI(4)P hydrolysis directs sterol/PI(4)P exchange by the ER-Golgi tether OSBP. *Cell*. 155(4):830–843

Metuzals J, Chang D, Hammar K, Reese TS. 1997. Organization of the cortical endoplasmic reticulum in the squid giant axon. *J Neurocytol*. 26(8):529–539

Min SW, Chang WP, Sudhof T. 2007. E-Syts, a family of membranous Ca2+-sensor proteins with multiple C2domains. *Proc. Natl. Acad. Sci. USA*. 104:3823–28

Ming G, Wong ST, Henley J, Yuan X, Song H, et al. 2002. Adaptation in the chemotactic guidance of nerve growth cones. Nature. 417(6887):411–418

Misura KM, Scheller RH, Weis WI. 2000. Three-dimensional structure of the neuronal-Sec1-syntaxin 1a complex. Nature. 404(6776):355–362

Mohammadi AS, Phan NT, Fletcher JS, Ewing AG. 2016. Intact lipid imaging of mouse brain samples: MALDI, nanoparticle-laser desorption ionization, and 40 keV argon cluster secondary ion mass spectrometry. *Anal. Bioanal. Chem.* 408(24):6857–6868

Montecucco C, Schiavo G. 1994. Mechanism of action of tetanus and botulinum neurotoxins. Mol. Microbiol. 13(1):1–8

Moreau K, Ravikumar B, Renna M, Puri C, Rubinsztein DC. 2011. Autophagosome precursor maturation requires homotypic fusion. Cell. 146(2):303–317

Moser von Filseck J, Čopič A, Delfosse V, Vanni S, Jackson CL, et al. 2015a. INTRACELLULAR TRANSPORT. Phosphatidylserine transport by ORP/Osh proteins is driven by phosphatidylinositol 4-phosphate. *Science*. 349(6246):432–436

Moser von Filseck J, Vanni S, Mesmin B, Antonny B, Drin G. 2015b. A phosphatidylinositol-4-phosphate powered exchange mechanism to create a lipid gradient between membranes. *Nat. Commun.* 6:6671

Müller P, Herrmann A. 2002. Rapid transbilayer movement of spin-labeled steroids in human erythrocytes and in liposomes. *Biophys. J.* 82(3):1418–1428

Muñiz M, Riezman H. 2000. Intracellular transport of GPI-anchored proteins. *EMBO J.* 19(1):10–15

Murphy SE, Levine TP. 2016. VAP, a Versatile Access Point for the Endoplasmic Reticulum: Review and analysis of FFAT-like motifs in the VAPome. *Biochim. Biophys. Acta*. 1861(8 Pt B):952–961

Nair U, Klionsky DJ. 2011. Autophagosome biogenesis requires SNAREs. Autophagy. 7(12):1570–1572

Nakamura MT, Yudell BE, Loor JJ. 2014. Regulation of energy metabolism by long-chain fatty acids. *Prog. Lipid Res.* 53:124–144

Neef AB, Schultz C. 2009. Selective fluorescence labeling of lipids in living cells. *Angew. Chem. Int. Ed. Engl.* 48(8):1498–1500

Nguyen TT, Lewandowska A, Choi JY, Markgraf DF, Junker M, et al. 2012. Gem1 and ERMES do not directly affect phosphatidylserine transport from ER to mitochondria or mitochondrial inheritance. *Traffic*. 13(6):880–890

Nickel W, Seedorf M. 2008. Unconventional mechanisms of protein transport to the cell surface of eukaryotic cells. Annu. Rev. Cell Dev. Biol. 24:287–308

Nishimura Y, Hayashi M, Inada H, Tanaka T. 1999. Molecular cloning and characterization of mammalian homologues of vesicle-associated membrane protein-associated (VAMP-associated) proteins. *Biochem. Biophys. Res. Commun.* 254(1):21–26

Novick P, Field C, Schekman R. 1980. Identification of 23 complementation groups required for post-translational events in the yeast secretory pathway. Cell. 21(1):205–215

Novikoff PR, Novikoff AB, Quintana N, Hauw JJ. 1971. GOLGI APPARATUS, GERL, AND LYSOSOMESOF NEURONS IN RAT DORSAL ROOT GANGLIA,STUDIED BY THICK SECTION ANDTHIN SECTION CYTOCHEMISTRY. *J. Cell Biol.* 50:859–886

Oksdath M, Guil AFN, Grassi D, Sosa LJ, Quiroga S. 2017. The Motor KIF5C Links the Requirements of Stable Microtubules and IGF-1 Receptor Membrane Insertion for Neuronal Polarization. Mol. Neurobiol. 54(8):6085–6096

Osen-Sand A, Catsicas M, Staple JK, Jones KA, Ayala G, et al. 1993. Inhibition of axonal growth by SNAP-25 antisense oligonucleotides in vitro and in vivo. Nature. 364(6436):445–448

Osen-Sand A, Staple JK, Naldi E, Schiavo G, Rossetto O, et al. 1996. Common and distinct fusion proteins in axonal growth and transmitter release. J. Comp. Neurol. 367(2):222–234

Park Y, Seo JB, Fraind A, Pérez-Lara A, Yavuz H, et al. 2015. Synaptotagmin-1 binds to PIP(2)-containing membrane but not to SNAREs at physiological ionic strength. Nat. Struct. Mol. Biol. 22(10):815–823

Perler FB, Davis EO, Dean GE, Gimble FS, Jack WE, et al. 1994. Protein splicing elements: inteins and exteins--a definition of terms and recommended nomenclature. Nucleic Acids Res. 22(7):1125–1127

Petkovic M, Jemaiel A, Daste F, Specht CG, Izeddin I, et al. 2014. The SNARE Sec22b has a non-fusogenic function in plasma membrane expansion. *Nat. Cell Biol.* 16(5):434–444

Pfenninger KH, Friedman LB. 1993. Sites of plasmalemmal expansion in growth cones. Brain Res. Dev. Brain Res. 71(2):181–192

Pfenninger KH, Laurino L, Peretti D, Wang X, Rosso S, et al. 2003. Regulation of membrane expansion at the nerve growth cone. J. Cell Sci. 116(Pt 7):1209–1217

Pfenninger KH. 2009. Plasma membrane expansion: a neuron's Herculean task. Nat. Rev. Neurosci. 10(4):251–261

Pichler H, Gaigg B, Hrastnik C, Achleitner G, Kohlwein SD, et al. 2001. A subfraction of the yeast endoplasmic reticulum associates with the plasma membrane and has a high capacity to synthesize lipids. *Eur. J. Biochem.* 268(8):2351–2361

Piper M, Anderson R, Dwivedy A, Weinl C, van Horck F, et al. 2006. Signaling mechanisms underlying Slit2-induced collapse of Xenopus retinal growth cones. Neuron. 49(2):215–228

Porter KR, Palade GE. 1957. STUDIES ON THE ENDOPLASMIC RETICULUM III. ITS FORM AND DISTRIBUTION IN STRIATED MUSCLE CELLS. *J Biophys Biochem Cytol*

Posse de Chaves E, Vance DE, Campenot RB, Vance JE. 1995. Axonal synthesis of phosphatidylcholine is required for normal axonal growth in rat sympathetic neurons. J. Cell Biol. 128(5):913–918

Prinz WA. 2010. Lipid trafficking sans vesicles: where, why, how? *Cell*. 143(6):870–874

Prinz WA. 2014. Bridging the gap: membrane contact sites in signaling, metabolism, and organelle dynamics. *J. Cell Biol.* 205(6):759–769

Rabouille C. 2017. Pathways of unconventional protein secretion. Trends Cell Biol. 27(3):230–240

Racchetti G, Lorusso A, Schulte C, Gavello D, Carabelli V, et al. 2010. Rapid neurite outgrowth in neurosecretory cells and neurons is sustained by the exocytosis of a cytoplasmic organelle, the enlargeosome. J. Cell Sci. 123(Pt 2):165–170

Ramakrishnan S, Bera M, Coleman J, Krishnakumar SS, Pincet F, Rothman JE. 2019. Synaptotagmin oligomers are necessary and can be sufficient to form a Ca2+ -sensitive fusion clamp. FEBS Lett. 593(2):154–162

Raychaudhuri S, Im YJ, Hurley JH, Prinz WA. 2006. Nonvesicular sterol movement from plasma membrane to ER requires oxysterol-binding protein-related proteins and phosphoinositides. *J. Cell Biol.* 173(1):107–119

Raychaudhuri S, Prinz WA. 2010. The diverse functions of oxysterol-binding proteins. *Annu. Rev. Cell Dev. Biol.* 26:157–177

Reim K, Mansour M, Varoqueaux F, McMahon HT, Südhof TC, et al. 2001. Complexins regulate a late step in Ca2+-dependent neurotransmitter release. Cell. 104(1):71–81

Reinisch KM, De Camilli P. 2016. SMP-domain proteins at membrane contact sites: Structure and function. *Biochim. Biophys. Acta*. 1861(8 Pt B):924–927

Renvoisé B, Blackstone C. 2010. Emerging themes of ER organization in the development and maintenance of axons. *Curr. Opin. Neurobiol.* 20(5):531–537

Resh MD. 2016. Fatty acylation of proteins: The long and the short of it. *Prog. Lipid Res.* 63:120–131

Rizo J, Südhof TC. 1998. C2-domains, structure and function of a universal Ca2+-binding domain. *J. Biol. Chem.* 273(26):15879–15882

Rizo J. 2018. Mechanism of neurotransmitter release coming into focus. Protein Sci. 27(8):1364–1391

Rodriguez OC, Schaefer AW, Mandato CA, Forscher P, Bement WM, Waterman-Storer CM. 2003. Conserved microtubule-actin interactions in cell movement and morphogenesis. Nat. Cell Biol. 5(7):599–609

Rosenbluth ack. 1962. Subsurface cisterns and their relationship to the neuronal plasma membrane. *J. Cell Biol.* 13:405–431

Rossi V, Banfield DK, Vacca M, Dietrich LEP, Ungermann C, et al. 2004. Longins and their longin domains: regulated SNAREs and multifunctional SNARE regulators. Trends Biochem. Sci. 29(12):682–688

Rothemund PW. 2006. Folding DNA to create nanoscale shapes and patterns. *Nature*. 440(7082):297–302

Rothman JE, Krishnakumar SS, Grushin K, Pincet F. 2017. Hypothesis - buttressed rings assemble, clamp, and release SNAREpins for synaptic transmission. FEBS Lett. 591(21):3459–3480

Rothman JE, Lenard J. 1977. Membrane asymmetry. *Science*. 195(4280):743–753

Saheki Y, Bian X, Schauder CM, Sawaki Y, Surma MA, et al. 2016. Control of plasma membrane lipid homeostasis by the extended synaptotagmins. Nat. Cell Biol. 18(5):504–515

Saito T, Nakatsuji N. 2001. Efficient gene transfer into the embryonic mouse brain using in vivo electroporation. Dev. Biol. 240(1):237–246

Saliba AE, Vonkova I, Gavin AC. 2015. The systematic analysis of protein-lipid interactions comes of age. *Nat. Rev. Mol. Cell Biol.* 16(12):753–761

Sargiacomo M, Sudol M, Tang Z, Lisanti MP. 1993. Signal transducing molecules and glycosyl-phosphatidylinositol-linked proteins form a caveolin-rich insoluble complex in MDCK cells. *J. Cell Biol.* 122(4):789–807

Schaaf G, Ortlund EA, Tyeryar KR, Mousley CJ, Ile KE, et al. 2008. Functional anatomy of phospholipid binding and regulation of phosphoinositide homeostasis by proteins of the sec14 superfamily. *Mol. Cell*. 29(2):191–206

Schaefer AW, Kabir N, Forscher P. 2002. Filopodia and actin arcs guide the assembly and transport of two populations of microtubules with unique dynamic parameters in neuronal growth cones. J. Cell Biol. 158(1):139–152

Schauder CM, Wu X, Saheki Y, Narayanaswamy P, Torta F, et al. 2014. Structure of a lipid-bound extended synaptotagmin indicates a role in lipid transfer. *Nature*. 510(7506):552–555

Schekman R. 2002. Lasker Basic Medical Research Award. SEC mutants and the secretory apparatus. *Nat. Med.* 8(10):1055–1058

Schelski M, Bradke F. 2017. Neuronal polarization: From spatiotemporal signaling to cytoskeletal dynamics. Mol. Cell. Neurosci. 84:11–28

Schiavo G, Matteoli M, Montecucco C. 2000. Neurotoxins affecting neuroexocytosis. Physiol. Rev. 80(2):717–766

Schoch S, Deák F, Königstorfer A, Mozhayeva M, Sara Y, et al. 2001. SNARE function analyzed in synaptobrevin/VAMP knockout mice. Science. 294(5544):1117–1122

Schulte C, Racchetti G, D'Alessandro R, Meldolesi J. 2010. A new form of neurite outgrowth sustained by the exocytosis of enlargeosomes expressed under the control of REST. Traffic. 11(10):1304–1314

Sclip A, Bacaj T, Giam LR, Südhof TC. 2016. Extended Synaptotagmin (ESyt) Triple Knock-Out Mice Are Viable and Fertile without Obvious Endoplasmic Reticulum Dysfunction. PLoS One. 11(6):e0158295

Scudieri P, Caci E, Venturini A, Sondo E, Pianigiani G, et al. 2015. Ion channel and lipid scramblase activity associated with expression of TMEM16F/ANO6 isoforms. J. Physiol. (Lond.). 593(17):3829–3848

Shelly M, Cancedda L, Heilshorn S, Sumbre G, Poo M-M. 2007. LKB1/STRAD promotes axon initiation during neuronal polarization. Cell. 129(3):565–577

Shenoy-Scaria AM, Dietzen DJ, Kwong J, Link DC, Lublin DM. 1994. Cysteine3 of Src family protein tyrosine kinase determines palmitoylation and localization in caveolae. *J. Cell Biol.* 126(2):353–363

Shevchenko A, Simons K. 2010. Lipidomics: coming to grips with lipid diversity. *Nat. Rev. Mol. Cell Biol.* 11(8):593–598

Shi L, Shen Q-T, Kiel A, Wang J, Wang H-W, et al. 2012. SNARE proteins: one to fuse and three to keep the nascent fusion pore open. Science. 335(6074):1355–1359

Shi S-H, Jan LY, Jan Y-N. 2003. Hippocampal neuronal polarity specified by spatially localized mPar3/mPar6 and PI 3-kinase activity. Cell. 112(1):63–75

Shimizu T. 2009. Lipid mediators in health and disease: enzymes and receptors as therapeutic targets for the regulation of immunity and inflammation. *Annu. Rev. Pharmacol. Toxicol.* 49:123–150

Shin J, Lou X, Kweon D-H, Shin Y-K. 2014. Multiple conformations of a single SNAREpin between two nanodisc membranes reveal diverse pre-fusion states. Biochem. J. 459(1):95–102

Shore Gordon, Tata Jamshed. 1977. Two fractions of rough endoplasmicreticulum from rat liver. *J. Cell biol.* 72:714–725

Simons K, Ikonen E. 1997. Functional rafts in cell membranes. *Nature*. 387(6633):569–572

Singer SJ, Nicolson GL. 1972. The Fluid Mosaic Model of the Structure of Cell Membranes. . *Science*. 175:720–731

Skehel PA, Martin KC, Kandel ER, Bartsch D. 1995. A VAMP-binding protein from Aplysia required for neurotransmitter release. *Science*. 269(5230):1580–1583

Skibbens JE, Roth MG, Matlin KS. 1989. Differential extractability of influenza virus hemagglutinin during intracellular transport in polarized epithelial cells and nonpolar fibroblasts. *J. Cell Biol.* 108(3):821–832

Sleight RG, Pagano RE. 1983. Rapid appearance of newly synthesized phosphatidylethanolamine at the plasma membrane. *J. Biol. Chem.* 258(15):9050–9058

Smith DH. 2009. Stretch growth of integrated axon tracts: extremes and exploitations. Prog. Neurobiol. 89(3):231–239

Soboloff J, Rothberg BS, Madesh M, Gill DL. 2012. STIM proteins: dynamic calcium signal transducers. *Nat. Rev. Mol. Cell Biol.* 13(9):549–565

Söllner T, Bennett MK, Whiteheart SW, Scheller RH, Rothman JE. 1993a. A protein assembly-disassembly pathway in vitro that may correspond to sequential steps of synaptic vesicle docking, activation, and fusion. Cell. 75(3):409–418

Söllner T, Whiteheart SW, Brunner M, Erdjument-Bromage H, Geromanos S, et al. 1993b. SNAP receptors implicated in vesicle targeting and fusion. Nature. 362(6418):318–324

Sosa L, Dupraz S, Laurino L, Bollati F, Bisbal M, et al. 2006. IGF-1 receptor is essential for the establishment of hippocampal neuronal polarity. Nat. Neurosci. 9(8):993–995

Spacek J, Harris KM. 1997. Three-dimensional organization of smooth endoplasmic reticulum in hippocampal CA1 dendrites and dendritic spines of the immature and mature rat. *J. Neurosci.* 17(1):190–203

Sparvero LJ, Amoscato AA, Dixon CE, Long JB, Kochanek PM, et al. 2012. Mapping of phospholipids by MALDI imaging (MALDI-MSI): realities and expectations. *Chem Phys Lipids*. 165(5):545–562

Spillane M, Ketschek A, Donnelly CJ, Pacheco A, Twiss JL, Gallo G. 2012. Nerve growth factor-induced formation of axonal filopodia and collateral branches involves the intra-axonal synthesis of regulators of the actin-nucleating Arp2/3 complex. J. Neurosci. 32(49):17671–17689

Steck TL, Ye J, Lange Y. 2002. Probing red cell membrane cholesterol movement with cyclodextrin. *Biophys. J.* 83(4):2118–2125

Stefan CJ, Manford AG, Baird D, Yamada-Hanff J, Mao Y, Emr SD. 2011. Osh proteins regulate phosphoinositide metabolism at ER-plasma membrane contact sites. *Cell*. 144(3):389–401

Stefan CJ, Manford AG, Emr SD. 2013. ER-PM connections: sites of information transfer and inter-organelle communication. *Curr. Opin. Cell Biol.* 25(4):434–442

Steiner P, Sarria JCF, Huni B, Marsault R, Catsicas S, Hirling H. 2002. Overexpression of neuronal Sec1 enhances axonal branching in hippocampal neurons. Neuroscience. 113(4):893–905

Südhof TC, Rizo J. 2011. Synaptic vesicle exocytosis. Cold Spring Harb. Perspect. Biol. 3(12):

Südhof TC, Rothman JE. 2009. Membrane fusion: grappling with SNARE and SM proteins. Science. 323(5913):474–477

Sutton RB, Fasshauer D, Jahn R, Brunger AT. 1998. Crystal structure of a SNARE complex involved in synaptic exocytosis at 2.4 A resolution. Nature. 395(6700):347–353

Suzuki J, Fujii T, Imao T, Ishihara K, Kuba H, Nagata S. 2013. Calcium-dependent phospholipid scramblase activity of TMEM16 protein family members. J. Biol. Chem. 288(19):13305–13316

Suzuki J, Umeda M, Sims PJ, Nagata S. 2010. Calcium-dependent phospholipid scrambling by TMEM16F. Nature. 468(7325):834–838

Tabata H, Nakajima K. 2001. Efficient in utero gene transfer system to the developing mouse brain using electroporation: visualization of neuronal migration in the developing cortex. Neuroscience. 103(4):865–872

Tafesse FG, Huitema K, Hermansson M, van der Poel S, van den Dikkenberg J, et al. 2007. Both sphingomyelin synthases SMS1 and SMS2 are required for sphingomyelin homeostasis and growth in human HeLa cells. *J. Biol. Chem.* 282(24):17537–17547

Takeshima H, Hoshijima M, Song LS. 2015. Ca^{2+} microdomains organized by junctophilins. *Cell Calcium*. 58(4):349–356

Takeshima H, Komazaki S, Nishi M, Iino M, Kangawa K. 2000. Junctophilins: a novel family of junctional membrane complex proteins. *Mol. Cell*. 6(1):11–22

Tanaka T, Yamaguchi H, Kishimoto Y, Gould RM. 1987. Lipid metabolism in various regions of squid giant nerve fiber. Biochim. Biophys. Acta. 922(1):85–94

Tareste D, Roux A. 2018. Common energetic and mechanical features of membrane fusion and fission machineries. In Physics of Biological Membranes, eds. P Bassereau, P Sens, pp. 421–469. Cham: Springer International Publishing

Tohda C, Nakanishi R, Kadowaki M. 2006. Learning deficits and agenesis of synapses and myelinated axons in phosphoinositide-3 kinase-deficient mice. Neurosignals. 15(6):293–306

Urbani L, Simoni RD. 1990. Cholesterol and vesicular stomatitis virus G protein take separate routes from the endoplasmic reticulum to the plasma membrane. *J. Biol. Chem.* 265(4):1919–1923

van Bergeijk P, Adrian M, Hoogenraad CC, Kapitein LC. 2015. Optogenetic control of organelle transport and positioning. Nature. 518(7537):111–114

van Beuningen SFB, Will L, Harterink M, Chazeau A, van Battum EY, et al. 2015. TRIM46 controls neuronal polarity and axon specification by driving the formation of parallel microtubule arrays. Neuron. 88(6):1208–1226

van Meer G, Voelker DR, Feigenson GW. 2008. Membrane lipids: where they are and how they behave. *Nat. Rev. Mol. Cell Biol.* 9(2):112–124

van Vliet AR, Giordano F, Gerlo S, Segura I, Van Eygen S, et al. 2017. The ER Stress Sensor PERK Coordinates ER-Plasma Membrane Contact Site Formation through Interaction with Filamin-A and F-Actin Remodeling. Mol. Cell. 65(5):885–899.e6

Vance JE, Aasman EJ, Szarka R. 1991. Brefeldin A does not inhibit the movement of phosphatidylethanolamine from its sites for synthesis to the cell surface. *J. Biol. Chem.* 266(13):8241–8247

Vance JE, Pan D, Vance DE, Campenot RB. 1991. Biosynthesis of membrane lipids in rat axons. J. Cell Biol. 115(4):1061–1068

Vance JE. 1990. Phospholipid synthesis in a membrane fraction associated with mitochondria. *J. Biol. Chem.* 265(13):7248–7256

Vance JE. 2014. MAM (mitochondria-associated membranes) in mammalian cells: lipids and beyond. *Biochim. Biophys. Acta*. 1841(4):595–609

Vega IE, Hsu SC. 2001. The exocyst complex associates with microtubules to mediate vesicle targeting and neurite outgrowth. J. Neurosci. 21(11):3839–3848

Vitriol EA, Zheng JQ. 2012. Growth cone travel in space and time: the cellular ensemble of cytoskeleton, adhesion, and membrane. Neuron. 73(6):1068–1081

Vogt L, Giger RJ, Ziegler U, Kunz B, Buchstaller A, et al. 1996. Continuous renewal of the axonal pathway sensor apparatus by insertion of new sensor molecules into the growth cone membrane. Curr. Biol. 6(9):1153–1158

Walch-Solimena C, Blasi J, Edelmann L, Chapman ER, von Mollard GF, Jahn R. 1995. The t-SNAREs syntaxin 1 and SNAP-25 are present on organelles that participate in synaptic vesicle recycling. J. Cell Biol. 128(4):637–645

Walther TC, Farese RV. 2012. Lipid droplets and cellular lipid metabolism. *Annu. Rev. Biochem.* 81:687–714

Wang B, Pan L, Wei M, Wang Q, Liu W-W, et al. 2015. FMRP-Mediated Axonal Delivery of miR-181d Regulates Axon Elongation by Locally Targeting Map1b and Calm1. Cell Rep. 13(12):2794–2807

Wang G, Nola S, Bovio S, Bun P, Coppey-Moisan M, et al. 2018. Biomechanical Control of Lysosomal Secretion Via the VAMP7 Hub: A Tug-of-War between VARP and LRRK1. iScience. 4:127–143

Wang J, Bello O, Auclair SM, Wang J, Coleman J, et al. 2014. Calcium sensitive ring-like oligomers formed by synaptotagmin. Proc. Natl. Acad. Sci. USA. 111(38):13966–13971

Warnock DE, Lutz MS, Blackburn WA, Young WW, Baenziger JU. 1994. Transport of newly synthesized glucosylceramide to the plasma membrane by a non-Golgi pathway. *Proc. Natl. Acad. Sci. USA*. 91(7):2708–2712

Weir ML, Xie H, Klip A, Trimble WS. 2001. VAP-A binds promiscuously to both v- and tSNAREs. Biochem. Biophys. Res. Commun. 286(3):616–621

Weninger K, Bowen ME, Choi UB, Chu S, Brunger AT. 2008. Accessory proteins stabilize the acceptor complex for synaptobrevin, the 1:1 syntaxin/SNAP-25 complex. Structure. 16(2):308–320

Weninger K, Bowen ME, Chu S, Brunger AT. 2003. Single-molecule studies of SNARE complex assembly reveal parallel and antiparallel configurations. Proc. Natl. Acad. Sci. USA. 100(25):14800–14805

West M, Zurek N, Hoenger A, Voeltz GK. 2011. A 3D analysis of yeast ER structure reveals how ER domains are organized by membrane curvature. *J. Cell Biol.* 193(2):333–346

Wilson DW, Wilcox CA, Flynn GC, Chen E, Kuang WJ, et al. 1989. A fusion protein required for vesicle-mediated transport in both mammalian cells and yeast. Nature. 339(6223):355–359

Winkle CC, Gupton SL. 2016. Membrane trafficking in neuronal development: ins and outs of neural connectivity. Int. Rev. Cell Mol. Biol. 322:247–280

Witte H, Bradke F. 2008. The role of the cytoskeleton during neuronal polarization. Curr. Opin. Neurobiol. 18(5):479–487

Wojnacki J, Galli T. 2016. Membrane traffic during axon development. Dev. Neurobiol. 76(11):1185–1200

Wolf W, Kilic A, Schrul B, Lorenz H, Schwappach B, Seedorf M. 2012. Yeast Ist2 recruits the endoplasmic reticulum to the plasma membrane and creates a ribosome-free membrane microcompartment. *PLoS One*. 7(7):e39703

Wong LH, Levine TP. 2017. Wong and Levine_Tubular lipid binding proteins (TULIPs) growing everywhere. *Cell Mol Biol Res*. 1864:1439–49

Wood D.W., Harcum S.W., Belfort G. (2005) Industrial Applications of Intein Technology. In: Belfort M., Wood D.W., Stoddard B.L., Derbyshire V. (eds) Homing Endonucleases and Inteins. Nucleic Acids and Molecular Biology, vol 16. Springer, Berlin, Heidelberg

Wu MM, Buchanan J, Luik RM, Lewis RS. 2006. Ca2+ store depletion causes STIM1 to accumulate in ER regions closely associated with the plasma membrane. *J. Cell Biol.* 174(6):803–813

Wu SJ, Niknafs YS, Kim SH, Oravecz-Wilson K, Zajac C, et al. 2017. A Critical Analysis of the Role of SNARE Protein SEC22B in Antigen Cross-Presentation. Cell Rep. 19(13):2645–2656

Wu Y, Whiteus C, Xu CS, Hayworth KJ, Weinberg RJ, et al. 2017. Contacts between the endoplasmic reticulum and other membranes in neurons. *Proc. Natl. Acad. Sci. USA*. 114(24):E4859–E4867

Xiao Q, Hu X, Wei Z, Tam KY. 2016. Cytoskeleton molecular motors: structures and their functions in neuron. Int. J. Biol. Sci. 12(9):1083–1092

Xu J, Bacaj T, Zhou A, Tomchick DR, Südhof TC, Rizo J. 2014. Structure and Ca^{2+}-binding properties of the tandem C_2 domains of E-Syt2. *Structure*. 22(2):269–280

Yang H, Kim A, David T, Palmer D, Jin T, et al. 2012. TMEM16F forms a Ca2+-activated cation channel required for lipid scrambling in platelets during blood coagulation. Cell. 151(1):111–122

Yao J, Sasaki Y, Wen Z, Bassell GJ, Zheng JQ. 2006. An essential role for beta-actin mRNA localization and translation in Ca2+-dependent growth cone guidance. Nat. Neurosci. 9(10):1265–1273

Yoder MD, Thomas LM, Tremblay JM, Oliver RL, Yarbrough LR, Helmkamp GM. 2001. Structure of a multifunctional protein. Mammalian phosphatidylinositol transfer protein complexed with phosphatidylcholine. *J. Biol. Chem.* 276(12):9246–9252

Yoshimura T, Arimura N, Kaibuchi K. 2006. Signaling networks in neuronal polarization. J. Neurosci. 26(42):10626–10630

Yoshimura T, Kawano Y, Arimura N, Kawabata S, Kikuchi A, Kaibuchi K. 2005. GSK-3beta regulates phosphorylation of CRMP-2 and neuronal polarity. Cell. 120(1):137–149

Yu H, Liu Y, Gulbranson DR, Paine A, Rathore SS, Shen J. 2016. Extended synaptotagmins are Ca2+-dependent lipid transfer proteins at membrane contact sites. Proc. Natl. Acad. Sci. USA. 113(16):4362–4367

Zakharenko S, Popov S. 1998. Dynamics of axonal microtubules regulate the topology of new membrane insertion into the growing neurites. J. Cell Biol. 143(4):1077–1086

Zanetti MN, Bello OD, Wang J, Coleman J, Cai Y, et al. 2016. Ring-like oligomers of Synaptotagmins and related C2 domain proteins. Elife. 5:

Zhang L, Yan F, Zhang S, Lei D, Charles MA, et al. 2012. Structural basis of transfer between lipoproteins by cholesteryl ester transfer protein. *Nat. Chem. Biol.* 8(4):342–349

Zhen Y, Stenmark H. 2015. Cellular functions of Rab GTPases at a glance. J. Cell Sci. 128(17):3171–3176

Zhou F-Q, Waterman-Storer CM, Cohan CS. 2002. Focal loss of actin bundles causes microtubule redistribution and growth cone turning. J. Cell Biol. 157(5):839–849

Zhou Q, Zhou P, Wang AL, Wu D, Zhao M, et al. 2017. The primed SNARE-complexin-synaptotagmin complex for neuronal exocytosis. Nature. 548(7668):420–425

Zimmerberg J, Chernomordik LV. 1999. Membrane fusion. *Adv. Drug Deliv. Rev.* 38(3):197–205

Zylbersztejn K, Galli T. 2011. Vesicular traffic in cell navigation. FEBS J. 278(23):4497–4505

Zylbersztejn K, Petkovic M, Burgo A, Deck M, Garel S, et al. 2012. The vesicular SNARE Synaptobrevin is required for Semaphorin 3A axonal repulsion. J. Cell Biol. 196(1):37–46